ISSN 2500-1388 (Print)
ISSN 2618-754X (Online)

НАУКА и ИННОВАЦИИ в медицине

2025
Том 10
Volume
Выпуск 3
Issue

SCIENCE and INNOVATIONS in medicine

www.innoscience.ru

16+

SAMARA STATE MEDICAL UNIVERSITY

SCIENCE & INNOVATIONS IN MEDICINE

NAUKA I INNOVATSII V MEDITSINE

Volume 10 | Issue 3 | 2025 | Founded in 2016

QUARTERLY PEER-REVIEWED MEDICAL JOURNAL

Founder and Publisher
Samara State Medical University

Registered by the Federal Service for Supervision of Communications, Information Technology and Mass Media (Roskomnadzor) 06.06.2016. Registration number FS 77-65957

ISSN 2500-1388 (Print)
ISSN 2618-754X (Online)

Publication frequency: quarterly.

Indexation
DOAJ
Russian Science Citation Index (eLibrary.ru)
Cyberleninka
Google Scholar
Ulrich's Periodicals Directory
Dimensions
Crossref

Journal archive:
www.innoscience.ru
Archive and current issues are in open access.

Articles submission:
https://innoscience.ru/2500-1388/author/submit/1
Author Guidelines:
https://innoscience.ru/2500-1388/about/submissions

Publisher and editorial office address:
89 Chapaevskaya st., Samara, Russia, 443099.
Tel.: + 7 (846) 374 10 04.
E-mail: edition@innoscience.ru

Executive editor: Alla V. Stefanskaya (e-mail: a.v.stefanskaya@samsmu.ru)
Translator: Konstantin M. Kalinin
Proofreader: Inna N. Chainikova
Layout editor: Tat'yana I. Ovchinnikova

Signed for printing: 24.08.2025
Publication 31.08.2025
Printed by: LLC "Prime"
12 Baikalsky lane,
Samara, Russia, 443079.
Tel.: +7 (846) 922 62 90.
Order: No0385.

САМАРСКИЙ ГОСУДАРСТВЕННЫЙ МЕДИЦИНСКИЙ УНИВЕРСИТЕТ

НАУКА И ИННОВАЦИИ В МЕДИЦИНЕ
SCIENCE AND INNOVATIONS IN MEDICINE

Том 10 | Выпуск 3 | 2025 | Издается с 2016 г.

НАУЧНО-ПРАКТИЧЕСКИЙ РЕЦЕНЗИРУЕМЫЙ ЖУРНАЛ

Учредитель и издатель
ФГБОУ ВО СамГМУ Минздрава России

Зарегистрирован Федеральной службой по надзору в сфере связи, информационных технологий и массовых коммуникаций (Роскомнадзор) 06.06.2016. Регистрационный № ФС 77-65957

ISSN 2500-1388 (Print)
ISSN 2618-754X (Online)

Периодичность: 4 номера в год.

Журнал включен в Перечень ведущих научных журналов и изданий ВАК (К2)

Индексация
DOAJ
Российский Индекс Научного Цитирования (eLibrary.ru)
Cyberleninka
Google Scholar
Ulrich's Periodicals Directory
Dimensions
Crossref

Архив номеров: www.innoscience.ru
Открытый доступ к архивам и текущим номерам.

Прием статей в журнал:
https://innoscience.ru/2500-1388/author/submit/1
Правила публикации авторских материалов:
https://innoscience.ru/2500-1388/about/submissions

Адрес издателя и редакции:
ул. Чапаевская, 89, г. Самара, Россия, 443099.
Тел.: + 7 (846) 374 10 04.
E-mail: edition@innoscience.ru

Зав. редакцией: Стефанская А.В. (e-mail: a.v.stefanskaya@samsmu.ru)
Переводчик: Калинин К.М.
Корректор: Чайникова И.Н.
Верстка: Овчинникова Т.И.

Подписано в печать: 24.08.2025
Выход в свет 31.08.2025
Отпечатано: ООО «Прайм».
Байкальский пер., 12, г. Самара, Россия, 443079.
Тел.: +7 (846) 922 62 90.
Формат 60 × 90⅛. Печать офсетная.
Заказ №0385.
Усл. печ. л. 9.
Тираж 250 экз.

CONTENTS / СОДЕРЖАНИЕ

Original research | Оригинальное исследование
DOI: https://doi.org/10.35693/SIM685730

Histomorphometry as a method for assessing the healing of tubular bone fractures

Vitalii N. Morozov[1], Viktoriya P. Pecherskaya[2], Ekaterina S. Novik[1], Elena N. Morozova[1]

[1]Belgorod National Research University (Belgorod, Russian Federation)
[2]Yakovlevskaya Central District Hospital (Belgorod Region, Stroitel, Russian Federation)

Abstract

Aim – to carry out a quantitative assessment of the healing of tubular bone fracture modeled by applying a hole defect in it and to analyze existing methods of bone regenerate morphometry.

Material and methods. The data were obtained on 30 white mature rats, which had a hole defect made in the tibiae. Morphological and morphometric studies of the regenerate were performed on the 3rd, 10th, 15th, 24th and 45th days after surgery on histological sections.

Results. Microscopically the tibial regenerate in mature rats is characterized by the presence of hematoma from 3rd to 10th days, as well as granulation tissue from 3rd to 24th days, fibroreticular tissue, woven bone from 3rd to 45th days, and lamellar bone, from 10th to 45th days of reparative osteogenesis. Along with the well-known structures of the bone regenerate, muscle fibers have been identified in its granulation tissue. Due to the peculiarities of the structural organization of fibroreticular tissue, woven and lamellar bones and their localization in the regenerate, it is proposed to distinguish organized and unorganized layers in the first, and typical and atypical (disorganized) components in the rest. Histomorphometry was used to obtain data on the actual values of the areas of hematoma, granulation, fibroreticular tissue, woven and lamellar bones on 3rd, 10th, 15th, 24th, 45th days after fracture modeling, their percentages to the total area of the regenerate and the dynamics of their changes from one period to another.

Conclusion. The histomorphometry data of the tibial regenerate on the 3rd, 10th, 15th, 24th and 45th days after surgery, as well as the revealed features of its histostructure, supplement the available information on bone fracture healing and can be used for fundamental medicine.

Keywords: tubular bone, regenerate, hematoma, granulation tissue, fibroreticular tissue, woven bone, lamellar bone, morphometry, technique.

Conflict of interest: nothing to disclose.

Citation
Morozov VN, Pecherskaya VP, Novik ES, Morozova EN. **Histomorphometry as a method for assessing the healing of tubular bone fractures.** *Science and Innovations in Medicine.* 2025;10(3):178-187. DOI: https://doi.org/10.35693/SIM685730

Information about authors
***Vitalii N. Morozov** – MD, Dr. Sci. (Medicine), Associate professor, Associate professor of the Department of Human Anatomy and Histology.
ORCID: 0000-0002-1169-4285
E-mail: vitaliyymorozov85@mail.ru
Viktoriya P. Pecherskaya – neurologist of the neurological department for the treatment of patients with stroke.
ORCID: 0000-0003-1615-4904
E-mail: konshina.viktory@yandex.ru
Ekaterina S. Novik – laboratory assistant at the Department of Human Anatomy and Histology.
ORCID: 0009-0007-7489-0260
E-mail: sidekser@mail.ru
Elena N. Morozova – MD, Cand. Sci. (Medicine), Associate professor, Associate professor of the Department of Human Anatomy and Histology.
ORCID: 0000-0002-6117-080X
E-mail: tiger2910@rambler.ru
Corresponding Author

Received: 18.06.2025
Received: 20.07.2025
Published: 11.08.2025

Гистоморфометрия как метод оценки заживления переломов трубчатых костей

В.Н. Морозов[1], В.П. Печерская[2], Е.С. Новик[1], Е.Н. Морозова[1]

[1]ФГАОУ ВО «Белгородский государственный национальный исследовательский университет» Министерства высшего образования и науки РФ (Белгород, Российская Федерация)
[2]ОГБУЗ «Яковлевская центральная районная больница» (Белгородская область, г. Строитель, Российская Федерация)

Аннотация

Цель – осуществить количественную оценку заживления перелома трубчатой кости, смоделированного путем нанесения в ней сквозного дефекта, и провести анализ существующих методик морфометрии костного регенерата.

Материал и методы. Данные получены на 30 белых половозрелых крысах, которым наносился сквозной дырчатый дефект в большеберцовых костях. Морфологическое и морфометрическое изучение регенерата осуществляли на 3, 10, 15, 24, 45-е сутки после операции на гистологических срезах.

Результаты. Исследование регенерата большеберцовой кости половозрелых крыс микроскопически характеризуется наличием гематомы на 3 и 10-е сутки, а также грануляционной ткани – на 3–24-е сутки, фиброретикулярной, грубоволокнистой тканей – на 3–45-е сутки и пластинчатой ткани – на 10–45-е сутки репаративного остеогенеза. Наряду с общеизвестными структурами регенерата в его грануляционной ткани выявлены мышечные волокна. В связи с особенностями структурной организации фиброретикулярной, грубоволокнистой, пластинчатой тканей и их локализацией в регенерате предложено выделить в первой организованный и неорганизованный слои, а в остальных – типичный и нетипичный (разрушающийся) компоненты. Методом гистоморфометрии получены данные о фактических значениях площадей гематомы, грануляционной, фиброретикулярной, грубоволокнистой и пластинчатой тканей на 3, 10, 15, 24, 45-е сутки после моделирования перелома, их процентных отношениях к общей площади регенерата и динамике их изменений от одного срока к другому.

Заключение. Данные гистоморфометрии регенерата большеберцовой кости на 3, 10, 15, 24, 45-е сутки после операции, а также выявленные особенности его гистоструктуры расширяют и дополняют имеющуюся информацию по заживлению переломов костей и могут быть использованы для фундаментальной медицины.

Ключевые слова: трубчатая кость, регенерат, гематома, грануляционная ткань, фиброретикулярная ткань, грубоволокнистая ткань, пластинчатая ткань, морфометрия, метод.

Конфликт интересов: не заявлен.

Для цитирования:
Морозов В.Н., Печерская В.П., Новик Е.С., Морозова Е.Н. **Гистоморфометрия как метод оценки заживления переломов трубчатых костей.** *Наука и инновации в медицине.* 2025;10(3):178-187. DOI: https://doi.org/10.35693/SIM685730

Сведения об авторах
***Морозов Виталий Николаевич** – д-р мед. наук, доцент, доцент кафедры анатомии и гистологии человека.
ORCID: 0000-0002-1169-4285
E-mail: vitaliyymorozov85@mail.ru
Печерская В.П. – врач-невролог неврологического отделения для лечения больных с ОНМК.
ORCID: 0000-0003-1615-4904
E-mail: konshina.viktory@yandex.ru
Новик Е.С. – лаборант кафедры анатомии и гистологии человека.
ORCID: 0009-0007-7489-0260
E-mail: sidekser@mail.ru
Морозова Е.Н. – канд. мед. наук, доцент, доцент кафедры анатомии и гистологии человека.
ORCID: 0000-0002-6117-080X
E-mail: tiger2910@rambler.ru
Автор для переписки

Получено: 18.06.2025
Одобрено: 20.07.2025
Опубликовано: 11.08.2025

INTRODUCTION

According to the statistics, in the Russian Federation traumas rank second after cardiovascular diseases and first among causes of early disablement in patients aged below 60 [1]. This makes the question of traumatism especially important [2]. Considering the social and economic consequences the state incurs due to its citizens' traumas, the research into problems of reparative regeneration of bones seems vital.

The healing of bone fractures is a complex multistaged process the assessment of which involves clinical signs and X-ray, ultrasonic [3], morphologic (light microscopy and histomorphometry), as well as laboratory methods (identification of bone metabolism markers).

AIM

To carry out a quantitative assessment of the healing of tubular bone fracture modeled by applying a hole defect in it and to analyze existing methods of bone regenerate morphometry.

MATERIAL AND METHODS

The study used 30 sexually mature male outbred white rats weighing 200-210 g (6 animals per experimental time point). The fracture of the tibia was modeled by making a through hole defect (2.2 mm) with an electrical tool consisting of a hard alloy burr for the angled handpiece (JSC "OEZ Vladmiva", Belgorod, Russian Federation) and X-Smart endo motor with tip and reduction gearbox (Dentsply, Maillefer, Switzerland) in the proximal section of the diaphysis under ether anesthesia [4]. Postoperative observation time points (days 3, 10, 15, 24, and 45) were established based on key stages of reparative osteogenesis according to Korzh N.A. and Deduh N.V. (2006) [5]. For the purposes of histological research, a fragment of the tibia between the proximal epiphysis and diaphysis was excised. The specimens were fixed in 10% neutral buffered formalin, decalcified in 5% formic acid solution, dehydrated through a graded series of isopropyl alcohol, and embedded in homogenized Histomix paraffin medium. Histological sections (5-6 μm thick) were prepared and stained with hematoxylin-eosin and Masson's trichrome. Visual assessment of histological changes in the media, measurement of their structural components, and photographing were performed on the hardware-software system consisting of a personal computer (Nis-Elements BR 4.60.00 software), Nikon Eclipse Ni microscope and Nikon DS-Fi3 digital camera (Nikon Corporation, Japan). The measurements of the morphometric parameters of the bone regenerate were performed in the NDP.view2 software kit (Hamamatsu Photonics K.K., EU, Japan, UK, USA). The numeric data was uploaded to a licensed program JASP (v. 0.19.1.0, The JASP Team, Amsterdam) to perform descriptive statistics (calculation of the median and the quartiles). The same program was used to test the normality of data distribution using the Shapiro-Wilk test. Considering the data distribution different from normal, to compare the independent groups in various times of experiment, the Mann-Whitney U-test was used to establish statistically significant changes. The confidence interval for values was 95%.

RESULTS

On day 3 of the experiment, in the area of the defect a section of a hematoma is visualized, surrounded by granular and fibroreticular tissue (**Fig. 1**), with foci of woven bone visualized in the latter.

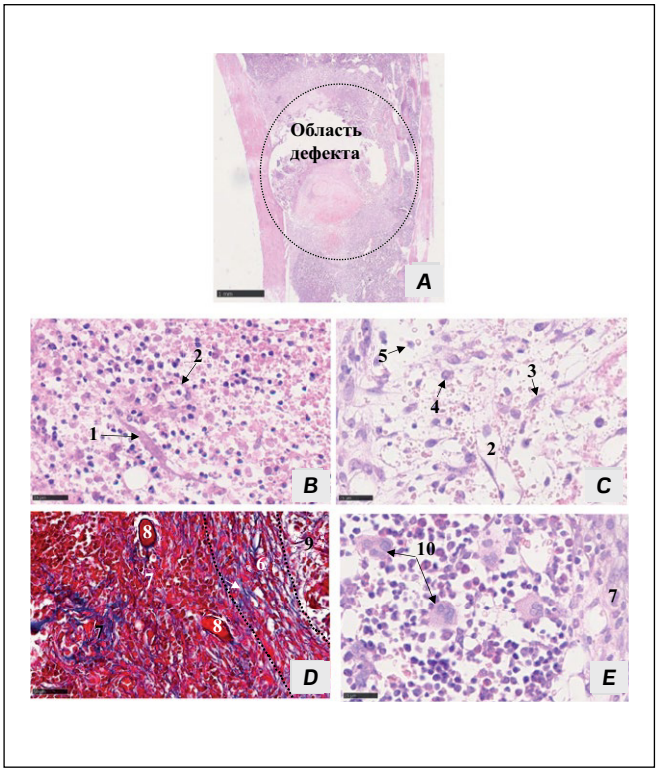

Figure 1. *Tibial bone regeneration site after applying a hole defect in it on the 3rd day of the experiment: A – area of the tibia with regenerate, B – hematoma in which remnants of muscle fibers (1) with vessels (2), C – granulation tissue containing a vessel (2), fibroblast (3), macrophage (4), lymphocyte (5), D – area of an organized (6) and non-insular disorganized (7) fibroreticular tissue containing areas of typical woven bone (8) that adhere to granulation tissue (9), E – area of non-insular disorganized fibroreticular tissue in contact with red bone marrow, 10 – megakaryocytes. Staining: hematoxylin-eosin (A-C, E), according to Masson (D).*

Рисунок 1. *Участок регенерата большеберцовой кости после нанесения в ней сквозного дырчатого дефекта на третьи сутки эксперимента: А – участок большеберцовой кости с регенератом, Б – гематома, в которой встречаются остатки мышечных волокон (1) с сосудами (2), В – грануляционная ткань, содержащая сосуд (2), фибробласт (3), макрофаг (4), лимфоцит (5), Г – участок организованной (6) и безостровковой неорганизованной (7) фиброретикулярной ткани, содержащий участки типичной грубоволокнистой ткани (8), которые прилежат к грануляционной ткани (9), Д – участок безостровковой неорганизованной фиброретикулярной ткани, контактирующий с красным костным мозгом, 10 – мегакариоциты. Окраска: гематоксилин-эозин (А-В, Д), по Массону (Г).*

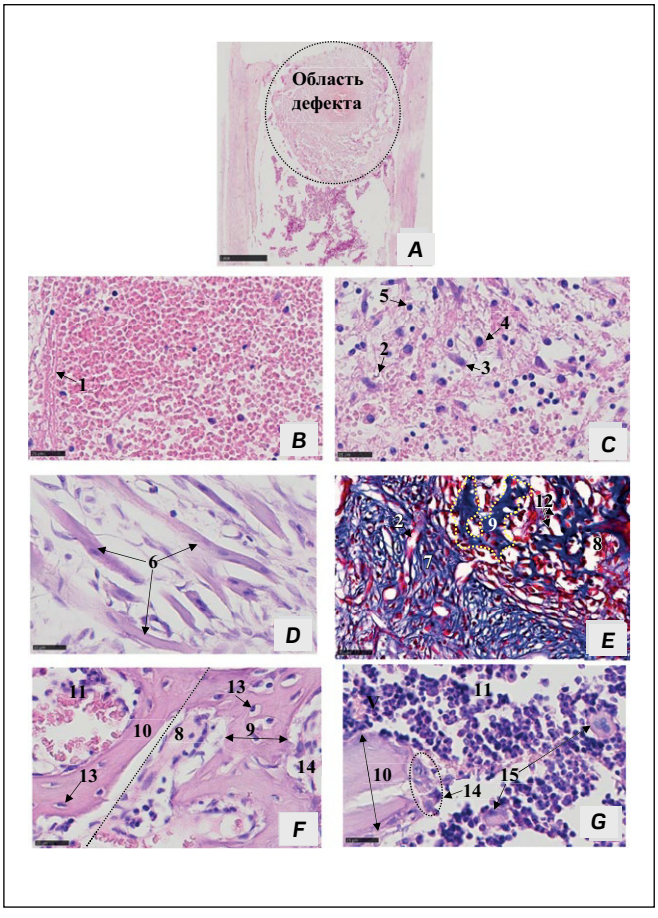

Figure 2. *The tibial bone regeneration site after applying a hole defect in it on the 10th day of the experiment: A – area of the tibia with regenerate, B – hematoma containing fibrin fibers (1), C – granulation tissue containing a vessel (2), fibroblast (3), macrophage (4), lymphocyte (5), D – area of granulation tissue with muscle fibers (6), E – organized (7) and insular (8) disorganized fibroreticular tissue containing areas of typical woven bone (9), F – section of typical woven bone surrounding bone marrow cavities with insular disorganized fibroreticular tissue, turning into typical lamellar bone (10) surrounding bone marrow cavities with red bone marrow (11), G – area of typical lamellar bone of the regenerate with red bone marrow surrounding it, 12 – osteoblasts, 13 – osteocyte, 11 – bone marrow cavity with red bone marrow, 12 – bone trabeculae of typical lamellar bone, 14 – osteoclast, 15 – megakaryocytes. Staining: hematoxylin-eosin (A-D, F, G), according to Masson (E).*

Рисунок 2. *Участок регенерата большеберцовой кости после нанесения в ней сквозного дырчатого дефекта на 10-е сутки эксперимента: А – участок большеберцовой кости с регенератом, Б – гематома, содержащая фибриновые волокна (1), В – грануляционная ткань, содержащая сосуд (2), фибробласт (3), макрофаг (4), лимфоцит (5), Г – участок грануляционной ткани с мышечными волокнами (6), Д – участок организованной (7) и островковой (8) неорганизованной фиброретикулярной ткани, содержащий участки типичной грубоволокнистой ткани (9), Е – участок типичной грубоволокнистой ткани, окружающей костно-мозговые полости с островковой неорганизованной фиброретикулярной тканью, переходящий в типичную пластинчатую ткань (10), окружающую костно-мозговые полости с красным костным мозгом (11), Ж – участок типичной пластинчатой костной ткани регенерата с окружающим регенерат красным костным мозгом, 12 – остеобласты, 13 – остеоцит, 11 – костно-мозговая полость с красным костным мозгом, 12 – костные трабекулы типичной пластинчатой костной ткани, 14 – остеокласт, 15 – мегакариоциты. Окраска: гематоксилин-эозин (А-Г, Е, Ж), по Массону (Д).*

In the hematoma area, fibrin mesh is visualized that fragments the area, separate it from the granular tissue and prevent proliferation of the blood corpuscles into the neighboring tissue. Within the mesh, debris of or deteriorating blood corpuscles are visualized, muscle fibers and fractured fragments of bone. Individual vessels are visualized on the periphery of the hematoma.

In the granular tissue around the hematoma, the cells are distributed loosely. The cellular composition is diverse. Fibroblasts, macrophages, lymphocytes, poorly differentiated cells, and capillaries in various cross-sections are identified.

The fibroreticular tissue is represented by a disorganized accumulation of cells and fibers, with vessels located between them. It should be noted that

there are more cells than fibers, and the structural components of the fibroreticular tissue surrounding the granulation tissue are arranged along it in the form of a layer (organized layer of fibroreticular tissue). On the compact bone side, the structural components of the fibroreticular tissue are arranged in bundles oriented in various directions (disorganized non-islet layer of fibroreticular tissue), and between them appear elongated areas of coarse fibrous tissue. These areas are surrounded by osteoblasts and consist of loosely arranged collagen fiber bundles organized into fascicles.

The compact bone area adjacent to the defect region contains lacunae without osteocytes. The red bone marrow in contact with this area contains large megakaryocytes.

The histomorphometry of the regenerate of tibia on day 3 of the experiment showed that its total area was 10.480 [10.317;10.710] mm^2, the area of the hematoma in the regenerate was 6.250 [5.942;6.513] mm^2, the area of the granular tissue was 1.790 [1.698;1.875] mm^2, area of fibroreticular tissue was 1.615 [1.530;1.685] mm^2, coarse fibrous bone tissue, 0.885 [0.807;0.932] mm^2, which, in percentage of the total area of the regenerate was 60%, 17%, 15% and 8%, respectively.

Structurally, the defect area on day 10 of the experiment is similar to that of day 3, but on the periphery of fibroreticular tissue, lamellar tissue appears (**Fig. 2**). It is to be noted that the regenerate tissues form evenly along the entire circumference of the defect area.

In terms of structure and location, the hematoma area, granulation and fibroreticular tissue are similar to those on day 3 of the experiment; at the same time, granulation tissue contained isolated muscle fibers displaying striations.

From the lamellar tissue side, coarse fibrous tissue appears as branched, interconnected irregularly shaped areas surrounding clusters of fibroreticular tissue, which forms an island-like disorganized layer. These areas of fibroreticular tissue are formed by loose clusters of collagen fiber, fibroblasts and fibrocytes, and change into densely packed groups of collagen fiber with similar cells and osteoclasts forming trabecula of lamellar tissue. The spaces between the clusters of the former are filled with fibroreticular tissue, and between the groups of the latter, with red bone marrow. On the surface of trabecula of the lamellar bone, osteoclasts are identified.

It is to be noted that on the periphery of the regenerate, areas of coarse fibrous tissue and lamellar bone tissue start deteriorating (matching in structure the failing fractured bone in the hematoma area on day 3 of the experiment, with osteoclasts identified in the surface of failing structures), and in their places, bone marrow cavities remain filled with fibroreticular tissue or red bone marrow, respectively. Thus, it is possible to identify the typical coarse fibrous tissue, lamellar bone tissue with constant structure, and non-typical, modified tissue with deteriorating or deteriorated structural components.

The specific features of structural components of the bone surrounding the regenerate in the defect area remain the same, as on day 3.

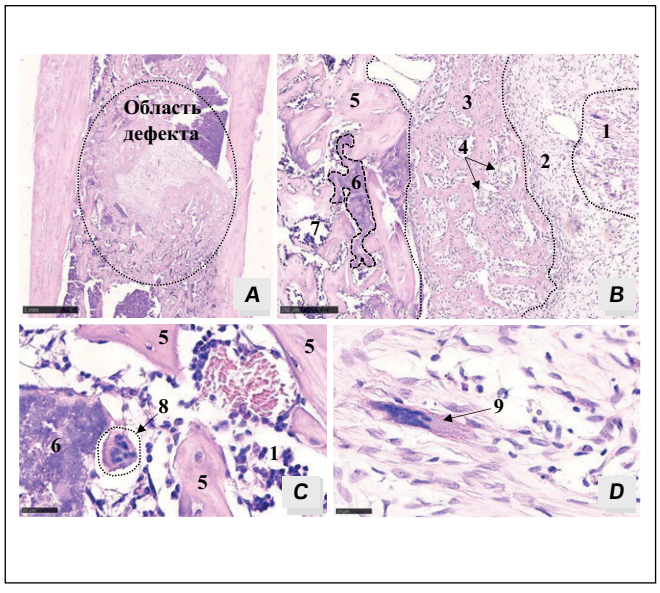

Figure 3. *Tibial bone regeneration site after applying a hole defect in it on the 15th day of the experiment: A – area of the tibia with regenerate, B – area of regenerate with granulation tissue (1), with organized fibroreticular tissue (2), with typical woven bone (3) containing bone marrow cavities with insular disorganized fibroreticular tissue (4), with typical (5) and atypical (6) lamellar bone surrounding cavities with red bone marrow (7), C – regenerate site containing typical and atypical lamellar bone surrounding bone marrow cavities with red bone marrow, D – granulation tissue site, 8 – osteoclast, 9 – muscle fiber. Staining: hematoxylin-eosin.*

Рисунок 3. *Участок регенерата большеберцовой кости после нанесения в ней сквозного дырчатого дефекта на 15-е сутки эксперимента: А – участок большеберцовой кости с регенератом, Б – участок регенерата с грануляционной тканью (1), с организованной фиброретикулярной тканью (2), с типичной грубоволокнистой тканью (3), содержащей костно-мозговые полости с островковой неорганизованной фиброретикулярной тканью (4), с типичной (5) и нетипичной (6) пластинчатой тканью, окружающими полости с красным костным мозгом (7), В – участок регенерата, содержащий типичную и нетипичную пластинчатую ткань, окружающую костно-мозговые полости с красным костным мозгом, Г – участок грануляционной ткани, 8 – остеокласт, 9 – мышечное волокно. Окраска: гематоксилин-эозин.*

On day 10 of the experiment, the total area of the regenerate was 11.500 [11.343;11.665] mm^2; the area occupied by the hematoma in the regenerate was 0.140 [0.115;0.165] mm2; the area taken by the granulation tissue was 0.890 [0.813;1.020] mm2; the area of fibroreticular tissue was 2.370 [2.295;2.625] mm^2; coarse fibrous bone tissue, 1.720 [1.662;1.823] mm^2; lamellar bone tissue, 3.630 [3.507;3.730] mm^2; bone marrow cavities, 2.535 [2.450;2.710] mm^2; the respective percentages being 1%, 8%, 21%, 15%, 32%, 23% of the total area of the regenerate. In comparison to day 3, on the 10th day of the experiment the total area of the regenerate increased by 1.09% (p=0.004), the area of the hematoma decreased by 97.77% (p=0.002), the area of the granulation tissue, by 48.93% (p=0.002). The area of fibroreticular tissue increased by 56.58% (p=0.002), and the area of coarse fibrous bone tissue, by 201.139% (p=0.005).

The area of the defect on day 15 of the experiment differs from that on the 3rd and 10th day by the lack of the hematoma. It is to be noted that the regenerate

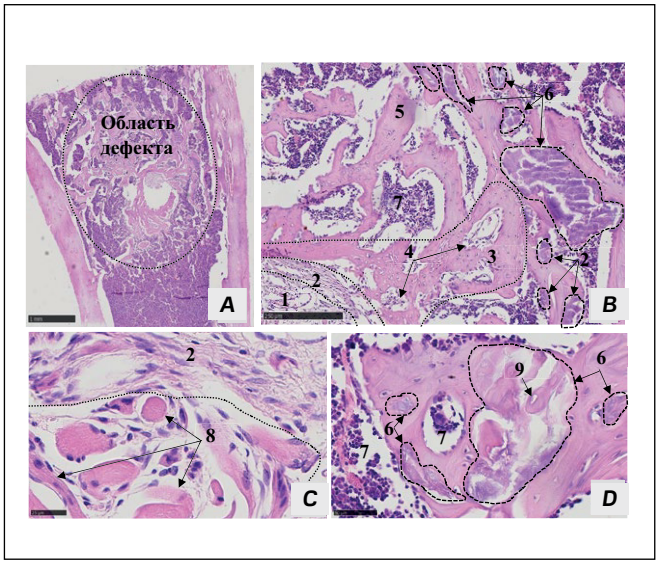

Figure 4. *Tibial bone regeneration site after applying a hole defect in it on the 24th day of the experiment: A – area of the tibia with regenerate, B – area of regenerate with granulation tissue (1), with organized fibroreticular tissue (2), with typical woven bone (3) containing bone marrow cavities with insular disorganized fibroreticular tissue (4), with typical (5) and atypical (6) lamellar bone surrounding cavities with red bone marrow (7), C – area of granulation tissue with organized fibroreticular tissue, D – regenerate site containing typical and atypical lamellar bone surrounding bone marrow cavities with red bone marrow, 8 – muscle fiber in granulation tissue, 9 – empty lacuna. Staining: hematoxylin-eosin.*

Рисунок 4. *Участок регенерата большеберцовой кости после нанесения в ней сквозного дырчатого дефекта на 24-е сутки эксперимента: А – участок большеберцовой кости с регенератом, Б – участок регенерата с грануляционной тканью (1), с организованной фиброретикулярной тканью (2), с типичной грубоволокнистой тканью (3), содержащей костно-мозговые полости с островковой неорганизованной фиброретикулярной тканью (4), с типичной (5) и нетипичной (6) пластинчатой тканью, окружающими полости с красным костным мозгом (7), В – участок грануляционной ткани с организованной фиброретикулярной тканью, Г – участок регенерата, содержащий типичную и нетипичную пластинчатую ткань, окружающую костно-мозговые полости с красным костным мозгом, 8 – мышечное волокно в грануляционной ткани, 9 – пустая лакуна. Окраска: гематоксилин-эозин.*

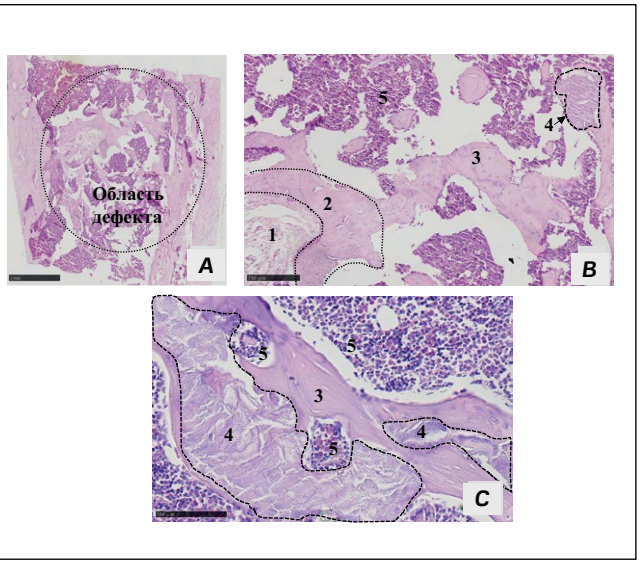

Figure 5. *The tibial bone regeneration site after applying a hole defect in it on the 45th day of the experiment (А, Б): A – area of the tibia with regenerate, B – area of regenerate with organized fibroreticular tissue (1), with typical woven bone (2), with typical (3) and atypical (4) lamellar bone surrounding cavities with red bone marrow (5), C – area of regenerate containing typical and atypical lamellar bone surrounding bone marrow cavities with red bone marrow. Staining: hematoxylin-eosin.*

Рисунок 5. *Участок регенерата большеберцовой кости после нанесения в ней сквозного дырчатого дефекта на 45-е сутки эксперимента: А – участок большеберцовой кости с регенератом, Б – участок регенерата с организованной фиброретикулярной тканью (1), с типичной грубоволокнистой тканью (2), с типичной (3) и нетипичной (4) пластинчатой тканью, окружающими полости с красным костным мозгом (5), В – участок регенерата, содержащий типичную и нетипичную пластинчатую ткань, окружающую костно-мозговые полости с красным костным мозгом. Окраска: гематоксилин-эозин.*

tissues form evenly on the entire circumference of the defect area.

In terms of structure and position, the area of granular, fibroreticular, coarse fibrous and lamellar tissues is similar to that on the 10th day of the experiment. At the same time, granulation tissue contained isolated muscle fibers displaying striations. In the latter, clusters of nuclei are seen in one of the sections of sarcoplasm (**Fig. 3**). The organized layer of fibroreticular tissue directly borders typical coarse fibrous tissue, while the island-like disorganized layer is located within cavities of the latter.

It is to be noted that both the typical and non-typical (deteriorating) lamellar bone tissue (similar morphological picture is seen on day 10), and on the place of the latter bone marrow cavities remain filled with red bone marrow. Near the non-typical lamellar bone tissue, osteoclasts are identified.

On day 15 of the experiment, the total area of the regenerate is 10.210 [10.105;10.503] mm^2; the area taken by granular tissue was 0.770 [0.637;0.858] mm^2, fibroreticular tissue, 2.445 [2.308;2.508] mm^2; coarse fibrous bone tissue, 2.065 [1.987;2.165] mm^2; lamellar bone tissue, 2.160 [2.032;2.295] mm^2; bone marrow cavities, 2.925 [2.768;3.052] mm2. The percentages from the total area of the regenerate are 7%, 23%, 20%, 21%, 29%, respectively. As compared to the 10th day, on the 15th day of the experiment the total area of the regenerate decreased by 10.08% (p=0.004), area of granular tissue, by 17.30% (p=0.180), area of fibroreticular tissue, by 2.51% (p=0.937). The area of coarse fibrous bone tissue increased by 17.64% (p=0.013), area of lamellar bone tissue decreased by 40.22% (p=0.002), and the area of bone marrow cavities increased by 13.55% (p=0.026).

On day 24 of the experiment, similar to day 15, the defect area differs from what it was on day 3 and day 10, namely, the hematoma is lacking. It is to be noted that the regenerate tissue form evenly along the entire circumference of the defect area. In terms of structure and position, the areas of granular, fibroreticular, coarse fibrous and lamellar bone tissue are similar to those on the 15th day of the experiment. In the granular tissue, individual muscle fibers are identified with signs of striation. The organized layer of fibroreticular tissue directly borders on the typical coarse fibrous tissue, and the insular non-organized layer is located in the cavities of the latter.

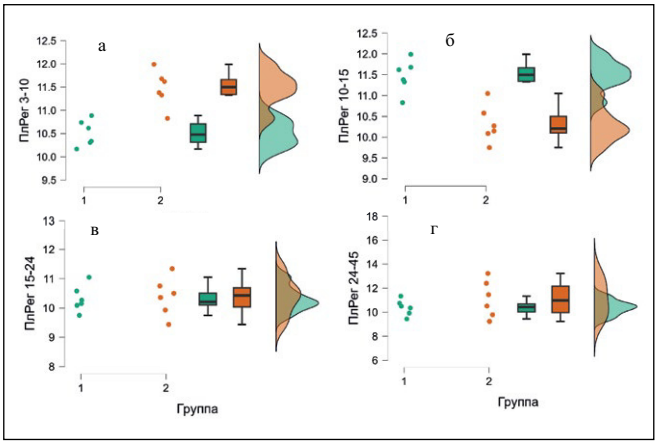

Figure 6. *"Rain cloud" graph reflecting the dynamics of changes in the area of tibial regenerate during different phases of reparative osteogenesis (a – from 3 to 10 days, b – from 10 to 15 days, c – from 15 to 24 days, d – from 24 to 45 days).*

Рисунок 6. *График «Дождевые облака», отражающий динамику изменений площади регенерата большеберцовых костей в течение разных фаз репаративного остеогенеза (а – с 3 по 10 сутки, б – с 10 по 15 сутки, в – с 15 по 24 сутки, г – с 24 по 45 сутки).*

On the periphery of the regenerate, both typical and non-typical lamellar bone tissue are identified (similar morphological picture is seen on day 15), and in the place of the latter, bone marrow cavities remain that are filled with red bone marrow (**Fig. 4**).

On the 24th day of the experiment, the total area of the regenerate was 10.430 [10.037;10.688] mm^2; the area under granular tissue, 0.655 [0.592;0.748] mm^2; fibroreticular tissue, 0.430 [0.405;0.485] mm^2; coarse fibrous bone tissue, 0.575 [0.505;0.638] mm^2; lamellar bone tissue, 2.115 [2.092;2.242] mm^2; bone marrow cavities, 6.505 [6.030;7.107] mm^2. This comprises the following percentages of the total regenerate area: 6%, 4%, 6%, 21%, 63%, respectively. As compared to the 15th day of the experiment, on the 24th day the total area of the regenerate increased by 0.69% (p=0.818), the area of granular tissue decreased by 12.56% (p=0.296), the area of fibroreticular tissue, by 81.64% (p=0.002), the area of coarse fibrous bone tissue, by 62.41% (p=0.002), the area of lamellar bone tissue, by 0.62% (p=0.748), and the area of bone marrow cavities increased by 224.79% (p=0.002).

The defect area on the 45th day of the experiment differs from that on the 24th day by the absence of granular tissue (**Fig. 5**). It is to be noted that the regenerate tissue form evenly along the entire circumference of the defect area. In terms of structure and position, the areas of fibroreticular, coarse fibrous and lamellar bone tissue are similar to those on the 24th day of the experiment.

On the periphery of the regenerate, both typical and non-typical lamellar bone tissue are identified (similar morphological picture is seen on day 24), and in the place of the latter, bone marrow cavities remain that are filled with red bone marrow.

On the 45th day, the total area of the regenerate is 10.990 [9.973;12.173] mm^2; the area under fibroreticular tissue, 0.420 [0.368;0.495] mm^2; coarse fibrous tissue, 0.400 [0.368;0.495] mm^2; lamellar tissue, 2.850 [2.732;3.042] mm^2; bone marrow cavities, 7.320 [6.505;8.210] mm^2, corresponding to 4%, 4%, 26%, 66% of the total area of the regenerate, respectively. In comparison with the 24th day, the total area of the regenerate on the 45th day increased by 6.95% (p=0.485) (Fig. 6), the area of fibroreticular tissue decreased by 2.65% (p=0.873), the area of coarse fibrous bone tissue, by 29.65% (p=0.009), the area of lamellar bone tissue increased by 33.31% (p=0.002), and the area of bone marrow cavities, by 12.93% (p=0.240).

DISCUSSION

Reparative osteogenesis exhibits distinct progression patterns in different types of bone fractures. Results from manual and automated measurements can vary significantly, making it essential to account for the morphometry equipment type, software used and staining method.

A.T. Silant'eva *et al.* (2003) evaluate the process of formation of regenerate forming between the proximal and distal ends of canine tibiae following transverse fracture, based on calculation of the regenerate compaction coefficient (amount of cortical plate in the transversal section of the regenerate), coefficient of the regenerate form (ratio of the transversal dimensions of the regenerate and the transversal dimensions of the fractured bone), coefficient of the regenerate structure (amount of bone sections in the total area of the regenerate), density index of the compact and spongy bone tissue (amount of matter of compact and spongy bone tissue on the regenerate section). These values are used to calculate the dynamic parameters of osteogenesis: index of amount of bone matter in the regenerate prior to formation of the cortical plate and on the stage of its formation [6].

V.V. Annikov *et al.* (2005) modeled transverse tibial fractures in rabbits and used an ocular grid on histological sections to determine the ratio of newly formed bone volume to other tissue types (connective and cartilage), relative area taken by the latter, ratio of length of bone trabecula occupied with active osteoblasts to their total length, and its cellular composition (amount of histocytes, fibroblasts, total number of osteoblasts and inflammatory cells) [7].

N.V. Deduh *et al.* (2009) used the model of a through hole defect in the distal metaphysis of the tibia in rats following G.G. Avtandilov's morphometry method and suggest measuring the number of tissue basophils, neutrophils, plasmocytes, lymphocytes, fibroblasts and poorly differentiated cells on the first, second and third days after fracture, and measuring the area of granular, fibroreticular, coarse fibrous and lamellar bone tissue, native bone and detritus, as well as bone marrow, on the 5th, 7th, 14th, 21st and 28th days [8].

A.V. Slisarenko *et al.* (2013) evaluated the morpho-functional condition of the regenerate on the 7th, 15th and 24th day after making the hole defect in the middle of diaphysis of tibiae by measuring such histomorphometric parameters as percentage of fibroblasts, macrophages, lymphocytes, plasmocytes, neutrophils, poorly

differentiated cells in the total amount of cells, as well as percentage of granular, fibroreticular, coarse fibrous and lamellar bone tissue. Morphometric measurements were performed in the SEO imageLab software suite using the histological sections stained with hematoxylin-eosin and using the Romanowsky-Giemsa method [9].

N.O. Ashukina *et al.* (2013) used histological sections of the regenerate (Van Gieson's staining with hematoxylin-eosin) forming in the hole defect of the middle diaphysis of the tibia in rats, to measure the relative area of the hematoma, bone, fibroreticular, granular tissue and bone marrow with the square ocular grid of the microscope to calculate their percentage from the total area of all tissues in the defect region. The measurements were taken on the 3rd, 7th, 14th and 21st says after making the model fracture of the tibia [10].

V.Yu. Lebedinsky *et al.* (2015) and I.N. Mikhailov et al. (2015), in their rabbit experiments, proposed calculating the following morphometric parameters for distraction regenerate of the ulna and radius: relative vascular volume, tissue structure volumes (with quantification of cellular and extracellular matrix components), and the ratio of ossified to non-ossified structures. The authors suggested such morphometric indices as vessel-to-tissue ratio, cell-to-tissue ratio, ossification index. The first two of these are the ratios of relative volume of vessels and cells to the amount of tissue structures; the third represents the ratio of ossified to non-ossified structures. In the latter, the amount of cells and intercellular matter were measured. The measurements were taken using an ocular grid and systems of image analysis on sections stained with hematoxylin-eosin [11-13].

P.E. Kovalchuk *et al.* (2015), after modeling a fracture in the proximal femoral metaphysis by creating a through-hole defect, proposed quantifying the percentage of defect filling with newly formed bone tissue at days 7, 15, and 30 of reparative osteogenesis. The authors measured this parameter planimetrically on digital images of histological sections using a measurement grid and expressed the results as percentages [14].

O.V. Korenkov (2016) proposed evaluating the healing of a hole defect in the rat tibial diaphyses by calculating the ratio of bone and connective tissue area to the total defect area using image analysis software ("Video-Test" and "Video-Size"). The analysis was performed on 15th and 30th days after the fracture on hematoxylin-eosin-stained histological sections [15].

M.S. Shpakovsky *et al.* (2016) propose the following as morphometric parameters of healing of the fracture of the femoral neck in rabbits: surface area of bone trabecula, numeric density of osteoblasts, osteocytes, osteoclasts, vessels, proliferating osteoblasts, and endothelium cells. The measurements were taken on the 7th, 14th, 30th, and 60th days post-operation on sections stained with hematoxylin-eosin and Van Gieson's method using the Axioplan 2 imaging software suite (Carl Zeiss, Germany) [16].

V.D. Shyshchuk *et al.* (2018) proposed measuring the cellular composition of the regenerate on the third day after making the through defect in the middle of diaphysis of tibiae in rats, namely, measuring the amount of fibroblasts, neutrophils, lymphocytes, plasmocytes, macrophages, poorly differentiated cells; on the 15th and 24th days, measurement of percentage of granular, fibroreticular, coarse fiber and lamellar bone tissue. In the two latter cases, thickness of bone trabecula was measured in the center and on the periphery of the regenerate, total area and diameter of vessels was measured in all cases. The morphometric measurements were performed in the software suites "Video test 5.0" and "Video Size 5.0" using histological sections stained with hematoxylin-eosin (15th and 24th days) and with Romanowsky-Giemsa method (3rd day) [17].

E.N. Gorbach (2019) investigated morphometric parameters of blood vessels in the proximal and distal bone fragments, corresponding regions of the regenerate, and the intervening zone in dogs following a modeled transverse fracture in the middle diaphysis of the tibia. Analyzing the histological sections stained with hematoxylin-eosin, and orcein using the Taenzer-Unna method in the "VideoTesT-Morphology 4.0" (Russia) software suite, the author measured the diameter of vessels and numeric density of arterial and venous vessels and calculated the number of arteria, arterioles, venules and veins [18].

D.I. Suchkov *et al.* (2019) modeled a fenestrated defect in the mid-third of the rat femur and measured the following parameters: number of vessels, amount and ratio of cells of osteocitarian differon (osteocytes, osteoblasts, osteoclasts), area of the bone marrow, fibrous tissue, amount of inflammatory cells and foreign cells. The authors performed their measurements in the ImageJ software suite (NIH, USA) using histological sections stained with hematoxylin-eosin and Van Gieson's method on the 14th, 21st and 28th days after modeling the fracture [19].

E.A. Nadyrov *et al.* (2019) propose measuring the following morphometric parameters in tibial bone regenerate of rats: area of necroses, granular tissue, bone trabecula on histological sections stained with hematoxylin-eosin [20].

Analysis of modern scientific literature has shown the absence up to the present time of a unified approach to the methodology of assessing tubular bone fracture healing, which can be associated with researchers choosing different biological objects for study (modeling), methods of fracture modeling, methodological approaches to morphometry and different time points for studying the forming regenerate. In the early stages after the fracture (day three) the measurements concern the hematoma and its cellular composition, and in later stages (day 10 and on), the parameters of forming tissues that gradually replace one another (granular, finroreticular, coarse fibrous and lamellar bone tissue) and their structural components.

Granulation tissue is a type of connective tissue that develops at the site of a fibrin clot, beginning from the peripheral portions of the hematoma. Its principal cells are fibroblasts, myofibroblasts coming from both the nearby connective tissues and differentiating from

progenitor cells or mesenchymal stem cells migrating to the fracture area. The amorphous matter of the granular tissue is characteriszed with a high degree of hydration in which the collagen fibers consist of type 3 collagen (faster synthesis with lower mechanical strength) without the presence of elastic fibers. Along with the formation of amorphous matter and collagen fibers, neo-formation of blood capillaries occurs [21].

As the fracture healing progresses, due to proliferation of fibroblastic differon cells and gradual maturation of collagen fibers (replacement of type 3 collagen with type 1 collagen) fibroreticular tissue is forming represented by randomly oriented bands of these cells and fibers. In the peripheral regions of the regenerate, as the osteoreparation process progresses, areas of coarse fibrous bone tissue appear, characterized by an organized arrangement of variably thick collagen fiber bundles aligned along the stress lines of the bone. They serve as the foundation of formation of trabecula of coarse fibrous bone tissue, in which the number of osteocytes and the dimensions of the lacunae in which they localize is higher than in the mature lamellar bone tissue. Whereas the space between the forming trabecula of coarse fibrous bone tissue is filled with fibroreticular tissue, in the lamellar bone tissue the similar spaces are filled with bone marrow [22].

Analysis of the histomorphometric parameters measured by the authors at different time points of reparative osteogenesis demonstrates their significance in quantitative assessment of tubular bone fracture healing. The dynamics of changes of such parameters as the amount of fibroblasts, poorly differentiated cells in the hematoma area among the total amount of cells, numeric density of vessels, and the percentage of forming granular tissue followed by fibroreticular tissue, coarse fibrous bone tissue and lamellar bone tissue, reflects the normal consistent staged process of regenerate formation from early stages to later, and the exclusion of one components from the process inevitably results in quantitative changes in the others. Thus, disruption of normal blood supply in the fracture area leads to osteogenesis turning to formation of cartilage tissue that does not have the same strength properties as the mature bone tissue. Our study established the presence of muscle fibers with transverse striation in the structure of granular tissue, which probably are not involved in the confinement and shrinkage of the hematoma area due to their contractile properties, and which may provide the granular tissue with the mechanical strength that the type 3 collagen lacks.

Other cells of the hematoma play an important role in the processes of its structural reorganization. The macrophages, similar to lymphocytes, synthesize and secrete angiogenic and cellular growth factors initiating fibroplasia and neo-formation of blood vessels in the fracture area. Endothelial cells can serve as a source of osteogenic progenitor cells and secrete endothelial growth factors that stimulate their proliferation. Like macrophages, endothelial cells also release platelet-derived growth factor, which promotes fibroblast proliferation, collagen synthesis, and chemotaxis of both mesenchymal stem cells and inflammatory lineage cells. The role of macrophages, along with neutrophils, is to be considered in the phagocytosis of the cellular detritus and bacteria in the fracture area [23]. Consequently, the quantified proportion of the aforementioned cell types within the total hematoma cell population serves as an indicator of the intensity of hematoma structural reorganization and formation of tissue-specific structures.

After the trauma, the fracture area is known to be surrounded by clusters of activated platelets that release the platelet growth factor, endothelial growth factor, insulin-like growth factor 1 and 2, beta-transforming growth factor. The first and the last stimulate chemotaxis, proliferation and differentiation of ostheogenic lineage cells [24].

In developing coarse fibrous bone and subsequent lamellar bone tissues, the dynamics of changes in parameters such as the quantity and ratio of osteocytic differon cells (osteocytes, osteoblasts, osteoclasts) provide crucial information about bone tissue neo-formation in the fracture area. Specifically, one example of a balance criterion of neo-formation and bone resorption may be the ratio of areas taken by osteoclasts vs. the area taken by osteoblasts, and ratio of osteoblast vs. osteoclast amounts [25].

CONCLUSIONS

1. The study of the regenerate of tibia of sexually mature rats provided microscopic evidence of the presence of the hematoma on days 3 to 10, granular tissue on days 3 to 24, fibroreticular and coarse fibrous bone tissue on days 3 to 45, and lamellar bone tissue on days 10 to 45 of reparative osteogenesis.

2. Our own data on actual values of their areas on days 3, 10, 15, 24, 45 after modeling the fracture, their percentage from the total area of regenerate and dynamics of their changes from one stage to another aligns with the information on quantitative assessment of bone regenerate available in the literature, and augment it.

3. Along with the generally known structures present in the regenerate, muscle fibers were identified in its granular tissue. Considering the specifics of structural organization of fibroreticulat, coarse fibrous and lamellar bone tissue and their localization in the regenerate, we suggest identifying the organized and non-organized in the first type of tissue, and typical and non-typical (deteriorating) components in other types of tissues. Future research will focus on developing quantitative assessment methods for these parameters and recommending their inclusion in standardized histomorphometric protocols for bone regenerate analysis, which will have significant implications for fundamental medicine.

ADDITIONAL INFORMATION	ДОПОЛНИТЕЛЬНАЯ ИНФОРМАЦИЯ
Ethical expertise. State Establishment "Sent Luke Lugansk State Medical University", Bioethics Commission, 25.03.2022, Protocol No. 2.	***Этическая экспертиза.*** Проведение исследования одобрено комиссией по биоэтике ГУ «Луганский государственный медицинский университет имени Святителя Луки» (протокол №2 от 25.03.2022 г.).
Study funding. The study was the authors' initiative without external funding.	***Источник финансирования.*** Работа выполнена по инициативе авторов без привлечения финансирования.
Conflict of interest. The authors declare that there are no obvious or potential conflicts of interest associated with the content of this article.	***Конфликт интересов.*** Авторы декларируют отсутствие явных и потенциальных конфликтов интересов, связанных с содержанием настоящей статьи.
Contribution of individual authors. Morozov V.N.: development of the concept, design of the study, editing of the text of the article. Pecherskaya V.P., Novik E.S.: search and analysis of literature, conducting an experiment, interpretation of results of histological research, statistical data processing, writing of the text of the article. Morozova E.N.: participation in histological processing of samples, writing and editing of the article. All authors gave their final approval of the manuscript for submission, and agreed to be accountable for all aspects of the work, implying proper study and resolution of issues related to the accuracy or integrity of any part of the work.	***Участие авторов.*** Морозов В.Н. – разработка концепции, дизайна исследования, редактирование текста статьи. Печерская В.П., Новик Е.С. – поиск и анализ литературы, проведение эксперимента, интерпретация результатов гистологического исследования, статистическая обработка данных, написание текста статьи. Морозова Е.Н. – участие в гистологической обработке образцов, написании и редактировании статьи. Все авторы одобрили финальную версию статьи перед публикацией, выразили согласие нести ответственность за все аспекты работы, подразумевающую надлежащее изучение и решение вопросов, связанных с точностью или добросовестностью любой части работы.

REFERENCES / ЛИТЕРАТУРА

1. Shcherbak NP, Mansurov DSh, Dorofeev YuL, et al. Features of the organization of traumatological care in the regions of the Russian Federation (A Scientific Review). *Physical and Rehabilitation Medicine*. 2021;3(3):62-72. [Щербак Н.П., Мансуров Д.Ш., Дорофеев Ю.Л., и др. Особенности организации травматологической помощи в регионах Российской Федерации. *Физическая и реабилитационная медицина*. 2021;3(3):62-72]. DOI: 10.26211/2658-4522-2021-3-3-62-72

2. Vasilyeva LS, Slivnitsyna NV, Shevchenko OI, et al. Clinical and psychological features of combined trauma in participants of military actions. *Polytrauma*. 2024;2:55-61. [Васильева Л.С., Сливницына Н.В., Шевченко О.И., и др. Клинико-психологические особенности сочетанной травмы участников военных действий. *Политравма*. 2024;2:55-61]. DOI: 10.24412/1819-1495-2024-2-55-61

3. Mikhanov VA, Kolosova NI, Polyakova VS, et al. The method to measure the evolution healing fractures of the tubular bones of rats in the experiment. *Journal of Anatomy and Histopathology*. 2017;6(1):58-62. [Миханов В.А., Колосова Н.И., Полякова В.С., и др. Способ количественной оценки динамики заживления переломов трубчатых костей крыс в эксперименте. *Журнал анатомии и гистопатологии*. 2017;6(1):58-62]. DOI: 10.18499/2225-7357-2017-6-1-58-62

4. Luzin VI, Ivchenko DV, Pankrat'ev AA. A technique for modeling bone defects in laboratory animals. *Ukraïns'kij medichnij al'manah*. 2005;8(2):162. (In Russ.). [Лузин В.И., Ивченко Д.В., Панкратьев А.А. Методика моделирования костного дефекта у лабораторных животных. *Український медичний альманах*. 2005;8(2):162].

5. Korzh NA, Deduh NV. Reparative bone regeneration: a modern view of the problem. Stages of regeneration. *Orthopaedics Traumatology and Prosthetics*. 2006;1:76-84. (In Russ.). [Корж Н.А., Дедух Н.В. Репаративная регенерация кости: современный взгляд на проблему. Стадии регенерации. *Ортопедия, травматология и протезирование*. 2006;1:76-84].

6. Silant'eva TA, Chirkova AM, Erofeev SA. Method of histomorphometric examination of distractive osteogenesis. Patent RF №2213963 C2, published Date of publication. 10.10.2003. (In Russ.). [Силантьева Т.А., Чиркова А.М., Ерофеев С.А. Способ гистоморфометрического исследования дистракционного остеогенеза. Патент РФ №2213963 С2, опубл. 10.10.2003].

7. Annikov VV, Slesarenko NA. Experimental research on the possibility of optimizing of reparative osteogenesis. *Veterinarnaja praktika*. 2005;1:14-18. (In Russ.). [Анников В.В., Слесаренко Н.А. Морфометрическая характеристика костного регенерата при его оптимизации с помощью аллопланта. *Ветеринарная практика*. 2005;1:14-18].

8. Dєduh NV, Nikol'chenko OA. Bone regeneration in Alimentary osteoporosis (experimental study). *Orthopaedics Traumatology and Prosthetics*. 2009;2(575):34-40. (In Ukrainian). [Дєдух Н.В., Нікольченко О.А. Регенерація кістки при аліментарному остеопорозі (експериментальне дослідження). *Ортопедия, травматология и протезирование*. 2009;2(575):34-40].

9. Slisarenko OV, Bumeister VI. Reparative Osteogenesis under Dehydration. *Tavricheskiy Mediko-Biologicheskiy Vestnik*. 2013;16(1-1):222-224. [Слисаренко А.В., Бумейстер В.И. Течение репаративного остеогенеза в условиях обезвоживания организма. *Таврический медико-биологический вестник*. 2013;16(1-1):222-224].

10. Ashukina NO, Diedukh NV, Geleta MM. Features of reparative osteogenesis in femur diaphyseal defects under condition of hypothyroidism modeling. *Tavricheskiy Mediko-Biologicheskiy Vestnik*. 2013;16(1-1):9-12. (In Ukrainian). [Ашукіна Н.О., Дєдух Н.В., Гелета М.М. Особливості репаративного остеогенезу в діафізарних дефектах стегнових кісток щурів за умов моделювання гіпотиреозу. *Таврический медико-биологический вестник*. 2013;16(1-1):9-12].

11. Lebedinskiy VYu, Puseva ME, Netesin ES, et al. Dynamics of quantitative parameters of regeneration in the experiment. *Sibirskij medicinskij zhurnal (Irkutsk)*. 2015;137(6):98-100. [Лебединский В.Ю., Пусева М.Э., Нетесин Е.С., и др. Динамика количественных параметров регенерации в эксперименте. *Сибирский медицинский журнал (Иркутск)*. 2015;137(6):98-100].

12. Lebedinskiy VYu, Puseva ME, Netesin ES, et al. Qualitative characteristics of distraction forelimb bone graft in rabbits in experiment. *Acta Biomedica Scientifica*. 2015;5(105):62-65. [Лебединский В.Ю., Пусева М.Э., Нетесин Е.С., и др. Количественная характеристика дистракционного регенерата костей предплечья кролика в эксперименте. *Acta Biomedica Scientifica*. 2015;5(105):62-65]. URL: https://www.actabiomedica.ru/jour/article/view/116

13. Mikhailov IN, Lebedinskiy VYu, Puseva ME, et al. Distraction forearm bone graft characteristics in experiment with stimulation of biologically active points. *Acta Biomedica Scientifica*. 2015;5(105):66-71. [Михайлов И.Н., Лебединский В.Ю., Пусева М.Э., и др. Характеристика дистракционного регенерата костей предплечья в эксперименте при стимуляции БАТ. *Acta Biomedica Scientifica*. 2015;5(105):66-71]. URL: https://www.actabiomedica.ru/jour/article/view/117

14. Kovalchuk PYe, Hasko MV, Tuliuliuk SV. Reparative osteogenesis in normal conditions and in micronutrient iodine and selenium deficiency. *Mezhdunarodnyj jendokrinologicheskij zhurnal*. 2015;3(67):61-64. (In Ukrainian). [Ковальчук П.Е., Гаська М.В., Тулюлюк С.В. Репаративний остеогенез у нормі та за умов дефіциту мікроелементів йоду та селену. *Международный эндокринологический журнал*. 2015;3(67):61-64].

15. Korenkov OV. Morphological peculiarities of bone healing in the place of experimental cortical defect of long bone of rats in the conditions of natural hydroxyapatite implantation. *Orthopaedics Traumatology and Prosthetics*. 2016;1(602):84-88. [Кореньков О.В. Морфологічні особливості загоєння дефекту коркового шару довгої кістки щурів за умов імплантації природного гідроксилапатиту. *Ортопедия, травматология и протезирование*. 2016;1(602):84-88]. DOI: 10.15674/0030-59872016184-88

16. Shpakovskiy MS, Budaev AV, Razumov AS, et al. Cytomorphometric and immunohistochemical results of regenerate bone after intraosseous injection of the drug "Perftoran" at the osteosynthesis of femoral neck fractures (experimental study). *Journal of New Medical Technologies*. 2016;1:127-134. [Шпаковский М.С., Будаев А.В., и др. Результаты цитоморфометрического и иммуногистохимического исследований костного регенерата после внутрикостного введения препарата «Перфторан» при остеосинтезе переломов

шейки бедренной кости (экспериментальное исследование). *Вестник новых медицинских технологий*. 2016;1:127-134]. DOI: 10.12737/18566

17. Shyshchuk VD, Redko SI, Ogienko MN, et al. Disturbances of Reparative Osteogenesis in the Hypovolemia and their Correction in Experiment. *Novosti Khirurgii*. 2018;26(5):526-534. [Шищук В.Д., Редько С.И., Огиенко М.Н., и др. Нарушения репаративного остеогенеза при дегидратации и их коррекция в эксперименте. *Новости хирургии*. 2018;26(5):526-534]. DOI: 10.18484/2305-0047.2018.5.526

18. Gorbach YeN. Morphometric analysis of blood vessels of tibial regenerate in tibia automatic lengthening at an increased rate. *Morphology*. 2018;153(1):33-38. [Горбач Е.Н. Морфометрический анализ сосудов регенерата большеберцовой кости при автоматическом удлинении голени с повышенным темпом. *Морфология*. 2018;153(1):33-38]. DOI: https://doi.org/10.17816/morph.398184

19. Suchkov DI, Pavlov AV, Vinogradov AA, et al. Bone Regeneration in the Application of a New Device for Osteosynthesis in the Experiment. *Acta Biomedica Scientifica*. 2019;4(1):155-161. [Сучков Д.И., Павлов А.В., Виноградов А.А., и др. Морфологические особенности костного регенерата при применении нового устройства для погружного остеосинтеза в эксперименте. *Acta Biomedica Scientifica*. 2019;4(1):155-161]. DOI: 10.29413/ABS.2019-4.1.24

20. Nadyrov EA, Nikolaev VI, Kirilenko SI, et al. The Morphological Characteristics of Bone Tissue Regeneration in the Application of Bone Grafting Auto-Mixture. *Health and Ecology Issues*. 2019;4(62):57-62. [Надыров Э.А., Николаев В.И., Кириленко С.И., и др. Морфологическая характеристика регенерации костной ткани при использовании трансплантационной костной аутосмеси. *Проблемы здоровья и экологии*. 2019;4(62):57-62].

21. Nikonorova VG, Krishtop VV, Rumyantseva TA. Granulation tissue as a type of connective tissue (review). *Journal of Medical and Biological Research*. 2022;10(2):167-179. [Никонорова В.Г., Криштоп В.В., Румянцева Т.А. Грануляционная ткань как разновидность соединительных тканей (обзор). *Журнал медико-биологических исследований*. 2022;10(2):167-179]. DOI: 10.37482/2687-1491-Z098

22. Guliuk AG, Zhelnin EV. Relationship of osteogenesis markers with processes of posttraumatic regeneration of alveolar bone. *Fundamental research*. 2013;7-3:534-539. [Гулюк А.Г., Желнин Е.В. Взаимосвязь маркеров остеогенеза и процессов посттравматической регенерации альвеолярной кости у крыс. *Фундаментальные исследования*. 2013;7-3:534-539]. URL: https://fundamental-research.ru/en/article/view?id=32050

23. Remedios A. Bone and bone healing. *Vet Clin North Am Small Anim Pract*. 1999;29(5):1029-44. DOI: 10.1016/s0195-5616(99)50101-0

24. Serbest S, Tiftikci U, Tosun HB, et al. Is there a relationship between fracture healing and mean platelet volume? *Ther Clin Risk Manag*. 2016;12:1095-1099. DOI: 10.2147/TCRM.S108790

25. Volkov AV, Bolshakova GB. Bone histomorphometry in regenerative medicine. *Clinical and Experimental Morphology*. 2013;3(7):65-72. [Волков А.В., Большакова Г.Б. Гистоморфометрия костной ткани в регенеративной медицине. *Клиническая и экспериментальная морфология*. 2013;3(7):65-72].

Original research | Оригинальное исследование
DOI: https://doi.org/10.35693/SIM646547

Morphological evaluation of decellularized lyophilized amniotic membrane

Kseniya E. Kuchuk[2], Larisa T. Volova[1], Iosif V. Novikov[1], Evgenii S. Milyudin[1]

[1]Samara State Medical University (Samara, Russian Federation)
[2]Samara Regional Clinical Ophthalmological Hospital named after T.I. Eroshevsky (Samara, Russian Federation)

Abstract

Aim – to study the morphological structure of lyophilized amniotic membrane preliminarily subjected to physical decellularization.

Material and methods. An experimental study of the preservation of the anatomical structure of lyophilized amniotic membrane was performed on four groups of amniotic membrane fragments. Group 1: AM impregnated with glycerin and dried over silica gel; Group 2: AM impregnated with glycerin, treated ultrasonically and lyophilized; Group 3: AM treated ultrasonically and lyophilized; Group 4: native AM without preservation. The biomaterial was studied using light microscopy and scanning electron microscopy.

Results. Physical methods of influencing biological tissue have an expected effect on cell viability and allow obtaining a completely decellularized amniotic membrane. Additional treatment with glycerol before physical action on biological tissue for the purpose of decellularization does not have a significant effect on the preservation of cellular structures. It should only be noted that in the amniotic membrane impregnated with glycerol, more fragments of epithelial cell membranes are preserved and the basement membrane is more preserved.

Conclusion. The decellularization method developed by us using physical methods does not introduce any chemicals into the processed biomaterial that can have an unpredictable effect on regenerating tissues. Preservation of the amniotic membrane by lyophilization allows obtaining a morphologically integral, elastic and durable biomaterial.

Keywords: amniotic membrane, decellularization, lyophilization, morphology of lyophilized amniotic membrane.

Conflict of interest: nothing to disclose.

Citation
Kuchuk KE, Volova LT, Novikov IV, Milyudin ES. **Morphological evaluation of decellularized lyophilized amniotic membrane.** *Science and Innovations in Medicine*. 2025;10(3):188-194. DOI: https://doi.org/10.35693/SIM646547

Information about authors
Kseniya E. Kuchuk – MD, ophthalmologist, head of the tissue procurement and preservation department.
ORCID: 0009-0003-2986-5913
E-mail: kuchukke@rambler.ru
Larisa T. Volova – MD, Dr. Sci. (Medicine), Professor, Director of the "BioTech" Research Institute.
ORCID: 0000-0002-8510-3118
E-mail: l.t.volova@samsmu.ru
Iosif V. Novikov – MD, Cand. Sci. (Medicine), assistant of the Department of Traumatology, Orthopedics and Extreme Surgery named after Academician of the Russian Academy of Sciences A.F. Krasnov.
ORCID: 0000-0002-6855-6828
E-mail: p111aa@yandex.ru
***Evgenii S. Milyudin** – MD, Dr. Sci. (Medicine), Associate professor, Department of Operative Surgery and Clinical Anatomy with a course in Medical Information Technologies.
ORCID: 0000-0001-7610-7523
E-mail: e.s.milyudin@samsmu.ru
Corresponding Author

Received: 23.01.2025
Accepted: 21.03.2025
Published: 10.04.2025

Оценка морфологической структуры децеллюляризованной человеческой амниотической мембраны

К.Е. Кучук[2], Л.Т. Волова[1], И.В. Новиков[1], Е.С. Милюдин[1]

[1]ФГБОУ ВО «Самарский государственный медицинский университет» Минздрава России (Самара, Российская Федерация)
[2]ГБУЗ «СОКОБ имени Т.И. Ерошевского» (Самара, Российская Федерация)

Аннотация

Цель – изучить морфологическую структуру лиофилизированной амниотической мембраны, предварительно подвергнутой децеллюляризации физическим методом.

Материал и методы. Экспериментальное исследование сохранности анатомической структуры лиофилизированной амниотической мембраны (АМ) было выполнено на четырех группах фрагментов амниотической мембраны. Первая группа – АМ, пропитанная глицерином и высушенная над силикагелем; вторая группа – АМ, пропитанная глицерином и обработанная ультразвуком, лиофилизированная; третья группа – АМ, обработанная ультразвуком и лиофилизированная; четвертая группа – нативная АМ, не консервированная.

Выполнено изучение биоматериала с помощью световой микроскопии и сканирующей электронной микроскопии.

Результаты. Физические методы воздействия на биологическую ткань ожидаемо оказывают влияние на жизнеспособность клеток и позволяют получить полностью децеллюляризованную амниотическую мембрану. Дополнительная обработка АМ глицерином перед физическим воздействием с целью децеллюляризации достоверно не способствует

сохранению клеточных структур. При этом необходимо отметить, что в амниотической мембране, пропитанной глицерином, после физического воздействия сохраняется значимо больше фрагментов мембран эпителиальных клеток и более сохранна базальная мембрана.
Выводы. Разработанный нами метод децеллюляризации с использованием физических методов не подразумевает внесения в обрабатываемый биоматериал каких-либо химических веществ, которые впоследствии могут оказать непредсказуемое воздействие на окружающие имплантированную АМ регенерирующие ткани. Также консервация АМ предложенным способом лиофилизации позволяет получить морфологически целостный, эластичный и прочный биоматериал для регенеративной медицины.
Ключевые слова: амниотическая мембрана, децеллюляризация, лиофилизация, морфология лиофилизированной амниотической мембраны.
Конфликт интересов: не заявлен.

Для цитирования:
Кучук К.Е., Волова Л.Т., Новиков И.В., Милюдин Е.С. **Оценка морфологической структуры децеллюляризованной человеческой амниотической мембраны.** *Наука и инновации в медицине.* 2025;10(3):188-194.
DOI: https://doi.org/10.35693/SIM646547

Сведения об авторах
Кучук К.Е. – врач-офтальмолог, заведующая отделением заготовки и консервации тканей.
ORCID: 0009-0003-2986-5913
E-mail: kuchukke@rambler.ru
Волова Л.Т. – д-р мед. наук, профессор, директор НИИ «БиоТех».
ORCID: 0000-0002-8510-3118
E-mail: l.t.volova@samsmu.ru

Новиков И.В. – канд. мед. наук, ассистент кафедры травматологии, ортопедии и экстремальной хирургии имени академика РАН А.Ф. Краснова.
ORCID: 0000-0002-6855-6828
E-mail: p111aa@yandex.ru
***Милюдин Евгений Сергеевич** – д-р мед. наук, доцент кафедры оперативной хирургии и клинической анатомии с курсом медицинских информационных технологий.
ORCID: 0000-0001-7610-7523
E-mail: e.s.milyudin@samsmu.ru
Автор для переписки

Список сокращений
АМ – амниотическая мембрана.

Получено: 23.01.2025
Одобрено: 21.03.2025
Опубликовано: 10.04.2025

INTRODUCTION

In regenerative medicine, one of unique biomaterials is used widely: the amniotic membrane (AM). It is a conglomeration of a monolayer of epithelial cells on the basal membrane and the stroma consisting of three layers. The biologically active substances present in all the layers of the AM ensure activation of regenerative processes and cell proliferation, and accelerate their migration [1–4]. Before being used, the donor biomaterial is subjected to compulsory pre-treatment. First, the AM surface is washed from blood and mucus clots. This is generally accepted practice. The subsequent processing of the amniotic membrane with various chemical agents for disinfection (NB: disinfection in this case!), protection of the biomaterial from excessive damage during preservation, and subsequent preservation is differently assessed by researchers in terms of necessity, effectiveness, and impact on the preservation of biologically active substances in the biomaterial [5]. Many specialists prefer using native or cryopreserved AM, as in these cases, the cells remain viable and the anatomical structure of the biomaterial is practically undamaged [6–9]. However, since native AM cannot be stored and there is a risk of using infected material, the method of choice for utilizing AM in regenerative medicine is cryopreservation.

It should be noted that the use of chemical substances during cryopreservation in glycerol-containing media, the application of antibacterial agents for disinfection, as well as freezing and thawing processes may significantly alter both the structure and viability of cryopreserved AM [9]. Other common AM preservation methods (specifically drying over silica gel or lyophilization) entail complete loss of cellular viability, decellularization, and potential disruption of morphological structure while maintaining the biomaterial's anatomical integrity [10, 11], which many authors consider a critical factor for successful application in reconstructive surgeries [11–13].

When creating tissue-engineered constructs, researchers prefer using decellularized AM as a biological scaffold for cultured cells. Decellularization is a process aimed at removing cells from tissue while preserving the extracellular matrix and its three-dimensional structure [7, 14, 15], utilizing various cell-disruption methods. All decellularization methods can be classified into three types based on the primary disruptive factor: physical, chemical and biological. Physical methods are found in the majority of protocols of primary tissue treatment. They entail the use of rotators, shakers or direct perfusion chambers that provide accelerated fluid exchange with an effect on cell membranes to break the cells and their nuclei. More often, researchers use chemical agents: sodium dodecyl sulfate, an anionic surfactant capable of protein denaturation and dissolution of cell membranes. Organic acids are also used, specifically, peracetic acid that decomposes and removes nucleic acids. Decellularization of biomaterial is also possible with the use of spirits and chelating agents [16, 17].

The simplest physical method of decellularization is the process of multiple alternating freezing and thawing, under which cell membranes rupture by crystals of ice, and the cells lose their viability. Immersion in hypertonic solution resulting in osmotic stress and damage to cell membranes is also regarded as a physical method [17, 18]. However, the most efficient physical method of decellularization is ultrasonic impact, since the high efficiency of cell structure destruction by sonic energy is augmented by the mechanical purification of biomaterial from cellular debris [14].

AIM

Study the morphological structure of lyophilized amniotic membrane preliminarily subjected to physical decellularization.

MATERIAL AND METHODS

An experimental study of the anatomical structure preservation of lyophilized amniotic membrane was conducted on four groups of amniotic membrane fragments. The biomaterial, after washing in running water to remove blood clots, was cut into 1×1 cm fragments and divided into four groups. Group 1 (10 fragments): the amniotic membrane was impregnated with glycerol, placed in frames over silica gel and dried. Group 2 (12 fragments): the amniotic membrane was impregnated

with glycerol and treated with low-frequency ultrasound at 24–40 kHz in an ultrasonic bath “Sapfir” TTK (“Sapfir” LLC, Moscow, Russia) with subsequent lyophilization. Group 3(10 fragments): the amniotic membrane was treated with low-frequency ultrasound at 24–40 kHz in an ultrasonic bath “Sapfir” TTK (“Sapfir” LLC, Moscow, Russia) with subsequent lyophilization, without glycerol impregnation. Group 4 (control group) consisted of 10 fragments of native amniotic membrane studied without additional treatment and conservation.

The material was lyophilized (vacuum-dried by sublimation) on the ALPHA2-4LSC sublimation machine (Martin Christ Gefriertrocknungsanlagen GmbH, Osterode am Harz, Germany).

Morphological studies were conducted after fixing the biomaterial in 12% neutral buffered formalin, processing through an alcohol series, and embedding in celloidin. No fewer than 500 sections were made from different biomaterial samples. The sections were stained with hematoxylin-eosin or picrofuchsin using Van Gieson’s method. The images of stained preparations were analyzed with the visualization system comprising an Olympus BX41 research microscope (“Olympus”, Japan), digital color camera “ProgRes CF” and a personal computer with Morphology 5.2 software suite (“VideoTesT”, Russia).

Scanning electronic microscopy (SEM) of the amniotic membrane after conservation were performed with the raster electronic microscope JEOLJSM-6390 A Analysis Station (Japan). For the purposes of this study, the fragments of biomaterial were fixed with 2.5% water solution of glutaric aldehyde and processed through an alcohol series. After processing through an ethanol solution of increasing concentration and drying at room temperature for 24 hours, gold or carbon was sputter-coated onto the biomaterial to enhance the required surface conductivity for scanning electron microscopy.

The obtained results were processed with statistical methods in the SPSS_Statistics software suite.

The work was performed with the approval from the Committee for Bioethics of the Samara State Medical University (Excerpt from the Protocol No. 206 dated 18 March 2020).

RESULTS

The active agent for decellularization was selected based on the anatomic and histological structure and dimensions of the biomaterial. The low-frequency ultrasonic impact may remove particles of the blood, and the wave effect and cavitation may likely damage all cellular structures of the amniotic membrane since the thickness of the native biomaterial is not more than 0.5 mm. Considering that the criteria of efficiency of decellularization are not determined at present, we prepared morphological preparations. We believe that decellularized donor organs should not contain unaffected cells and cellular components.

From the macroscopic perspective, the biomaterial of all three experimental groups had the appearance of tissue paper, elastic and velvety to the touch. The samples from Group 3 of lyophilized amniotic membrane without glycerol impregnation turned out to have a more matte and non-uniform surface than the samples from Groups 1 and 2 that had been impregnated with glycerol.

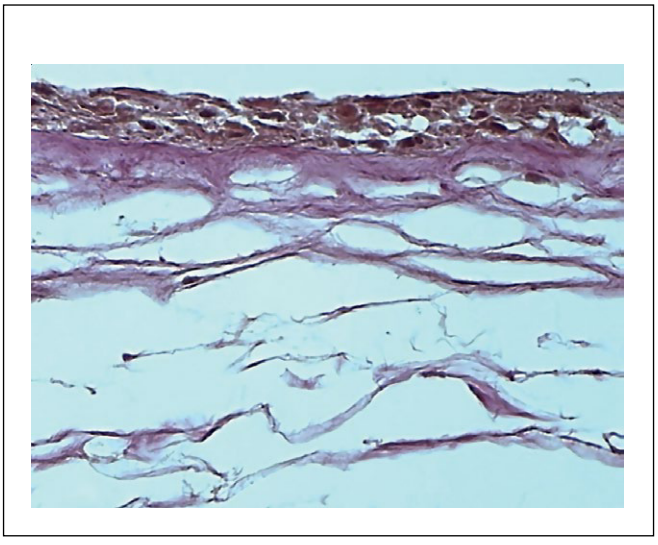

Figure 1. *Native amniotic membrane preparation. Stained with picrofuchsin. Magnification x400.*

Рисунок 1. *Препарат нативной амниотической мембраны. Окраска пикрофуксином. Ув. х400.*

The morphological preparation of the native amniotic membrane shows a completely preserved epithelial layer with viable cells and a multitude of pinosomes (**Fig. 1**). Adjacent to the basement membrane lies the compact layer, composed of tightly interwoven collagen fibers, followed by the fibroblast layer: a loose arrangement with fibroblasts interspersed among reticular fiber networks. The spongy layer consists of delicate, randomly oriented reticular fibers.

In histological preparations of the first group (silica-dried amniotic membrane after preliminary glycerol impregnation), an almost homogeneous band is observed, where distinguishing the epithelial and compact layers becomes difficult (**Fig. 2**). Focal areas show severely flattened cell nuclei. The stromal compact layer appears as a homogeneous acellular oxyphilic band. Nuclear shadows are frequently visible in the fibroblast layer. Persisting fibroblast nuclei exhibit rod-shaped morphology. The spongy layer is markedly flattened, identifiable by multidirectional oxyphilic-stained fibers. Morphometric

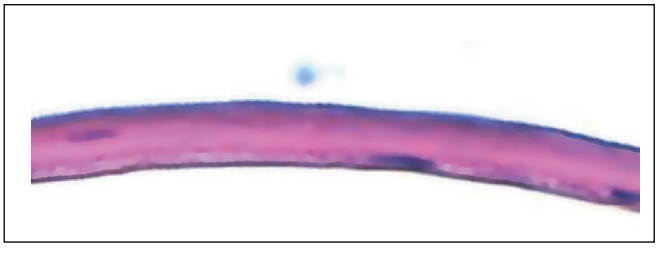

Figure 2. *Amniotic membrane preparation preserved by drying over silica gel after preliminary treatment with glycerol. Stained with hematoxylin and eosin. Magnification x400.*

Рисунок 2. *Препарат амниотической мембраны, консервированной путем высушивания над силикагелем после предварительной обработки глицерином. Окраска гематоксилин-эозином. Ув. х400.*

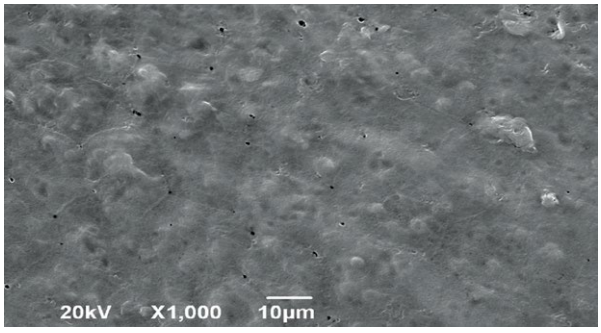

Figure 3. *Electron microscopic image of the amniotic membrane in a scanning electron microscope. Epithelial surface of the amniotic membrane preparation dried with silica and pre-impregnated with glycerol. Magnification x1000.*

Рисунок 3. *Электронно-микроскопическое изображение амниотической мембраны в сканирующем электронном микроскопе. Эпителиальная поверхность препарата амниотической мембраны силиковысушенной с предварительным пропитыванием глицерином. Ув. х1000.*

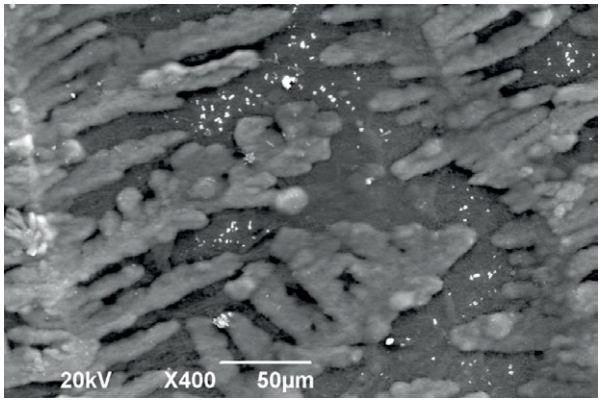

Figure 4. *Electron microscopic image of the amniotic membrane in a scanning electron microscope. Spongy layer of the amniotic membrane preparation dried with silica and preliminary impregnation with glycerin. Magnification x400.*

Рисунок 4. *Электронно-микроскопическое изображение амниотической мембраны в сканирующем электронном микроскопе. Спонгиозный слой препарата амниотической мембраны силиковысушенной с предварительным пропитыванием глицерином. Ув. х400.*

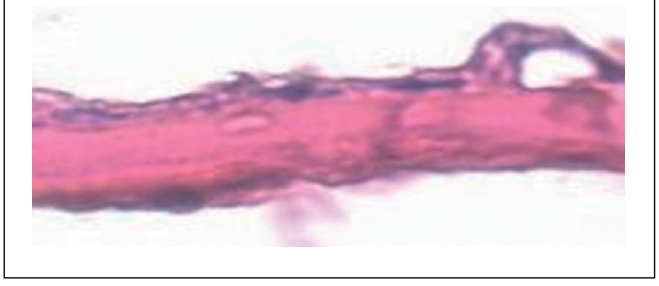

Figure 5. *Amniotic membrane preparation preserved by lyophilization after preliminary treatment with glycerol. Stained with hematoxylin and eosin. Magnification x400.*

Рисунок 5. *Препарат амниотической мембраны, консервированной путем лиофилизации после предварительной обработки глицерином. Окраска гематоксилин-эозином. Ув. х400.*

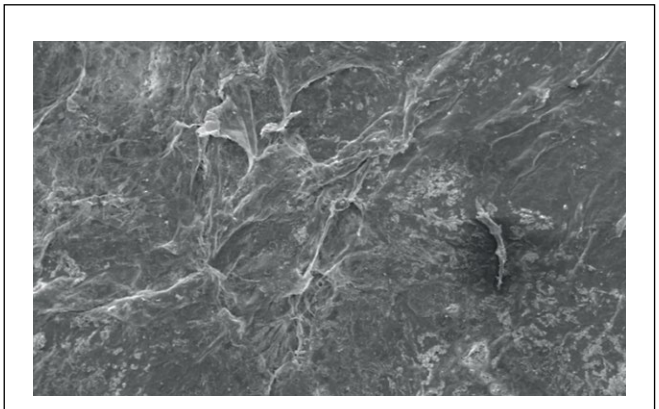

Figure 6. *Electron microscopic image of amniotic membrane in a scanning electron microscope. Epithelial surface of a lyophilized amniotic membrane preparation with preliminary impregnation with glycerol. Magnification x5*

Рисунок 6. *Электронно-микроскопическое изображение амниотической мембраны в сканирующем электронном микроскопе. Эпителиальная поверхность препарата лиофилизированной амниотической мембраны с предварительным пропитыванием глицерином. Ув. х50..*

analysis of total graft thickness (n=55) in lyophilized glycerol-impregnated amniotic membrane yielded a mean measurement of 6.9184 μm.

Raster electronic microscopy confirmed preservation of the epithelial layer in samples from Group 1 (**Fig. 3**). The epithelial layer represented by partially affected cells adjoins the substratum on the entire surface of the biomaterial. Individual defects are seen, restricted by cell contours.

Raster electronic microscopy of the amniotic membrane dried over silica gel from the side of the spongy layer confirms that significant changes occur in the loose connective tissue layer of the stroma, specifically, the spongy layer becomes smoothed. It is important to note the presence of homogeneous amorphous substrates forming dendritic patterns along multidirectional reticular fibers (**Fig. 4**).

The detailed study of the histological preparations of Group 2 offers a clear view of the epithelial layer (**Fig. 5**). In isolated areas, focal destruction of epithelial cells is observed. In preserved cells, nuclear pyknosis and chromatin condensation into conglomerates are evident. The basement membrane is damaged in regions of focal epithelial cell destruction. The compact layer appears in some areas as a homogeneous acellular oxyphilic band, while in others fibers are visible. The spongy layer is also preserved but compacted, with loss of structural organization. The morphometry of the total thickness of samples (n=48) of lyophilized amniotic membrane impregnated with glycerol yielded a mean measurement of 10.236 μm.

Scanning electron microscopy revealed, in a clearer way, the destruction of the epithelial layer, absence of viable cellular structures, and damage with partial desquamation of the basement membrane.

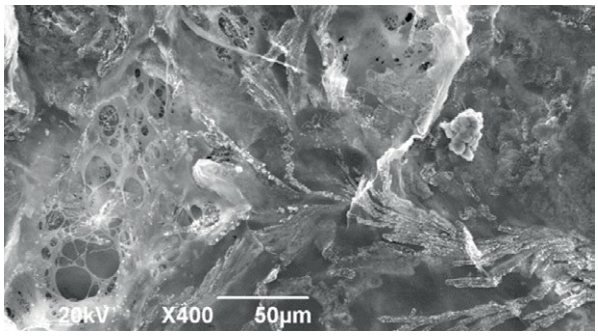

Figure 7. *Electron microscopic image of amniotic membrane in a scanning electron microscope. Spongy layer of a lyophilized amniotic membrane preparation with preliminary impregnation with glycerol. Magnification x400.*

Рисунок 7. *Электронно-микроскопическое изображение амниотической мембраны в сканирующем электронном микроскопе. Спонгиозный слой препарата лиофилизированной амниотической мембраны с предварительным пропитыванием глицерином. Ув. х400.*

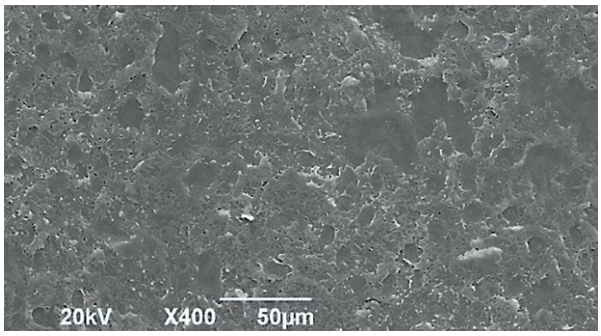

Figure 9. *Electron microscopic image of amniotic membrane in a scanning electron microscope. Epithelial surface of a lyophilized amniotic membrane preparation without preliminary impregnation with glycerol. Magnification x400.*

Рисунок 9. *Электронно-микроскопическое изображение амниотической мембраны в сканирующем электронном микроскопе. Эпителиальная поверхность препарата лиофилизированной амниотической мембраны без предварительного пропитывания глицерином. Ув. х400.*

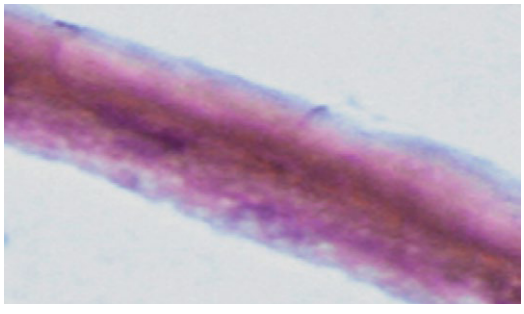

Figure 8. *Amniotic membrane preparation preserved by lyophilization without glycerol treatment. Hematoxylin and eosin staining. Magnification x400.*

Рисунок 8. *Препарат амниотической мембраны, консервированной путем лиофильной сушки без обработки глицерином. Окраска гематоксилин-эозином. Ув. х400.*

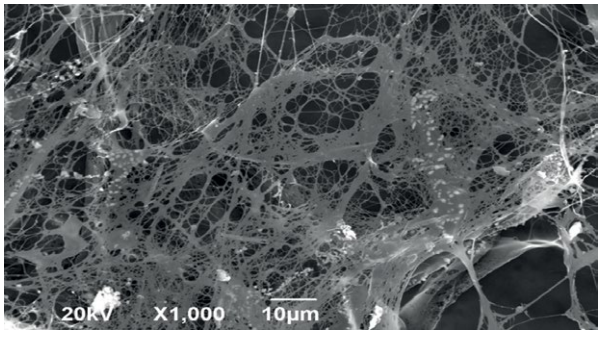

Figure 10. *Electron microscopic image of amniotic membrane in a scanning electron microscope. Spongy layer of the preparation of lyophilized amniotic membrane without preliminary impregnation with glycerol. Magnification x1000.*

Рисунок 10. *Электронно-микроскопическое изображение амниотической мембраны в сканирующем электронном микроскопе. Спонгиозный слой препарата лиофилизированной амниотической мембраны без предварительного пропитывания глицерином. Ув. х1000.*

The spongy layer is represented with denser connective fibers, on which homogenous structure-less substrates are visualized, attached in clusters (**Fig. 7**).

The epithelial layer in histological preparations of Group 3 of samples appears as a flattened homogeneous oxyphilic layer (**Fig. 8**). Isolated chromatin conglomerates from destroyed epithelial cell nuclei are observed.

The basement membrane is uneven in thickness and partially absent. The compact layer exhibits a dense homogeneous structure. The fibroblast layer is nearly devoid of cellular elements. Isolated nuclei of destroyed fibroblasts appear as rod-shaped shadows. No chromatin conglomerates are present. The spongy layer is flattened. Morphometric analysis of total graft thickness (n=44) in lyophilized non-glycerinated amniotic membrane yielded a mean measurement of 10.026 µm.

Scanning electron microscopy of preserved amniotic membrane samples from Group 3 revealed the following: the epithelial layer consists of minor cellular membrane fragments and the basement membrane that is desquamated across most of the examined surface. At higher magnification, the basement membrane appears as sparse fragments with curled edges, exposing the underlying stromal layer (**Fig. 9**).

The spongy layer in this sample group shows the least damage. Collagen fibers are thin, multidirectional, and loosely arranged. This preparation clearly demonstrates the end-to-end porosity of the biomaterial. The isolated homogeneous formations attached to collagen fibers are present (**Fig. 10**).

DISCUSSION

The histological study of the amniotic membrane showed significant differences of the morphological

landscape depending on the preliminary (pre-conservation) treatment of the biomaterial. In those cases where decellularization was not performed and the silica gel drying method was used without biomaterial freezing stages, the epithelial layer with preserved nuclei and cell membranes was visualized.

Studies of the amniotic membrane fragments subjected to decellularization by low-frequency ultrasound in Groups 2 and 3 reveal complete destruction of cellular structures and almost complete removal of cell components. In the histological samples, complete destruction of epithelial layer cells and partial destruction of the basement membrane with exposure of the stroma and formation of trabecular architectonic of the biomaterial are observed. Such changes are more manifested in the preparations not impregnated with glycerol before lyophillization.

In the decellularized tissue, the extracellular matrix remained unchanged. No swelling or other pathological changes in the structure, architectonic, fiber orientation, and tinctorial properties of the connective tissue were observed.

Thus, the methods of physical treatment of biological tissue provide an expected impact on the cell viability and allow production of a completely decellularized amniotic membrane. Impregnation with glycerol before physical treatment of the biological tissue with the aim of decellularization has no significant effect on the preservation of cellular structures. It remains to be noted that the decellularized lyophilized amniotic membrane impregnated with glycerol preserves more fragments of membranes of epithelial cells, and the basement membrane is also preserved to a greater extent.

CONCLUSIONS

The decellularization method we developed using physical approaches introduces no chemical substances into the processed biomaterial that could unpredictably affect regenerating tissues.

AM conservation through lyophilization yields morphologically intact, elastic, and durable biomaterial.

ADDITIONAL INFORMATION	ДОПОЛНИТЕЛЬНАЯ ИНФОРМАЦИЯ
Study funding. The study was the authors' initiative without external funding.	***Источник финансирования.*** Работа выполнена по инициативе авторов без привлечения финансирования.
Conflict of interest. The authors declare that there are no obvious or potential conflicts of interest associated with the content of this article.	***Конфликт интересов.*** Авторы декларируют отсутствие явных и потенциальных конфликтов интересов, связанных с содержанием настоящей статьи.
Compliance with Ethical Standards. The study was approved by the Bioethics Committee of Samara State Medical University (extract from protocol No. 206 dated March 18, 2020).	***Соответствие нормам этики.*** Исследование одобрено комитетом по биоэтике Самарского государственного медицинского университета (выписка из протокола №206 от 18 марта 2020 г.).
Contribution of individual authors. K.E. Kuchuk: processing andconservation of biomaterial, text preparation. L.T. Volova: development of the concept and design of the study, analysis of the obtained data. I.V. Novikov: analysis of obtained data, preparation of text. E.S. Milyudin: collection of material, analysis of obtained data, editing of text. The authors gave their final approval of the manuscript for submission, and agreed to be accountable for all aspects of the work, implying	***Участие авторов.*** К.Е. Кучук – обработка и консервация биоматериала, подготовка текста. Л.Т. Волова – разработка концепции и дизайна исследования, анализ полученных данных. И.В. Новиков – анализ полученных данных, подготовка текста. Е.С. Милюдин – сбор материала, анализ полученных данных, редактирование текста. Все авторы одобрили финальную версию статьи перед публикацией, выразили согласие нести ответственность за все аспекты работы, подразумевающую надлежащее изучение и решение вопросов, связанных с точностью или добросовестностью любой части работы.

REFERENCES / ЛИТЕРАТУРА

1. Meller D, Pires RT, Mack RJ, et al. Amniotic membrane transplantation for acute chemical or thermal burns. *Ophthalmology*. 2000;107(5):980-9; discussion 990. DOI: 10.1016/s0161-6420(00)00024-5

2. Niknejad H, Peirovi H, Jorjani M, et al. Properties of the amniotic membrane for potential use in tissue engineering. *Eur Cell Mater*. 2008;15:88-99. DOI: 10.22203/ecm.v015a07

3. Pollard SM, Aye NN, Symonds EM. Scanning electron microscope appearances of normal human amnion and umbilical cord at term. *Br J Obstet Gynaecol*. 1976;83(6):470-7. DOI: 10.1111/j.1471-0528.1976.tb00868.x

4. Adds PJ, Hunt CJ, Dart JK. Amniotic membrane grafts, "fresh" or frozen? A clinical and in vitro comparison. *Brit J Ophthalmol*. 2001;85(8):905-7. DOI: 10.1136/bjo.85.8.905

5. Aleksandrova OI, Gavrilyuk IO, Mashel TV, et al. On preparation of amniotic membrane as a scaffold for cultivated cells to create corneal bioengineering constructs. *Saratov Journal of Medical Scientific Research*. 2019;15(2):409-413. [Александрова О.И., Гаврилюк И.О., Машель Т.В., и др. К вопросу о подготовке амниотической мембраны в качестве скаффолда для культивируемых клеток при создании биоинженерных конструкций роговицы. *Саратовский научно-медицинский журнал*. 2019;15(2):409-413]. URL: https://ofmntk.ru/files/upload/2019215.pdf

6. Li H, Niederkorn JY, Neelam S, et al. Immunosuppressive Factors Secreted by Human Amniotic Epithelial Cells. *Invest Ophthalmol Vis Sci*. 2005;46(3):900-907. DOI: 10.1167/iovs.04-0495.

7. Koizumi NJ, Inatomi TJ, Sotozono CJ, et al. Growth factor mRNA and protein in preserved human amniotic membrane. *Curr Eye Res*. 2000;20(3):173-7. PMID: 10694891

8. Riau AK, Beuerman RW, Lim LS, Mehta JS. Preservation, sterilization and de-epithelialization of human amniotic membrane for use in ocular surface reconstruction. *Biomaterials*. 2010;31(2):216-25. DOI: 10.1016/j.biomaterials.2009.09.034

9. Adds PJ, Hunt CJ, Dart JK. Amniotic membrane grafts, "fresh" or frozen? A clinical and *in vitro* comparison. *Br J Ophthalmol*. 2001;85(8):905-7. DOI: 10.1136/bjo.85.8.905

10. Milyudin ES. Technology of preservation of the amniotic membrane by drying with silica gel. *Technologies of living systems*. 2006;3(3):44-49. (In Russ.). [Милюдин Е.С. Технология консервации амниотической мембраны путем высушивания над силикагелем. *Технологии живых систем*. 2006;3(3):44-49].

11. Milyudin ES, Kuchuk KE, Bratko OV. Preserved amniotic membrane in a small tissue-engineering complex of the anterior corneal epithelium. *Perm Medical Journal*. 2016;33(5):47-54. [Милюдин Е.С., Кучук К.Е., Братко О.В. Консервированная амниотическая мембрана в структуре тканеинженерного комплекса переднего эпителиального слоя роговицы. *Пермский медицинский журнал*. 2016;33(5):47-54]. DOI: 10.17816/pmj33547-53

12. Kim JC, Tseng SCG. Transplantation of preserved human amniotic membrane for surface reconstruction in severly damaged rabbit corneas. *Cornea*. 1995;14:473-484. PMID: 8536460

13. Koizumi N, Fullwood NJ, Bairaktaris G, et al. Quantock Cultivation of Corneal Epithelial Cells on Intact and Denuded Human Amniotic Membrane. *Investigative Ophthalmology & Visual Science*. 2000;41:2506-2513. PMID: 10937561

14. Lin CH, Hsia K, Su CK, et al. Sonication-Assisted Method for Decellularization of Human Umbilical Artery for Small-Caliber Vascular Tissue Engineering. *Polymers (Basel)*. 2021;13(11):1699. DOI: 10.3390/polym13111699

15. Melkonyan KI, Rusinova TV, Kozmai YaA, Asyakina AS. Assessment of Nuclear Material Elimination by Different Methods of Dermis Decellularization. *Journal Biomed*. 2021;17(3E):59-63. [Мелконян К.И., Русинова Т.В., Козмай Я.А., Асякина А.С. Оценка элиминации ядерного материала при различных методах децеллюляризации дермы. *Биомедицина*. 2021;17(3E):59-63]. DOI: 10.33647/2713-0428-17-3E-59-63

16. Murphy SV, Skardal A, Nelson RAJr, et al. Amnion membrane hydrogel and amnion membrane powder accelerate wound healing in a full thickness porcine skin wound model. *Stem Cells Transl Med*. 2020;9(1):80-92. DOI: 10.1002/sctm.19-0101

17. Startseva OI, Sinelnikov ME, Babayeva YuV, Trushenkova VV. Decellularization of organs and tissues. *Pirogov Russian Journal of Surgery*. 2019;(8):59-62. [Старцева О.И., Синельников М.Е., Бабаева Ю.В., Трущенкова В.В. Децеллюляризация органов и тканей. *Хирургия. Журнал им. Н.И. Пирогова*. 2019;(8):59-62]. DOI: 10.17116/hirurgia201908159

18. Tovpeko DV, Kondratenko AA, Astakhov AP, et al. Decellularization of organs and tissues as a key stage in the creation of biocompatible material. *Bulletin of the Military Innovation Technopolis "Era"*. 2023;4(4):342-346. [Товпеко Д.В., Кондратенко А.А., Астахов А.П., и др. Децеллюляризация органов и тканей как ключевой этап создания биосовместимого материала. *Вестник Военного инновационного технополиса «Эра»*. 2023;4(4):342-346]. DOI: 10.56304/S2782375X23040150 EDN: IHEIWC

Technical report | Технический отчет
DOI: https://doi.org/10.35693/SIM639885

Features of the application of the digital clinical calculator of cardiovascular risk in elderly patients

Nikolai A. Pervyshin
Samara State Medical University (Samara, Russian Federation)

Abstract

Aim – evaluation of the features of using a digital clinical calculator for an objective assessment of the cardiovascular risk in elderly patients in a routine outpatient practice.

Material and methods. The methodology for calculating the value of cardiovascular risk used in the calculator is based on the recommendations for the prevention of CVD of the European Society of Cardiology (2021). The program provides the functionality of calculating the personalized quantitative value of the probability of fatal and non-fatal cardiovascular events over a period of 10 years.

Results. The calculator matrix uses five significant initial variables: patient's age, gender, smoking, systolic blood pressure and low-density lipoprotein cholesterol. The program provides for use directly in outpatient settings, works in any browser, does not require downloading to a device, can be used in a mobile phone version, and allows the user to form a conclusion for printing and saving on electronic media.

Conclusion. The calculation of an objective numerical indicator of risk of CVD, which lends itself to accurate mathematical and statistical assessment, allows the calculator to be used to solve the following tasks: monitoring and reclassification of cardiovascular risk in elderly patients, a weighted assessment of indications for correction of modifying factors and intensification of treatment, dynamic control of the effectiveness of the treatment methods used; the result of the calculator is stored as an electronic medical document. The program can be used in any medical information system as a module of the medical decision support system through the integration subsystem.

Keywords: elderly patient, cardiovascular risk, clinical calculator, digital assessment method, evidence-based medicine, medical decision support system.

Conflict of interest: nothing to disclose.

Citation
Pervyshin NA. **Features of the application of the digital clinical calculator of cardiovascular risk in elderly patients.** *Science and Innovations in Medicine.* 2025;10(3):195-200.
DOI: https://doi.org/10.35693/SIM639885

Information about author
Nikolai A. Pervyshin – MD, Cand. Sci. (Medicine), assistant of the Department of Endocrinology and Geriatrics, endocrinologist of the highest category.
ORCID: 0000-0002-9609-2725
E-mail: n.a.pervyshin@samsmu.ru

Received: 27.10.2024
Received: 07.03.2025
Published: 23.03.2025

Особенности прикладного применения цифрового клинического калькулятора кардиоваскулярного риска у пациентов пожилого возраста

Н.А. Первышин
ФГБОУ ВО «Самарский государственный медицинский университет» Минздрава России (Самара, Российская Федерация)

Аннотация

Цель – определить особенности применения цифрового клинического калькулятора объективной оценки значения кардиоваскулярного риска пожилого пациента в условиях рутинной амбулаторной практики.

Материал и методы. Методология расчета значения кардиоваскулярного риска, использованная в калькуляторе, основана на рекомендациях по профилактике ACC3 Европейского общества кардиологов (2021). Программа позволяет рассчитать персонализированное количественное значение вероятности фатального и нефатального сердечно-сосудистого события в течение 10 лет.

Результаты. Матрица калькулятора использует пять существенных исходных переменных: возраст пациента, пол, курение, систолическое артериальное давление и уровень холестерина липопротеидов невысокой плотности. Программа предусматривает применение непосредственно в условиях амбулаторного приема, работает в любом браузере, не требует скачивания на устройство, может быть использована в версии для мобильного телефона, позволяет формировать заключение для вывода на печать и сохранения на электронном носителе.

Заключение. Расчет объективного численного показателя риска ACC3, который поддается точной математической и статистической оценке, позволяет применять калькулятор для решения следующих задач: мониторинга и реклассификации кардиоваскулярного риска пожилого пациента, взвешенной оценки показаний к коррекции модифицирующих факторов и интенсификации лечения, динамического контроля эффективности применяемых методов лечения; результат работы калькулятора сохраняется в виде электронного медицинского документа; программа может быть использована в любой медицинской информационной системе в качестве модуля системы поддержки принятия врачебных решений через подсистему интеграции.

Ключевые слова: пожилой пациент, кардиоваскулярный риск, клинический калькулятор, цифровой метод оценки, доказательная медицина, система поддержки принятия врачебных решений.

Конфликт интересов: не заявлен.

Для цитирования:
Первышин Н.А. **Особенности прикладного применения цифрового клинического калькулятора кардиоваскулярного риска у пациентов пожилого возраста.** *Наука и инновации в медицине*. 2025;10(3):195-200.
DOI: https://doi.org/10.35693/SIM639885

Сведения об авторе
Первышин Николай Александрович – канд. мед. наук, врач-эндокринолог высшей категории, ассистент кафедры эндокринологии и гериатрии.
ORCID: 0000-0002-9609-2725
E-mail: n.a.pervyshin@samsmu.ru

Список сокращений
АССЗ – атеросклеротические сердечно-сосудистые заболевания, ХС неЛВП – фракция холестерина липопротеидов невысокой плотности; РКИ – рандомизированное контролируемое исследование, САД – систолическое артериальное давление, СД – сахарный диабет, ТГ – триглицериды; ХБП – хроническая болезнь почек, ХСН – хроническая сердечная недостаточность.

Получено: 27.10.2024
Одобрено: 07.03.2025
Опубликовано: 23.03.2025

INTRODUCTION

The global demographic trend of ageing population is a serious challenge faced by the modern healthcare system. According to WHO information, by the year 2050 the share of people aged over 60 may reach 38% and become greater than the share of people aged 10–24 (2.1 billion vs. 2.0 billion) [1]. In 2018, the number of elderly people in the total population of the Russians reached 25.4%[1]; according to the official forecast, in 20 the number will exceed 37.3 million people (26.9% of the population)[2].

The average elderly patient with atherosclerotic cardiovascular diseases (ASCVD) and chronic heart failure (CHF), which may be regarded as a clinical outcome, tends to be considerably older, much like the overall population. The data of large national and international randomized controlled trials (RCTs) with long-term prospective follow-up confirm this fact, e.g. EPOCH CHF in the Russian Federation [2] and the study of Claire A. Lawson *et al*. (2020) in Great Britain [3]. They demonstrated significant dynamics of increase of average age of CHF patients; particularly, in Great Britain, the relative share of people aged over 60 in the CHF cohort reached 65%. This emphasized the importance of evaluation of cardiovascular risks in elderly patients.

The European Society of Cardiology (ESC) suggests personalized phased strategies of management for individual patients optimized in accordance with the ASCVD risk evaluation using the SCORE2 and SCORE2-OP scales.

Whereas the SCORE scale, used earlier, evaluated the 10-year risk of ASCVD death, the SCORE2 considers a wider range of clinical outcomes including not only mortality rates from ASCVD, but morbidity outcomes as well (non-fatal myocardial infarction, non-fatal stroke) [4]. This approach provides a more precise picture of the adverse burden of the cardiovascular pathology on the patient's condition.

For patients aged over 70, a separate scale SCORE2-OP was developed [5] that included the so-called 'competing risks'. A 'competing risk' is vital in the older age, since it provides a significant impact on the relative survival of patients without ASCVD in the general cohort of older patients, which results in the corruption of the evaluation of the actual 10-year risk of ASCVD upwards [6].

It is to be noted that the proper use of the SCORE2 and SCORE2-OP scales is limited exclusively to a group of healthy patients. According to the ESC consensus, this group includes outwardly healthy individuals without confirmed ASCVD, type II diabetes mellitus (T2DM), chronic kidney disease (CKD) and other severe comorbidities that were not treated before or whose clinical condition remained stable for several years. At the same time, the recommendations make it a point that the SCORE2 algorithm may be recommended for use in patients with comorbid pathologies, other risk modifiers, and clinical conditions, including T2DM, as the all-purpose tool for the objective assessment of cardiovascular risks and clarification of efficiency of various therapeutic measures with systematic follow-up [7].

Thus, one of the initial logical prerequisites of the ESC is that any therapeutic intervention affects the risk of ASCVD development. Since the SCORE2 and SCORE2-OP algorithms provide for an objective quantitative assessment of ASCVD risks, the medical impact is assessed from the position of measuring its value. Thus, the cardiovascular risk is seen as a dynamic calculation indicator that requires regular follow-up and re-classification depending on the treatment methods, correction of risk factors and clinical condition of the patient [8, 9]. Of course, personalized phased approach to assessment of ASCVD risk increases the workload on the doctor and requires extra working time. Systematic assessment of ASCVD risk under the SCORE2 algorithm in the conditions of limited time of a hospital admission poses some difficulties for the medical practitioner. This justifies the high practical value of the calculator we developed.

AIM

Evaluation of the features of using a digital clinical calculator for an objective assessment of the cardiovascular risk in elderly patients in a routine outpatient practice.

MATERIAL AND METHODS

The methodology of calculation of cardiovascular risks in elderly patients used in the calculator is based on the ESC recommendations as amended in 2021 [10], validated in the Russian Federation [11].

SCORE2 and SCORE2-OP scales are deeply formalized; therefore, only five principal factors of cardiovascular risks are used as independent variables (4 clinical and anamnestic and 1 laboratory): age, sex, smoking status, systolic blood pressure (BP), and non-high-density cholesterol level (non-HDL-C) (**Table 1**).

[1] Federal Service of National Statistics. Senior citizens (demographic indicators). Link valid as of 26.06.2024. Available online: https://www.gks.ru/folder/13877
[2] Updated demographic forecast of the Russian Statistics Agency until the year 2046. Available online: https://rosstat.gov.ru/folder/313/document/220709

The calculator processes the input data and finds the numeric value of the probability of development of fatal or non-fatal cardiovascular event (infarction or stroke) within 10 years in per cent, indicated in the respective cells of the SCORE2 and SCORE2-OP tables, which determines the patient's belonging to some group of cardiovascular risk or other.

Individuals aged 60–69: ≥10% is 'very high risk', an absolute indication for treatment of ASCVD risk factors; 5–10% stands for 'high risk' that requires correction of ASCVD risk factors with consideration to risk modifiers, lifetime risk and lifetime benefit of treatment, as well as the patient's preferences; below 5% stands for 'moderate risk' that does not require correction of risk factors, as a rule.

Individuals aged 70: ≥ 15% is 'very high risk', an absolute indication for treatment of ASCVD risk factors; 7.5–15% stands for 'high risk' that requires correction of ASCVD risk factors with consideration to risk modifiers, lifetime risk and lifetime benefit of treatment, as well as possible sarcopenia, poly-pragmasy and the patient's preferences; below 7.5% stands for 'moderate risk' that does not require correction of risk factors, as a rule.

For those clinical cases, in which the non-HDL-C level values are not available to the doctor, the calculator provides an alternative method. Since the non-HDL-C levels have been used in wide clinical practice only recently, not all medical institutions measure it within a standard lipid profile. For this purpose, the calculator integrates a module to calculate the value using the inverse Friedewald equation [12]. The following are used as independent laboratory values: LDL-C and triglyceride (TG) levels. The laboratory method of measurement the LDL-C and TG levels is a part of standard outpatient monitoring in dyslipidemia. The direct Friedewald equation is used to calculate the LDL-C levels based on the total cholesterol, triglyceride and HDL-C values, calculated in the vast majority of laboratories. The precision of LDL-C level measurement is comparable with reference methods provided that the following conditions are met: TG plasma concentration below 4.5 mmol/L; LDL level above 1.3 mmol/L, which is taken into account in the argument ranges of the calculator [13].

The algorithm for calculating cardiovascular risk in elderly patients is based on a risk scale validated in Russia for very high-risk countries [14]. The SCORE2 and SCORE2-OP charts are geographically calibrated according to national ASCVD mortality rates and categorize countries into four risk groups: low-risk countries, moderate-risk countries, high-risk countries, and very high-risk countries. Russia is classified in the fourth group (very high risk).

Variable	Unit	Range
Age	Years	60–120
Sex	Nominal	M/F
Smoking status	Nominal	Y/N
Systolic BP	mmHg	99–180
non-HDL-C	mmol/L	3.0–6.9

Table 1. *Essential features of the clinical calculator of cardiovascular risk in elderly patients*

Таблица 1. *Существенные признаки клинического калькулятора значения кардиоваскулярного риска у пожилых пациентов*

The calculator has limitations in practical application and cannot be used to calculate individual cardiovascular risk values in the following cases: for patients younger than 60 years; for hyperaldosteronism; for familial hypercholesterolemia; for plasma TG greater than 4.5 mmol/L; for plasma LDL less than 1.3 mmol/L.

The calculator has limitations in practical application and cannot be used to calculate individual cardiovascular risk values in the following cases: in patients younger than 60 years; in hyperaldosteronism; in familial hypercholesterolemia; in plasma TG concentration greater than 4.5 mmol/L; in plasma LDL concentration less than 1.3 mmol/L.

RESULTS AND DISCUSSION

When clinically applying the calculator, several critical considerations must be addressed, particularly for elderly patients. The stratification of the population into two age groups (60-69 years [15] and ≥70 years [5]), as implemented in the original study, results in abrupt increases in threshold values for defining moderate-, high-, and very-high-risk categories in individuals aged 70 and above. This occurs because calculated cardiovascular risk values in the ≥70 cohort nearly always exceed general population thresholds, rendering them inadequate for risk stratification purposes. Moreover, when assessing the lifetime benefit of therapeutic intervention in terms of additional years lived without ASCVD, this benefit objectively demonstrates lower magnitude in very elderly populations. While the LIFE-CVDK[1] scale enables calculation of cardiovascular disease-free life expectancy accounting for comorbidities and specific pharmacological interventions (statins, anticoagulants), unfortunately, this tool does not support the Russian language.

A patient's assignment to a specific risk category primarily determines the optimal intensity of therapeutic intervention. Since the patient's age is a fixed value at any given time, a reasonable assessment of decision-making thresholds in actual clinical practice requires physicians to conduct a comprehensive evaluation of geriatric status and maintain clinical flexibility, particularly for patients now over the 70-year age threshold.

The determination of a particular risk category in an individual patient does not mean unconditional and automatic initiation or intensification of drug therapy. The physician must necessarily take into account other factors affecting the risk of ASCVD in old age, in particular the category of the patient's functional dependence, as well as the presence of such specific geriatric syndromes as senile asthenia, sarcopenia, and polymorbidity [16]. The higher risk stratification threshold in the 70+ cohort helps avoid overtreatment and polypharmacy, which is particularly common in very elderly multimorbid patients. Another key

[1] Available online: https://u-prevent.com/calculators/lifeCvd

clinical rationale for separating the over-70 group in the algorithm is the significant weakening of the correlation gradient between ASCVD risk and classical modifiable risk factors, such as non-HDL cholesterol levels and systolic blood pressure, with advancing age [17].

Despite the fact that SCORE2 algorithms are designed to assess cardiovascular risk in apparently healthy individuals, their absolute value remains important and relevant even for patients with comorbidities (T2DM, CKD, CAD), as they enable tracking of risk category transitions (e.g., from “very high” to “high”) when applying specific treatment methods (e.g., when intensifying lipid-lowering therapy). This calculator specifically emphasizes calculating the quantitative probability of adverse cardiovascular events (expressed as a percentage) rather than assigning patients to formalized risk categories (a qualitative characteristic). This approach is particularly relevant for very high ASCVD-risk countries. An objective numerical indicator lends itself better to mathematical and statistical evaluation, enabling its application across a wide range of practical tasks, from balanced assessment of indications for modifying factor correction to dynamic monitoring of pharmacotherapy effectiveness.

A key advantage of the calculator is that all source independent variables are included in the standard follow-up protocol for elderly patients [18] and are recorded by physicians during routine outpatient visits. When digitization tools are used[1], the calculator may be used as a module of medical decision-making support system and calculate the values of cardiovascular risk in elderly patients automatically in the process of provision of outpatient medical care. Given that the obtained data are stored and systematized in digital format, this addresses the need for systematic monitoring and reclassification of ASCVD risk categories based on the patient's current clinical status, while trends in absolute risk values provide insights into the effectiveness of administered treatments.

The calculator is registered at the Federal Institute of Industrial Property[2]. It is written using the TypeScript language, the size of the program code is 500 Kb; it has no specific requirements to hardware and software; the program requires no installation and can work on any computer with a browser (Google Chrome 127 and higher, Mozilla Firefox 128 and higher), or an a mobile phone. The calculator is available for doctors of any specialization on the website of doctors’ digital assistants[3] or through the QR-code for mobile devices (**Fig. 1**).

Reliability of the calculator was verified through validation using clinical cases from routine outpatient practice.

Clinical case. From the outpatient visit sample, a male patient XXX1955 aged 69 years was randomly selected, with a harmful habit (smoking), SBP 155 mmHg, LDL-C level 3.5 mmol/L, TG level 2.3 mmol/L; calculated non-HDL-C level using the inverse Friedewald formula: 4.5 mmol/L.

The personalized cardiovascular risk value (probability of fatal and non-fatal cardiovascular events over a 10-year period) was calculated at 33% (**Fig. 2**).

To demonstrate the capabilities of the calculator for objective ASCVD risk monitoring, the personalized risk score was recalculated for the same patient XXX1955 after modifying factor adjustment. The therapeutic interventions (smoking cessation and optimization of antihypertensive therapy) reduced the probability of fatal/

Figure 1. *QR code of the CVD Risk Assessment Calculator for elderly patients.*

Рисунок 1. *QR-код калькулятора определения значения кардиоваскулярного риска пожилых пациентов.*

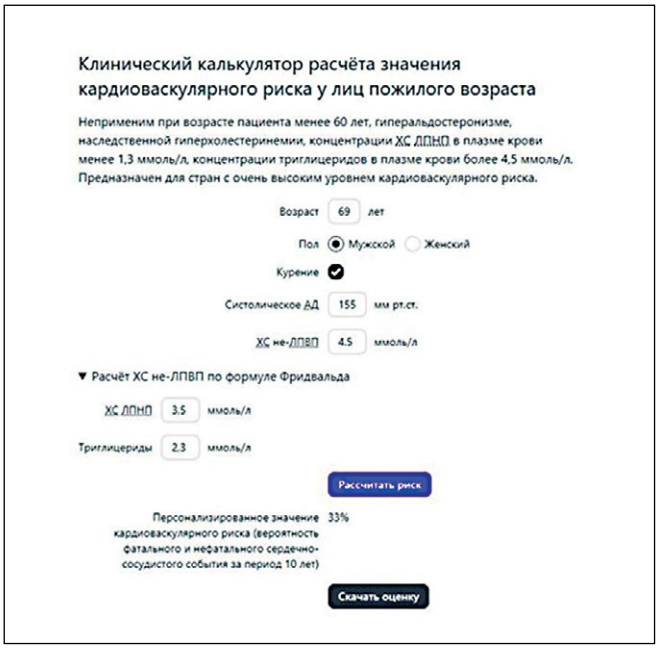

Figure 2. *A clinical example of the application CVD Risk Assessment Calculator for elderly patients.*

Рисунок 2. *Клинический пример прикладного применения калькулятора оценки риска ACCЗ пожилых пациентов.*

[1] Pervyshin N.A., Bulgakova S.V.,Galkin R.A., Zeleno L.S., Shamin E.A., Panshin A.S. Client-server application “Endocrinologist’s Automated Workplace for Outpatient Visits (ARME 3.0)”. Certificate of state registration of software for personal computers No. 2023665315 dated 14.07.2023. Available online: https://fips.ru/EGD/08c33405-6b4b-44f2-85a9-09fefade5fcc

[2] Pervyshin N.A. Clinical calculator for the calculation of cardiovascular risk in elderly patients. Certificate of state registration of software for personal computers No. 2024668302 dated 06.08.2024. Available online: https://fips.ru/EGD/20c2c0e3-c0e0-4f6a-9af6-95ed5bd1e461

[3] Available online: https://кафэндгер.рф/Клинические_калькуляторы/Геронтология/Риск_SCORE2

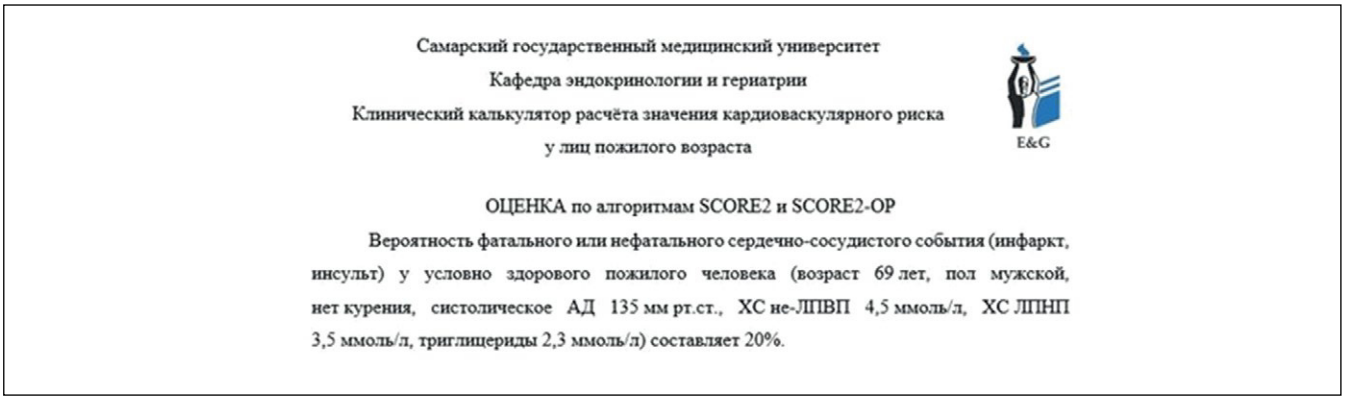
Самарский государственный медицинский университет
Кафедра эндокринологии и гериатрии
Клинический калькулятор расчёта значения кардиоваскулярного риска
у лиц пожилого возраста
E&G
ОЦЕНКА по алгоритмам SCORE2 и SCORE2-OP
Вероятность фатального или нефатального сердечно-сосудистого события (инфаркт, инсульт) у условно здорового пожилого человека (возраст 69 лет, пол мужской, нет курения, систолическое АД 135 мм рт.ст., ХС не-ЛПВП 4,5 ммоль/л, ХС ЛПНП 3,5 ммоль/л, триглицериды 2,3 ммоль/л) составляет 20%.

Figure 3. *Protocol for assessing the value of cardiovascular risk in an elderly patient.*

Рисунок 3. *Протокол оценки значения кардиоваскулярного риска пожилого пациента.*

non-fatal cardiovascular events in the patient XXX1955 by 13% to 20%, clearly demonstrating its effectiveness. Furthermore, this tangible outcome helps physicians convincingly motivate patients to continue treatment and adhere to recommendations, thereby ensuring compliance, a particularly crucial factor for elderly patients [19].

Personalized cardiovascular risk assessment results can be downloaded from the calculator as a Microsoft Word (.docx) file to a personal computer or mobile device. Physicians can either save this file as an electronic medical record or print it for inclusion in paper-based outpatient charts or medical histories (**Fig. 3**).

Practical application of the calculator in routine clinical practice enables dynamic assessment of personalized metrics that may be used both as an objective tool for determining optimal therapeutic strategies in specific elderly patients and as an indicator of their medical and economic effectiveness.

CONCLUSIONS

1. Assessment of the probability of fatal and non-fatal cardiovascular events over a 10-year period reflects the overall burden of negative impact of ASCVDs on a patient's health status with more accuracy than mortality indicators.

2. Assessment of cardiovascular risk is of special importance for elderly patients: in making a decision on therapeutic intervention, the doctor must take into account the specific geriatric syndromes: senile asthenia, sarcopenia, cognitive disorders and polymorbidity as well as poly-pragmasy mediated by them.

3. The objective digital assessment of numerical cardiovascular risk values using a validated methodology allows using the calculator for weighted assessment of indications for modifying factors correction, intensification of drug therapy, as well as for dynamic control of treatment effectiveness.

4. The results of the calculation are available for download as an outpatient chart protocol and are also saved as an electronic medical record, enabling their use in other MIS as a clinical decision support system module via the integration subsystem.

ADDITIONAL INFORMATION	ДОПОЛНИТЕЛЬНАЯ ИНФОРМАЦИЯ
Study funding. The study was the author's initiative without external funding.	***Источник финансирования.*** Работа выполнена по инициативе автора без привлечения финансирования.
Conflict of Interest. The author declares that there are no obvious or potential conflicts of interest associated with the content of this article.	***Конфликт интересов.*** Автор декларирует отсутствие явных и потенциальных конфликтов интересов, связанных с содержанием настоящей статьи.

REFERENCES / ЛИТЕРАТУРА

1. Rudnicka E, Napierała P, Podfigurna A, et al. The World Health Organization (WHO) approach to healthy ageing. *Maturitas*. 2020;139:6-11. DOI: 10.1016/j.maturitas.2020.05.018

2. Polyakov DS, Fomin IV, Belenkov YuN, et al. Chronic heart failure in the Russian Federation: what has changed over 20 years of follow-up? Results of the EPOCH-CHF study. *Kardiologiia*. 2021;61(4):4-14. [Поляков Д.С., Фомин И.В., Беленков Ю.Н., и др. Хроническая сердечная недостаточность в Российской Федерации: что изменилось за 20 лет наблюдения? Результаты исследования ЭПОХА-ХСН. *Кардиология*. 2021;61(4):4-14]. DOI: 10.18087/cardio.2021.4.n1628

3. Lawson C, Zaccardi F, Squire I, et al. Risk Factors for Heart Failure: 20-Year Population-Based Trends by Sex, Socioeconomic Status and Ethnicity. *Circulation*. 2020;13(2):e006472. DOI: 10.1161/CIRCHEARTFAILURE.119.006472:e006472

4. Tregubov AV, Tregubova AA, Alekseeva IV, et al. Comparison of the results of cardiovascular risk assessment using the SCORE and SCORE2 scales. *The Journal of Atherosclerosis and Dyslipidemias*. 2021;3(48):41-47. [Трегубов А.В., Трегубова А.А., Алексеева И.В., и др. Опыт применения шкал SCORE и SCORE2 для оценки риска сердечно-сосудистых осложнений у жителей Российской Федерации. *Атеросклероз и дислипидемии*. 2021;3(48):41-47]. DOI: 10.34687/2219-8202.JAD.2022.03.0005

5. SCORE2-OP working group and ESC Cardiovascular risk collaboration. SCORE2-OP risk prediction algorithms: estimating incident cardiovascular event risk in older persons in four geographical risk regions. *Eur Heart J*. 2021;42(25):2455-2467. DOI: 10.1093/eurheartj/ehab312

6. Visseren FLJ, Mach F, Smulderst YM, et al. 2021 ESC Guidelines on cardiovascular disease prevention in clinical practice. *Russian Journal of Cardiology*. 2022;27(7):5155. [Виссерен Ф.Л.Дж.,

Мах Ф., Смулдерс Ю.М., и др. 2021 Рекомендации ESC по профилактике сердечно-сосудистых заболеваний в клинической практике. *Российский кардиологический журнал*. 2022;27(7):5155]. DOI: 10.15829/1560-4071-2022-5155

7. Zairova AR, Rogoza AN, Oshchepkova EV, et al. SCORE2 cardiovascular risk stratification of an urban adult population sample and evaluation of its effectiveness based on 5-year follow-up. *Cardiovascular Therapy and Prevention*. 2025;24(1):4184. [Заирова А.Р., Рогоза А.Н., Ощепкова Е.В., и др. Стратификация сердечно-сосудистого риска с использованием шкалы SCORE2 в популяционной выборке взрослого городского населения и оценка ее эффективности по результатам 5-летнего наблюдения. *Кардиоваскулярная терапия и профилактика*. 2025;24(1):4184]. DOI: 10.15829/1728-8800-2025-4184

8. Bakulin GG, Serezhina EK, Obrezan AG. Topical issues of cardiovascular risk scales application in cardiovascular disease clinical practice. *Cardiology: News, Opinions, Training*. 2023;11(3):43-52. [Бакулин Г.Г., Сережина Е.К., Обрезан А.Г. Актуальные вопросы применения в клинической практике шкал кардиоваскулярного риска у пациентов с сердечно-сосудистой патологией. *Кардиология: Новости. Мнения. Обучение*. 2023;11(3):43-52]. DOI: 10.33029/2309-1908-2023-11-3-43-52

9. Jennings G, Raffoul N, Nelson M. Assessing and communicating cardiovascular disease risk: a practical summary of the 2023 guideline. *Aust Prescr*. 2024;47:57-63. DOI: 10.18773/austprescr.2024.014

10. 2021 ESC Guidelines on cardiovascular disease prevention in clinical practice: Developed by the Task Force for cardiovascular disease prevention in clinical practice with representatives of the European Society of Cardiology and 12 medical societies with the special contribution of the European Association of Preventive Cardiology (EAPC). *Eur Heart J*. 2022;43(42):4468. DOI: 10.1093/eurheartj/ehac458

11. Svinin GE, Kutsenko VA, Shalnova SA, et al. Validation of SCORE2 on a sample from the Russian population and adaptation for the very high cardiovascular disease risk region. *PLoS One*. 2024;19(4):e0300974. [Свинин Г.Е., Куценко В.А., Шальнова С.А., и др. Валидация SCORE2 на выборке из российской популяции и адаптация для региона с очень высоким риском сердечно-сосудистых заболеваний. *PLoS One*. 2024;19(4):e0300974]. DOI: 10.1371/journal.pone.0300974

12. *Clinical guidelines: Lipid metabolism disorders*. ICD coding: E78.0-4. Eds. by Yezhov MV, Kukharchuk VV, Sergienko IV, et al. M., 2023. (In Russ.). [*Клинические рекомендации: Нарушения липидного обмена*. Кодирование по МКБ: Е78.0-4. Под ред. Ежова М.В., Кухарчук В.В., Сергиенко И.В., и др. М., 2023]. URL: https://cr.minzdrav.gov.ru/schema/752_1

13. Penson P, Martin SS, Henney NC, et al. Comparison of LDL-C calculation by friedewald and martin/hopkins methods in 12,243 adults from the United States of America. *Eur Heart J*. 2020;41(2):2932. DOI: 10.1093/ehjci/ehaa946.2932

14. Navarese EP, Lansky AJ, Kereiakes DJ, et al. Cardiac mortality in patients randomised to elective coronary revascularisation plus medical therapy or medical therapy alone: a systematic review and meta-analysis. *Eur Heart J*. 2021;42(45):4638-4651. DOI: 10.1093/eurheartj/ehab246

15. SCORE2 working group and ESC Cardiovascular risk collaboration. SCORE2 risk prediction algorithms: new models to estimate 10-year risk of cardiovascular disease in Europe. *Eur Heart J*. 2021;42:2439-2454. DOI: 10.1093/eurheartj/ehab309

16. *Clinical guidelines: Frailty*. Eds. by Tkacheva ON, Kotovskaya YuV, Runikhina NK, et al. M., 2024. (In Russ.). [*Клинические рекомендации: Старческая астения*. Под ред. Ткачевой О. Н., Котовской Ю.В., Рунихиной Н.К., и др. М., 2024]. URL: https://cr.minzdrav.gov.ru/schema/613_2

17. Kannel WB. Coronary heart disease risk factors in the elderly. *The American journal of geriatric cardiology*. 2002;11(2):101-107. DOI: 10.1111/j.1076-7460.2002.00995.x

18. *Clinical guidelines: Type 2 diabetes mellitus in adults*. Eds. by Dedov II, Shestakova MV, Mayorov AYu, et al. M., 2022. (In Russ.). [*Клинические рекомендации: Сахарный диабет 2 типа у взрослых*. Под ред. Дедова И.И., Шестаковой М.В., Майорова А.Ю., и др. М., 2022]. URL: https://cr.minzdrav.gov.ru/recomend/290_2

19. Lukina YuV, Kutishenko NP, Martsevich SYu, et al. Methodological recommendations: "Adherence to drug therapy in patients with chronic non-communicable diseases. Addressing the problem in a number of clinical situations". *Russian Journal of Preventive Medicine*. 2020;23(3-2):42-60. [Лукина Ю.В., Кутишенко Н.П., Марцевич С.Ю., и др. Методические рекомендации: «Приверженность к лекарственной терапии у больных хроническими неинфекционными заболеваниями. Решение проблемы в ряде клинических ситуаций». *Профилактическая медицина*. 2020;23(3-2):42-60]. DOI: 10.17116/profmed20202303242

Review | Научный обзор
DOI: https://doi.org/10.35693/SIM688475

Possibilities and prospects of echocardiographic diagnostics of regional contractility disorders of the left ventricular myocardium in patients with chronic ischemic heart disease

Tatyana O. Nikolaeva, Vera V. Mazur, Evgenii S. Mazur
Tver State Medical University (Tver, Russian Federation)

Abstract

Currently, the primary method for identifying transient disorders of local contractility of the left ventricular myocardium in patients with coronary atherosclerosis remains visual assessment of myocardial contractility under physical or pharmacological stress testing. Visual assessment of myocardial contractility, especially in stress tests, requires extensive experience in conducting such studies. However, visual assessment by even the most experienced operator remains subjective. Consequently, a principal focus in diagnosing left ventricular regional wall motion abnormalities has been, and remains, the development of methods for objective quantitative assessment of functional status across different left ventricular myocardial segments. A significant success in this area was the development of speckle-tracking echocardiography technique, which allows for a quantitative assessment of myocardial deformation during its contraction and relaxation.

The review presents the results of studies indicating that the determination of left ventricular myocardial deformation indices may become an alternative to the traditional method, devoid of such disadvantages as the subjectivity of visual information perception and very high requirements for the operator's qualification level. Deepening knowledge about the mechanisms, clinical significance of various myocardial deformation indices, the improvement of both the speckle-tracking echocardiography technique itself and the algorithms of automated processing of data creates a real prospect for its introduction into clinical practice as the main method for identifying transient disorders of local left ventricular contractility in patients with hemodynamically significant coronary atherosclerosis.

Keywords: chronic ischemic heart disease, stress-echocardiography, speckle tracking echocardiography technology, regional myocardial contractility disorders, longitudinal systolic deformation of the left ventricle, myocardial postsystolic shortening.

Conflict of interest: nothing to disclose.

Citation
Nikolaeva TO, Mazur VV, Mazur ES. **Possibilities and prospects of echocardiographic diagnostics of regional contractility disorders of the left ventricular myocardium in patients with chronic ischemic heart disease.** *Science and Innovations in Medicine.* 2025;10(3):201-210. DOI: https://doi.org/10.35693/SIM688475

Information about authors
***Tatyana O. Nikolaeva** – MD, Cand. Sci. (Medicine), Associate professor,
Head of the Department of internal diseases.
ORCID: https://orcid.org/0000-0002-1103-5001
E-mail: nikolaevato@mail.ru
Vera V. Mazur – MD, Dr. Sci. (Medicine), Associate professor,
Professor the Department of Hospital Therapy and Occupational Diseases.
ORCID: https://orcid.org/0000-0003-4818-434X
E-mail: vera.v.mazur@gmail.com
Evgenii S. Mazur – MD, Dr. Sci. (Medicine), Professor,
Head of the Department of Hospital Therapy and Occupational Diseases.
ORCID:https://orcid.org/0000-0002-8879-3791
E-mail: mazur-tver@mail.ru
Corresponding Author

Received: 01.07.2025
Accepted: 08.08.2025
Published: 12.08.2025

Возможности и перспективы эхокардиографической диагностики нарушений локальной сократимости миокарда левого желудочка при хронической ишемической болезни сердца

Т.О. Николаева, В.В. Мазур, Е.С. Мазур
ФГБОУ ВО «Тверской государственный медицинский университет» Минздрава России
(Тверь, Российская Федерация)

Аннотация

В настоящее время основным методом выявления транзиторных нарушений локальной сократимости миокарда левого желудочка у больных с коронарным атеросклерозом служит визуальная оценка сократимости миокарда при физической или фармакологической нагрузке. Визуальная оценка сократительной способности миокарда, особенно в нагрузочных пробах, требует большого опыта в проведении такого рода исследований. Однако зрительная оценка даже самого опытного оператора по-прежнему не лишена субъективизма. В связи с этим одним из магистральных направлений диагностики нарушений локальной сократимости левого желудочка была и остается разработка методов объективной количественной оценки функционального состояния различных участков миокарда левого желудочка. Существенным успехом на этом пути стало создание методики отслеживания серого пятна (speckle-tracking эхокардиография), позволяющей получить количественную оценку деформации миокарда при его сокращении и расслаблении.

В обзоре представлены результаты исследований, свидетельствующие, что определение показателей деформации миокарда левого желудочка может стать альтернативой традиционному методу, лишенной таких его недостатков, как субъективизм восприятия визуальной информации и очень высокие требования к уровню квалификации оператора. Углубление знаний о механизмах и клиническом значении различных показателей деформации миокарда, наряду с совершенствованием как самой методики speckle-tracking эхокардиографии, так и алгоритмов автоматизированной обработки получаемых с ее помощью данных, создает реальную перспективу ее внедрения в клиническую практику в качестве основного метода выявления транзиторных нарушений локальной сократимости миокарда левого желудочка у больных с гемодинамически значимым коронарным атеросклерозом.

Ключевые слова: хроническая ишемическая болезнь сердца, стресс-эхокардиография, нарушения локальной сократимости миокарда, технология speckle tracking echocardiography, продольная систолическая деформация левого желудочка, постсистолическое укорочение миокарда.

Конфликт интересов: не заявлен.

Для цитирования:
Николаева Т.О., Мазур В.В., Мазур Е.С. **Возможности и перспективы эхокардиографической диагностики нарушений локальной сократимости миокарда левого желудочка при хронической ишемической болезни сердца.** *Наука и инновации в медицине*. 2025;10(3):201-210.
DOI: https://doi.org/10.35693/SIM688475

Сведения об авторах
***Николаева Татьяна Олеговна** – канд. мед. наук, доцент, заведующая кафедрой пропедевтики внутренних болезней.
ORCID: 0000-0002-1103-5001
E-mail: nikolaevato@mail.ru
Мазур В.В. – д-р мед. наук, доцент, профессор кафедры госпитальной терапии и профессиональных болезней.
ORCID: 0000-0003-4818-434X
E-mail: vera.v.mazur@gmail.com
Мазур Е.С. – д-р мед. наук, профессор, заведующий кафедрой госпитальной терапии и профессиональных болезней.
ORCID: 0000-0002-8879-3791
E-mail: mazur-tver@mail.ru

Список сокращений
ГПС – глобальный продольный стрейн; ИБС – ишемическая болезнь сердца; КАГ – коронарная ангиография; НЛС – нарушение локальной сократимости; ОВ – огибающая ветвь; ПКА – правая коронарная артерия; ПМЖВ – передняя межжелудочковая ветвь; ПСИ – постсистолический индекс; ПСУ – постсистолическое укорочение; ТИМ – транзиторная ишемия миокарда; ЭхоКГ – эхокардиография; AUC – площадь под кривой; РПС – региональный продольный стрейн.

Автор для переписки

Получено: 01.07.2025
Одобрено: 08.08.2025
Опубликовано: 12.08.2025

INTRODUCTION

One of the principal tasks of echocardiographic examination (EchoCG) is to identify disorders of regional contractility (RCD) of the left ventricle myocardium that may be caused by a number of cardiovascular diseases [1]. The most common cause of RCD is the coronary heart disease (CHD), specifically, the ischemic necrosis (infarction) of the myocardium followed by replacement of the necrotized section of the myocardium with connective tissue. The reason for deterioration of the myocardial contractility may be not only necrosis but also the persistent reduction of blood supply to the section of the myocardium to the level sufficient to maintain the viability of myocardiocytes, but insufficient for them to perform their contractile function (hibernating myocardium) [2]. Considerably less frequently, ILC stems from other causes, e.g. amyloid deposition [3].

In the above mentioned cases, RCDs are persistent, i.e. present over a long period regardless of the work performed by the heart. The reason for transient RCDs is the transitory myocardial ischemia (TMI), most frequently arising out of impossibility of adequate blood supply of the myocardium under the increasing cardiac load. The morphological substrate of TMI is typically hemodynamically significant atherosclerosis of the coronary arteries. At the same time, restricted myocardial blood supply under stress may also result from compression of the coronary arteries (so-called “myocardial bridging”) or from the loss of the ability of coronary arteries to dilate in response to increased blood flow velocity (Syndrome X). The onset of TMI at rest might stem from a spasm of the coronary artery (vasospastic angina) [4]. Thus, identification of RCDs is only the first step of the diagnostic process whose task is the identification of causes of their onset.

This review article provides an analysis of the modern possibilities offered by EchoCG in the diagnostics and differential diagnostics of persistent and transient RCDs of the left ventricle myocardium.

Methodology of search for sources. The search for literature was performed in the Russian Science Citation Index (RSCI) and PubMed databases using the following keywords: speckle tracking echocardiography, stress-echocardiography and regional myocardial contractility disorders, or global longitudinal strain of the left ventricle, or myocardial postsystolic shortening. The total number of analyzed papers was 3215. The conditions for the selection of journal articles and other materials were as follows: year of publication: not earlier than 2010; focus on the use of speckle tracking echocardiography during stress tests (stress-echocardiography). The final analysis included 36 selected articles.

VISUAL DIAGNOSTICS OF RCD

From the advent of EchoCG into clinical practice to the present, the major method of identifying RCDs is the visual comparison of contractile activity of various regions of the left ventricular myocardium [1]. Myocardial contractions come with an obvious thickening of the walls of the left ventricle and their shift to the ‘axis line’ of the left ventricle.

In the systolic period, the thickness of the interventricular septum and of the posterior wall of the left ventricle increases by more than 50%, and its transverse size decreases by at least 10% [5]. Visually, it is possible to ascertain a decrease of contractile activity of a certain myocardial region (hypokinesia), complete absence of contractility (akinesia), as well as systolic or systolic-diastolic protrusion of a

region of the myocardium (dyskinesia or aneurysm). While RCD may be present in some regions of the myocardium, increased contractile activity (hyperkinesia) may be observed in other regions. Contractile activity of various regions of the myocardium is often expressed in points: hyperkinesia – 0, normokinesis – 1, hypokinesia – 2, akinesia – 3, dyskinesia – 4, aneurysm – 5 [1].

In order to localize the identified changes, three diagrams of segmental division of the left ventricle are proposed: 16-segment, 17-segment and 18-segment. The 17-segment diagram is now the most widely used, with 6 segments on the basal level, 6 on the medial, and 5 on the apical (**Fig. 1**).

On the same figure, the scheme of blood supply to the left ventricle is shown, proposed by M.D Cerqueira *et al*. (2002) [6]. Depending on the specific features of coronary anatomy, the 9th segment may receive blood from the anterior interventricular branch (*Ramus interventricularis anterior,* RIVA) or the right coronary artery (RCA), 6th, 12th and 16th from the RIVA or from the circumflex branch (CB), and the 5th and 11th from the CB or RCA. Mismatch between RCD and the perfusion territory of a specific coronary artery suggests a non-ischemic etiology, such as deposition of foreign material in the affected myocardial segment.

In order to identify transient RCDs, tests under physical or pharmacological stress are performed under EchoCG control (stress-EchoCG). Exercise stress testing utilizes a cycle ergometer or treadmill, while pharmacological stress testing employs dobutamine infusion. In either case, heart rate increases as does the myocardium demand of oxygen, which, in the event of impossibility of adequate increase of coronary perfusion, results in the onset of TMI and transient RCDs. Modern ultrasonic devices are equipped with a so-called stress system that simultaneously displays the recording of the systolic part of the cardiac cycle at rest and under stress, which significantly facilitates identification of transient RCDs.

Exercise stress testing on an upright (seated) cycle ergometer and especially on a treadmill provides good modeling of actual conditions leading to the onset of TMI but does not allow visual tracking of the contractile activity of the myocardium under stress. Such a possibility arises when the supine (recumbent) cycle ergometer is used; however, due to the non-physiologic nature of the load, it had not become widely employed.

The dobutamine infusion test is less physiologic but provides ideal conditions for a continuous visual assessment of the contractile capacity of the myocardium. At the same time, low-dosage dobutamine infusion test allows identification of the hibernating (viable but not contracting) myocardium. Dobutamine stimulation causes such myocardium to contract, which confirms its viability. Identification of the hibernating myocardium is highly important for the decision-making as to feasibility of revascularization after an infarction [2, 5].

It is to be emphasized that a visual assessment of the contractile capacity of the myocardium, especially in stress tests, requires vast experience in making such examinations. It is officially considered that the results of 50 first examinations performed by an aspiring operator have no diagnostic value [5]. At the same time, an assessment performed even by a highly experienced operator remains subjective, which is

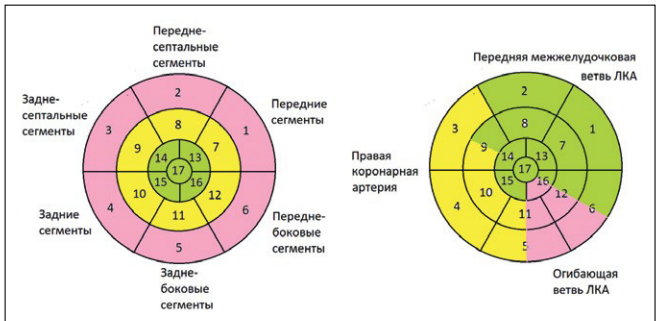

Anterior septal segments Posterior septal segments Anterior segments Posterior segments Anterior lateral segments Posterior lateral segments	Anterior interventricular branch of the LCA Right coronary artery Circumflex branch of the LCA

Figure 1. *Diagram of segmental division and blood supply of the segments of the left ventricle. On the left is a diagram of the segmental division of the left ventricle (pink: basal level, yellow: medial level, green: apical level). On the right: diagram of blood supply to the left ventricle (LCA: left coronary artery).*

Рисунок 1. *Схема сегментарного деления и кровоснабжения сегментов левого желудочка. Слева – схема сегментарного деления левого желудочка (розовый цвет – базальный уровень, желтый – медиальный, зеленый – апикальный). Справа – схема кровоснабжения левого желудочка (ЛКА – левая коронарная артерия).*

confirmed by characteristics of the stress-EchoCG as a predictor of identification of hemodynamically significant coronary atherosclerosis. According to the data from the leading medical centers, the sensitivity and specificity of the stress test is approx. 85–90%, i.e. one in every ten cases of identification of RCD, and one in every ten cases when RCD is deemed absent under stress, are erroneous [5]. Therefore, one of the major trends in the development of EchoCG has been, and remains, the work on methods of objective assessment of contractile capacity of different regions of the left ventricular myocardium. A significant achievement in this area was the development of the speckle-tracking echocardiography that provides quantitative assessment of the myocardium deformation in its contraction and relaxation [7–10].

LONGITUDINAL SYSTOLIC MYOCARDIAL DEFORMATION

During systole, the left ventricle shortens, contracts, and twists along its longitudinal axis, resulting in longitudinal, radial, and circumferential deformation of each myocardial segment. The myocardial deformation comes with a change in the distance between its neighboring points, which enables quantitative assessment of the deformation by comparing the distance between the points in the beginning and the end of systole. These measurements can be obtained using various methods, such as tissue Doppler imaging. However, speckle-tracking echocardiography, a gray-scale pattern tracking technology, is currently considered the gold standard for assessing myocardial deformation. This technology allows for an assessment of all three components of systolic deformation whose diagnostic value may vary in different clinical situations [11]. However, only the longitudinal systolic deformation is recommended for use in present-day clinical practice [12]. This review focuses only on this type of myocardial deformation,

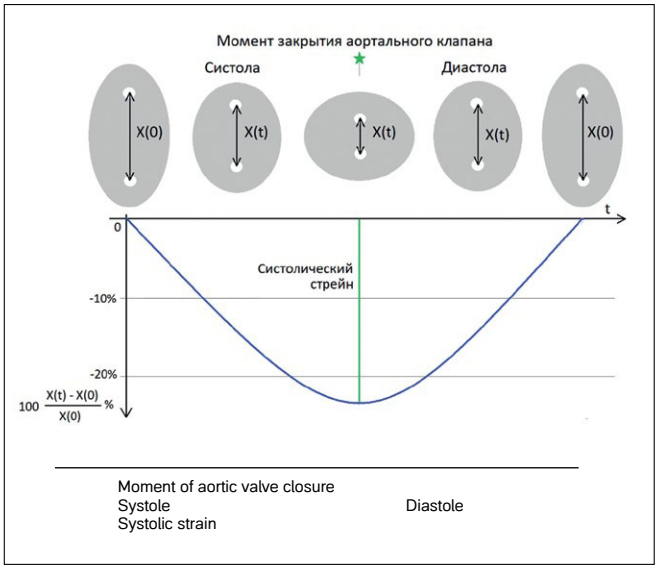

Figure 2. *Changes in the distance between adjacent points of the myocardium and the longitudinal systolic strain index (longitudinal systolic strain) throughout the cardiac cycle (diagram).*

Рисунок 2. *Изменение расстояния между близлежащими точками миокарда и показателя продольной систолической деформации (продольного систолического стрейна) на протяжении кардиоцикла (схема).*

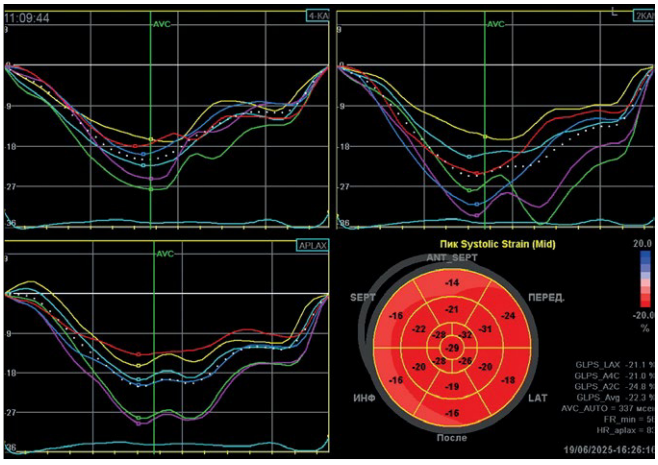

Figure 3. *Results of measuring the longitudinal systolic strain of the left ventricle using the speckle-tracking echocardiography method. Graphs of strain changes throughout the cardiac cycle in all 17 segments of the left ventricle are presented. Strain values at the moment of aortic valve closure are shown on the color map.*

Рисунок 3. *Результаты измерения продольного систолического стрейна левого желудочка методом speckle-tracking эхокардиографии. Представлены графики изменения стрейна на протяжении кардиоцикла во всех 17 сегментах левого желудочка. Значения стрейна в момент закрытия аортального клапана отражены на цветовой карте.*

and the term systolic deformation (systolic strain) shall mean the longitudinal systolic deformation (longitudinal systolic strain).

Speckle-tracking technology allows for making a graph of changes in the distance between the two neighboring points of the myocardium during the cardiac cycle (**Fig. 2**). This distance reaches its maximum in the end of the diastole, when the myocardium is fully relaxed. During the systole, the distance between the tracked points decreases, and upon the end of contraction, it starts increasing. At the same time, the difference between the current and the initial distance during the systole increases, and decreases during the diastole. The percent ratio of this difference at the moment of closure of the aortic valve to the initial distance is used for the qualitative assessment of the systolic myocardial deformation (strain).

During myocardial contraction, the distance between the tracked points decreases, and so the systolic strain is a negative value. However, in the description and statistical processing of the results, the absolute value of the strain is used: the greater the contraction of the myocardium, the greater the value.

The graph of myocardial deformation during the cardiac cycle is created for each of the 17 segments of the left ventricle, and the values of segmental strain at the moment of closure of aortic valve are shown on a color map commonly referred to as the 'bull's eye' (**Fig. 3**). Transition from intense red to intense blue marks the decrease of contractive capacity of the myocardium, from hyperkinesia to dyskinesia.

The color map gives a visual representation of the contractive capacity of various regions of the left ventricular myocardium, for which reason it is often used in educational materials and descriptions of clinical cases. For a generalized assessment of the map data, some indicators are used that represent the contractive capacity of the myocardial segments belonging to a specific region (regional longitudinal strain, RLS). In most cases, regional indicators are calculated as the average value of strain in segments of that region. Specifically, it is shown that in healthy individuals at rest the average strain value in the basal segments is lower than in the apical, while at stress these differences become more pronounced [13].

Studying of the relation of RCD with myocardial ischemia usually involves calculation of average values of longitudinal strain in the regions belonging to perfusion areas of some or other coronary artery (Fig. 1, right). This approach was used in the study of M.K. Smedsrud *et al.* (2012) [14] that included 86 patients with recurrent chest pains. The study did not include patients with prior verified CHD. Speckle-tracking echocardiography at rest was performed before the coronary angiography (CAG), the results of which allowed identification of patients with and without hemodynamically significant coronary stenosis (>50%). It was found that the average values of RLS in patients with hemodynamically significant stenosis were in average 2.2% lower than in the alternative group (17.9±3.5% vs. 20.1±2.9%, p = 0.015). At the same time, the predictive capacity of decreased RLS with respect to identification of hemodynamically significant stenosis by CAG was rather low: the area under the curve (AUC) was 0.67 (95% CI 0.52–0.82).

A similar approach was used in several other studies that confirmed the presence of statistically significant RLS at rest in patients with and without hemodynamically significant coronary stenosis [15]. Assessment of predictive capacity of RLS in these studies was virtually the same (AUC from 0.72 to 0.75), however, the values of the cutoff varied within a broad range (12.6…18.3%), which precludes consideration of RLS at rest as a predictor for identification of hemodynamically significant coronary stenosis.

Regional longitudinal strain during physical or pharmacological stress may provide a more reliable predictor

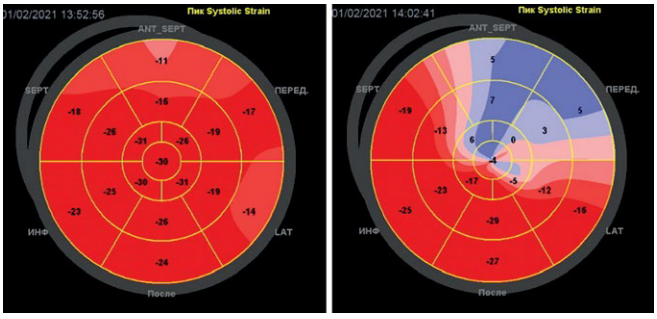

Figure 4. *Left ventricular strain in a patient with hemodynamically significant stenosis of the anterior interventricular branch (LAD) of the left coronary artery before (left) and after (right) dosed physical exercise. Before the exercise, the average longitudinal strain value in the blood supply zone of the LAD is -22%, after the exercise – +2.1%. A positive value of systolic longitudinal strain indicates that the myocardium is stretched during systole, i.e. is in the state of dyskinesis.*

Рисунок 4. *Стрейн левого желудочка у пациента с гемодинамически значимым стенозом передней межжелудочковой ветви (МПЖВ) левой коронарной артерии до (слева) и после (справа) дозированной физической нагрузки. До нагрузки среднее значение продольного стрейна в зоне кровоснабжения ПМЖВ равно -22%, после нагрузки – +2,1%. Положительное значение систолического продольного стрейна свидетельствует, что миокард во время систолы растягивается, то есть находится в дискинезе.*

of hemodynamically significant coronary stenoses than measurements at rest (**Fig. 4**).

Indeed, the study of S.I. Farag *et al*. (2020) [16] showed an almost complete matching of results of assessment of the availability and localization of the hemodynamically significant atherosclerosis on the color map after dobutamine stress testing, and CAD data. The agreement coefficient (kappa) was 0.819, significantly exceeding the kappa coefficient for agreement with visual assessment of RCD during stress echocardiography compared to coronary angiography results (kappa 0.663). The sensitivity of RCD assessment with the color map of the regional longitudinal strain with respect to identification of the hemodynamically significant atherosclerosis was 95%, its specificity was 90%; the respective values of the visual assessment of RCD were 86% and 85%. The results of the study confirm the perspectives of studying the RLS under stress in the diagnostics of transitory myocardial ischemia; however, we found no other papers on this topic in the available literature. Much more frequent were the papers studying the diagnostic capacity of the global longitudinal strain (GLS).

GLS is calculated as the arithmetic mean of the strain values in all segments of the left ventricle. In healthy individuals at rest, the GLS is nearing 20%, and under stress, it increases by approx. 5 percent points. After exercise test on a cycle ergometer, GLS of 67 healthy individuals aged between 23 and 80 increased from the base level of 20.1 ± 1.8% to 25.4 ± 2.0%, p<0.0001 [13]. In 46 patients without CHD but with risk factors of its development (arterial hypertension, Diabetes mellitus, hyperlypidemia, positive family history), the global strain grew to 25 ± 3% (p<0.05) [17]. Administration of dobutamine also leads to GLS growth in healthy individuals less pronounced than under physical stress [18].

GLS reflects contractile capacity of the left ventricular myocardium on the whole, i.e. provides the same information as the ejection fraction; at the same time, it has higher sensitivity and reproducibility in the assessment of the systolic function of the left ventricle [19, 20]. Thus, determination of GLS is recommended for the control of the systolic function of the left ventricle in the use of cardiotoxic drugs, specifically, during chemotherapy of oncological diseases [21, 22], and new diagnostic algorithms to identify heart failure with preserved ejection fraction and diagnostics of the diastolic function of the left ventricle [23–25].

Some studies show that the GLS values at rest differ in patients with and without hemodynamically significant coronary atherosclerosis. A systematic review of these studies showed that the differences in GLS at rest in patients with stenosis (n = 397) and without stenosis (n = 381) are 2 percent points (17.2 ± 2.6 vs. 19.2 ± 2.8%, p <0.0001), AOC varies from 0.68 to 0.80, and the threshold level for the prediction of hemodynamically significant stenosis varies from 17.4 to 19.7%, with sensitivity from 51% to 81% and specificity from 58% to 81% [15]. Based on the obtained data, the authors of the review concluded that GLS at rest has only minor capacity in the prediction of hemodynamically significant stenosis in patients with acute or recurrent chest pains.

A similar conclusion stems from the results of later studies. Thus, in the study of A.I. Stepanova *et al*. (2021) [26], GLS at rest demonstrated no predictive significance with respect to coronary atherosclerosis generally or with respect to severe coronary atherosclerosis (Gensini score ≥35). In the former case, the AOC was 0.52 (95% CI 0.42–0.63, p = 0.59), while in the latter it was 0.63 (CI 0.47–0.73, p = 0.12). However, in some papers, GLS at rest shows very high predictive capacity with respect to hemodynamically significant stenosis of coronary arteries. For example, in the above mentioned study of S.I. Farag *et al.* (2020) [16], the area under curve for GLS at rest was 0.827 (95% CI 0.732–0.921), and in the study of S. Qin et al. [27] it was 0.973.

The studies focusing on prognostic capacity of GLS under physical or pharmacological stress [28–32] demonstrate more uniform results. In the study of A.I. Stepanova et al. (2021) [26], the area under curve for GLS under physical stress as predictor of identification of severe coronary atherosclerosis (Gensini score ≥ 35) was 0.76 (95% CI 0.63–0.89; p <0.001), and the sensitivity and specificity for GLS below 16.9% was 80% and 70%, respectively. In the study of S.I. Farag *et al*. (2020) [16], similar values for global strain under dobutamine stress were 0.837 (95% CI 0.748–0.927), 82.4 and 78.3% for GLS below 12.5%.

In the assessment of results of studies of predictive capacity of GLS with respect to hemodynamically significant coronary atherosclerosis one needs to consider that GLS provides an assessment of the contractive capacity of the left ventricular myocardium on the whole. Its decrease may be related to persistent or transient regional contractility disorders and with a number of other reasons, e.g. type II diabetes mellitus [33, 34], the prevalence of which among patients with severe coronary atherosclerosis is quite high. In the above mentioned study of S.I. Farag *et al*. (2020) [16], 59% of examined patients had the concomitant diabetes mellitus. At the same time, according to C. Philouze *et al*.

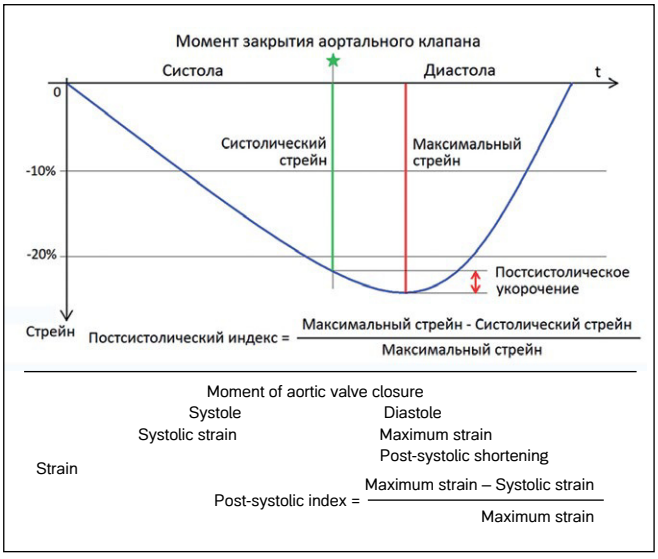

Figure 5. *Schematic representation of the longitudinal strain change graph, in which the maximum longitudinal strain is observed after the completion of left ventricular systole.*

Рисунок 5. *Схематическое изображение графика изменения продольного стрейна, на котором максимальный продольный стрейн отмечается после завершения систолы левого желудочка.*

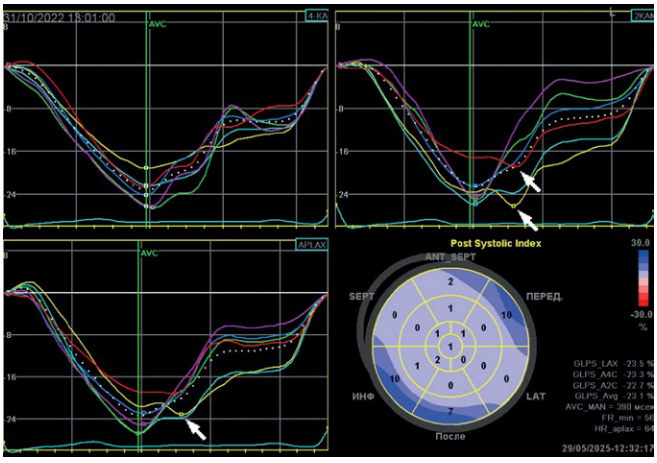

Figure 6. *Results of calculation of the postsystolic index. The graphs of strain changes in 17 segments of the left ventricle during the cardiac cycle are presented. The systolic longitudinal strain corresponds to the point of intersection of the graph with the vertical line AVC (aortic valve closure), reflecting the moment of closure of the aortic valve. Arrows indicate the maximum longitudinal strain recorded after the completion of systole. Segments in which postsystolic shortening is recorded are highlighted in saturated blue on the color map.*

Рисунок 6. *Результаты расчета постсистолического индекса. Представлены графики изменения стрейна в 17 сегментах левого желудочка на протяжении кардиоцикла. Систолическому продольному стрейну соответствует точка пересечения графика с вертикальной прямой AVC (aortic valve closure), отражающей момент закрытия аортального клапана. Стрелки указывают на максимальный продольный стрейн, зарегистрированный после завершения систолы. Сегменты, в которых зарегистрировано постсистолическое укорочение, выделены на цветовой карте насыщенным синим цветом.*

(2018) [35], the increase of GLS under dobutamine stress in patients with diabetes mellitus was much less marked than in healthy individuals. In the control group, GLS under stress increased on average by 3.4 percent points (from 20.8 ± 2.3 to 24.2 ± 2.5%), and in the diabetes group, just by 1 percent point (from 20.2 ± 2.7 to 21.2 ± 2.4%). The authors believe that the mild increase of GLS could be the excessive deposit of epicardial fat in diabetes patients: being a source of proinflammatory and profibrotic cytokines, it adversely affects the contractile capacity of cardiomyocytes [36].

The study of M.J. Mansour *et al*. (2018) [31], the results of stress-echocardiography with speckle tracking were compared not only with CAG data on the severity of coronary atherosclerosis, but also with the presence of concomitant diseases in the patient (cerebrovascular diseases, diabetes mellitus, arterial hypertension), and cardiovascular risk factors (smoking and dyslipidemia). It was found that the lower values of GLS at rest and under stress were identified not only in patients with marked coronary atherosclerosis, but also in patients with multiple concomitant conditions and risk factors which, in the authors' opinion, indicates a subclinical dysfunction of the left ventricle caused by those conditions. Based on the obtained information, the authors conclude that the higher values of GLS allow exclusion of hemodynamically significant stenosis, whereas the lower values of strain provide no foundation for its diagnostics.

As a sensitive marker of disorder of the global systolic function of the left ventricle, the GLS can hardly become an effective means of diagnosing regional contractility disorders. Assessment of longitudinal strain in the perfusion regions under stress seems to be more promising, but, as we mentioned earlier, this problem requires further research. Moreover, the assessment of global and regional longitudinal strain has some limitations related to the image quality and some rhythm disorders (e.g., ventricular bigeminy).

POST-SYSTOLIC SHORTENING

The systole of the left ventricle finishes at the moment of aortic valve closure. By that time, the majority of segments reach the state of maximum contraction and begin elongating. However, some segments continue contracting even after the systole of the ventricle is over. This phenomenon is referred to as 'post-systolic shortening' (PSS). Quantitative values of the PSS is the difference between the maximum and systolic strain (PSS = maximum longitudinal strain – systolic longitudinal strain) and the post-systolic index (PSI), that is the percentage of this difference from the maximum longitudinal strain (PSI% = PSS/ maximum longitudinal strain, **Fig. 5**).

PSI is calculated for each segment of the left ventricle and is represented on the color map (**Fig. 6**). In order to analyze the obtained data, the average PSI value is calculated in all segments of the left ventricle (global PSI) or in the segments referring to perfusion are of some coronary artery or other (regional PSI).

According to P. Brainin *et al*. (2019) [37], in healthy individuals PSS is registered on average in 80% segments of the left ventricle. At the same time, the median PSS is 0.4% [interquartile range 0.2; 0.8%], and the median PSI is 2% [0.7; 4.8%]. The mechanism of physiological PSS is related to the measurement of geometry of the left ventricle at the stage of isovolumic relaxation, i.e. in the period from the closure of aortic valve to the opening of the mitral valve. At this stage, the cavity of the left ventricle turns

from elongated on the longitudinal axis to near spherical in shape. Singe the surface area of a sphere is less than the area of any non-spherical body of the same volume, the area of the myocardium surrounding the cavity of the left ventricle and the distance between its neighboring points decrease. Therefore, the physiological PSS is shortening, not the contraction, of the myocardium.

From the clinical perspective, the PSS phenomenon is interesting because the reason for its onset might be myocardial perfusion disorder. In some experimental studies on animals it was shown that the occlusion of the coronary artery results in the lowering of the longitudinal strain and increase of the PSI in the perfusion area of that artery, and the restoration of the blood supply is accompanied by a quick restoration of the strain and relatively slow return to baseline levels of PSS indices. The phenomenon of delayed recovery of PSS indices after ischemia resolution has been termed "ischemic memory" [8, 38].

The relation of PSS and TMI has been demonstrated in several studies involving stress-echocardiography with dobutamine or exercise stress [38–40]. Thus, the work of A.I. Stepanova et al. (2022) [39] showed, that in the individuals without coronary atherosclerosis (Gensini score = 0), moderate (<0 Gensini score <35) and severe (Gensini score ≥35) coronary atherosclerosis at rest, the global PSI did not have statistically significant difference and was 2.0 [0.9; 4.1], 2.1 [1.3; 4.2] and 2.7 [1.9; 5.2]%, respectively. After a predefined exercise on the treadmill, the global PSI increased to 3.8 [2.2; 6.8], 3.4 [2.2; 6.2] and 8.9 [3.8; 10.7]%, respectively, which resulted in the appearance of statistically significant differences between patients with and without severe coronary atherosclerosis ($p = 0.012$). The area under curve for global PSI as a predictor of severe coronary atherosclerosis was 0.74 (95% CI 0.63–0.85; $p < 0.001$), and the sensitivity and specificity of the criterion 'global PSI > 4.9%' was 75% and 61%.

Similar results were arrived at in the study of E. Rumbinaite et al. (2020 [40], where stress echocardiography under dobutamine stress was performed for 83 patients with pre-test chance of CAD, in 45 of which CAG identified hemodynamically significant stenosis of coronary arteries. Initially, the global PSI in patients with and without stenosis was 4.59 ± 3.04 and 4.07 ± 1.37% ($p = 0.32$), and under dobutamine stress it increased respectively to 10.46 ± 3.42 and 5.23 ± 1.96% ($p = 0.02$). The area under curve for global PSI under stress was 0.724 ($p = 0.04$), the sensitivity and specificity of the criterion 'global PSI > 6.46%' was 70% and 74%.

This study focused not only on the global but on regional PSIs on the perfusion areas of three coronary arteries as well. Initially, in the perfusion area of the anterior intraventricular branch the regional PSI in patients with and without hemodynamically significant stenosis was 6.87 ± 3.32 and 4.65±2.32%, respectively; after dobutamine stress, 11.59 ± 5.21 and 6.43 ± 3.21 ($p = 0.02$). In the perfusion area of the right coronary artery, the respective initial values of PSI were 6.51 ± 3.14 and 4.58 ± 2.42% ($p = 0.34$), under stress: 10.71 ± 4.21 and 5.59 ± 2.46 ($p = 0.03$). In the basin of the circumflex branch of the left coronary artery, the initial PSI values were 6.65 ± 3.14 and 5.01 ± 2.34% ($p = 0.53$), under stress: 7.13 ± 4.16 and 5.78 ± 2.67% ($p = 0.18$). Thus, dobutamine stress results in the increase of both the global PSI and the regional PSI in the perfusion area of the affected artery, yet the initial values of the regional PSI and their increase under stress differ in various vascular areas. Obviously, these differences form additional complications for the interpretation of results of assessment of the regional PSI.

The possibility of using the changes in the PSI under stress to identify individuals with hemodynamically significant coronary atherosclerosis may be considered proven; at the same time, a number of problems remain unanswered.

First, we should mention the lack of a generally recognized criterion of diagnosing the pathological PSS. Quite frequently, PSI value above 20% is used as this criterion, which was suggested to diagnose pathological PSS using the data of Doppler tissue examination. At the same time, we already mentioned that in the patients with hemodynamically significant atherosclerosis the PSI in the perfusion area of the affected artery under stress increases to approx. 10%. The PSI increase in this case is, without doubt, pathological, but it is not anywhere near 20%. Thus, the question of diagnostic criteria of pathological PSS remains unanswered and requires further research.

In the majority of studies focusing on the correlation of PSS with myocardial ischemia, considerably high sensitivity of PSI increase as the sign of myocardial ischemia was demonstrated; however, its specificity requires further research: pathological PSS is identified in the hypertrophic, dilatation and stress cardiomyopathy, arterial hypertension and aortic stenosis [41]. It is evident that in order to use the PSI in clinical practice a criterion for differential diagnosis of ischemia- and non-ischemia-mediated changes of that indicator.

Another question in need of further research is that of the mechanisms of development of pathological PSS, and these include the following: 1) delayed start of contraction of a segment of myocardium due to late arrival of the excitation wave; 2) delayed contraction of the affected (e.g., ischemic) section of the myocardium; 3) deformation of the section of the myocardium that lost its contractile capacity during contraction and relaxation of the myocardium around.

A visual representation of the role of disorders of intraventricular conductivity in the development of PSS is shown in the color maps shown in **Fig. 7** built in the course of intracardial electrical stimulation of various sections of the conductive system. Evidently, intraventricular conduction disturbances virtually preclude the identification of PSS from other origins. It is plausible that local abnormalities in intraventricular conduction contribute to the development of pathological PSS in ischemic myocardial regions, though this hypothesis requires further investigation.

Delayed myocardial contraction is indicated as the cause of PSS in the outcomes of the study of C. Eek *et al.* (2011) [42], where indices of longitudinal strain and PSS in the area of affected coronary artery were compared before and after revascularization in patients with non-ST-segment elevation myocardial infarction. It was found that after revascularization the recovery of the systolic function occurs in those segments in which marked PSS was registered on the background of acute ischemia. This result enabled the authors to conclude that registration of PSS in the segments perfused by the affected coronary arteries shows preserved viability of the ischemic myocardium.

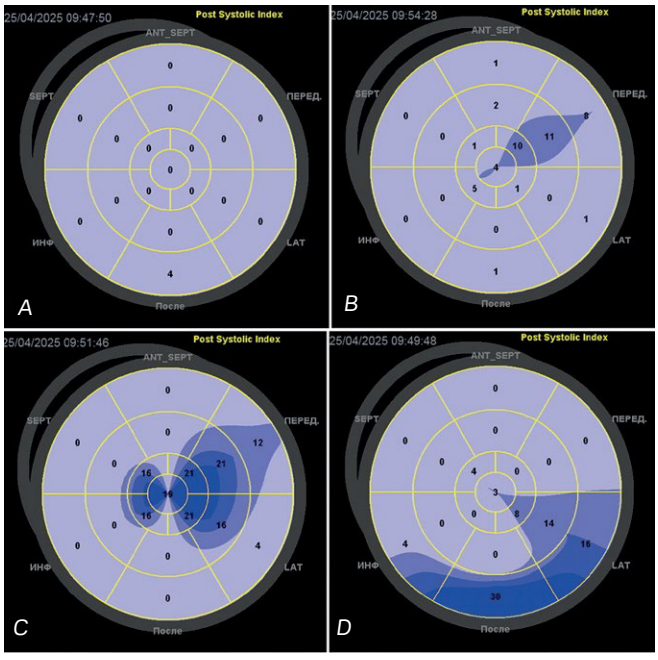

Figure 7. *Effects of the excitation wave propagation path along the left ventricle on the post-systolic contraction. A: sinus rhythm, B: electrical cardiac stimulation in the His bundle region, C: in the region of the middle third of the interventricular septum, D: in the region of the apex of the right ventricle.*

Рисунок 7. *Влияния пути распространения волны возбуждения по левому желудочку на постсистолическое сокращение. А – синусовый ритм, Б – электрокардиостимуляция в области пучка Гиса, В – в области средней трети межжелудочковой перегородки, Г – в области верхушки правого желудочка.*

However, in the similarly designed studies of C. Terkelsen *et al*. (2007) [43] and P. Brainin et al. (2018) [44], dynamic follow-up did not identify recovery of the systolic function of the segments with marked PSS. Moreover, they identified a correlation of PSS with the further development of heart failure, which shows non-viability of the myocardial section with a marked PSS and enables connection of the phenomenon with the deformation of the myocardial section that lost its contractile capacity during relaxation of the muscular tissue around.

The mechanism of the onset of PSS in the myocardium incapable of contraction is easily understood on the example of a myocardial area in the state of dyskinesis. During the systole, this section protrudes beyond the contour of the left ventricle which results in the increase of area of that section and increase of distance between its neighboring points. During the diastole, the protrusion disappears, and the area of the dyskinetic section and the distance between its neighboring points decrease: this is registered as the PSS.

Thus, the question of development of pathologic PSS is directly related to the clinical interpretation of this phenomenon and, beyond doubt, is worthy of further research. This might be confirmed by results of speckle-tracking echocardiography shown in **Fig. 8.** In the patient with 95% stenosis of the circumflex branch of the LCA in the physical stress test, RCD (hypokinesia) in the basal and the medial posterior lateral segments were identified visually. At the same time, the values of the longitudinal systolic strain during the stress increased in all segments including the perfusion area of the affected artery (**Fig. 8 A, C**), which contradicts the results of visual assessment of the stress test and the CAG data. Yet the post-systolic index in the perfusion area of the circumflex branch of the LCA increased from 0 to 27% (**Fig. 8 B, D**), thus confirming the adequacy of visual assessment of the stress test. Based on the available knowledge of mechanisms of development and clinical significance of changes of indices of deformation under physical stress, it does not seem possible to explain the results of this study.

CONCLUSION

Currently, the assessment of left ventricular deformation parameters during physical or pharmacological stress cannot be considered a replacement for the conventionally used visual evaluation of regional contractility dysfunction. At the same time, more knowledge on the mechanisms and clinical significance if carious mechanisms of deformation of the myocardium, as well as development of the very method of speckle-tracking echocardiography and algorithms of automated processing of data thus obtained, forms a realistic perspective of its implementation in clinical practice as the principal method of identification of transitory RCDs in patients with hemodynamically significant coronary atherosclerosis.

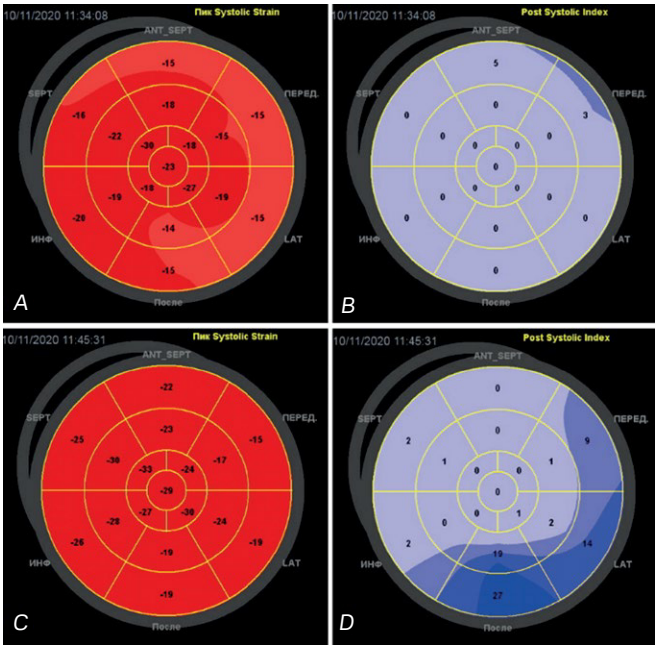

Figure 8. *Results of speckle-tracking echocardiography at rest (A, B) and after dosed physical exercise (C, D) in a patient with 95% stenosis of the circumflex branch of the left coronary artery.*

Рисунок 8. *Результаты speckle-tracking эхокардиографии в покое (А, Б) и после дозированной физической нагрузки (В, Г) у пациента с 95% стенозом огибающей ветви левой коронарной артерии.*

ADDITIONAL INFORMATION	ДОПОЛНИТЕЛЬНАЯ ИНФОРМАЦИЯ
Study funding. The study was the authors' initiative without external funding.	***Источник финансирования.*** Работа выполнена по инициативе авторов без привлечения финансирования.
Conflict of interest. The authors declare that there are no obvious or potential conflicts of interest associated with the content of this article.	***Конфликт интересов.*** Авторы декларируют отсутствие явных и потенциальных конфликтов интересов, связанных с содержанием настоящей статьи.
Compliance with Ethical Standards. The study was approved by the local Ethics Committee of the Tver State Medical University of the Ministry of Health of the Russian Federation, Protocol No.4 dated 16.04.2025).	***Соответствие нормам этики.*** Исследование одобрено локальным этическим комитетом ФГБОУ ВО Тверской ГМУ Минздрава России (протокол №4 от 16.04.2025 г.)
Contribution of individual authors. Nikolaeva T.O.: contribution to obtaining, analyzing literature data and writing of the text of the article. Mazur V.V.: contribution to obtaining results, editing of the text of the article, provision of illustrative material from the author's archive. Mazur E.S.: development of the article concept, data analysis, making significant important edits to the manuscript in order to increase the scientific value of the article. The authors gave their final approval of the manuscript for submission, and agreed to be accountable for all aspects of the work, implying proper study and resolution of issues related to the accuracy or integrity of any part of the work.	***Участие авторов.*** Николаева Т.О. – вклад в получение, анализ данных литературы и написание текста статьи. Мазур В.В. – вклад в получение результатов, редактирование текста статьи, предоставление иллюстративного материала из авторского архива. Мазур Е.С. – разработка концепции статьи, анализ данных, внесение в рукопись существенно важной правки с целью повышения научной ценности статьи. Все авторы одобрили финальную версию статьи перед публикацией, выразили согласие нести ответственность за все аспекты работы, подразумевающую надлежащее изучение и решение вопросов, связанных с точностью или добросовестностью любой части работы.

REFERENCES / ЛИТЕРАТУРА

1. Lang RM, Badano LP, Mor-Avi V, et al. Recommendations for cardiac camber quantification by echocardiography in adults: an update from the American Society of Echocardiography and the European Association of Cardiovascular Imaging. *Eur Heart J Cardiovasc Imaging*. 2015;16:233-271. DOI: 10.1093/ehjci/jev014

2. Vrints ChJ, Andreotti F, Koskinas KC, et al. 2024 ESC Guidelines for the management of chronic coronary syndromes: Developed by the task force for the management of chronic coronary syndromes of the European Society of Cardiology (ESC) Endorsed by the European Association for Cardio-Thoracic Surgery (EACTS). *European Heart Journal*. 2024;45(36):3415-3537. DOI: 10.1093/eurheartj/ehae177

3. Dzhioeva ON. Functional methods of amyloid cardiomyopathy diagnostic in practice and in expert centers: A review. *Terapevticheskii Arkhiv (Ter. Arkh.)*. 2023;95(1):96-102. [Джиоева О.Н. Функциональная диагностика амилоидной кардиомиопатии в условиях практики и экспертных центров. *Терапевтический архив*. 2023;95(1):96-102]. DOI: 10.26442/00403660.2023.01.202081

4. Barbarash OL, Karpov YuA, Panov AV, et al. 2024 Clinical practice guidelines for Stable coronary artery disease. *Russian Journal of Cardiology*. 2024;29(9):6110. [Барбараш О.Л., Карпов Ю.А., Панов А.В., и др. Стабильная ишемическая болезнь сердца. Клинические рекомендации 2024. *Российский кардиологический журнал*. 2024;29(9):6110]. DOI: 10.15829/1560-4071-2024-6110

5. Pellikka PA, Arruda-Olson A, Chaudhry FA, et al. Guidelines for Performance, Interpretation, and Application of Stress Echocardiography in Ischemic Heart Disease: From the American Society of Echocardiography. *J Am Soc Echocardiogr*. 2020; 33(1):1-41.e8. DOI: 10.1016/j.echo.2019.07.001

6. Cerqueira MD, Weissman NJ, Dilsizian V, et al. Standardized myocardial segmentation and nomenclature for tomographic imaging of the heart: a statement for heartcare professionals from the Cardiac Imaging Committee of the Council on Clinical Cardiology of the American Heart Association. *Circulation*. 2002;105:539-542. DOI: 10.1161/hc0402.102975

7. Stepanova AI, Alekhin MN. Capabilities and limitation of speckle tracking stressechocardiography. *Siberian Journal of Clinical and Experimental Medicine*. 2019;34(1):10-17. [Степанова А.И., Алехин М.Н. Возможности и ограничения спекл-трекинг стресс-эхокардиографии. *Сибирский медицинский журнал*. 2019;34(1):10-17]. DOI: 10.29001/2073-8552-2019-34-1-10-17

8. Alekhin MN, Stepanova AI. Echocardiography in the Assessment of Postsystolic Shortening of the Left Ventricle Myocardium of the Heart. *Kardiologiia*. 2020;60(12):110-116. [Алехин М.Н., Степанова А.И. Эхокардиография в оценке постсистолического укорочения миокарда левого желудочка сердца. *Кардиология*. 2020;60(12):110-116.]. DOI: 10.18087/cardio.2020.12.n1087

9. Oleynikov VE, Smirnov YuG, Galimskaya VA, et al. New capabilities in assessing the left ventricular contractility by two-dimensional speckle tracking echocardiography. *Siberian Journal of Clinical and Experimental Medicine*. 2020;35(3):79-85. [Олейников В.Э., Смирнов Ю.Г., Галимская В.А., и др. Новые возможности оценки сократимости левого желудочка методом двухмерной speckle tracking эхокардиографии. *Сибирский журнал клинической и экспериментальной медицины*. 2020;35(3):79-85]. DOI: 10.29001/2073-8552-2020-35-3-79-85

10. Tyurina LG, Khamidova LT, Ryubalko NV, et al. Role of speckle-tracking echocardiography in diagnosis and further prognosis of coronary heart disease. *Medical alphabet*. 2023;(16):7-18. [Тюрина Л.Г., Хамидова Л.Т., Рыбалко Н.В., и др. Роль спекл-трэкинг-эхокардиографии в современной диагностике и прогнозе при коронарной недостаточности. *Медицинский алфавит*. 2023;(16):7-18]. DOI: 10.33667/2078-5631-2023-16-7-18

11. Shvets DA, Povetkin SV. Limitations of diagnosis of ischemic left ventricular dysfunction using the values of strain, twist and untwist in patients with myocardial infarction of various localization. *Kardiologiia*. 2024;64(3):55-62. [Швец Д.А., Поветкин С.В. Возможности диагностики ишемической дисфункции левого желудочка с помощью значений деформации, показателей вращения у больных инфарктом миокарда различной локализации. *Кардиология*. 2024;64(3):55-62]. DOI: 10.18087/cardio.2024.3.n2253

12. Voigt J-U, Pedrizzetti G, Lysyansky P, et al. Definition for a common standard for 2D speckle tracking echocardiography: a consensus document of the EACVI/ASE/Industry Task Force to standardize deformation imaging. *Eur Heart J Cardiovask Imaging*. 2015;16:1-11. DOI: 10.1093/ehjci/jeu184

13. Larsen AH, Clemmensen TS, Wiggers H, Poulsen SH. Left Ventricular Myocardial Contractile Reserve during Exercise Stress in Healthy Adults: A Two-Dimensional Speckle-Tracking Echocardiographic Study. *J Am Soc Echocardiogr*. 2018;31(10):1116-1126. DOI: 10.1016/j.echo.2018.06.010

14. Smedsrud MK, Sarvari S, Haugaa KH, et al. Duration of myocardial early systolic lengthening predicts the presence of significant coronary artery disease. *J Am Coll Cardiol*. 2012;60:1086-93. DOI: 10.1016/j.jacc.2012.06.022

15. Norum BI, Ruddox V, Edvardsen T, Otterstad JE. Diagnostic accuracy of left ventricular longitudinal function by speckle tracking echocardiography to predict significant coronary artery stenosis. A systematic review. *BMC Medical Imaging*. 2015;15(1):25-36. DOI: 10.1186/s12880-015-0067-y

16. Farag SI, El-Rabbat K, Mostafa SA, et al. The predictive value of speckle tracking during dobutamine stress echocardiography in patients with chronic stable angina. *Indian Heart Journal*. 2020;72:40-45. DOI: 10.1016/j.ihj.2020.03.001

17. Leitman M, Tyomkin V, Peleg E, et al. Speckle tracking imaging in normal stress echocardiography. *J Ultrasound Med*. 2017;36:717-724. DOI: 10.7863/ultra.16.04010

18. Lancellotti P, Pellikka PA, Budts W, et al. The clinical use of stress echocardiography in non-ischaemic heart disease: recommendations from the European Association of Cardiovascular Imaging and the American Society of Echocardiography. *J Am Soc Echocardiogr*. 2017;30:101-138. DOI: 10.1093/ehjci/jew190

19. Yingchoncharoen T, Agarwal S, Popovic ZB, Marwick TH. Normal ranges of left ventricular strain: a meta-analysis. *J Am Soc Echocardiogr*. 2013;26:1850191. DOI: 10.1016/j.echo.2012.10.008

20. Trusov YA, Shchukin YuV, Limareva LV. Prediction of adverse outcomes in the long-term follow-up period in patients with chronic heart failure who have suffered a myocardial infarction. *Science and Innovations in Medicine*. 2025;10(2):119-127. [Трусов Ю.А., Щукин Ю.В., Лимарева Л.В. Прогнозирование неблагоприятных исходов в отдаленном периоде наблюдения у пациентов с хронической

сердечной недостаточностью, перенесших инфаркт миокарда. *Наука и инновации в медицине*. 2025;10(2):119-127]. DOI: 10.35693/SIM655825

21. Galyavich AS, Tereshchenko SN, Uskach TM, et al. 2024 Clinical practice guidelines for Chronic heart failure. *Russian Journal of Cardiology*. 2024;29(11):6162. [Галявич А.С., Терещенко С.Н., Ускач Т.М., и др. Хроническая сердечная недостаточность. Клинические рекомендации 2024. Российский кардиологический журнал. 2024;29(11):6162]. DOI: 10.15829/1560-4071-2024-6162

22. Thavendiranathan P, Poulin F, Lim KD, et al. Use of Myocardial Strain Imaging by Echocardiography for the Early Detection of Cardiotoxicity in Patients During and After Cancer Chemotherapy: A Systematic Review. *J Am Coll Cardiol*. 2014; 63:2751-68. DOI: 10.1016/j.jacc.2014.01.073

23. Pieske P, Tschöpe C, De Boer RA, et al. How to diagnose heart failure with preserved ejection fraction: The HFA-PEFF diagnostic algorithm: A consensus recommendation from the Heart Failure Association (HFA) of the European Society of Cardiology (ESC). *Eur J Heart Fail*. 2019;40:3297-3317. DOI: 10.1093/eurheartj/ehz641

24. Robinson S, Ring L, Oxborough D, et al. The assessment of left ventricular diastolic function: guidance and recommendations from the British Society of Echocardiography. *Echo Res Pract*. 2024;11(1):16. DOI: 10.1186/s44156-024-00051-2

25. Germanova OA, Reshetnikova YuB, Efimova EP. *Modern methods of assessment of diastolic function of the left ventricle*. Samara, 2024. (In Russ.). [Германова О.А., Решетникова Ю.Б., Ефимова Е.П. *Современные методы оценки диастолической функции левого желудочка*. Самара, 2024].

26. Stepanova AI, Radova NF, Alekhin MN. Speckle tracking stress echocardiography on treadmill in assessment of the functional significance of the degree of coronary artery disease. *Kardiologiia*. 2021;61(3):4-11. [Степанова А.И., Радова Н.Ф., Алехин М.Н. Спекл-трекинг стресс-эхокардиография с использованием тредмил-теста в оценке функциональной значимости степени стеноза коронарных артерий. *Кардиология*. 2021;61(3):4-11]. DOI: 10.18087/cardio.2021.3.n1462

27. Qin S, Cao X, Zhang R, Liu H. Predictive value of speckle tracking technique for coronary artery stenosis in patients with coronary heart disease. *Am J Transl Res*. 2023;15(9):5873-5881. PMID: 37854206; PMCID: PMC10579018

28. Rumbinaitė E, Žaliaduonytė-Pekšienė D, Vieželis M, et al. Dobutamine-stress echocardiography speckle-tracking imaging in the assessment of hemodynamic significance of coronary artery stenosis in patients with moderate and high probability of coronary artery disease. *Medicina*. 2016;52(6):331-339. DOI: 10.1016/j.medici.2016.11.005

29. Nishi T, Funabashi N, Ozawa K, et al. Regional layer-specific longitudinal peak systolic strain using exercise stress two-dimensional speckle-tracking echocardiography for the detection of functionally significant coronary artery disease. *Heart and Vessels*. 2019;34(8):1394-403. DOI: 10.1007/s00380-019-01361-w

30. Park JH, Woo JS, Ju S, et al. Layer-specific analysis of dobutamine stress echocardiography for the evaluation of coronary artery disease. *Medicine*. 2016;95(32):e4549-4557. DOI: 10.1097/MD.0000000000004549

31. Mansour MJ, Al-Jaroudi W, Hamoui O, et al. Multimodality imaging for evaluation of chest pain using strain analysis at rest and peak exercise. *Echocardiography*. 2018;35(8):1157-63. DOI: 10.1111/echo.13885

32. Ejlersen JA, Poulsen SH, Mortensen J, May O. Diagnostic value of layerspecific global longitudinal strain during adenosine stress in patients suspected of coronary artery disease. *The International Journal of Cardiovascular Imaging*. 2017;33(4):473-80. DOI: 10.1007/s10554-016-1022-x

33. Liu JH, Chen Y, Yuen M, et al. Incremental prognostic value of global longitudinal strain in patients with type 2 diabetes mellitus. *Cardiovasc Diabetol*. 2016;15:22-27. DOI: 10.1186/s12933-016-0333-5

34. Wierzbowska-Drabik K, Trzos E, Kurpesa M, et al. Diabetes as an independent predictor of left ventricular longitudinal strain reduction at rest and during dobutamine stress test in patients with significant coronary artery disease. *Eur Heart J Cardiovasc Imaging*. 2018;19(11):1276-1286. DOI: 10.1093/ehjci/jex315

35. Philouze C, Obert P, Nottin S, et al. Dobutamine stress echocardiography unmasks early left ventricular dysfunction in asymptomatic patients with uncomplicated type 2 diabetes: a comprehensive two-dimensional speckle-tracking imaging study. *J Am Soc Echocardiogr*. 2018;31(5):587-597. DOI: 10.1016/j.echo.2017.12.006

36. Serrano-Ferrer J, Crendal E, Walther G, et al. Effects of lifestyle intervention on left ventricular regional myocardial function in metabolic syndrome patients from the RESOLVE randomized trial. *Metabolism*. 2016;65:1350-1360. DOI: 10.1016/j.metabol.2016.05.006

37. Brainin P, Biering-Sørensen SR, Møgelvang R, et al. Post-systolic shortening: normal values and association with validated echocardiographic and invasive measures of cardiac function. *The International Journal of Cardiovascular Imaging*. 2019;35(2):327-37. DOI: 10.1007/s10554-018-1474-2

38. Brainin P, Hoffmann S, Fritz-Hansen T, et al. Usefulness of Postsystolic Shortening to Diagnose Coronary Artery Disease and Predict Future Cardiovascular Events in Stable Angina Pectoris. *Journal of the American Society of Echocardiography*. 2018;31(8):870-879.e3. DOI: 10.1016/j.echo.2018.05.007

39. Stepanova AI, Radova NF, Alekhin MN. Diagnostic value of postsystolic shortening of the left ventricular myocardium assessed during speckle tracking stress echocardiography on the treadmill in patients with coronary artery disease. *Kardiologiia*. 2022;62(1):57-64. [Степанова А.И., Радова Н.Ф., Алехин М.Н. Диагностическое значение постсистолического укорочения миокарда левого желудочка у пациентов с ишемической болезнью сердца при speckle-tracking стресс-эхокардиографии с использованием тредмил-теста. *Кардиология*. 2022;62(1):57-64]. DOI: 10.18087/cardio.2022.1.n1724

40. Rumbinaite E, Karuzas A, Verikas D, et al. Detection of Functionally Significant Coronary Artery Disease: Role of Regional Post Systolic Shortening. *J Cardiovasc Echogr*. 2020;30(3):131-139. DOI: 10.4103/jcecho.jcecho_55_19

41. Brainin P. Myocardial Postsystolic Shortening and Early Systolic Lengthening: Current Status and Future Directions. *Diagnostics*. 2021;11:1428-36. DOI: 10.3390/diagnostics11081428

42. Eek C, Grenne B, Brunvand H, et al. Postsystolic shortening is a strong predictor of recovery of systolic function in patients with non-ST-elevation myocardial infarction. *European Journal of Echocardiography*. 2011;12(7):483-9. DOI: 10.1093/ejechocard/jer055

43. Terkelsen C, Hvitfeldt Poulsen S, Nørgaard BL, et al. Does Postsystolic Motion or Shortening Predict Recovery of Myocardial Function After Primary Percutanous Coronary Intervention? *Journal of the American Society of Echocardiography*. 2007;20(5):505-511. DOI: 10.1016/j.echo.2006.10.004

44. Brainin P, Haahr-Pedersen S, Sengeløv M, et al. Presence of post-systolic shortening is an independent predictor of heart failure in patients following ST-segment elevation myocardial infarction. *The International Journal of Cardiovascular Imaging*. 2018;34(5):751-60. DOI: 10.1007/s10554-017-1288-7

Technical report | Технический отчет
DOI: https://doi.org/10.35693/SIM643149

Remote assessment of treatment adherence based on the KP-25 questionnaire: a new telemedicine tool for remote compliance analysis

Andrei A. Garanin, Yurii A. Trusov

Samara State Medical University (Samara, Russian Federation)

Abstract

Aim – creation of a computer program using a modern programming language that allows remote assessment of patient treatment adherence based on the national KP-25 scale.

Material and methods. The program we developed was implemented using the modern programming language Python 3.8. This electronic assistant allows the user to automatically collect and systematize compliance data, conduct statistical analysis and store patient survey data. All these processes, depending on the operator's goals, can be carried out using local and cloud servers. If it is necessary to transfer data remotely, the program has the functionality to 'depersonalize' data about the respondent, which ensures safe and correct accumulation and storage of data.

Results. The program allows the user to evaluate 6 technical indicators calculated using formulas: importance of drug therapy, importance of medical support, importance of lifestyle modification, readiness for drug therapy, readiness for medical support, readiness for lifestyle modification. Calculation using integrated formulas also allows the user to display the result of the commitment calculation on the user's screen in four aspects: 1) commitment to lifestyle modification, 2) commitment to drug therapy, 3) commitment to medical support, 4) integral commitment to treatment. After the end of testing, the program saves the patient's answers to an Excel file located in the root folder of the program in the form of percentages, which are generated depending on the patient's response in accordance with the classical algorithm for interpreting the results of the questionnaire using integrated formulas.

Conclusion. This software product can potentially be used in the scientific process in conducting cohort and population-based studies aimed at assessing compliance in routine medical practice, as well as integrated into existing and promising medical information systems.

Keywords: treatment commitment, electronic assistant, COP-25 questionnaire, telemedicine, telemonitoring.

Conflict of interest: nothing to disclose.

Citation
Garanin AA, Trusov YuA. **Remote assessment of treatment adherence based on the KP-25 questionnaire: a new telemedicine tool for remote compliance analysis**. *Science and Innovations in Medicine*. 2025;10(3):211-217.
DOI: https://doi.org/10.35693/SIM643149

Information about authors
Andrei A. Garanin – MD, Cand. Sci. (Medicine), Director of the Research and Practice Center for Telemedicine.
ORCID: 0000-0001-6665-1533
E-mail: a.a.garanin@samsmu.ru

***Yurii A. Trusov** – MD, cardiologist at the SamSMU Clinics, assistant at the Department of Propaedeutic Therapy with a course in cardiology.
ORCID: 0000-0001-6407-3880
E-mail: yu.a.trusov@samsmu.ru
Corresponding Author

Received: 17.12.2024
Accepted: 04.02.2025
Published: 25.04.2025

Программа удаленной оценки приверженности лечению на основе опросника КОП-25: новый инструмент телемедицины для дистанционного анализа комплаентности

А.А. Гаранин, Ю.А. Трусов

ФГБОУ ВО «Самарский государственный медицинский университет» Минздрава России (Самара, Российская Федерация)

Аннотация

Цель – создание компьютерной программы с использованием современного языка программирования, позволяющей дистанционно оценивать приверженность лечению пациентов на основе отечественной шкалы КОП-25.

Материал и методы. Разработанная нами программа выполнена с использованием современного языка программирования Python 3.8. Данный электронный помощник позволяет в автоматическом режиме осуществлять сбор и систематизацию данных о комплаентности, проводить статистический анализ и хранить данные об анкетировании пациентов. Все эти процессы в зависимости от целей оператора могут осуществляться с использовнием локальных и облачных серверов. При необходимости передачи данных на расстоянии программа имеет функционал по «обезличиванию» данных о респонденте, что обеспечивает безопасное и корректное накопление и хранение данных.

Результаты. Программа позволяет оценивать шесть технических показателей, рассчитываемых по формулам: важность лекарственной терапии, важность медицинского сопровождения, важность модификации образа жизни, готовность к лекарственной терапии, готовность

к медицинскому сопровождению, готовность к модификации образа жизни. Расчет по интегрированным формулам также позволяет вывести на экран пользователя результат расчета приверженности по четырем аспектам: приверженность модификации образа жизни; приверженность лекарственной терапии; приверженность медицинскому сопровождению; интегральная приверженность лечению. После окончания тестирования программа сохраняет ответы пациента в файл Excel, расположенный в корневой папке программы, в виде процентов, которые порождаются в зависимости от ответа пациентов в соответствии с классическим алгоритмом интерпретации результатов вопросника по интегрированным формулам.

Заключение. Разработанный программный продукт потенциально может быть применен в научном процессе при проведении когортных и популяционных исследований, которые направлены на оценку комплаентности и в рутинной медицинской практике, а также интегрирован в существующие и перспективные медицинские информационные системы.

Ключевые слова: приверженность лечению, электронный помощник, опросник КОП-25, телемедицина, телемониторинг.

Конфликт интересов: не заявлен.

Для цитирования:
Гаранин А.А., Трусов Ю.А. **Программа удаленной оценки приверженности лечению на основе опросника КОП-25: новый инструмент телемедицины для дистанционного анализа комплаентности.** *Наука и инновации в медицине.* 2025;10(3):211-217. DOI: https://doi.org/10.35693/SIM643149

Сведения об авторах
Гаранин А.А. – канд. мед. наук, директор научно-практического центра дистанционной медицины.
ORCID: 0000-0001-6665-1533
E-mail: a.a.garanin@samsmu.ru
***Трусов Юрий Александрович** – врач-кардиолог Клиник СамГМУ, ассистент кафедры пропедевтической терапии с курсом кардиологии.
ORCID: 0000-0001-6407-3880
E-mail: yu.a.trusov@samsmu.ru
Автор для переписки

Список сокращений
ХНИЗ – хроническое неинфекционное заболевание; АГ – артериальная гипертензия; КОП – клиническая оценка приверженности; ССЗ – сердечно-сосудистое заболевание; ИМ – инфаркт миокарда; ИБС – ишемическая болезнь сердца; СД – сахарный диабет; ФП – фибрилляция предсердия; ХСН – хроническая сердечная недостаточность.

Получено: 17.12.2024
Одобрено: 04.02.2025
Опубликовано: 25.04.2025

INTRODUCTION

Adherence to treatment (compliance) can be characterized as a patient's measurable ability to follow medical prescriptions. It includes regular medication intake, lifestyle modifications, and observance of medical recommendations.

Comliance is critically important in achieving positive therapeutic results and, in many aspects, shapes the patient's health prognosis. According to World Health Organization experts, compliance with medical prescriptions is considered one of the most significant factors influencing public health [1, 2]. Focusing on treatment adherence can substantially enhance the effectiveness of healthcare initiatives and programs.

At the moment, the methods of therapeutic compliance evaluation may be divided into two main groups [3]: direct (analyses and direct supervision of medication intake) and indirect (use of various questionnaires and scales).

Although direct methods of evaluation of compliance with recommended treatment are very accurate, they are seldom used in routine clinical practices and are usually resorted to in clinical trials. Among alternate approaches, such as interviews, analysis of admissions, questionnaires the latter are considered the most economically viable to evaluate the patients' compliance with prescriptions [4].

In modern clinical practice, the emphasis is placed on questionnaires that enable quantitative assessment of treatment compliance levels. These tools are universal and applicable to patients with various diseases; they facilitate automated data collection and analysis, which makes them particularly convenient.

Among the well-known questionnaires use to evaluate compliance, MMAS-4 and MMAS-8 are worth a special mention. While MMAS-4 has limited sensitivitiy, specificity and reliability [5], its successor, the MMAS-8, shows significantly higher sensitivity values with a comparable level of specificity [6]. It is to be noted, however, that complete reliance on this new tool requires additional research. Despite such advantages as brevity and ease of use, the two questionnaires have several disadvantages: the evauation scale is qualitative, not quantitative; lack of possibilities to evaluate other aspects of compliance than medication intake.

In order to overcome the said restrictions, the Russian questionnaire for quantitative evaluation of treatment compliance was developed, the COP-25. Created in 2009, this tool was designed to evaluate compliance with instructions of patients with arterial hypertension, but found use in other fields of medicine [7]. Treatment compliance assessment is of particular importance in patients with chronic non-communicable diseases (CNCDs) within the framework of outpatient follow-up. The protocol published in 2015 provides a detailed description of treatment compliance analysis methods. Studies have demonstrated the high sensitivity, specificity, and reliability of the COP-25 questionnaire, making it a valuable tool in clinical practice.

Recent studies demonstrate that effective long-term monitoring can be achieved using telemedicine technologies [8–10]. However, the integration of information and communication technologies and telemedicine tools into routine clinical practice raises a number of challenges that require in-depth analysis and optimization to enhance healthcare quality and improve collaboration among all stakeholders.

AIM

Creation of a computer program using a modern programming language that allows remote assessment of patient treatment adherence based on the national COP-25 scale.

MATERIAL AND METHODS

The Scientific and Practical Center for Telemedicine at Samara State Medical University has developed software tools to assess treatment compliance using the Russian COP-25 scale. These tools comprise a software suite with three web applications. This solution enables healthcare providers

to efficiently and accurately collect patient adherence data during both in-person outpatient visits and telemedicine consultations.

Our program is written in the modern programming language, Python 3.8. The electronic assistant enables automated collection and systematization of data on patient compliance, perform statistical analysis and store data from patient questionnaires. These processes, depending on the operator's goals and objectives, may be performed on local and cloud-based servers. In case of necessity of long-distance data transfer, the program, has an option of depersonalization of the interviewee's data ensuring secure proper collection and storage of information.

Following the results of work on the electronic assistant, certificates of state registration of computer programs were obtained: "Program of remote quantitative evaluation of therapeutic compliance based on the COP-25 questionnaire" (registration No. 2024619892, registration date: 27.04.2024); "Program of remote quantitative evaluation of therapeutic compliance based on the COP-25 questionnaire" (registration No. 2024660040, registration date: 02.05.2024); "Questionnaire for the quantitative evaluation of therapeutic compliance: the COP-25 calculator" (registration No. 2024660243, registration date: 03.05.2024).

RESULTS AND DISCUSSION

Our program is designed for the remote quantitative evaluation of patients' compliance with therapy in the process of dynamic follow-up to perform scientific research, therapy or prevention; it is implemented based on the COP-25 questionnaire. To that end, the software package is installed to the disk specified by the user in the doctor's workstation. Once installed, the electronic assistant is launched by running the executable file (.exe). After launching, the program generates a window in the user's desktop with 25 questions from the classic variant of the COP-25 scale. Once all questions are answered, the program uses integrated formulas to automatically calculate the indicators of therapeutic compliance, shows the user the result of the interview with the score and their interpretation describing the patient's level of compliance with treatment (**Fig. 1**).

The program evaluates six technical indicators calculated using formulas: significance of drug therapy, significance of medical follow-up, significance of lifestyle modification, readiness to drug therapy, readiness to medical follow-up, readiness to lifestyle modification (**Table 1**).

The calculation using integrated formulas also enables output of the compliance calculation in four aspects: 1) compliance with lifestyle modification; 2) compliance with

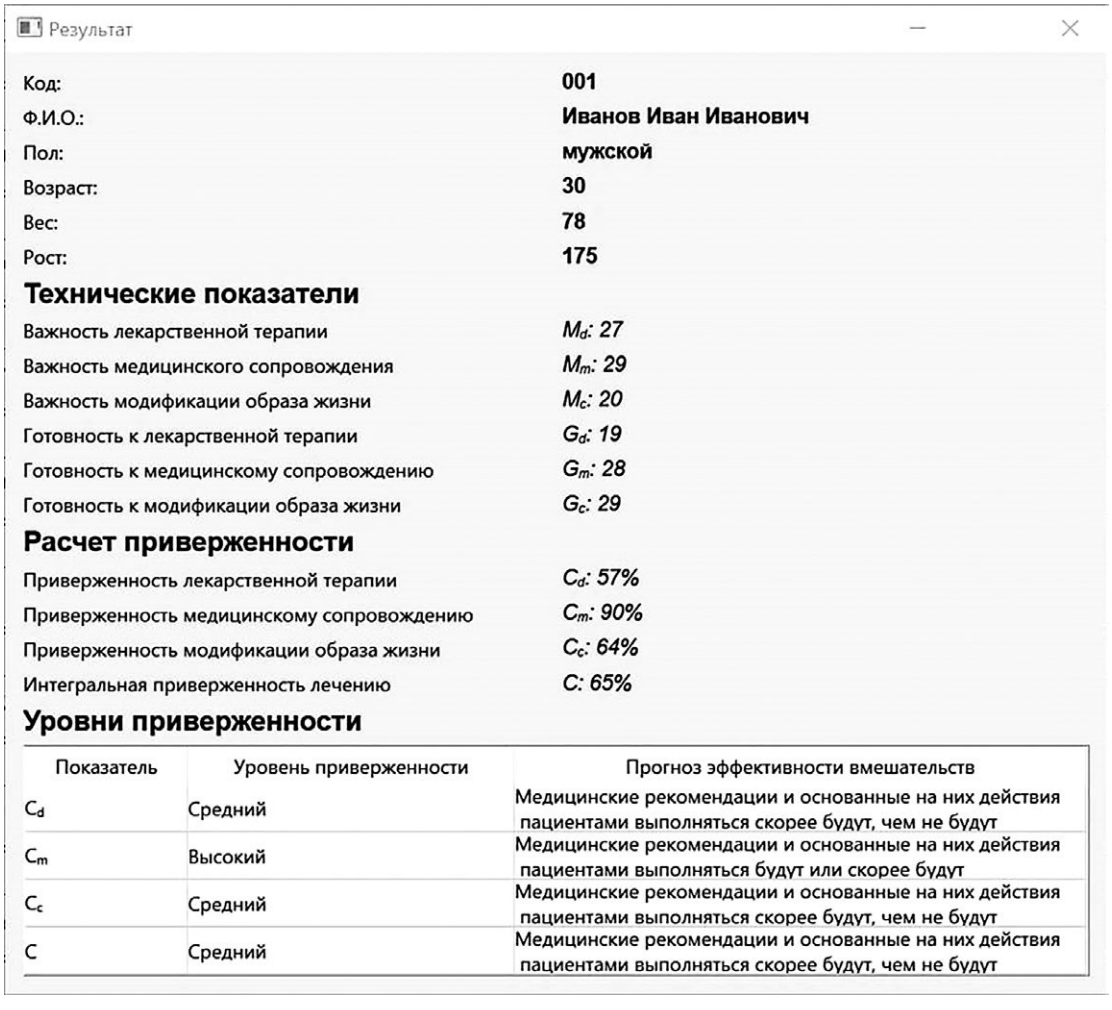

Figure 1. *Appearance of the doctor's electronic assistant based on the domestic scale KOP-25, generated by the core of the program when launched from the browser.*

Рисунок 1. *Внешний вид электронного помощника врача на основе отечественной шкалы КОП-25, порождаемого ядром программы при запуске из браузера.*

Indicator	Name	Question No. (sum of scores)
Significance of drug therapy	Md	2, 3, 4, 6, 14
Signigicance of medical follow-up	Mm	1, 5, 10, 11, 13
Significance of lifestyle modification	Mc	7, 8, 9, 12, 15
Readiness to drug therapy	Gd	16, 17, 18, 20, 21
Readiness to medical follow-up	Gm	16, 19, 20, 24, 25
Readiness to lifestyle modification	Gc	19, 22, 23, 24, 25

Table 1. *List of 6 technical indicators for the results of patient interviews using the electronic version of the KOP-25 questionnaire*

Таблица 1. *Оценка 6 технических показателей по результатам интервьюирования пациента с помощью электронного варианта опросника КОП-25*

drug therapy; 3) compliance with medical follow-up; 4) integral compliance with treatment.

The calculation of these values is performed using the following formulas.

Compliance with lifestyle modification:

$$Cc=1 \div \frac{((30 \div Mc) \times (60 \div Gc))}{2} \times 100 \quad (1),$$

where:
Cc – compliance with lifestyle modification, %
Mc – significance of lifestyle modification, points
Gc – readiness to lifestyle modification, points
Compliance with drug therapy:

$$Cd=1 \div \frac{((30 \div Md) \times (60 \div Gd))}{2} \times 100 \quad (2),$$

where:
Cd – compliance with drug therapy, %
Md – significance of drug therapy, points
Gd – readiness to drug therapy, points

Compliance with medical follow-up::

$$Cm=1 \div \frac{((30 \div Mm) \times (60 \div Gm))}{2} \times 100 \quad (3),$$

where:
Cm – compliance with medical follow-up, %
Mm – significance of medical follow-up, points
Gm – readiness to medical follow-up, points

Integral compliance with treatment:

$$C= \frac{(Cm+2Cc+3Cd)}{6} \quad (4),$$

where:
C – integral compliance with treatment
Cm – compliance with medical follow-up, %
Cc – compliance with lifestyle modification, %
Cd – compliance with drug therapy, %.

Upon completion of testing, the program saves the patient's answers in an Excel file in the root folder of the program as percentage values calculated depending on the answers of patients in accordance with the conventional algorithm of interpretation of questionnaire answers using integrated formulas. At the same time the doctor may perform a number of studies on a group of patients forming a database on their computer, and then perform a population analysis of therapeutic compliance, or compliance in a specific cohort or a specific patient. Moreover, the program enables any entitled observer to remotely evaluate compliance with therapy from any location and any computer connected to the Internet, thus providing the opportunity of mass remote evaluation of therapeutic compliance.

Following the interview with the patient using the COP-25 scale, the electronic assistant gives the doctor the possibility of recording and transferring the data as well as form a database. This assists in the making of a substantiated decision on prescription of drugs with consideration of evaluated compliance. Below are several options of use of our electronic assistant.

1. Deployment at a paramedic's workstation in rural health posts (RHPs) enables remote assessment of treatment compliance for RHP-visiting patients by physicians from central district hospitals or regional telemedicine centers during remote follow-up monitoring. This software solution also allows integration with regional medical information systems.

2. Development of a mobile application for patients under follow-up care, enabling self-assessment via the COP-25 questionnaire with subsequent automated treatment compliance evaluation, data transmission to the medical information system, and results analysis by the attending physician.

3. Development of a mobile application for industrial workers as part of occupational health initiatives, enabling periodic workplace assessment of treatment adherence using this digital tool among employees with chronic non-communicable diseases.

The important feature of this electronic assistant is the functionality of dynamic evaluation of compliance with the prescribed therapy, viz. analysis of efficacy of the treatment and adjustment of therapeutic plan over a long period of time. Not only does it register data on compliance but also compares results on different stages of treatment, which allows determining the trends and suggest more personalized treatment considering individual needs and behavior of the patient. This approach assists better outcomes of the therapy and improves overall patient satisfaction with treatment results. In outpatient and telemedicine practice, time constraints often limit thorough medical documentation. Digital assistants that streamline data entry and storage serve as valuable tools for optimizing clinician workflow.

The Scientific and Practical Center for Telemedicine at Samara State Medical University is conducting pilot studies to evaluate the efficacy of a digital assistant, particularly in remote follow-up monitoring. The research focuses on treatment adherence in patients with various chronic non-communicable diseases (CNCDs). This issue is of critical importance as many of these conditions require long-term therapy.

As per existing data, the level of non-complianc with treatment varies from 4 to 88%, and only about 50% of patients with CNCDs demonstrate long-term compliance. This emphasizes the need for development of efficient solutions to improve treatment compliance [11–14]. The electronic assistant may significantly influence the treatment outcomes not only from the new data, but also from evaluating the compliance dynamics in the long run. This enables the doctor respond to changes in the patients' behavior in a prompt way.

Modern technologies can significantly improve healthcare quality and physician-patient interaction, thereby enhancing treatment effectiveness. Treatment adherence assessment is particularly crucial for patients with cardiovascular diseases (CVDs), as these conditions represent the leading cause of disability and mortality. Circulatory system disorders frequently lead to severe complications, underscoring the need for adequate and consistent therapy. However, the national register REKVAZA, initiated in the Ryazan Region, identified a significant discrepancy between the medical prescriptions and modern clinical recommendations. This discrepancy emphasizes the importance of implementation of systems enabling doctors to supervise in a more closer manner the patients' compliance with treatment and meet the current clinical standards. It follows from the data that among 2548 outpatients with coronary heart disease (CHD) the statins, crucial for reducing the risk of cardiovascular accidents, were prescribed only in 28.7% cases. In the patients after a myocardial infarction (MI), this indicator was 42.3%, and in the patients after the second MI, 50%. In the patients with a cerebral stroke, this indicator was only 9.8%, and in patients with diabetes mellitus (DM), 18.9% [15]. These quantitative data emphasize the vital importance of a stricter adherence to recommendations once the therapy is prescribed, which would minimize the risk of potential complications and improve the quality of medical services. The EFFORT study addressed elderly patients aged over 65, of which 81.1% were in the age group of 65–74 years. These individuals suffered from arterial hypertension and had confirmed CHD, for which statin therapy is indicated. However, every third of them had MI, and 93% were diagnosed with arterial hypertension, which indicates the vulnerability of this age group and its need for special attention during treatment. Despite that, compliance with therapy is only significant in the initial stages of it. Active use of statins is typically observed during the first three months of treatment. With prolonged follow-up, compliance levels decline sharply. At three months, 34.2% of patients discontinue prescribed medications. Between four months and one year, this proportion increases to 69.9%, while compliance drops to 72.7% in the 1-5 year period. Regretfully, nearly 93.1% of patients discontinue therapy after five years, which represents a critical concern [16].

Multiple studies show that lack of compliance with intake of oral anticoagulants by patients with atrial fibrillation (AF) may decrease their efficiency in actual clinical practice. The systematic review and the metaanalysis by S. Salmasi et al. (2020) included 30 different studies and determined hat up to 30% patients with AF do not comply with the prescribed anticoagulant therapy [17]. This emphasizes the need to focus on compliance, for the lack of compliance with treatment may have an adverse effect on the health of patients increasing the risk of clot formation and strokes. Another group is patients with arterial hypertension who also demonstrate lack of compliance. According to some studies, 43 to 66% of patients do not follow the doctors' advise on the intake of antihypertensive drugs; moreover, one year after the start of therapy, 40 to 65% of patients stop taking the prescribed drugs [18–20].

Studies demonstrate that patients with poor compliance with intake of essential cardiac medications face a 10-40% increased hospitalization risk [21, 22]. R. Mathews et al. (2015) found that only 71% of 7,425 patients after percutaneous coronary intervention maintained prescribed treatment at 6-week follow-up, while 25% showed suboptimal compliance and 4% exhibited poor compliance [23]. Most alarmingly, over one-third of patients miss antiplatelet therapy twice weekly or more frequently, significantly elevating the risk of stent thrombosis and recurrent myocardial infarction..

The study of ST de Vries et al. Found that the experience of patients with Type 2 diabetes mellitus shows various levels of compliance with therapy. The most manifested problems were found in patients taking glucose-lowering medications: 37.6% of patients did not comply with the proper treatment regime. Every fifth patient demonstrated low compliance with antihypertensive and lipid-lowering drugs [24]. A similar study performed by M. Viana found that among patients with chronic heart failure (CHF) compliance with angiotensin-converting enzyme inhibitors (ACEIs) was high, while significantly lower compliance rates were observed for beta-blockers and diuretics.

On a side note, if information about only one type of drug were used to evaluate compliance with treatment, such classification would have been inaccurate in over 20% cases [25]. This emphasized the importance of an individual approach, in which it is important to evaluate compliance with each type of drug seperately.

CONCLUSION

Treatment adherence assessment in patients with chronic non-communicable diseases has become a critical aspect of clinical practice. This is particularly relevant in telemedicine consultations and remote health monitoring. Integrating digital tools for dynamic adherence evaluation into modern medical information systems may optimize diagnostic and therapeutic processes while improving patient compliance with prescribed therapy. The use of modern digital solutions plays a pivotal role in scientific research aiming at development and implementation of primary and secondary prevention of chronic non-communicable diseases. The accumulated data may be used in the future as the basis for datasets to be utilized in machine learning which, in its turn, may facilitate development of medical decision-making support systems. In this way, development of technologies aimed at enhancing evaluation of compliance opens new horizons not only for improving healthcare quality, but also for creating novel opportunities in scientific progress and clinical practice. This advancement may lead to more effective and personalized treatment approaches, including for patients with comorbidities.

ADDITIONAL INFORMATION	ДОПОЛНИТЕЛЬНАЯ ИНФОРМАЦИЯ
Study funding. The study was the authors' initiative without external funding.	***Источник финансирования.*** Работа выполнена по инициативе авторов без привлечения финансирования.
Conflict of Interest. The authors declare that there are no obvious or potential conflicts of interest associated with the content of this article.	***Конфликт интересов.*** Авторы декларируют отсутствие явных и потенциальных конфликтов интересов, связанных с содержанием настоящей статьи.
Contribution of individual authors. Garanin A.A.: setting of tasks, writing and editing of the article, testing of computer software. Trusov Yu.A.: writing of the computer program, writing of the article. All authors gave their final approval of the manuscript for submission, and agreed to be accountable for all aspects of the work, implying proper study and resolution of issues related to the accuracy or integrity of any part of the work.	***Участие авторов.*** Гаранин А.А. – постановка задач, написание и редактирование статьи, тестирование программы для ЭВМ. Трусов Ю.А. – написание программы для ЭВМ, написание статьи. Все авторы одобрили финальную версию статьи перед публикацией, выразили согласие нести ответственность за все аспекты работы, подразумевающую надлежащее изучение и решение вопросов, связанных с точностью или добросовестностью любой части работы.

REFERENCES / ЛИТЕРАТУРА

1. Nikolaev NA, Martynov AI, Skirdenko YuP, et al. Treatment management based on adherence: patient recommendation algorithms. Cross-disciplinary guidelines. *Medical news of North Caucasus*. 2020;15(4):461-468. [Николаев Н.А., Мартынов А.И., Скирденко Ю.П., и др. Управление лечением на основе приверженности: алгоритмы рекомендаций для пациентов. Междисциплинарные рекомендации. *Медицинский вестник Северного Кавказа*. 2020;15(4):461-468]. DOI: 10.14300/mnnc.2020.15109

2. World Health Organization. Adherence to long-term therapies: evidence for action. Available at: https: www.who.int/chp/knowledge/publications/adherence_report/en/

3. Lukina YuV, Kutishenko NP, Martsevich SYu, Drapkina OM. Questionnaires and scores for assessing medication adherence – advantages and disadvantages of the diagnostic method in research and actual clinical practice. *Cardiovascular therapy and prevention*. 2020;19(3):2562. [Лукина Ю.В., Кутишенко Н.П., Марцевич С.Ю. Опросники и шкалы для оценки приверженности к лечению – преимущества и недостатки диагностического метода в научных исследованиях и реальной клинической практике. *Кардиоваскулярная терапия и профилактика*. 2020;19(3):2562]. DOI: 10.15829/1728-8800-2020-2562

4. Drapkina OM, Livzan MA, Martynov AI, et al. First Russian consensus on quantitative assessment of adherence to treatment: main provisions, algorithms and recommendations. *Medical news of North Caucasus*. 2018;1(12):259. [Драпкина О.М., Ливзан М.А., Мартынов А.И., и др. Первый Российский консенсус по количественной оценке приверженности к лечению: основные положения, алгоритмы и рекомендации . *Медицинский вестник Северного Кавказа*. 2018;1(12):259]. DOI: 10.14300/mnnc.2018.13039

5. Morisky DE, Green LW, Levine DM. Concurrent and predictive validity of self-reported measure of medical adherence. *Med Care*. 1986;24:67-73. DOI: 10.1097/00005650-198601000-00007

6. Morisky DE, Ang A, Krousel-Wood M. Predictive validity of a medication adherence measure in an outpatient setting. *J Clin Hypertens (Greenwich)*. 2008;10(5):348-54. DOI: 10.1111/j.1751-7176.2008.07572.x

7. Nikolaev NA. Russian universal questionnaire of quantitative assessment of adherence to treatment (KOP-25). *Clinical Pharmacology and Therapy*. 2018;1(27):74. (In Russ.). [Николаев Н.А. Российский универсальный опросник количественной оценки приверженности к лечению (КОП-25). *Клиническая фармакология и терапия*. 2018;1(27):74]. URL: https://clinpharm-journal.ru/articles/2018-1/rossijskij-universalnyj-oprosnik-kolichestvennoj-otsenki-priverzhennosti-k-lecheniyu-kop-25/

8. Garanin AA, Mullova IS, Shkaeva OV, et al. Remote monitoring of outpatients discharged from the emergency cardiac care department. *Russian Journal of Cardiology*. 2022;27(3S):5072. [Гаранин А.А., Муллова И.С., Шкаева О.В., и др. Амбулаторный дистанционный мониторинг пациентов, выписанных из отделения неотложной кардиологии. *Российский кардиологический журнал*. 2022;27(3S):5072]. DOI: 10.15829/1560-4071-2022-5072

9. Drapkina OM, Korsunsky DV, Komkov DS, Kalinina AM. Prospects for developing and implementing remote blood pressure monitoring in patients under dispensary follow-up. *Cardiovascular Therapy and Prevention*. 2022;21(3):3212. [Драпкина О.М., Корсунский Д.В., Комков Д.С., и др. Перспективы разработки и внедрения дистанционного контроля уровня артериального давления пациентов, находящихся на диспансерном наблюдении. *Кардиоваскулярная терапия и профилактика*. 2022;21(3):3212]. DOI: 10.15829/1728-8800-2022-3212

10. Sirotina AS, Kobyakova OS, Deev IA, et al. Remote monitoring of health status. Analytical review. *Social aspects of population health*. 2022;68(2):1. [Сиротина А.С., Кобякова О.С., Деев И.А., и др. Удаленный мониторинг состояния здоровья. Аналитический обзор. *Социальные аспекты здоровья населения*. 2022;68(2):1]. DOI: 10.21045/2071-5021-2022-68-2-1

11. Sabaté E. Adherence to long-term therapies: evidence for action. Geneva (Switzerland): World Health Organization (WHO), 2003.

12. Chowdhury R, Khan H, Heydon E, et al. Adherence to cardiovascular therapy: a meta-analysis of prevalence and clinical consequences. *Eur Heart J*. 2013;34(38):2940. DOI: 10.1093/eurheartj/eht295

13. De Bacquer D, Astin F, Kotseva K, et al. Poor adherence to lifestyle recommendations in patients with coronary heart disease: results from the EUROASPIRE surveys. *Eur J Prev Cardiol*. 2022;29(2):383. DOI: 10.1093/eurjpc/zwab115

14. Pedretti RFE, Hansen D, Ambrosetti M, et al. How to optimize the adherence to a guideline-directed medical therapy in the secondary prevention of cardiovascular diseases: a clinical consensus statement from the European Association of Preventive Cardiology. *Eur J Prev Cardiol*. 2023;30(2):149. DOI: 10.1093/eurjpc/zwac204

15. Zagrebalny AV, Martsevich SYu, Lukyanov MM, et al. Quality of lipid-lowering therapy in outpatient practice: RECVAS Register data. *Russian Journal of Preventive Medicine*. 2016;19(1):9-14. [Загребальный А.В., Марцевич С.Ю., Лукьянов М.М., и др. Качество гиполипидемической терапии в амбулаторно-поликлинической практике: данные регистра РЕКВАЗА. *Профилактическая медицина*. 2016;19(1):9-14]. DOI: 10.17116/profmed20161919-14

16. Bubnova MG, Aronov DM, Deev AD. Statins in routine clinical care in elderly with hyperlipidemia and coronary heart disease. Russian program EFFORT. *Atherosclerosis and Dyslipidemia*. 2018;1(30):5-16. [Бубнова М.Г., Аронов Д.М., Деев А.Д. Терапия статинами в реальной клинической практике у пожилых пациентов с гиперлипидемией и коронарной болезнью сердца. Российская программа ЭФФОРТ. *Атеросклероз и дислипидемии*. 2018;1(30):5-16].

17. Salmasi S, Loewen PS, Tandun R. et al. Adherence to oral anticoagulants among patients with atrial fibrillation: a systematic review and meta-analysis of observational studies. *BMJ Open*. 2020;10(4):e034778. DOI: 10.1136/bmjopen-2019-034778

18. Corrao G, Zambon A, Parodi A, et al. Discontinuation of and changes in drug therapy for hypertension among newly-treated patients: a population-based study in Italy. *J Hypertens*. 2008;26:819-24. DOI: 10.1097/HJH.0b013e3282f4edd7

19. Degli Esposti E, Sturani A, Di Martino M. Long term persistence with antihypertensive drugs in new patients. *J Hum Hypertens*. 2002;16:439. DOI: 10.1038/sj.jhh.1001418

20. Fofanova TV, Ageev FT, Smirnova MD. Adherence to therapy in the outpatient setting: the ability to identify and assess the effectiveness of therapy. *Kardiologiia*. 2017;57(7):35-42. [Фофанова Т.В., Агеев Ф.Т., Смирнова М.Д. Приверженность к терапии в амбулаторных условиях: возможность выявления и оценка эффективности терапии. *Кардиология*. 2017;57(7):35-42]. DOI: 10.18087/cardio.2017.7.10004

21. Ho PM, Bryson CL, Rumsfeld JS. Medication adherence: its importance in cardiovascular outcomes. *Circulation*. 2009;119(23):3028-35. DOI: 10.1161/CIRCULATIONAHA.108.768986

22. Corrao G, Parodi A, Nicotra F, et al. Better compliance to antihypertensive medications reduces cardiovascular risk. *J Hypertens*. 2011;29:610-8. DOI: 10.1097/HJH. 0b013e328342ca97

23. Mathews R, Peterson ED, Honeycutt E, et al. Early Medication Nonadherence After Acute Myocardial Infarction: Insights into Actionable Opportunities From the TReatment with ADP receptor iNhibitorS: Longitudinal Assessment of Treatment Patterns and Events after Acute Coronary Syndrome (TRANSLATE-ACS) Study. *Circ Cardiovasc Qual Outcomes*. 2015;8(4):347-356. DOI: 10.1161/CIRCOUTCOMES.114.001223

24. de Vries ST, Keers JC, Visser R, et al. Medication beliefs, treatment complexity, and non-adherence to different drug classes in patients with type 2 diabetes. *J Psychosom Res*. 2014;76(2):134. DOI: 10.1016/j.jpsychores.2013.11.003

25. Viana M, Laszczynska O, Mendes S, et al. Medication adherence to specific drug classes in chronic heart failure. *J Manag Care Spec Pharm*. 2014;20(10):1018-26. DOI: 10.18553/jmcp.2014.20.10.1018

Technical report | Технический отчет
DOI: https://doi.org/10.35693/SIM624827

A postmortem interval estimation by cranioencephalic thermometry at a single discrete decrease in ambient temperature

German V. Nedugov
Samara State Medical University (Samara, Russia)

Abstract

Aim – to develop an estimation method and a computer program for determining the postmortem interval (PMI) by cranioencephalic temperature (CT) of a corpse under conditions of cooling with a single discrete decrease in ambient temperature.

Material and methods. We performed an analytical and finite element modeling of CT dynamics at a single discrete decrease in ambient temperature.

Results. A mathematical model has been developed for determining the PMI and the uncertainty of its estimates at a single discrete decrease in the ambient temperature. The constants' values of the model equation and their variances were determined on the basis of finite element modeling of CT dynamics under the specified cooling conditions. The computational algorithm of the specified method for determining PMI and limitations of its use were implemented in the Warm Bodies DSC program written on C#.

Conclusion. We can recommend using the developed method and software in forensic medicine to determine the PMI at a single discrete decrease in ambient temperature.

Keywords: corpse cooling, postmortem interval, cranioencephalic temperature.

Conflict of interest: nothing to disclose.

Citation
Nedugov G.V. **A postmortem interval estimation by cranioencephalic thermometry at a single discrete decrease in ambient temperature.** *Science and Innovations in Medicine.* 2025;10(3):218-223. DOI: https://doi.org/10.35693/SIM624827

Information about author
German V. Nedugov – Dr. Sci. (Medicine), Associate professor,
Head of the Department of Forensic Medicine.
ORCID: 0000-0002-7380-3766
E-mail: nedugovh@mail.ru

Received: 19.12.2023
Accepted: 09.03.2024
Published: 17.05.2024

Оценка давности наступления смерти методом краниоэнцефальной термометрии при однократном дискретном понижении внешней температуры

Г.В. Недугов
ФГБОУ ВО «Самарский государственный медицинский университет» Минздрава России (Самара, Россия)

Аннотация

Цель – разработка реализованного в формате компьютерной программы метода определения ДНС по КТ трупа в условиях его охлаждения при однократном дискретном понижении внешней температуры.

Материал и методы. Выполнено аналитическое и конечно-элементное моделирование динамики КТ при однократном дискретном понижении внешней температуры.

Результаты. Разработана математическая модель определения ДНС и неопределенности ее оценок при однократном дискретном понижении внешней температуры. Значения констант модельного уравнения и их дисперсий определены путем конечно-элементного моделирования динамики КТ в указанных условиях охлаждения. Вычислительный алгоритм данного метода определения ДНС и противопоказания к его применению реализованы на языке C# в виде программы Warm Bodies DSC.

Выводы. Разработанный метод и реализующее его приложение рекомендуются к использованию в судебно-медицинской практике для определения ДНС при однократном дискретном понижении внешней температуры.

Ключевые слова: охлаждение трупа, давность наступления смерти, краниоэнцефальная температура.

Конфликт интересов: не заявлен.

Для цитирования:
Недугов Г.В. **Оценка давности наступления смерти методом краниоэнцефальной термометрии при однократном дискретном понижении внешней температуры.** *Наука и инновации в медицине.* 2025;10(3):218-223.
DOI: https://doi.org/10.35693/SIM624827

Сведения об авторе
Недугов Герман Владимирович – д-р мед. наук, доцент,
заведующий кафедрой судебной медицины.
ORCID: 0000-0002-7380-3766
E-mail: nedugovh@mail.ru

Список сокращений
ДНС – давность наступления смерти;
КТ – краниоэнцефальная температура.

Получено: 19.12.2023
Одобрено: 09.03.2024
Опубликовано: 17.05.2024

INTRODUCTION

The 'gold standard' of estimating the postmortem interval (PMI) in the early postmortem period remains C. Henssge's method, the use of which requires a single measurement of rectal or cranioencephalic temperature (CT) [1–5]. This method is based on the phenomenological law of deep tissue cooling in corpses at constant ambient temperature, proposed in 1962 by researchers T.K. Marshall and F.E. Hoare, which takes the form of a transcendental equation:

$$\frac{T-T_a}{T_0-T_a} = \frac{p}{p-k}e^{-kt} - \frac{k}{p-k}e^{-pt}, \quad (1)$$

where T – current core body temperature of the corpse, °C; T_a – ambient temperature, °C; $T0$ – initial body temperature at the diagnostic point at the moment of death, °C; k – cooling constant, h^{-1}; p – temperature plateau constant, h^{-1}; t – TSD, h [6].

In his modification of the equation (1) C. Henssge used the analysis of a vast amount of empirical data to establish linear dependencies of the temperature plateau constant from the cooling constant, as well as mean statistical data of the latter in various conditions of cooling of the dead body [7, 8]. The most critical condition for the accuracy of this method, which significantly limits its practical application, is the constancy of ambient temperature. This specific circumstance has prompted a series of studies focused on adapting Henssge's method to variable ambient temperature conditions [9–11].

One of the forensically relevant patterns of ambient temperature variation in medico-legal practice is its single discrete decrease, referring to a one-time reduction in external temperature while maintaining constant temperature thereafter [12]. This generic change in the cooling conditions is usually seen in the corpse thermometry after it had been relocated from the place of discovery to a storage vault with different temperature conditions. In such situations, the ambient temperature before and after relocation or the corpse, time after the relocation before the thermometry, and the results of the thermometry are usually known [9]. After experimenting on manikins, L. Althaus and C. Henssge developed a phenomenological model of determining the PMI in the specific conditions of cooling based on the equation (1) and data of rectal thermometry [9]. This model was later optimized and implemented as a computer program. Apart from the measurement of changes in the temperature conditions, it considered changes in other conditions of cooling of the dead body, namely, the properties of its clothes and bed, as well as status of wind of water flow [12].

On the whole, the data obtained provided a solution for determination of the PMI by a single discrete decrease in the ambient temperature by rectal thermometry of the corpse. At the same time, in order to obtain valid evaluations of PMI based on rectal thermometry of the corpse, the initial ambient temperature conditions with its discrete decrease should not exceed 23.2 °C [9, 13]. For that reason, the approach proposed by L. Althaus and C. Henssge is not applicable if the initial ambient temperature is above the given threshold, which significantly limits the application of the method.

Unlike the case of rectal temperature, the dynamics of CT is characterized by lack of influence of external temperature on the linkage between the constants of thermal plateau and cooling, which is expressed as the following ratio for this diagnostic point:

$$p = 8{,}425k. \quad (2)$$

Moreover, evaluation of PMI by cranioencephalic thermometry does not require measurement of the mass of the corpse [7, 8, 13]. Notwithstanding these advantages, no technologies of PMI evaluation with single discrete decrease of ambient temperature by cranioencephalic thermometry of the corpse have been proposed. At the same time, the forensic expert practice requires such technologies whose calculation algorithms are implemented as computer programs.

AIM

To develop an estimation method and a computer program for determining the postmortem interval (PMI) by cranioencephalic temperature (CT) of a corpse under conditions of cooling with a single discrete decrease in ambient temperature.

MATERIAL AND METHODS

The methodological design of the study is to develop a phenomenological model of PMI determination with single discrete decrease of ambient temperature based on finite element modeling of CT dynamics with the given conditions of corpse cooling, the calculation algorithm of the model to be implemented as a computer program.

The mathematical model of the corpse core cooling involved two periods, the initial and the final, representing periods before and after changes in the cooling conditions, respectively. The model of CT dynamics in the final period of corpse cooling was based on the equation (1) with respect to linear correlation (2) of its constants. The value range of the constants in the equation (1) was determined by numeric search of solution of the Marshall-Hoare system of nonlinear equations (SNE) for double thermometry of the corpse:

$$\begin{cases} T_{0_2} = \dfrac{(T_1 - T_{a_2})(p-k)}{pe^{-kt_2} - ke^{-pt_2}}, \\ T_{0_2} = \dfrac{(T_2 - T_{a_2})(p-k)}{pe^{-k(t_2+\Delta t)} - ke^{-p(t_2+\Delta t)}}, \end{cases} \quad (3)$$

where Ta_2 – final ambient temperature, °C; t_2 – duration of the final period of cooling, h; T_1 – CT in the first thermometry of the corpse in the end of t_2 period, °C; T_2 – CT in the second thermometry of the corpse, °C; Δ_t – time between the thermometries of the corpse, h (**Fig. 1**).

To that end, roots of the equation

$$(T_1 - T_{a_2})\left(pe^{-k(t_2+\Delta t)} - ke^{-p(t_2+\Delta t)}\right) - (T_2 - T_{a_2})\left(pe^{-kt_2} - ke^{-pt_2}\right) = 0, \quad (4)$$

were found that would meet the various conditions of the specific type of cooling. The nonlinear optimization of the functions (4) obtained from the SNE (3) with constants k and p serving as variables was performed using the generalized reduced gradient method implemented in the "Solver" add-in of the Microsoft Office Excel 2016 spreadsheet processor.

The values of other indicators of the SNE (3) were found by computer modeling by finite element method for the

thermal field of the head in the conditions of convective heat exchange with the heat transfer factor of 6 W/(m²·K), for various combinations of the initial and final cooling periods in the absence of internal and external heat sources. The borderline values of parameters of these cooling conditions were as follows: initial period, 10–35 °C, final period, 4–11 °C, difference between the initial and final ambient temperatures was 2–26 °C; duration of the initial cooling period, 1–21 h, duration of the final cooling period, 1–10 h; the interval between the first and second thermometry of the corpse was 0.5–2 hours. The discretization step for ambient temperatures was 1°C, cooling period durations, 1 h, and time intervals between corpse thermometry measurements were 0.5 h. In total, 148 non-degenerate solutions to the SNEs (3) were found based on the generated data.

For the purposes of computer modeling of postmortem CT dynamics, a two-dimensional finite-element model of the cerebral head region was used. It was designed as a quadrant with 98 mm radius comprising uniformly distributed homogeneous layers: cutaneous-aponeurotic flap (5 mm), cranial vault bones (5 mm), subarachnoid space cerebrospinal fluid (2 mm), and brain tissue (86 mm). The thermophysical parameters of these biological tissues, procedures for establishing initial and postmortem temperature fields in the computational domain, and validation of the finite-element model were previously detailed in our work [14]. CT was defined as the temperature at the point with zero radial coordinate.

The finite element model of the postmortem thermal field of the head was constructed using the free version of ELCUT 6.5 (https://elcut.ru/free_soft_r.htm). The remaining calculation procedures were performed in Microsoft Excel (Office 2016 software suite). The mathematical analysis was performed in the free web application WolframAlpha (https://www.wolframalpha.com). The code of the program calculating PMI and error of the obtained estimates was written in C# using the free version of Microsoft Visual Studio (https://visualstudio.microsoft.com/ru/downloads).

RESULTS

In the initial cooling period, the CT dynamics progresses in accordance with equation (1) with constant values established by C. Henssge [7, 8, 13]. Provided that the CT value as of the moment of decrease of ambient temperature is available, it is possible to determine the duration of the initial cooling period, which represents the root of the implicitly defined equation

$$1{,}135e^{-0{,}127t_1} - 0{,}135e^{-1{,}07t_1} - \frac{T_{0_2} - T_{a_1}}{T_{0_1} - T_{a_1}} = 0, \qquad (5)$$

where t_1 – duration of the initial cooling period, h; T_{0_2} – CT at the moment of change of cooling regimes, °C; Ta_1 – initial ambient temperature, °C; T_{0_1} – initial CT as per recommendations of C. Henssge, taken to be 37.2 °C (**Fig. 1**).

Thus, the task of determining the PMI in the given conditions is reduced to the task of determining the CT at the moment of change of thermal modes of cooling.

Computer simulation of cooling under the considered conditions showed that during the final cooling period, CT dynamics also follow law (1), but with unknown individual values of cooling constants and temperature plateau.

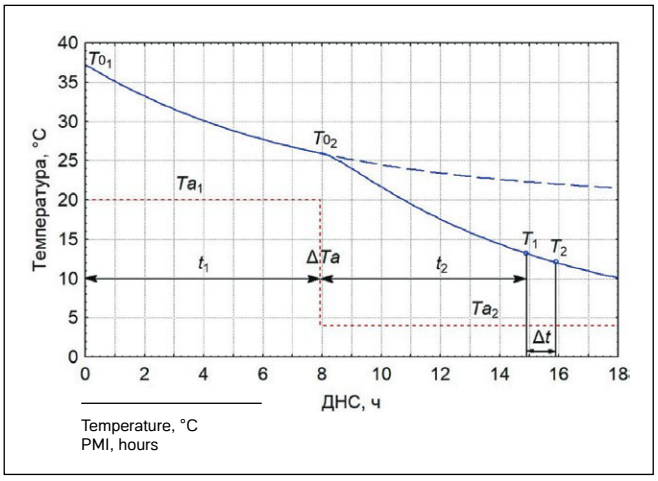

Figure 1. *Dynamics of cranioencephalic temperature on the example 1 (solid blue line). The red dashed line marks the dynamics of ambient temperature. The dashed blue line shows the conditional dynamics of cranioencephalic temperature in the absence of a change in cooling modes.*

Рисунок 1. *Динамика КТ для данных из примера 1 (сплошная синяя линия). Красной штриховой линией маркирована динамика внешней температуры. Штриховой синей линией показана условная динамика КТ при отсутствии смены режима охлаждения.*

To determine the ranges of constants k and p using the generalized reduced gradient method, a search was performed for solutions of equation (4) variants generated based on the finite-element model that satisfy given boundary conditions under various regimes of single discrete decreases in ambient temperature. This search showed that the average value of the k constant is 0.135 h^{-1}, and its dispersion, maximum in the first two hours of the final period of cooling, then drastically decreases decaying to zero after five hours (**Fig. 2**). The maximum deviation of the cooling constant from its average value in the period of 3 to 10 hours after the decrease of ambient temperature reached 0.007 h^{-1}.

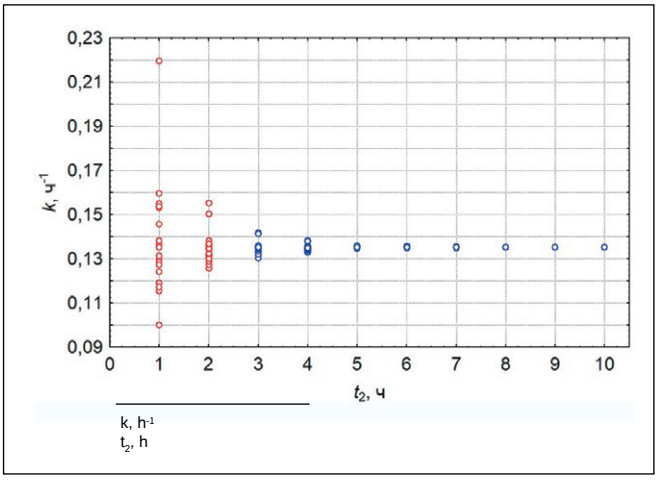

Figure 2. *Dependence of the cooling constant on the duration of the final cooling period according to finite element modeling of corpse cooling under various modes of a single discrete decrease in ambient temperature. The values of k at t_2 < 3 h and ΔTa < 6 °C are marked in red.*

Рисунок 2. *Зависимость константы охлаждения от продолжительности финального периода охлаждения по данным конечно-элементного моделирования охлаждения трупа при различных режимах однократного дискретного понижения внешней температуры. Красным маркированы значения k при t_2 < 3 ч и ΔTa < 6 °C.*

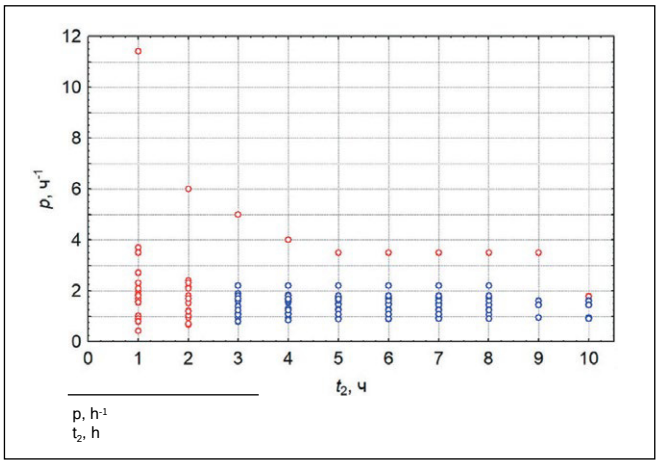

Figure 3. *The dependence of the temperature plateau constant on the duration of the final cooling period according to finite element modeling of corpse cooling under various modes of a single discrete decrease in ambient temperature. The values of p at t_2 < 3 h and ΔTa < 6 °C are marked in red.*

Рисунок 3. *Зависимость константы температурного плато от продолжительности финального периода охлаждения по данным конечно-элементного моделирования охлаждения трупа при различных режимах однократного дискретного понижения внешней температуры. Красным маркированы значения p при t_2 < 3 ч и ΔTa < 6 °C.*

The values of the p constant in the first two hours of the final cooling period, as well as with the difference ΔT_a of the initial and the final temperatures below 6 °C also demonstrated marked dispersion, whereas in other options of the studies cooling conditions the distribution of values of the constant was uniform with the average value being 1.4 h^{-1} and maximum deviation from the average at 0.8 h^{-1} (**Fig. 3**).

The obtained data allow using the established average values of both constants when determining CT at the moment of ambient temperature change via any of the SNEs (3). It is preferable to use the first equation for this purpose, as it contains fewer arguments and does not require repeated corpse thermometry for calculations. After calculating CT at the moment of ambient temperature shifts, the duration of the initial cooling period is determined by formula (5). Thus, the sought PMI represents the sum of the initial and final cooling periods: $t=t_2+t_1$, where t – PMI, h.

Example 1. The corpse was discovered in a room with an air temperature of 20.0 °C, then transported to the morgue and placed in a refrigeration chamber at 4.1 °C, where cranioencephalic thermometry was performed 7 hours after discovery. The CT measured 14.0 °C. It is necessary to determine PMI at the time of corpse thermometry.

As per SNE (3), at the moment of ambient temperature change the corpse CT was

$$T_{0_2} = \frac{(14-4{,}1)(1{,}4-0{,}135)}{1{,}4e^{-0{,}135\cdot 7}-0{,}135e^{-1{,}4\cdot 7}} = 27{,}115 \ \text{°C}.$$

Using the obtained CT value in the equation (5), we obtain the expression

$$1{,}135e^{-0{,}127t_1} - 0{,}135e^{-1{,}07t_1} - \frac{27{,}115-20}{37{,}2-20} = 0,$$

from which we calculate t_1 = 7.95 h. Therefore, the PMI at the moment of the corpse thermometry is

t = 7,95+7=14,95 h.

Due to the use of average values of the SNEs (3) constants, CT estimates obtained by the described method will inherently contain errors. The magnitude of these errors will be further influenced by inaccuracies in corpse thermometry and ambient temperature measurement, duration measurement errors of the final cooling period. According to the first SNE (3), the CT at the moment of cooling regime shifts can be treated as a function of

$$T_{0_2}=F(k, p, t_2, T_{a_2}, T_1) \qquad (6)$$

5 random variables. Assuming there are no mutual correlation among the errors of the arguments of this function, the variance of CT estimation errors is determined from the equation

$$\sigma^2_{T_{0_2}} = \left(\frac{\partial F}{\partial k}\right)^2\sigma^2_k + \left(\frac{\partial F}{\partial p}\right)^2\sigma^2_p + \left(\frac{\partial F}{\partial t_2}\right)^2\sigma^2_{t_2} + \left(\frac{\partial F}{\partial T_{a_2}}\right)^2\sigma^2_{T_{a_2}} + \left(\frac{\partial F}{\partial T_1}\right)^2\sigma^2_{T_1}, \qquad (7)$$

where σ^2 – error dispersion, and F is the function (6). With no information about standard deviations of errors being available, they should be set equal to one-third of the maximum permissible error of the corresponding parameter.

The uncertainty of estimates of the initial period t_1 according to data [12] is

$$\sigma_{t_1} = 2{,}0889e^{-1{,}1411Q},$$

where Q – non-dimensional temperature, in this case calculated as

$$Q = \frac{T_{0_2}-T_{a_1}}{T_{0_1}-T_{a_1}}.$$

The total variance of PMI estimation errors equals the sum of variance in initial cooling period duration errors, variance in final cooling period duration errors, and variance in CT estimation errors at the moment of ambient temperature regime shifts:

$$\sigma^2_t = \sigma^2_{t_1} + \sigma^2_{t_2} + \left(\frac{\partial f(t)}{\partial T_{0_2}}\right)^2\sigma^2_{T_{0_2}},$$

where $f(t)$ – implied function (5), the partial derivative of which for T02 is determined by the equation

$$\frac{\partial f(t)}{\partial T_{0_2}} = \left[(T_{a_1}-T_0)\left(0{,}14445e^{-1{,}07t_1} - 0{,}144145e^{-0{,}127t_1}\right)\right]^{-1}.$$

Knowing the error variance, one can calculate the tolerant interval of PMI:

$$PMI = t \pm \sigma_t \cdot z_{1-\alpha},$$

where t – PMI estimate, h; z – standard normal variable; α – level of significance..

Example 2. Determine the 95% tolerant interval of PMI for the data from Example 1, taking the absolute threshold errors of corpse thermometry and ambient temperature measurement as 0.1 °C and the final cooling period as 20 minutes (0.333 h).

x indicator	Value	Δx	σ	$\frac{\partial F}{\partial x}$	Product of squares
T_1, °C	14	0,1	0,033333	2,324753	0,006004972
Ta_2, °C	4,1	0,1	0,033333	-1,32475	0,001949966
t_2, ч	7	0,333333	0,111111	3,106631	0,119150105
k, $ч^{-1}$	0,135	0,007	0,002333	142,9162	0,111203002
p, $ч^{-1}$	1,4	0,8	0,266667	1,751952	0,218263764

Table 1. *Intermediate calculations of the cranioencephalic temperature error at the time of changing the temperature regimes of cooling the corpse*

Таблица 1. *Промежуточные расчеты погрешности КТ в момент смены температурных режимов охлаждения трупа*

The results of preliminary calculations of CT error variance at the time of cooling temperature shifts are shown in **Table 1**.

Summing up the products of squares, we find that the CT variance is 0.4566.

Since

$$Q = \frac{27{,}115 - 20}{37{,}2 - 20} = 0{,}4137,$$

then

$$\sigma_{t_1} = 2{,}0889e^{-1{,}1411 \cdot 0{,}4137} = 1{,}3029.$$

Therefore

$$\sigma_t = \sqrt{1{,}3029^2 + 0{,}1111^2 + 0{,}4566\left[(20 - 27{,}115)\left(0{,}14445e^{-1{,}07 \cdot 7{,}95} - 0{,}144145e^{-0{,}127 \cdot 7{,}95}\right)\right]^{-2}} = 1{,}51 \text{ ч.}$$

Multiplying the value of the standard normal variable of 1.960 by the standard PMI error variance, we calculate the 95% tolerant interval of the latter:

$$PMI = 14.95 \pm 2.95 \text{ h}.$$

The described computational algorithm was formalized in C# within the computer program Warm Bodies SDC (Certificate of State Registration of Computer Program No. 2023687943). Based on the proposed mathematical model, the application calculates PMI from corpse CT when there is a single discrete decrease in constant ambient temperature by 6 °C or more and a final cooling period duration of 3 to 10 hours. In addition to point estimates, the program determines two-sided interval estimates of PMI for the required confidence probability level. The calculated error magnitude includes inaccuracies arising from potential deviations of individual cooling conditions from statistical averages, as well as measurement errors of input parameters.

The maximum errors for the latter are set at 0.1°C for temperature parameters and 5% for the duration of the final cooling period. The application calculates the duration of the initial cooling period using Newton's iterative method. When degenerate cooling scenarios are detected, the program halts calculations and displays a corresponding warning window. To operate the program, the user must input the result of the single-time corpse CT measurement, initial and final ambient temperatures, time interval between the ambient temperature decrease and body thermometry, initial CT, and permissible error probability.

DISCUSSION

The computer modeling conducted in this study demonstrated that CT dynamics following a single discrete decrease in ambient temperature conform to the Marshall-Hoare equation (1). This cooling pattern under such conditions appears universal for all deep corpse tissues, as L. Althaus and C. Henssge observed the same phenomenon when studying rectal temperature dynamics [9]. However, due to the impossibility of establishing individual constants for equation (1) during the final cooling phase, these authors replaced equation (1) with their own empirical expression when developing their PMI determination method.

Unlike the approach of L. Althaus and C. Henssge, the method to determine CT at the moment of cooling temperature shifts suggested within this study uses the original Marshall-Hoare equation with the average values of cooling and thermal plateau constants obtained by computer modeling of a wider range of different variants of discrete decrease of ambient temperature. Additionally, the method provides for calculating uncertainty both in estimates of BT at the moment of cooling regime changes and in final estimates of PMI, based on variances of the constants of equation (1) and measurement errors of temperature and time parameters.

The use of the developed method may be limited due to possible discrepancies between real cooling conditions and those modeled in the computer experiment. The reasons for potential discrepancies include: 1) heat transfer through conduction when the cooling body part contacts other physical objects; 2) convection under non-standard conditions with different heat transfer coefficients; 3) thermo-physical properties of tissues in the cooling body region differing from model parameters.

However, the selected body part for the modeling of cooling (the head) demonstrates the highest resistance to the listed factors affecting PMI determination accuracy. This is because the shape of the head closely approximates a sphere, which has only one point of contact with a tangential plane. This circumstance allows neglecting heat conduction processes when the corpse's head rests on a flat surface. The anatomical structure of the head and its modeled tissue layers exhibits minimal variability. Additionally, the constants of equation (1) for non-standard cooling scenarios (presence of headwear, strong wind, liquid contact) can be refined through future finite-element modeling of corresponding cooling conditions. [15–17].

The developed method is contraindicated for use when the duration of the final cooling period is less than 3 hours and when the difference between initial and final ambient temperature regimes is less than 6°C. In the first case, the cooling process does not exhibit distinct exponential and temperature equilibration phases. In the second case, the temperature plateau phase is absent. These circumstances naturally lead to a mismatch between mathematical model (1) and actual cooling conditions, resulting in increased variance of equation (1) constants and greater errors in PMI estimates. These contraindications are easily manageable in practice. In the first case, it is sufficient to perform corpse thermometry after a longer period following its transfer to different cooling conditions. In the second case, it is

advisable to consider the ambient temperature as constant in calculations, equal to the average value of the sum of initial and final ambient temperatures, with a maximum measurement error of 3°C.

The contraindications also include limitations inherent to all thermometric PMI determination methods based on C. Henssge's modifications of equation (1), e.g., solar radiation, significant fluctuations of ambient temperature during initial and final cooling periods, marked deviations from normothermic thanatogenesis [7, 8, 13].

CONCLUSIONS

1. A method has been developed for determining PMI and the errors of its estimates based on corpse CT under cooling conditions with a single discrete decrease in ambient temperature.

2. The computational algorithm of the proposed PMI determination method and contraindications for its use are implemented in the Warm Bodies DSC application program.

3. The developed method and the computer program implementing it are recommended for use in forensic expert practice for thermometric PMI determination during single discrete decreases in ambient temperature.

ADDITIONAL INFORMATION	ДОПОЛНИТЕЛЬНАЯ ИНФОРМАЦИЯ
Study funding. The study was the author's initiative without external funding.	***Источник финансирования.*** Работа выполнена по инициативе автора без привлечения финансирования.
Conflict of interest. The author declares that there are no obvious or potential conflicts of interest associated with the content of this article.	***Конфликт интересов.*** Автор декларирует отсутствие явных и потенциальных конфликтов интересов, связанных с содержанием настоящей статьи.

REFERENCES / ЛИТЕРАТУРА

1. Hubig M, Muggenthaler H, Mall G. Confidence intervals in temperature-based death time determination. *Leg Med (Tokyo)*. 2015;17(1):48-51. DOI: 10.1016/j.legalmed.2014.08.002

2. Schweitzer W, Thali MJ. Computationally approximated solution for the equation for Henssge's time of death estimation. *BMC Med Inform Decis Mak*. 2019;19(1):201. DOI: 10.1186/s12911-019-0920-y

3. Potente S, Henneicke L, Schmidt P. Prism - A novel approach to dead body cooling and its parameters. *Forensic Sci Int*. 2021;325:110870. DOI: 10.1016/j.forsciint.2021.110870

4. Laplace K, Baccino E, Peyron PA. Estimation of the time since death based on body cooling: a comparative study of four temperature-based methods. *Int J Legal Med*. 2021;135(6):2479-2487. DOI: 10.1007/s00414-021-02635-7

5. Wei T, Abraham J, Wang Y. Comment on the Marshall-Hoare-Henssge model for estimating the time since death. *J Forensic Sci*. 2023;68(2):676-681. DOI: 10.1111/1556-4029.15218

6. Marshall TK, Hoare FE. Estimating the time of death. The rectal cooling after death and its mathematical expression. *J Forensic Sci*. 1962;7(1):56-81.

7. Henssge C. Death time estimation in case work. I. The rectal temperature time of death nomogram. *Forensic Sci Int*. 1988;38(3-4):209-236. DOI: 10.1016/0379-0738(88)90168-5

8. Henssge C. Rectal temperature time of death nomogram: dependence of corrective factors on the body weight under stronger thermic insulation conditions. *Forensic Sci Int*. 1992;54(1):51-66. DOI: 10.1016/0379-0738(92)90080-G

9. Althaus L, Henssge C. Rectal temperature time of death nomogram: sudden change of ambient temperature. *Forensic Sci Int*. 1999;99(3):171-178. DOI: 10.1016/s0379-0738(98)00188-1

10. Bisegna P, Henssge C, Althaus L, Giusti G. Estimation of the time since death: sudden increase of ambient temperature. *Forensic Sci Int*. 2008;176(2-3):196-199. DOI: 10.1016/j.forsciint.2007.09.007

11. Nedugov GV. Double exponential model of corpse cooling under conditions of linearly varying ambient temperature. *Russian Journal of Forensic Medicine*. 2021;7(4):19-28. (In Russ.). [Недугов Г.В. Двойная экспоненциальная модель охлаждения трупа в условиях линейно изменяющейся внешней температуры. *Судебная медицина*. 2021;7(4):19-28]. DOI: 10.17816/fm429

12. Nedugov GV. New computer technologies to determine postmortem interval by the Henssge method. *Russian Journal of Forensic Medicine*. 2021;7(3):152-158. (In Russ.). [Недугов Г.В. Новые компьютерные технологии определения давности наступления смерти по методу Henssge. *Судебная медицина*. 2021;7(3):152-158]. DOI: 10.17816/fm406

13. Henssge C, Madea B. Estimation of the time since death in the early post-mortem period. *Forensic Sci Int*. 2004;144(2-3):167-75. DOI: 10.1016/j.forsciint.2004.04.051

14. Nedugov GV. Estimation of the postmortem interval by the method of finite element modeling of postmortem heat transfer in human head. *Science & Innovations in Medicine*. 2022;7(3):179-185. [Недугов Г.В. Оценка давности наступления смерти методом конечно-элементного моделирования посмертного теплообмена головы. *Наука и инновации в медицине*. 2022;7(3):179-185]. DOI: 10.35693/2500-1388-2022-7-3-179-185

15. Schenkl S, Muggenthaler H, Hubig M, et al. Automatic CT-based finite element model generation for temperature-based death time estimation: feasibility study and sensitivity analysis. *Int J Legal Med*. 2017;131(3):699-712. DOI: 10.1007/s00414-016-1523-0

16. Subramaniam JS, Hubig M, Muggenthaler H, et al. Sensitivity of temperature-based time since death estimation on measurement location. *Int J Legal Med*. 2023;137(6):1815-1837. DOI: 10.1007/s00414-023-03040-y

17. Ullrich J, Weiser M, Shanmugam Subramaniam J, et al. The impact of anatomy variation on temperature based time of death estimation. *Int J Legal Med*. 2023;137(5):1615-1627. DOI: 10.1007/s00414-023-03026-w

Original research | Оригинальное исследование
DOI: https://doi.org/10.35693/SIM680762

Improving the quality of medical care for patients with 5q spinal muscular atrophy through the implementation of continuing professional education programs

Yan V. Vlasov[1], Timur S. Syunyakov[2, 3], Arsenii Ya. Gayduk[4, 5], Anastasiya V. Gazheva[5], Natalya N. Kamynina[5], Olga V. Pesneva[6], Tatyana B. Bukharova[7], Sergei S. Nikitin[7], Sergei I. Kutsev[7]

[1]All-Russian Union of Public Associations of Patients (Moscow, Russian Federation)
[2]Republican Specialized Scientific and Practical Medical Center of Mental Health (Tashkent, Republic of Uzbekistan)
[3]Psychiatric Clinic No. 1 named after N.A. Alekseev (Moscow, Russian Federation)
[4]Samara State Medical University (Samara, Russian Federation)
[5]National Research Institute of Public Health and Healthcare Management (Moscow, Russian Federation)
[6]MedConsul (Moscow, Russian Federation)
[7]Academician N.P. Bochkov Medical Genetic Research Center (Moscow, Russian Federation)

Abstract

Aim – to evaluate the effectiveness of the continuing professional education program "Multidisciplinary approach to managing patients with a confirmed diagnosis of 5q spinal muscular atrophy" (36 hours; hereinafter referred to as the SMA5q CPE Program) as a tool for improving the level of competence of doctors within multidisciplinary teams providing medical care to SMA5q patients.

Material and methods. The study used the materials completed by course teachers and students who had completed training under the SMA5q CPE Program. These materials included entrance control forms, final certification forms, and certification reports, which were provided by the Institute of Higher and Continuing Professional Education of the N.P. Bochkov Medical Genetic Research Center.

Results. As of January 2025, 136 students from 39 administrative entities of the Russian Federation had completed the training. During the final certification of the training program, all students demonstrated a relatively high level of competence in completing test tasks: 70-80% correct answers were given by 96 students, 81-90% by 36, 91-100% by 4. At least one control question was answered by 42 students, two by 85, and all three questions, by 9 doctors.

Conclusions. The SMA5q CPE Program has proven effective in improving the competencies of doctors who make up a multidisciplinary team. The implementation of this SMA5q CPE Program can increase the availability and effectiveness of high-cost pathogenetic therapy for patients with SMA5q.

Keywords: additional education program, 5q spinal muscular atrophy, SMA5q.
Conflict of interest: nothing to disclose.

Citation
Vlasov YaV, Syunyakov TS, Gayduk AYa, Gazheva AV, Kamynina NN, Pesneva OV, Bukharova TB, Nikitin SS, Kutsev SI. **Improving the quality of medical care for patients with 5q spinal muscular atrophy through the implementation of continuing professional education programs.** *Science and Innovations in Medicine.* 2025;10(3):224-231. DOI: https://doi.org/10.35693/SIM680762

Information about authors
Yan V. Vlasov – Dr. Sci. (Medicine), Professor, Co-Chair.
ORCID: 0000-0002-9471-9088
E-mail: jansams99@inbox.ru
Timur S. Syunyakov – Cand. Sci. (Medicine), Science Advisor.
ORCID: 0000-0002-4334-1601
E-mail: sjunja@gmail.com
***Arsenii Ya. Gayduk** – Acting Director of the International Scientific and Educational Center for Neuropsychiatry.
ORCID: 0000-0002-4015-3162
E-mail: a.j.gayduk@samsmu.ru
Anastasiya V. Gazheva – Cand. Sci. (Medicine), Associate Professor, Head of the Department for Coordination of Organizational and Methodological Work in Healthcare.
ORCID: 0000-0003-2665-5606
E-mail: karina.keri@mail.ru
Natalya N. Kamynina – Dr. Sci. (Medicine), Professor, Deputy Director for Research.
ORCID: 0000-0002-0925-5822
E-mail: kamyninaNN@zdrav.mos.ru
Olga V. Pesneva – CEO.
ORCID: 0009-0001-0152-8718
E-mail: pesnevaov@mail.ru
Tatyana B. Bukharova – Cand. Sci. (Biology), Leading Researcher of the Laboratory of Stem Cell Genetics.
ORCID: 0000-0003-0481-256X
E-mail: bukharova-rmt@yandex.ru
Sergei S. Nikitin – Dr. Sci. (Medicine), Professor, Head of the Department of Genetics of Neurological Diseases.
ORCID: 0000-0003-3292-2758
E-mail: maria_fnc@mail.ru
Sergei I. Kutsev – Dr. Sci. (Medicine), Professor, Academician of the Russian Academy of Sciences, Chief Specialist of the Ministry of Health of the Russian Federation in Medical Genetics, Director.
ORCID: 0000-0002-3133-8018
E-mail: kutsev@mail.ru
Corresponding Author

Received: 27.05.2025
Accepted: 05.08.2025
Published: 11.08.2025

Повышение уровня врачебных компетенций в области ведения пациентов со спинальной мышечной атрофией 5q с помощью внедрения программы дополнительного профессионального образования

Я.В. Власов[1], Т.С. Сюняков[2, 3], А.Я. Гайдук[4, 5], А.В. Гажева[5], Н.Н. Камынина[5], О.В. Песнева[6], Т.Б. Бухарова[7], С.С. Никитин[7], С.И. Куцев[7]

[1]НКО «Всероссийский союз общественных объединений пациентов» (Москва, Российская Федерация)
[2]Республиканский специализированный научно-практический медицинский центр психического здоровья (Ташкент, Республика Узбекистан)
[3]ГБУЗ «Психиатрическая клиника №1 имени Н.А. Алексеева» департамента здравоохранения г. Москвы (Москва, Российская Федерация)
[4]ФГБОУ ВО «Самарский государственный медицинский университет» Минздрава России (Самара, Российская Федерация)
[5]ГБУ «Национальный исследовательский институт организации здравоохранения и медицинского менеджмента» департамента здравоохранения г. Москвы (Москва, Российская Федерация)
[6]ООО «Медконсул» (Москва, Российская Федерация)
[7]Институт высшего и дополнительного профессионального образования ФГБНУ «Медико-генетический научный центр имени академика Н.П. Бочкова» (Москва, Российская Федерация)

Аннотация

Цель – оценка эффективности дополнительной программы образования «Многопрофильный подход к ведению пациентов с подтвержденным диагнозом спинальная мышечная атрофия 5q» (36 часов) (далее – Программа ДПО по СМА5q) в качестве инструмента повышения уровня компетенций врачей, входящих в многопрофильную бригаду по оказанию медицинской помощи пациентам со СМА5q.

Материал и методы. Использованы материалы, заполненные преподавателями курса и обучающимися, прошедшими подготовку по Программе ДПО по СМА5q. Указанные материалы представляли собой бланки входного контроля, бланки итоговой аттестации и аттестационные ведомости, которые были предоставлены Институтом высшего и дополнительного профессионального образования ФГБНУ «Медико-генетический научный центр имени академика Н.П. Бочкова».

Результаты. По состоянию на январь 2025 года подготовку прошли 136 обучающихся из 39 субъектов РФ. В ходе итоговой аттестации по обучающей программе все обучающиеся показали сравнительно высокий уровень компетенций при выполнении тестовых заданий: 70–80% правильных ответов дали 96 обучающихся, 81–90% – 36, 91–100% – 4. Как минимум на один контрольный вопрос ответили 42 обучающихся, на два – 85 и на все три вопроса – 9 врачей.

Выводы. Программа ДПО по СМА5q показала эффективность в повышении компетенций врачей, составляющих многопрофильную бригаду. Внедрение данной Программы ДПО по СМА5q способно повысить доступность и эффективность использования высокозатратной патогенетической терапии пациентов со СМА5q.

Ключевые слова: дополнительная программа образования, спинальная мышечная атрофия 5q, СМА5q.

Конфликт интересов: не заявлен.

Для цитирования:
Власов Я.В., Сюняков Т.С., Гайдук А.Я., Гажева А.В., Камынина Н.Н., Песнева О.В., Бухарова Т.Б., Никитин С.С., Куцев С.И. **Повышение уровня врачебных компетенций в области ведения пациентов со спинальной мышечной атрофией 5q с помощью внедрения программы дополнительного профессионального образования.** *Наука и инновации в медицине.* 2025;10(3):224-231.
DOI: https://doi.org/10.35693/SIM680762

Сведения об авторах
Власов Я.В. – д-р мед. наук, профессор, сопредседатель.
ORCID: 0000-0002-9471-9088
E-mail: jansams99@inbox.ru
Сюняков Т.С. – канд. мед. наук, советник по науке.
ORCID: 0000-0002-4334-1601
E-mail: sjunja@gmail.com
***Гайдук Арсений Янович** – и.о. директора Международного научно-образовательного центра нейропсихиатрии.
ORCID: 0000-0002-4015-3162
E-mail: a.j.gayduk@samsmu.ru
Гажева А.В. – канд. мед. наук, доцент, начальник отдела координации организационно-методической работы в здравоохранении.
ORCID: 0000-0003-2665-5606
E-mail: karina.keri@mail.ru
Камынина Н.Н. – д-р мед. наук, профессор, заместитель директора по научной работе.
ORCID: 0000-0002-0925-5822
E-mail: kamyninaNN@zdrav.mos.ru
Песнева О.В. – генеральный директор.
ORCID: 0009-0001-0152-8718
E-mail: pesnevaov@mail.ru
Бухарова Т.Б. – канд. биол. наук, ведущий научный сотрудник лаборатории генетики стволовых клеток.
ORCID: 0000-0003-0481-256X
E-mail: bukharova-rmt@yandex.ru
Никитин С.С. – д-р мед. наук, профессор, заведующий кафедрой генетики неврологических заболеваний.
ORCID: 0000-0003-3292-2758
E-mail: maria_fnc@mail.ru
Куцев С.И. – д-р мед. наук, профессор, академик РАН, главный внештатный специалист Минздрава РФ по медицинской генетике, директор.
ORCID: 0000-0002-3133-8018
E-mail: kutsev@mail.ru
Автор для переписки

Список сокращений
ДПО СМА5q – дополнительная программа образования «Многопрофильный подход к ведению пациентов с подтвержденным диагнозом спинальная мышечная атрофия 5q»; СМА5q – спинальная мышечная атрофия 5q; ОПОП – основная профессиональная образовательная программа; ПС – профессиональный стандарт; ФГОС – федеральный государственный образовательный стандарт; ОПК – общепрофессиональная компетенция; ПК – профессиональная компетенция.

Получено: 27.05.2025
Одобрено: 05.08.2025
Опубликовано: 11.08.2025

INTRODUCTION

Spinal muscle atrophy 5q (SMA5q) is a severe hereditary orphan life-threatening disease the progresses mostly in the early age [1–4]. In compliance with the Clinical recommendations for SMA5q (2024), a multidisciplinary team should be involved in the management of SMA5q patients [5–7].

The multidisciplinary team providing medical care to SMA5q patients should be headed by a neurologist[1], and pediatricians, physicians, orthopedic traumatologists, anesthesiologists and reanimatologisits, nutritionists, physiotherapists, physical and rehabilitation medicine specialists, as well as palliative care specialists should be on the team [8, 9].

Contents of academic disciplines	Competences to be created			
	Genetic specialists	Neurologists, physicians, general practitioners, orthopedic traumatologists, anesthesiologists and reanimatologists, pulmonologists, gastroenterologists, nutritionists, physiotherapists and specialists in sports medicine	Pediatricians	Specialists in medical rehabilitation, specialists in palliative care
"Hereditary SMA5q: etiopathogenesis, classification, specifics of clinical manifestations, diagnostics"	PC-5. Diagnostic activities: competency in identifying patients' pathological conditions, symptoms, disease syndromes, and nosological entities in accordance with the International Statistical Classification of Diseases and Related Health Problems. PC-6. Clinical practice: competency in managing and treating patients with hereditary disorders.	GPC-5. Competence in prescribing treatments for diseases and/or medical conditions, while monitoring therapeutic efficacy and safety. GPC-6. Competence in implementing and monitoring the effectiveness of medical rehabilitation interventions for diseases and/or health conditions, including through individualized rehabilitation or habilitation programs for persons with disabilities.	GPC-4. Competence in using medical products stipulated by the procedures of provision of medical care, and perform patient check-ups for diagnostic purposes. GPC-5. Competence in assessment of morpho-functional, physiological and pathological processes in the body in order to perform professional tasks.	GPC-4. Competence in examining patients to identify activity limitations and impairments of body functions and structures. GPC-5. Competence in prescribing procedures for the medical rehabilitation of patients with activity limitations and impairments of body functions and structures, and monitoring therapeutic efficacy and safety.
"Implementation of a multidisciplinary approach in provision of medical care to SMA5q patients"	PC-6. Clinical practice: competency in managing and treating patients with hereditary disorders. PC-9. Rehabilitation activities: competence in administering pharmacological and non-pharmacological therapy and other methods in need of medical rehabilitation.	GPC-6. Competence in implementing and monitoring the effectiveness of medical rehabilitation interventions for diseases and/or health conditions, including through individualized rehabilitation or habilitation programs for persons with disabilities. GPC-8. Способен проводить и контролировать эффективность мероприятий по профилактике и формированию здорового образа жизни и санитарно-гигиеническому просвещению населения.	GPC-6. Competence in organizing patient care, delivering primary healthcare, and coordinating professional decision-making during prehospital emergencies, disaster situations, epidemics, and mass casualty incidents. GPC-7. Competence in prescribing treatment and monitoring its therapeutic efficacy and safety. GPC-8. Competence in monitoring the efficiency of medical rehabilitation of patients, including through implementation of individual programs of rehabilitation and habilitation of pediatric patients with disabilities, evaluation of the patients' ability to perform labor activities.	GPC-4. Competence in examining patients to identify activity limitations and impairments of body functions and structures. GPC-5. Competence in prescribing procedures for the medical rehabilitation of patients with activity limitations and impairments of body functions and structures, and monitoring therapeutic efficacy and safety.
"Legal, ethical and coordination aspects of the multidisciplinary approach provision of medical care to SMA5q patients"	PC-5. Diagnostic activities: competency in identifying patients' pathological conditions, symptoms, disease syndromes, and nosological entities in accordance with the International Statistical Classification of Diseases and Related Health Problems. PC-6. Clinical practice: competency in managing and treating patients with hereditary disorders. PC-9. Rehabilitation activities: competence in administering pharmacological and non-pharmacological therapy and other methods in need of medical rehabilitation.	GPC-5. Competence in prescribing treatments for diseases and/or medical conditions, while monitoring therapeutic efficacy and safety. GPC-6. Competence in implementing and monitoring the effectiveness of medical rehabilitation interventions for diseases and/or health conditions, including through individualized rehabilitation or habilitation programs for persons with disabilities. GPC-8. Competence in delivery and monitoring efficiency of events aimed at disease prevention and promotion of healthy living, and sanitary and hygienic education of the population.	GPC-9. Competence in implementation of principled of quality management in professional activities. GPC-10. Competence in solving standard professional tasks using informational and bibliographic resources, biomedical terminology, and information-communication technologies while adhering to core data security requirements. GPC-1. Competence in the implementation of moral and legal norms, ethical and deontological principles in professional activities.	GPC-6. Competence in implementing and monitoring the effectiveness of medical rehabilitation interventions for diseases and/or health conditions, including through individualized rehabilitation or habilitation programs for persons with disabilities. GPC-8. Competence in analyzing medical and statistical information, keeping medical documentation, organization of activities of available medical personnel.

Table 1. *Sections of the CPE for SMA5q and their characteristics*
Таблица 1. *Разделы Программы ДПО по СМА5q и их характеристики*

[1] Clinical guidelines of the Ministry of Health of the Russian Federation "5q Proximal Spinal Muscular Atrophy", children, 2023, p. 67.
Clinical guidelines of the Ministry of Health of the Russian Federation "5q-associated Spinal Muscular Atrophy", adults, 2024, p. 77.

At the same time, some papers identified insufficient readiness of medical specialists to provide medical care to SMA5q patients based on the modern multifaceted approach [10–13]. Besides, our analysis of the Professional Standard "Neurologist" No.1240 (the PS)[1] showed that the document contains generalized data on job functions described as tentative working actions, required skill and knowledge. The specific knowledge required for the management of SMA5q patients are described in that document by way of mentioning the knowledge of "etiology, pathogenesis, diagnostics, clinical manifestations, …modern methods of treatment of… *general* diseases and (or) conditions of the nervous system" including "neuromuscular diseases". What diseases and conditions of the nervous system are 'general' and whether the SMA5q belongs to the same, is not specified in the PS.

The analysis of the Federal State Educational Standard 31.08.42 "Neurology"[2] (FSES) shows the possibility of an arbitrary approach of educational institutions towards development and implementation of the respective programs. According to the said FSES, "professional competences are determined by the educational institution proper based on the PSs compliant with the professional activities of the graduates" (FSES, paragraph 3.4). Here the authors of the FSES indicate that "from each of the chosen PSs, the educational institution selects one or several generalized job functions (GJF)", and the "GJF may be selected fully or partially". At the same time, paragraph 3.6 of the FSES determines unambiguously that the program of residency training for the specialization "Neurology" complies with the FSES if it provides to the graduate the competences in one of the spheres of professional activities (administrative, education, and healthcare, paragraph 1.12 of FSES) and in completion of tasks of one type (medical, scientific research, organizational and managerial, pedagogical, paragraph 1.13 of the FSES) [14].

We also studied the principal specialized educational programs (PSEP) of higher education: residency training programs for the specialization 31.08.42 "Neurology" of ten higher educational institutions for the period of 2021–2024. The analysis of PSEPs of Russian Universities for the specialization "Neurology" revealed that a dedicated class of four academic hours for the topic SMA5q was planned only in one out of ten academic programs; that SMA5q was mentioned in four out of ten academic programs in the context of a class on neuromuscular diseases; that neuromuscular diseases, without details, was found in the structure of other classes in three out of ten academic products.

Thus, the neurologists who received only the base education have insufficient competences to provide quality care to SMA5q patients [14]. Moreover, the advent of new diagnostic and therapeutic tools, and regular revision of guidelines for the management of such patients require delivery of additional educational activities for specialists involved in provision of medical care.

In order to improve the level of competence of doctors on the multidisciplinary team engaged in treatment and management of SMA5q patients, in the year 2022 the Institute of Higher and Continuing Professional Education of the N.P. Bochkov Medical Genetic Research Center developed and implemented the supplementary professional education program "Multidisciplinary approach to managing patients with a confirmed diagnosis of 5q spinal muscular atrophy" (36 hours; "the SMA5q CPE Program")[3].

AIM

To evaluate the effectiveness of the professional education program as a tool for improving the level of competence of doctors within multidisciplinary teams providing medical care to SMA5q patients.

MATERIAL AND METHODS

In the course of preparation of this article, the materials were used filled by the course tutors and trainees who underwent training for the SMA5q CPE Program. These materials included entrance control forms, final certification forms, and certification reports, which were provided by the Institute of Higher and Continuing Professional Education of the N.P. Bochkov Medical Genetic Research Center. The statistic analysis of the results was performed by methods of descriptive statistics, and diagrams were prepared in the STSS program (Syunyakov Timur Sergeevich Statistics analyzer).

The aim of the SMA5q CPE Program is to form the capacity and readiness of medical professionals of various specializations to identify pathological conditions, symptoms, syndromes, characteristic of the hereditary SMA5q in patients, to management and treatment of such patients, to use pharmacological and non-pharmacological therapy, as well as other methods.

The form of tuition was in-person training including remote educational technologies and electronic learning as simultaneous learning in the classroom.

The components of the academic program formulated as modules are presented in **Table 1**, and the contents of modules is shown in **Tables 2-4**.

The entrance control had 12 questions with four choice options. The qualification class included two forms of control, an interview and a test. The final testing included questions for each of the three modules: "Hereditary SMA5q: etiopathogenesis, classification, specifics of clinical manifestations, diagnostics" (12 open questions and 14 multiple-choice questions); "Implementation of a multidisciplinary approach in provision of medical care to SMA5q patients" (29 control questions and 45 test tasks); "Legal, ethical and coordination aspects of the multidisciplinary approach provision of medical care to SMA5q patients" (9 control questions and 12 test tasks). The test cards for the qualification class contained three control questions (one for each module) and fifteen test tasks.

[1] Approved by the Order of the Ministry of Labor and Social Protection of the Russian Federation dated 29 January 2019 No.51n, as amended 25 September 2023.
[2] Approved by the Order of the Ministry of Science and Higher Education of the Russian Federation dated 2 February 2022 No. 103.
[3] The Program is approved by the Education and methodology Commission of the IHCPE of Medical Genetic Research Center (Protocol No. 2 dated 06 May 2022); the first curriculum is approved by the Order of the Director of Medical Genetic Research Center dated 11 May 2022 No.19-DPO.

Topics, Elements and Sub-elements
Structure and functions of the peripheral neuromotor apparatus
Structure of peripheral motor neurons and principle of their functioning
Pathogenic mechanisms of hereditary spinal muscular atrophies and functional roles of disease-associated gene products
Classification of hereditary spinal muscular atrophies
Clinical and genetic characteristics of hereditary spinal muscular atrophies
Clinical, genetic and neurophysiological characteristics of SMA5q
Interpretation of results of neurophysiological examination in cases of suspected SMA5q
Differential diagnostics of hereditary spinal muscular atrophies with other groups of neuromuscular diseases
Medical and genetic counseling for families with a history of SMA5q
Principles of genealogy analysis in inherited disorders and genetic status determination for relatives of SMA5q probands
Approaches to prevention of recurrent cases
Methods of molecular genetic diagnostics of SMA5q
Molecular genetic foundations of SMA5q
Screening methods: requirements, limitations, possibilities
SMA5q diagnostic methods: requirements, limitations, possibilities
Methods used to diagnose SMA5q carrier status
Prenatal and pre-implantation SMA5q diagnostics
Summary on molecular genetic study of SMA5q

Table 2. *Contents of the module "SMA5q: etiopathogenesis, classification, features of clinical manifestations and diagnostics"*

Таблица 2. *Содержание модуля «СМА5q: этиопатогенез, классификация, особенности клинических проявлений и диагностика»*

Topics, Elements and Sub-elements
Respiratory function in SMA5q patients
Principles of modern approaches to organization and delivery of respiratory support for SMA5q patients
Criteria of monitoring efficiency of respiratory support
Diagnostics of acute respiratory disorders in SMA5q patients; methods of management of life-threatening situations
General approaches to home-based non-invasive ventilation (NIV)
Emergency and urgent care for acute conditions (e.g., decannulation, aspiration) and respiratory support in infectious diseases in SMA5q patients
Coordination of work of pulmonologists and respiratory support specialists in the multidisciplinary team managing SMA5q patients
Digestion function in SMA5q patients
Under-nourishment and problem of weight gain, growth and muscular development delay; causes of obesity in SMA5q
Correction of nutritive status and principles of nutritional support to provide adequate nutrition to SMA5q patients
Pathological disorders of the intestinal tract and their correction in in SMA5q patients
Prevention of aspiration syndrome in impaired deglutition in SMA5q patients
Prevention of acute conditions: aspiration, probe displacement and migration, feeding tube obstruction, peristomal infections, metabolic disorders in SMA5q patients
Musculoskeletal system in SMA5q patients
Diagnostics of pathological changes in the musculoskeletal system
Approaches to physiotherapeutic and orthopedic correction in children with SMA5q of various types
Orthopedic support: prevention and treatment, including surgical treatment, of spinal deformities, subdislocations/dislocations of the hip joint, contractures, osteoporosis-associated fractures
Orthopedic interventions in SMA5q patients
Physical and device-assisted contracture prevention, scoliosis, retention of movement range and prevention of pain syndrome
Practical skills of orthopedic support, rehabilitation procedures and physiotherapy
Coordination and provision of nutritive and respiratory support in patients with orthopedic devices, basics of cooperation between members of the multidisciplinary team
Home-based adaptation activities to ensure maximum independence of patients
Basic principles and methods of assessment of condition and treatment of SMA5q patients
Principles of assessment of SMA5q patients using motor function scales
Motor function scale in SMA5q (Hammersmith Functional Motor Scale Expanded (HFMSE)
Revised Upper Limb Module (RULM)
Children's Hospital of Philadelphia Infant Test of Neuromuscular Development, CHOP-INTEND
6-minute walking test in SMA5q patients (6MWT)
Modern approaches to pathogenetic therapy of SMA5q
Possibilities of gene therapy of SMA5q and methods of agent administration
Recommendations on choosing drugs for SMA5q gene therapy from the list of drugs registered in the Russian Federation: Nusinersen, Ridisplam, Onasemnogene abeparvovec
Long-term intrathecal therapy of SMA5q with Nusinersen
Regulations of oral drug use
Specifics of pathogenetic treatment of patients of AVL/NIV and feeding through the feeding tube
Rehabilitation procedures in patients with varied clinical manifestations
Principles of symptomatic therapy in SMA5q patients on pathogenetic therapy
Assessment of efficiency of pathogenetic therapy in compliance with standards as per generally accepted clinical scales
Palliative care of SMA5q patients
Definition and formalization of indication for palliative medial care to children and adults with SMA5q within the functions of the medical advisory commission of healthcare institutions
Principles of organization of outpatient and inpatient palliative care to patients with SMA5q, patient routing and interdisciplinary cooperation of specialists
Provision of medical devices for the support of organ and system functions to SMA5q patient
Principles of effective communication and psychosocial support of SMA5q pediatric patients and their family members. Principles of delivering bad news; methodology for shared decision-making between physicians and legal guardians in the provision of palliative medical care; educational and recreational needs of a child with SMA5q receiving palliative medical care

Table 3. *Contents of the module "Implementation of a multidisciplinary approach in providing medical care to patients with SMA5q"*

Таблица 3. *Содержание модуля «Реализация многопрофильного подхода в оказании медицинской помощи пациентам со СМА5q»*

Topics, Elements and Sub-elements
Ethical problems of medical and genetic care
Ethical principles of medical and genetic counseling; rights of patients
Ethics of genetic testing
Communication between doctors and patients or their legal representatives
Principles of delivering bad news
Psychological component of medical and genetic counseling
Legal aspects in provision of medical care to SMA5q patients
Fundamentals of legal regulation of procedures of medical care and provision of medicines to patients of SMA5q patients
Rights and obligations of patients and medical personnel implemented in the provision of medical care to SMA5q patients
Legal aspects and procedure of free medical care to SMA5q patients depending on terms and conditions of its provision within the state guarantee program
State programs of preferential provision of medicines
Rules and regulation for the prescription of drugs and specialized products of clinical nutrition and medical products
Special feature of medical care provided with telemedicine technologies
Procedure of communication of medical personnel with the "Krug Dobra" Foundation, "SMA Families" Foundation

Table 4. *Contents of the module "Legal, ethical and coordination aspects of a multidisciplinary approach in providing medical care to patients with SMA5q"*

Таблица 4. *Содержание модуля «Юридические, этические и координационные аспекты многопрофильного подхода при оказании медицинской помощи пациентам со СМА5q»*

Medical specialization	Number of trainees
Neurologists	78
Medical genetics specialists	37
Gastroenterologists	4
Pediatricians	4
Pulmonologists	3
Rehabilitation specialists	2
Orthopedic traumatologists	2
Physiotherapists	1
Physical rehabilitation specialists	1
Physicians	1
Anesthesiologists	1
Nutritionists	1
Palliative care specialists	1

Table 5. *Distribution of doctors trained under the SMA5q CPE by specialization*

Таблица 5. *Распределение врачей, прошедших обучение по Программе по специальностям*

RESULTS

As of January 2025, four groups of trainees received training under this program (136 medical specialists from 39 administrative units of the Russian Federation). The distribution of trainees by specializations and regions is presented in Tables 5, 6.

In the course of entrance control, less than 50% correct answers were given by 69 trainees; 51–70% by 42 trainees; 70–80% by 2 trainees; 23 more trainees did not participate in the entrance control. In the qualification testing of the training program, all trainees showed a relatively high level of competence while performing the test tasks: 70–80% of correct answers were given by 96 trainees; 81–90% by 36 trainees; 91–100% by 4 trainees. At least one control question was correctly answered by 42 trainees; two questions, by 85, and all three questions, by 9 medical specialists. The diagram comparing the results of entrance control and final testing is shown in **Fig. 1**.

Region of the country	No.	Region of Russia	No.
Orenburg Region	49	Belgorod Region	1
Volgograd Region	8	Voronezh Region	1
Moscow	8	Republic of Dagestan	1
Irkutsk Region	7	Izhevsk Region	1
Tyumen Region	7	Kemerovo Region	1
Republic of Bashkortostan	5	Kostroma Region	1
Krasnodar Region	4	Republic of Crimea	1
Moscow Region	4	Kurgan Region	1
Saratov Region	3	Leningrad Region	1
Tomsk Region	3	Magadan Region	1
Republic of Buryatia	2	Novgorod Region	1
Krasnoyarsk Region	2	Novosibirsk Region	1
Oryol Region	2	Omsk Region	1
Rostov Region	2	Penza Region	1
St.-Petersburg	2	Samara Region	1
Republic of North Ossetia-Alania	2	Sverdlovsk Region	1
Stavropol Region	2	Smolensk Region	1
Republic of Yakutia	2	Tver Region	1
Yaroslavl Region	2	Republic of Chechnya	1
Amur Region	1	**Total**	**136**

Table 6. *Distribution of the SMA5q CPE Program students by regions*

Таблица 6. *Распределение обучающихся Программы по регионам*

The trainees found the following questions the most difficult: module "Hereditary SMA5q: etiopathogenesis, classification, specifics of clinical manifestations, diagnostics", section "Clinical and genetic characteristics of hereditary spinal muscular atrophies" (6 correct answers in the entrance control and 101 correct answers in the final test); and from the module "Legal, ethical and coordination aspects of the multidisciplinary approach provision of medical care to SMA5q patients", section "Legal aspects in provision of medical care to SMA5q patients" (11 correct answers in the entrance control and 98 correct answers in the final test). The easiest were the questions related to clinical manifestations of the disease (module "Implementation of a multidisciplinary approach in provision of medical care to SMA5q patients", sections "Basic principles and methods of assessment of condition and treatment of SMA5q patients" and "Musculoskeletal system in SMA5q patients").

DISCUSSION

The first experience of delivery and the analysis of results of SMA5q CPE Program in 2023 showed that the specialists most interested in improving their qualification

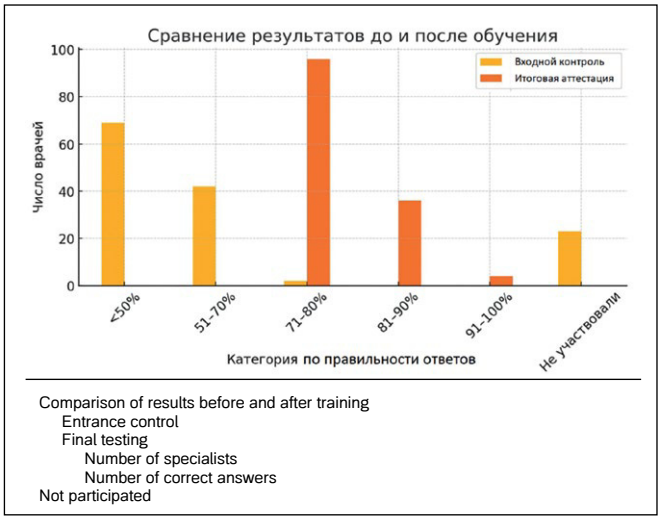

Figure 1. *Comparison diagram of the results of incoming inspection and final certification.*

Рисунок 1. *Диаграмма сравнения результатов входного контроля и итоговой аттестации.*

and gaining new competences in the orphan pathology in question are specialists in neurology and genetics. The demand for training under the SMA5q CPE Program from other specialists is relatively low, which might be related to the actual shortage of personnel in the regions and to the local normative and organizational deficit with respect to provision of medical care to SMA5q patients [15].

Mastering of the considered program provides the specialists of multidisciplinary teams with the necessary knowledge and skills in compliance with the federal state educational standards, and assists in obtaining the lacking skills that are needed to provide medical care to SMA5q patients not specified in the professional standards.

It proved difficult to compare the results of implementation of SMA5q CPE Program with similar programs in Russia and abroad: Elibrary.ru and Cyberleninka databases have no publications on the evaluation of educational programs on SMA5q and orphan diseases generally. PubMed lists only one publication describing a similar initiative [16].

CONCLUSION

The supplementary professional education program "Multidisciplinary approach to managing patients with a confirmed diagnosis of 5q spinal muscular atrophy" (36 hours) proved high efficiency in the improvement of professional competences of specialists of multidisciplinary teams working on provision of medical care to SMA5q patients. Improvement of quality of medical care to this category of patients requires organization of multidisciplinary teams in all administrative units of the Russian Federation, which in its turn calls for active cooperation from the federal and regional ministries and departments of health represented by the respective Chief Consultants thereof.

ADDITIONAL INFORMATION	ДОПОЛНИТЕЛЬНАЯ ИНФОРМАЦИЯ
Study funding. The study was the authors' initiative without external funding.	***Источник финансирования.*** Работа выполнена по инициативе авторов без привлечения финансирования.
Conflict of interest. The authors declare that there are no obvious or potential conflicts of interest associated with the content of this article.	***Конфликт интересов.*** Авторы декларируют отсутствие явных и потенциальных конфликтов интересов, связанных с содержанием настоящей статьи.
Contribution of individual authors. Vlasov Ya.V., Kutsev S.I.: initial idea for creating the manuscript and final proofreading of the text, participation in the development of the educational program, development of test and assessment materials. Sunyakov T.S.: decision making on the choice of statistical methods of analysis, formation of graphs and tables. Gaiduk A.Ya.: preparation of the primary text of the manuscript, participation in the development of the educational program, development of test and assessment materials. Gazheva A.V., Kamynina N.N.: recommendations on the presentation of materials and proofreading of the primary text. Pesneva O.V., Bukharova T.B., Nikitin S.S.: participation in the development of the educational program, development of test and assessment materials, interpretation of students' responses using a scoring system. The authors gave their final approval of the manuscript for submission, and agreed to be accountable for all aspects of the work, implying proper study and resolution of issues related to the accuracy or integrity of any part of the work.	***Участие авторов.*** Власов Я.В., Куцев С.И. – первичная идея создания рукописи и финальная корректура текста, участие в разработке образовательной программы, разработка тестовых и аттестационных материалов. Сюняков Т.С. – принятие решения о выборе статистических методов анализа, формирование графиков и таблиц. Гайдук А.Я. – подготовка первичного текста рукописи, участие в разработке образовательной программы, разработка тестовых и аттестационных материалов. Гажева А.В., Камынина Н.Н. – рекомендации по изложению материалов и корректура первичного текста. Песнева О.В., Бухарова Т.Б., Никитин С.С. – участие в разработке образовательной программы, разработка тестовых и аттестационных материалов, интерпретация ответов обучающихся по балльной системе. Все авторы одобрили финальную версию статьи перед публикацией, выразили согласие нести ответственность за все аспекты работы, подразумевающую надлежащее изучение и решение вопросов, связанных с точностью или добросовестностью любой части работы.

REFERENCES / ЛИТЕРАТУРА

1. Nishio H, Niba ETE, Saito T, et al. Spinal muscular atrophy: the past, present, and future of diagnosis and treatment. *Int J Mol Sci*. 2023;24(15):11939. DOI: 10.3390/ijms241511939

2. Yeo CJJ, Tizzano EF, Darras BT. Challenges and opportunities in spinal muscular atrophy therapeutics [published correction appears in Lancet Neurol. 2024;23(3):e7. DOI: 10.1016/S1474-4422(24)00050-4.]. *Lancet Neurol*. 2024;23(2):205-218. DOI: 10.1016/S1474-4422(23)00419-2

3. Ramdas S, Oskoui M, Servais L. Treatment options in spinal muscular atrophy: a pragmatic approach for clinicians. *Drugs*. 2024;84(7):747-762. DOI: 10.1007/s40265-024-02051-2

4. Giess D, Erdos J, Wild C. An updated systematic review on spinal muscular atrophy patients treated with nusinersen, onasemnogene abeparvovec (at least 24 months), risdiplam (at least 12 months) or combination therapies. *Eur J Paediatr Neurol*. 2024;51:84-92. DOI: 10.1016/j.ejpn.2024.06.004

5. Kutsev SI, Nikitin SS, Dadali EL, et al. *Spinal muscular atrophy 5q. Clinical and genetic characteristics, molecular genetic diagnostics and etiopathogenetic treatment*. M., 2024. (In Russ.). [Куцев С.И., Никитин С.С., Дадали Е.Л., и др. *Спинальная мышечная атрофия 5q. Клинико-генетическая характеристика, молекулярно-генетическая диагностика и этиопатогенетическое лечение*. М., 2024].

6. Voronin SV, Zakharova EYu, Baydakova GV, et al. Advanced neonatal screening for hereditary diseases in Russia: first results and future prospects. *Pediatria n.a. G.N. Speransky*. 2024;103(1):16-29. [Воронин С.В., Захарова Е.Ю., Байдакова Г.В., и др. Расширенный неонатальный скрининг на наследственные заболевания в России: первые итоги и перспективы. *Педиатрия им. Г.Н. Сперанского*. 2024;103(1):16-29]. DOI: 10.24110/0031-403X-2024-103-1-16-29

7. Komarov IA, Malakhova AR, Vasilyeva TP, et al. Socioeconomic efficiency of neonatal screening for spinal muscular atrophy in the Russian Federation. *Neuromuscular Diseases*. 2023;13(3):25-32. [Комаров И.А.,

Малахова А.Р., Васильева Т.П., и др. Социально-экономическая эффективность проведения неонатального скрининга на спинальную мышечную атрофию в Российской Федерации. *Нервно-мышечные болезни*. 2023;13(3):25-32. DOI: 10.17650/2222-8721-2023-13-3-25-32

8. Kutsev SI, Nikitin SS, Ryabykh OS, et al. *Spinal muscular atrophy 5q. Multidisciplinary approach to management of patients with confirmed diagnosis of spinal muscular atrophy 5q*. M., 2024. (In Russ.). [Куцев С.И., Никитин С.С., Рябых О.С., и др. *Спинальная мышечная атрофия 5q. Многопрофильный подход к ведению пациентов с подтвержденным диагнозом спинальная мышечная атрофия* 5q. М., 2024].

9. Keinath MC, Prior DE, Prior TW. Spinal Muscular Atrophy: Mutations, Testing, and Clinical Relevance. *Appl Clin Genet*. 2021;14:11-25. DOI: 10.2147/TACG.S239603

10. Vitkovskaya IP. Study of legal literacy of doctors as an indicator of adequate humanitarian assistance to children suffering from orphan diseases. *Problems of standardization in health care*. 2018;9-10:41-50. [Витковская И.П. Изучение юридической грамотности врачей как показателя адекватной гуманитарной помощи детям, страдающим орфанными болезнями. *Проблемы стандартизации в здравоохранении*. 2018;9-10:41-50]. DOI: 10.26347/1607-2502201809-10041-050

11. Kutsev SI. Path of a patient with a rare diagnosis: regulatory documents and organization of the process of treatment and diagnosis of an orphan disease in the Russian Federation. *Neuromuscular Diseases*. 2017;7(4):61-63. [Куцев С.И. Путь пациента с редким диагнозом: нормативные документы и организация лечебно-диагностического процесса при орфанном заболевании в Российской Федерации. *Нервно-мышечные болезни*. 2017;7(4):61-63]. DOI: 10.17650/2222-8721-2017-7-4-61-63

12. Beisenbayeva GG, Ryskulova AR, Izbassarova ASh, et al. Analysis of doctors' knowledge on the diagnosis and treatment of spinal muscle atrophy using a developed validated questionnaire. *Phthisiopulmonology*. 2024;4:264-272. [Бейсенбаева Г.Г., Рыскулова А.Р., Избасарова А.Ш., и др. Анализ знаний врачей по диагностике и лечению спинальной мышечной атрофии с помощью разработанного валидированного опросника. *Фтизиопульмонология*. 2024;4:264-272]. DOI: 10.26212/2227-1937.2025.97.65.036

13. Vitkovskaya IP, Pechatnikova NL, Utkin SA, et al. *Registers of rare (orphan) diseases. Algorithm for providing information about a patient with a rare (orphan) disease to the regional segment of the federal register: method. recommendations*. M., 2017. (In Russ.). [Витковская И.П., Печатникова Н.Л., Уткин СА., и др. *Регистры редких (орфанных) заболеваний. Алгоритм предоставления сведений о пациенте с редким (орфанным) заболеванием в региональный сегмент федерального регистра: метод. рекомендации*. М., 2017].

14. Gayduk AJ, Gazheva AV, Pesneva OV, et al. Comparative analysis of the contentof professional and educational standards for the program "Neurology" in the context of the competence of neurologists regarding the management of patients with spinal muscular atrophy 5q. *Vestnik Roszdravnadzora*. 2025;4:83-88. [Гайдук А.Я., Гажева А.В., Песнева О.В., и др. Сравнительный анализ содержания профессионального и образовательного стандартов по программе «Неврология» в рамках исследования компетентности врачей-неврологов относительно вопросов ведения пациентов со спинальной мышечной атрофией 5q. *Вестник Росздравнадзора*. 2025;4:83-88].

15. Gayduk AYa, Gazheva AV, Pesneva OV, et al. Regulatory problems of the rehabilitation organization for patients with spinal muscular atrophy 5q in Russia. *Current problems of health care and medical statistics*. 2023;3:655-667. [Гайдук А.Я., Гажева А.В., Песнева О.В., и др. Проблемы нормативно-правового регулирования организации проведения реабилитационных мероприятий пациентам со спинальной мышечной атрофией 5q в России. *Современные проблемы здравоохранения и медицинской статистики*. 2023;3:655-667]. DOI: 10.24412/2312-2935-2023-3-655-667

16. Tizzano EF, Christie-Brown V, Baranello G, et al. Clinical Trial Readiness for Spinal Muscular Atrophy: Experience of an International Educational-Training Initiative. *Journal of Neuromuscular Diseases*. 2022;9(6):809-820. DOI: 10.3233/JND-221538

Original research | Оригинальное исследование
DOI: https://doi.org/10.35693/SIM687668

Advantages of mesenteric approach to pancreatoduodenectomy for pancreatic head cancer with invasion of great vessels

Mikael G. Abgaryan, Aleksei G. Kotelnikov, Aleksandr N. Polyakov, Ivan G. Avdyukhin, Omar A. Egenov, Henian Sun, Ivan S. Stilidi

N.N. Blokhin National Medical Research Center of Oncology
(Moscow, Russian Federation)

Abstract

Aim – to compare standard and mesenteric approaches to surgical treatment of patients with pancreatic head cancer invading the portal and/or superior mesenteric veins and to evaluate their advantages.

Material and methods. Surgical treatment of 192 patients with pancreatic head cancer with portal and/or superior mesenteric vein invasion was performed. In 43 (22.4%) cases, pancreatoduodenal resection was performed through the mesenteric approach, in the remaining 149 (77.3%) patients, the standard approach to surgical treatment was used.

Results. The median duration of operations with the mesenteric approach was 290 min., with the standard one, 300 min., the median blood loss was 1120 ml and 1800 ml, respectively, p=0.0002. No statistically significant differences in the long-term treatment results were found for mesenteric and standard approaches: progression of pancreatic head adenocarcinoma was diagnosed in 48.8% and 49%, respectively; the median overall survival was 24.5 months and 22.3 months; the median progression-free survival was 21.3 months and 22.1 months, respectively. Analysis of long-term treatment results depending on the type of approach and the degree of radicality of surgical intervention showed that the incidence of local relapse with standard access in non-radically operated patients is significantly higher (40.6% vs 7.7%, p = 0.001).

Conclusion. The advantages of the mesenteric approach over the standard approach to surgical treatment of patients with pancreatic head cancer with portal and/or superior mesenteric vein invasion are as follows: 1) it makes it possible to assess the prevalence and operability of the tumor as early as at the beginning of the surgical intervention; 2) it ensures a significantly higher frequency of operations in the R0 volume; 3) it ensures significantly less blood loss during surgery; 4) after circular resection of the main veins it provides more opportunities to perform end-to-end plastic surgery, which reduces the risk of thrombosis due to the formation of only one anastomosis and reduces the time of clamping of the main veins, reducing the risk of liver and intestinal ischemia.

Keywords: mesenteric approach; pancreatic head cancer; pancreaticoduodenectomy; portal vein resection; superior mesenteric vein resection.

Conflict of interest: nothing to disclose.

Citation
Abgaryan MG, Kotelnikov AG, Polyakov AN, Avdyukhin IG, Egenov OA, Sun Henian, Stilidi IS. **Advantages of mesenteric approach to pancreatoduodenectomy for pancreatic head cancer with invasion of great vessels.** *Science and Innovations in Medicine.* 2025;10(3):232-236.
DOI: https://doi.org/10.35693/SIM687668

Information about authors
Mikael G. Abgaryan – Cand. Sci. (Medicine), Senior Researcher, Oncologist of the Department of Abdominal Oncology No. 1 of the N.N. Trapeznikov Research Institute of Clinical Oncology.
ORCID: 0000-0001-8893-1894
E-mail: abgaryan.mikael@gmail.com
Aleksei G. Kotelnikov – Dr. Sci. (Medicine), Leading Researcher of the Department of Abdominal Oncology No. 2 (Hepatopancreatobiliary Zone Tumors) of the N.N. Trapeznikov Research Institute of Clinical Oncology.
ORCID: 0000-0002-2811-0549
E-mail: kotelnikovag@mail.ru
Aleksandr N. Polyakov – Cand. Sci. (Medicine), Senior Researcher of the Department of Abdominal Oncology No. 2 (Hepatopancreatobiliary Zone Tumors) of the N.N. Trapeznikov Research Institute of Clinical Oncology.
ORCID: 0000-0001-5348-5011
E-mail: dr.alexp@gmail.com
Ivan G. Avdyukhin – oncologist of the Department of Abdominal Oncology No. 1 of the N.N. Trapeznikov Research Institute of Clinical Oncology.
ORCID: 0000-0002-3524-1037
E-mail: ivan.avdyukhin@yandex.ru
***Omar A. Egenov** – Cand. Sci. (Medicine), Oncologist, Department of the Abdominal Oncology No. 2 (Hepatopancreatobiliary Zone Tumors) of the N.N. Trapeznikov Research Institute of Clinical Oncology.
ORCID: 0000-0002-8681-7905
E-mail: egenov.omar@mail.ru
Henian Sun – oncologist of the Department of Abdominal Oncology No. 1 of the N.N. Trapeznikov Research Institute of Clinical Oncology.
ORCID: 0000-0001-5574-0047
E-mail: sunalaric@gmail.com
Ivan S. Stilidi – Academician of the Russian Academy of Sciences, Dr. Sci. (Medicine), Director.
ORCID: 0000-0002-0493-1166
E-mail: biochimia@yandex.ru
Corresponding Author

Received: 01.07.2025
Accepted: 05.08.2025
Published: 12.08.2025

Преимущества брыжеечного доступа к панкреатодуоденальной резекции при раке головки поджелудочной железы с инвазией магистральных сосудов

М.Г. Абгарян, А.Г. Котельников, А.Н. Поляков, И.Г. Авдюхин, О.А. Егенов, Хэнянь Сунь, И.С. Стилиди

ФГБУ «Национальный медицинский исследовательский центр онкологии имени Н.Н. Блохина» Минздрава России (Москва, Российская Федерация)

Аннотация

Цель – сравнить стандартный и брыжеечный доступы к хирургическому лечению больных раком головки поджелудочной железы, инвазирующим воротную и/или верхнюю брыжеечную вены, и оценить их преимущества.

Материал и методы. Проведено хирургическое лечение 192 больных раком головки поджелудочной железы с инвазией воротной и/или верхней брыжеечной вены. В 43 (22,4%) случаях панкреатодуоденальную резекцию выполнили через брыжеечный доступ, у остальных 149 (77,3%) пациентов использовали стандартный подход к хирургическому лечению.

Результаты. Медиана длительности операций с брыжеечным доступом составила 290 мин., со стандартным – 300 мин., медиана кровопотери – соответственно 1120 мл и 1800 мл, p=0,0002. Статистически значимых различий отдаленных результатов лечения при брыжеечном и стандартном доступах не выявлено: прогрессирование аденокарциномы головки поджелудочной железы диагностировано соответственно у 48,8% и 49%, медиана общей выживаемости составила 24,5 мес. и 22,3 мес., медиана выживаемости без прогрессирования – 21,3 мес. и 22,1 мес. соответственно. Анализ отдаленных результатов лечения в зависимости от вида доступа и степени радикальности хирургического вмешательства показал, что частота развития местного рецидива при стандартном доступе у нерадикально оперированных больных достоверно выше (40,6% vs 7,7%, p=0,001).

Заключение. Преимущества брыжеечного доступа перед стандартным подходом к хирургическому лечению больных раком головки поджелудочной железы с инвазией воротной и/или верхней брыжеечной вены заключаются в следующем: 1) дает возможность оценить распространенность и операбельность опухоли уже в начале хирургического вмешательства; 2) обеспечивает достоверно более высокую частоту выполнения операций в объеме R0; 3) обеспечивает достоверно меньшую кровопотерю во время операции; 4) после циркулярной резекции магистральных вен дает больше возможностей выполнить пластику «конец в конец», что снижает риск развития тромбоза за счет формирования только одного анастомоза и уменьшает время пережатия магистральных вен, уменьшая риск ишемии печени и кишечника.

Ключевые слова: брыжеечный доступ; рак головки поджелудочной железы; панкреатодуоденальная резекция; резекция воротной вены; резекция верхней брыжеечной вены.

Конфликт интересов: не заявлен.

Для цитирования:
Абгарян М.Г., Котельников А.Г., Поляков А.Н., Авдюхин И.Г., Егенов О.А., Сунь Хэнянь, Стилиди И.С. **Преимущества брыжеечного доступа к панкреатодуоденальной резекции при раке головки поджелудочной железы с инвазией магистральных сосудов.** *Наука и инновации в медицине.* 2025;10(3):232-236.
DOI: https://doi.org/10.35693/SIM687668

Сведения об авторах

Абгарян М.Г. – канд. мед. наук, старший научный сотрудник, врач-онколог отделения абдоминальной онкологии №1 НИИ Клинической онкологии имени академика РАН и РАМН Н.Н. Трапезникова.
ORCID: 0000-0001-8893-1894
E-mail: abgaryan.mikael@gmail.com

Котельников А.Г. – д-р мед. наук, ведущий научный сотрудник отделения абдоминальной онкологии №2 (опухолей гепатопанкреатобилиарной зоны) НИИ Клинической онкологии имени академика РАН и РАМН Н.Н. Трапезникова.
ORCID: 0000-0002-2811-0549
E-mail: kotelnikovag@mail.ru

Поляков А.Н. – канд. мед. наук, старший научный сотрудник отделения абдоминальной онкологии №2 (опухолей гепатопанкреатобилиарной зоны) НИИ Клинической онкологии имени академика РАН и РАМН Н.Н. Трапезникова.
ORCID: 0000-0001-5348-5011
E-mail: dr.alexp@gmail.com

Авдюхин И.Г. – врач-онколог отделения абдоминальной онкологии №1 НИИ Клинической онкологии имени академика РАН и РАМН Н.Н. Трапезникова.
ORCID: 0000-0002-3524-1037
E-mail: ivan.avdyukhin@yandex.ru

***Егенов Омар Алиевич** – канд. мед. наук, врач-онколог отделения абдоминальной онкологии №2 (опухолей гепатопанкреатобилиарной зоны) НИИ Клинической онкологии имени академика РАН и РАМН Н.Н. Трапезникова.
ORCID: 0000-0002-8681-7905
E-mail: egenov.omar@mail.ru

Сунь Хэнянь – врач-онколог отделения абдоминальной онкологии №1 НИИ Клинической онкологии имени академика РАН и РАМН Н.Н. Трапезникова.
ORCID: 0000-0001-5574-0047
E-mail: sunalaric@gmail.com

Стилиди И.С. – академик РАН, профессор, д-р мед. наук, директор.
ORCID: 0000-0002-0493-1166
E-mail: biochimia@yandex.ru

Автор для переписки

Список сокращений

ПЖ – поджелудочная железа; ПДР – панкреатодуоденальная резекция; ВБВ – верхняя брыжеечная вена; ВВ – воротная вена.

Получено: 01.07.2025
Одобрено: 05.08.2025
Опубликовано: 12.08.2025

INTRODUCTION

The literature contains very few reports on the mesenteric approach for surgical treatment of pancreatic head cancer. The first publication on the mesenteric approach to pancreatoduodenal resection appeared as late as in 1993. Japanese surgeons A. Nakao *et al*. suggested the mesenteric approach using the principal rule of oncological surgery as the guide: minimal contact with the tumor prior to its mobilization and vessel ligation [1]. The authors developed an approach through the root of the transverse mesocolon to sequentially expose the branches of the superior mesenteric artery. This provided the possibility of evaluating the resectability of the tumor as early as on the start of the surgical intervention, dissecting the tissue from the side not affected by the tumor, ligate the lower pancreoduodenal artery and other branches of the superior mesenteric artery in the early stages of the surgery, perform lymphadenectomy around the superior mesenteric artery and the superior mesenteric vein (SMV), facilitated the reconstruction of the portal vein in the formation of the end-to-end anastomosis, facilitated decrease of venous congestion in the area of the pancreatic head, minimize the intraoperative blood loss and improve the possibilities of performing the radical resection of the tumor [2, 3]. In 2007, I. Gockel *et al*. [4] reported the use of mesenteric approach to perform the total resection of the 'mesopancreas'. This anatomic term has been mentioned in the literature only in the recent years similarly to the term 'mesorectum' and the surgery of total mesorectumectomy in colorectal cancer [4]. No final definition of the 'mesopancreas' has been formed to date despite the fact that the Japanese classification of pancreatic cancer [5] contains a detailed description of the anatomy of extrapancreatic neural plexi. In the literature, 'mesopancreas' is in many cases identified as the 'reproportal plate' [6–8], referring to the retroperitoneal adipose tissue located posterior to the pancreas and the portal vein and anterior to the aorta, between the origins of the superior mesenteric artery and the celiac trunk. This is not absolutely true from the anatomical standpoint, since microscopically it is the adipose tissue and the neural plexi of the pancreatic head (PLphI and PLphII), limited by the visceral arteries and not covered with fascia [9–12]. However, the term 'mesopancreas' is important from the clinical and surgical perspectives, since resection of the entire aforementioned complex of tissues is actually a radical resection [10, 13, 14].

Considering the clinical relevance of this issue and the near absence of studies comparing mesenteric and standard approaches for surgical treatment of pancreatic head cancer, we present the results of our investigation.

AIM

To compare standard and mesenteric approaches to surgical treatment of patients with pancreatic head cancer invading the portal and/or superior mesenteric veins and to evaluate their advantages.

MATERIAL AND METHODS

This study includes a retrospective analysis of 192 patients' records who had undergone surgical treatment of the pancreatic head invading the portal and/or superior mesenteric veins at the N.N. Blokhin National Medical Research Center of Oncology of the Ministry of Health of Russia in 2002-2023. In 43 (22.4%) cases, pancreatoduodenal resection was performed through the mesenteric approach, in 149 (77.3%) patients, the standard approach to surgical treatment was used. Mesenteric approach was used in 2 (12.5%) of the 16 patients with resection of the portal vein; in 15 (18.1%) of 83 patients with resection of the superior mesenteric vein; in 26 of 93 patients (28%), with resection of both major veins (portal and superior mesenteric veins).

Circular resection of the principal veins was performed in 36 (83.7%) patients using mesenteric approach and 108 (72.5%) patients using standard approach, the median length of resection was 4 cm (from 1.5 to 8 cm) and 3 cm (from 0.5 to 1 cm), respectively, with a statistically significant difference between medians, p=0.0009 (Table 1).

The reconstruction of the principal veins in these patients was performed as follows:

1) End-to-end anastomosis in 21 (48.8%) and 76 (51%) patients, median length: 3 cm (from 1.5 to 7 cm) and 2 cm (from 0.5 to 4.5 cm), respectively, with a statistically significant difference between medians, p=0.007;

2) Autovenous prosthetic repair in 2 (4.7%) and 4 (2.7%) patients, median length: 4.5 cm (4 and 5 cm) and 3.5 cm (from 2 to 4 cm);

3) Gore-Tex synthetic prosthetic repair in 13 (30.2%) and 28 (18.8%) patients, with credible difference between groups, p=0.083. The median lengths were 5 cm and 3 cm, respectively, with a statistically significant difference between medians, p=0.006.

Partial wall resection was performed in 7 (16.3%) and 41 (27.5%) patients, with median resection lengths of 2 cm and 1.5 cm, respectively. For reconstruction, a running suture technique was used, with median suture lengths of 2 cm and 1.5 cm for each group.

RESULTS

The histological study identified adenocarcinoma in all 192 patients included in the study. The R0 tumor resection rate, confirmed histologically, was 97.7% (n=42) with the mesenteric approach and credibly exceeded this value in the standard approach to surgery: only 78.5% (n=117, p=0.001). R1 surgeries were performed in 2.3% (n=1) patients with mesenteric approach and 19.5% (n=29, p=0.003) with standard approach; R2 surgeries, in 0% and 2%, respectively. The medians of surgery durations in the mesenteric and standard approaches were near similar, 290 and 300 minutes, respectively; at the same time, the median blood loss in the mesenteric approach is credibly lower, 1120 ml vs. 1800 ml, p=0.0002. The blood loss under mesenteric approach varied from 200 ml to 3200 ml, with the standard approach, from 50 ml to 8500 ml.

We identified no statistically significant differences in the remote outcomes of treatment of patients with pancreatic head cancer with invasion of major veins regardless of the type of surgical approach. Progression of adenocarcinoma of the pancreatic head was diagnosed in 48.8% (n=21) patients with mesenteric approach and in 49% (n=73) patients with standard approach. The local recurrence rate was 14% (n=6) and 14.8% (n=22) respectively, the mortality rate was 55.8% (n=24) and 56.4% (n=84), the median survival rate was 24.5 months and 22.3 months, the median progression-free survival was 21.3 months and 22.1 months. At the moment of the study completion, 41.9% (n=18) of patients with mesenteric approach and 42.3% (n=63) with standard approach remained alive without evidence of disease; tumor progression was observed in 2.3% (n=1) and 1.3% (n=2) of patients, respectively/ Deaths occurred due to surgical complications: 9.3% (n=4) and 8.7% (n=13); or disease progression 46.5% (n=20) and 47.7% (n=71).

Since we found no statistically significant differences in long-term treatment outcomes based on surgical approach, we evaluated its impact in combination with the degree of radical

Parameter		Approach type			
		Standard (n=149)		Mesenteric (n=43)	
		Abs.	%	Abs.	%
Portal and/or superior mesenteric vein resection type					
Circular	Type	108	72,5	36	83,7
	Length, cm (min-max)	3 [2,5; 4] (0,5-10)		4* [3; 5,8 (1,5-8,0) *0,0009*	
Partial wall	Type	41	27,5	7	16,3
	Length, cm (min-max)	1,5 [1; 2] (0,5-3,5)		2 [1,5; 2,5] (0,5-2,5)	
Portal and/or superior mesenteric vein reconstruction type					
Running suture Median length, cm (min-max)		41	27,5	7	16,3
		1,5 [1; 2] (0,5-3,5)		2 [1,5; 2,5] (0,5-2,5)	
End-to-end Median length, cm (min-max)		76	51,0	21	48,8
		2,5 [2; 3,5] (0,5-4,5)		3 [2,5; 5,0] (1,5-7)* *0,007*	
Autovenous prosthesis Median length, cm (min-max)		4	2,7	2	4,7
		3,0 [2,5; 3,5] (2-4)		4,5 [4; 5] (4-5)	
Synthetic prosthesis Median length, cm (min-max)		28	18,8	13	30,2 *0,083*
				5 [4; 6] (3-8)* *0,006*	
Degree of radicality of the surgery					
R0		117	78,5	42	97,7* *0,001*
R1		29	19,5	1	2,3* *0,003*
R2		3	2,0	-	-
Медиана длительности операции, мин. (мин-макс)		300 [255; 360] (190-640)		290 [240; 330] (190-460)	
Медиана кровопотери, мл (мин-макс)		1800 [900; 3000] (50,0-8500,0)		1120* [700; 1500] (200,0-3200,0) *0,0002*	

***Statistically significant differences as compared to the standard approach, p<0.05*

Table 1. *Characteristics of standard and mesenteric approaches to surgical treatment of patients with cancer of the head of the pancreas with invasion of the major veins*

Таблица 1. *Характеристика стандартного и брыжеечного доступов к хирургическому лечению больных раком головки ПЖ с инвазией магистральных вен*

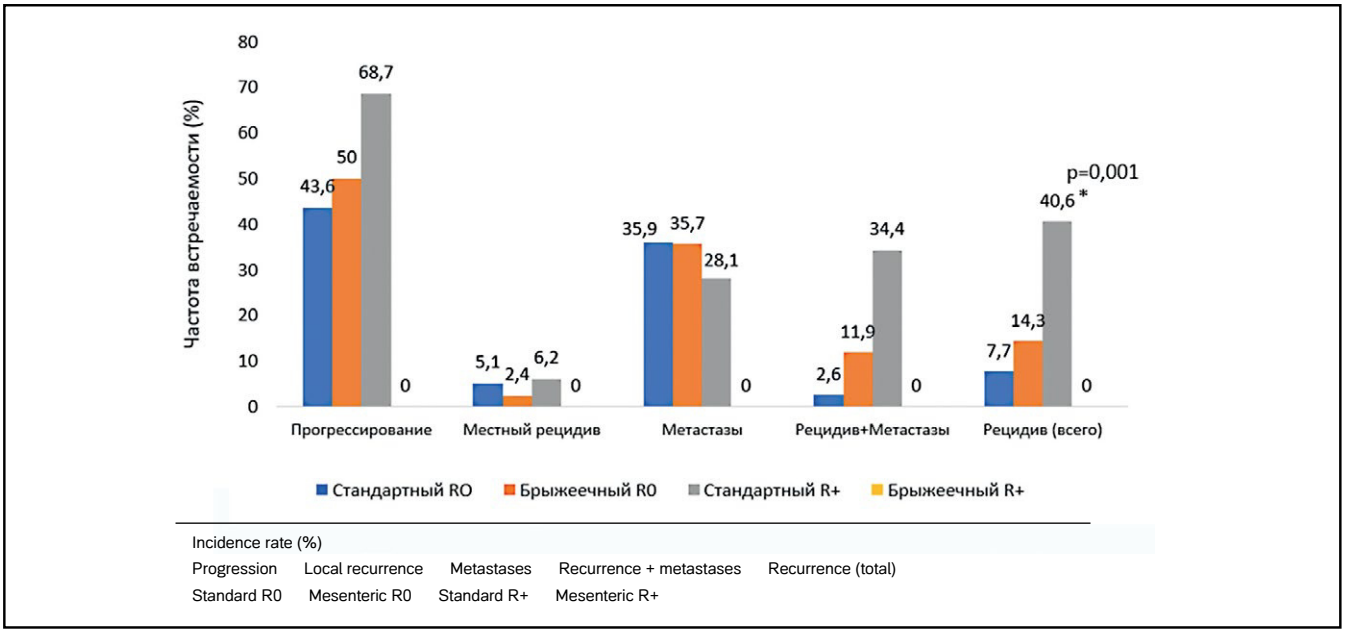

resection (Fig. 1). This approach allowed identification of a credibly more frequent development of local recurrences in non-radically operated patients with standard approach (40.6% vs. 7.7%, p=0.001).

Figure 1. *Types and frequency of progression of pancreatic head cancer with invasion of the major veins depending on access to surgical treatment and the degree of its radicality.*

Рисунок 1. *Виды и частота прогрессирования рака головки ПЖ с инвазией магистральных вен в зависимости от доступа к хирургическому лечению и степени его радикальности.*

DISCUSSION

Considering many years of clinical practice, this comparative study of mesenteric versus standard approaches for pancreatic head cancer with portal vein and/or superior mesenteric vein invasion demonstrates clear advantages of the mesenteric technique. Although the mesenteric approach required higher qualification of the operating surgeon, it gives the opportunity of performing radical surgeries credibly more frequently (p=0.001). We were able to perform R0 resection of the tumor invading the major veins in 97.7% patients, whereas similar radical surgeries using the standard approach were possible only in 78.5% patients.

The mesenteric approach also demonstrates a definitive advantage of significantly reduced intraoperative blood loss (p=0.0002). In our study, median blood loss in patients with mesenteric approach was 1200 ml, whereas in the standard approach it reached 1800 ml. Maximum individual blood loss in mesenteric approach was 3200 ml, whereas in the standard approach is was 2.6 times higher at 8500 ml. We believe that the reduced blood loss results from the ability provided by the mesenteric approach to assess tumor extent and resectability early in the operation, to ligate vessels feeding the tissues of the operating area, e.g. gastroduodenal and pancreaticoduodenal arteries.

Our analysis of the options of resection and reconstruction of major veins depending on the approach to the operating field showed that the mesenteric approach provides wide opportunities of end-to-end reconstruction of the portal vein and/or superior mesenteric vein without using the prosthetic after circular resection. Formation of only one anastomosis significantly reduces the risk of thrombosis development. In the mesenteric approach, we formed the end-to-end anastomosis in the statistically greater resection length (p=0.007), which in individual cases reached 7 cm.

We identified no statistically significant effect of the approach on the long-term outcomes of surgical treatment of pancreatic head cancer with invasion into major veins. However, the analysis of long-term outcomes depending on the approach type and degree of radicality of surgery showed a credibly more frequent development of local recurrence in the standard approach in non-radically operated patients (40.6% vs. 7.7%, p=0.001). It is to me mentioned that by the end of the study the single non-radically operated patient with mesenteric approach survived without signs of tumor progression for 12 months after the surgery and adjuvant chemotherapy.

CONCLUSION

The advantages of mesenteric approach to surgical treatment of patients with pancreatic head cancer with invasion into portal and/or superior mesenteric vein were identified as follows: 1) possibility of assessing tumor extent and operability early in the procedure, 2) credibly more frequent R0 surgeries performance, 3) credibly reduced intraoperative blood loss, 4) more opportunities of end-to-end major vein reconstruction after the circular resection, which decreases the risk of thrombosis by forming just one anastomosis and reduces the time of compression of major veins, thus lowering the risk of ischemia of the liver and the intestines.

ADDITIONAL INFORMATION	ДОПОЛНИТЕЛЬНАЯ ИНФОРМАЦИЯ
Ethical Approval Statement. The article was performed as part of the dissertation "Angioplasty operations in abdominal oncology" for the degree of Doctor of Medical Sciences. The thesis topic was approved by the Scientific Council of the Scientific Research Institute of Clinical Oncology n.a. Academician of the Russian Academy of Sciences and the Russian Academy of Medical Sciences N.N. Trapeznikov, Blokhin National Research Medical Center of Oncology, Ministry of Health of the Russian Federation.	***Этическая экспертиза.*** Статья выполнена в рамках диссертации «Ангиопластические операции в абдоминальной онкологии» на соискание ученой степени доктора медицинских наук. Тема диссертации утверждена на ученом совете НИИ Клинической онкологии имени академика РАН и РАМН Н.Н. Трапезникова ФГБУ НМИЦ онкологии имени Н.Н. Блохина Минздрава России.
Study funding. The study was the authors' initiative without external funding.	***Источник финансирования.*** Работа выполнена по инициативе авторов без привлечения финансирования.
Conflict of interest. The authors declare that there are no obvious or potential conflicts of interest associated with the content of this article.	***Конфликт интересов.*** Авторы декларируют отсутствие явных и потенциальных конфликтов интересов, связанных с содержанием настоящей статьи.
Contribution of individual authors. Abgaryan M.G., Avdyukhin I.G., Egenov O.A., Sun H.: data collection, analysis and interpretation, preparation of the text of the article. Stilidi I.S.: study concept and design. Kotelnikov A.G., Polyakov A.N.: editing of the article. The authors gave their final approval of the manuscript for submission, and agreed to be accountable for all aspects of the work, implying proper study and resolution of issues related to the accuracy or integrity of any part of the work.	***Участие авторов.*** Абгарян М.Г., Авдюхин И.Г., Егенов О.А., Сунь Х. – сбор, анализ и интерпретация данных, подготовка текста статьи. Стилиди И.С. – концепция и дизайн работы. Котельников А.Г., Поляков А.Н. – редактирование текста статьи. Все авторы одобрили финальную версию статьи перед публикацией, выразили согласие нести ответственность за все аспекты работы, подразумевающую надлежащее изучение и решение вопросов, связанных с точностью или добросовестностью любой части работы.

REFERENCES / ЛИТЕРАТУРА

1. Nakao A, Takagi H. Isolated pancreatectomy for pancreatic head carcinoma using catheter bypass of the portal vein. *Hepato-Gastroenterology*. 1993;40(5):426-429.

2. Nakao A, Harada A, Nonami T, et al. Lymph node metastases in carcinoma of the head of the pancreas region. *The British Journal of Surgery*. 1995;82(3):399-402. DOI: 10.1002/bjs.1800820340

3. Kuroki T, Eguchi S. No-touch isolation techniques for pancreatic cancer. *Surg Today*. 2017;47(1):8-13. DOI: 10.1007/s00595–016–1317–5

4. Gockel I, Domeyer M, Wolloscheck T, et al. Resection of the mesopancreas (RMP): a new surgical classification of a known anatomical space. *World Journal of Surgical Oncology*. 2007;5:44. DOI: 10.1186/1477-7819-5-44

5. Ishida M, Fujii T, Kishiwada M, et al. Japanese classification of pancreatic carcinoma by the Japan Pancreas Society: Eighth edition. *Journal of Hepato-Biliary-Pancreatic Sciences*. 2024;31(11):755. DOI: 10.1002/JHBP.12056

6. Adham M, Singhirunnusorn J. Surgical technique and results of total mesopancreas excision (TMpE) in pancreatic tumors. *European Journal of Surgical Oncology*. 2012;38(4):340-345. DOI: 10.1016/J.EJSO.2011.12.015

7. Pandanaboyana S, Loveday B, Windsor JA. Artery First Approach to Pancreatic Cancer Resection: A Review of the Evidence for Benefit. *J Pancreas (Online)*. 2017;18(5):369-371. URL: https://www.primescholars.com/articles/artery-first-approach-to-pancreatic-cancer-resection-a-review-of-the-evidence-for-benefit-99162.html

8. Pessaux P, Varma D, Arnaud JP. Pancreaticoduod enectomy: superior mesenteric "artery-first" approach. *J Gastrointest Surg*. 2006;10(4):607-11. DOI: https://doi.org/10.1016/j. gassur.2005.05.001

9. Bouassida M, Mighri MM, Chtourou MF, et al. Retroportal lamina or mesopancreas? Lessons learned by anatomical and histological study of thirty three cadaveric dissections. *International Journal of Surgery (London, England)*. 2013;11(9):834-836. DOI: 10.1016/j.ijsu.2013.08.009

10. Weitz J, Rahbari N, Koch M, Büchler MW. The "artery-first" approach for resection of pancreatic head cancer. *J Am Coll Surg*. 2010;210(2):e1-4. DOI: 10.1016/j.jamcollsurg.2009.10.019

11. Sanjay P, Takaori K, Govil S, et al. "Artery-first" approaches to pancreatoduodenectomy. *Br J Surg*. 2012;99(8):1027-35. DOI: 10.1002/bjs.8763

12. Inoue Y, Saiura A, Tanaka M, et al. Technical Details of an Anterior Approach to the Superior Mesenteric Artery During Pancreaticoduodenectomy. *J Gastrointest Surg*. 2016;20:1769-1777. DOI: 10.1007/s11605-016-3214-z

13. Gaedcke J, Gunawan B, Grade M, et al. The mesopancreas is the primary site for R1 resection in pancreatic head cancer: relevance for clinical trials. *Langenbeck's Archives of Surgery*. 2010;395(4):451-458. DOI: 10.1007/s00423-009-0494-8

14. Peparini N, Chirletti P. Mesopancreas: a boundless structure, namely R1 risk in pancreaticoduodenectomy for pancreatic head carcinoma. *European Journal of Surgical Oncology: The Journal of the European Society of Surgical Oncology and the British Association of Surgical Oncology*. 2013;39(12):1303-1308. DOI: 10.1016/j.ejso.2013.10.012

Original research | Оригинальное исследование
DOI: https://doi.org/10.35693/SIM686422

Prediction of recurrence-free survival in patients with renal cell carcinoma and tumor thrombosis of the renal and inferior vena cava of levels I–II using an extended Cox model and machine learning methods

Musabek K. Mirzabekov[1], Nikolai D. Tikhonskii[2], Mikhail I. Shkolnik[1], Oleg A. Bogomolov[1], Nina V. Trukhacheva[2]

[1]Russian Scientific Center for Radiology and Surgical Technologies named after Academician A.M. Granov (Saint Petersburg, Russian Federation)
[2]Altai State Medical University (Barnaul, Russian Federation)

Abstract

Aim – to compare the predictive accuracy of Cox regression and machine learning (ML) methods regarding recurrence-free survival in patients with locally advanced renal cell carcinoma after radical treatment. Additionally, to investigate an extended Cox model in which the risk function is formed using a neural network approximator (DeepSurv).

Material and methods. This study conducted a retrospective analysis of data from patients diagnosed with renal cell carcinoma who underwent radical nephrectomy with thrombectomy from the renal and inferior vena cava between 2007 and 2024 at the Federal State Budgetary Institution "RSC for Radiology and Surgical Technologies named after Academician A.M. Granov". The study included 100 patients (54 men and 46 women). The median age was 61.5 years (IQR: 59.7–63). Of the total observations, disease progression was recorded in 41 cases, while in the remaining 59 cases, the data were censored. The models were evaluated based on the concordance index (C-index) and interpreted using SHAP analysis.

Results. The DeepSurv neural network model demonstrated higher predictive accuracy on the test dataset compared to the classical Cox model (C-index: 0.8056 vs. 0.7917, respectively). This indicates a superior ability of DeepSurv to rank patients by individual risk of disease progression. Using SHAP analysis, the key predictors contributing most significantly to the prognosis were identified: tumor size, ISUP grade, level of tumor thrombosis, and histological tumor type. The DeepSurv model enabled the capture of complex nonlinear interactions between features, thereby improving both the interpretability and clinical applicability of the results.

Conclusion. The obtained data confirm the feasibility of using machine learning methods for personalized prognosis and optimization of monitoring strategies in patients with RCC.

Keywords: recurrence-free survival, renal cell carcinoma, tumor thrombosis, Cox model, DeepSurv, machine learning, SHAP, prognosis, oncourology.
Conflict of interest: nothing to disclose.

Citation
Mirzabekov MK, Tikhonskii ND, Shkolnik MI, Bogomolov OA, Trukhacheva NV. **Prediction of recurrence-free survival in patients with renal cell carcinoma and tumor thrombosis of the renal and inferior vena cava of levels I–II using an extended Cox model and machine learning methods.** *Science and Innovations in Medicine.* 2025;10(3):237-242.
DOI: https://doi.org/10.35693/SIM686422

Information about authors
Musabek K. Mirzabekov – postgraduate student.
ORCID: 0009-0003-8365-7672
E-mail: musabek.mirzabekoff@yandex.ru
Nikolai D. Tikhonskii – lecturer at the Department of Physics and Informatics.
ORCID: 0009-0001-3077-1776
E-mail: wirelessm8@mail.ru
Mikhail I. Shkolnik – MD, Dr. Sci. (Medicine), chief researcher, Professor.
ORCID: 0000-0003-0589-7999
E-mail: shkolnik_phd@mail.ru
Oleg A. Bogomolov – MD, Cand. Sci. (Medicine), senior researcher, Associate professor.
ORCID: 0000-0002-5860-9076
E-mail: urologbogomolov@gmail.com
***Nina V. Trukhacheva** – Cand. Sci. (Pedagogics), Associate professor of the Department of Physics and Informatics.
ORCID: 0000-0002-7894-4779
E-mail: tn10@mail.ru
Corresponding Author

Received: 30.05.2025
Accepted: 13.07.2025
Published: 12.08.2025

Прогнозирование безрецидивной выживаемости больных с почечно-клеточным раком и опухолевым тромбозом почечной и нижней полой вены I–II уровней с использованием расширенной модели Кокса и методов машинного обучения

М.К. Мирзабеков[1], Н.Д. Тихонский[2], М.И. Школьник[1], О.А. Богомолов[1], Н.В. Трухачева[2]

[1]ФГБУ «Российский научный центр радиологии и хирургических технологий имени академика А.М. Гранова» Минздрава России (Санкт-Петербург, Российская Федерация)
[2]ФГБОУ ВО «Алтайский государственный медицинский университет» Минздрава России (Барнаул, Российская Федерация)

Аннотация

Цель – сравнить прогностическую точность регрессии Кокса и методов машинного обучения (ML) в отношении безрецидивной выживаемости пациентов с местно-распространенным почечно-клеточным раком после радикального лечения, а также исследовать расширенную модель Кокса, в которой функция риска формируется с использованием нейросетевого аппроксиматора (DeepSurv).

Материал и методы. В данном исследовании был проведен ретроспективный анализ данных пациентов с диагнозом «почечно-клеточный рак», перенесших радикальную нефрэктомию с тромбэктомией из почечной и нижней полой вены в период с 2007 по 2024 годы в ФГБУ «РНЦРХТ им. акад. А.М. Гранова». В исследование включены 100 пациентов (54 мужчины и 46 женщин). Медианный возраст составил 61,5 года (IQR: 59,7–63). Из общего числа наблюдений в 41 случае было зафиксировано прогрессирование заболевания, в остальных 59 случаях данные были цензурированные. Оценка моделей проводилась на основе индекса конкордации (C-index) и интерпретировалась с использованием SHAP-анализа.

Результаты. Нейросетевая модель DeepSurv продемонстрировала более высокую прогностическую точность на тестовой выборке по сравнению с классической моделью Кокса (C-index: 0,8056 против 0,7917 соответственно). Это свидетельствует о лучшей способности модели DeepSurv ранжировать пациентов по индивидуальному риску прогрессирования. С помощью SHAP-анализа установлены ключевые предикторы, вносящие наибольший вклад в прогноз: размер опухоли, степень злокачественности (ISUP-грейд), уровень опухолевого тромбоза и морфологический тип опухоли. Модель DeepSurv позволила учесть сложные нелинейные взаимодействия между признаками, что повысило интерпретируемость и клиническую применимость результатов.

Заключение. Полученные данные подтверждают целесообразность применения методов машинного обучения для персонализированного прогноза и оптимизации тактики наблюдения у больных с почечно-клеточным раком.

Ключевые слова: безрецидивная выживаемость, почечно-клеточный рак, опухолевый тромбоз, модель Кокса, DeepSurv, машинное обучение, SHAP, прогноз, онкоурология.

Конфликт интересов: не заявлен.

Для цитирования:
Мирзабеков М.К., Тихонский Н.Д., Школьник М.И., Богомолов О.А., Трухачева Н.В. **Прогнозирование безрецидивной выживаемости больных с почечно-клеточный раком и опухолевым тромбозом почечной и нижней полой вены I–II уровней с использованием расширенной модели Кокса и методов машинного обучения.** *Наука и инновации в медицине.* 2025;10(3):237-242. DOI: https://doi.org/10.35693/SIM686422

Сведения об авторах
Мирзабеков М.К. – аспирант.
ORCID: 0009-0003-8365-7672
E-mail: musabek.mirzabekoff@yandex.ru
Тихонский Н.Д. – преподаватель кафедры физики и информатики.
ORCID: 0009-0001-3077-1776
E-mail: wirelessm8@mail.ru
Школьник М.И. – д-р мед. наук, главный научный сотрудник, профессор.
ORCID: 0000-0003-0589-7999
E-mail: shkolnik_phd@mail.ru
Богомолов О.А. – канд. мед. наук, старший научный сотрудник, доцент.
ORCID: 0000-0002-5860-9076
E-mail: urologbogomolov@gmail.com
***Трухачева Нина Васильевна** – канд. пед. наук. доцент кафедры физики и информатики.
ORCID: 0000-0002-7894-4779
E-mail: tn10@mail.ru
Автор для переписки

Получено: 30.05.2025
Одобрено: 13.07.2025
Опубликовано: 12.08.2025

INTRODUCTION

Prediction of recurrence-free survival in patients with renal cell carcinoma after radical surgery is an important task of urologic oncology. The accuracy of assessment of individual progression risk determines both the scheme of post-surgery supervision and the need for adjuvant therapy.

Traditionally, medical studies use the Cox proportionate risk model based on the supposition of linear impact of covariates on the risk function logarithm is used to analyze the time to event:

$$h(t|X) = h_0(t) \cdot e^{\sum b_i X_i} \quad (1)$$

where $h_0(t)$ –base risk function; $\sum b_i X_i$ – linear combination of predictors [1].

At the same time, the classic Cox model has several limitations, especially in the context of complex biomedical data. The main limitation is the suggestion of linearity and additivity of covariate influence on the risk function logarithm. This restricts its capability to model nonlinear or interacting effects, which is critically important for the analysis of heterogeneous oncological populations, e.g. patients with tumor thrombosis of the venous system.

The development of machine learning methods opened the possibility of flexible approximation of the dependence of the risk function from predictors without the need of strict prerequisites of its form [2-4]. Specifically, the DeepSurv neural network architecture is an extension of the Cox model, in which the linear prediction index ir replaced with the output of the multilayer neural network:

$$h(t) = h_0(t)\, e^{g(w_j, x_i)} \quad (2)$$

where $h_0(t)$ is the base risk function; $g(w_j, X_i)$ – result of the work of the neural network on predictors X_i and weighted coefficients w_j. Such a model retains the interpretable structure of the risk function, but demonstrates a significantly higher flexibility in accounting for nonlinear and highly dimensional correlations between the variables.

The use of DeepSurv allows for identification of implicit dependencies, unevident for the classic Cox regression, especially with complex clinical and morphological interactions in place. The question of interpretability remains a highly important aspect as well. This study additionally uses the SHAP method (SHapley Additive exPlanations) that allows for a quantitative assessment of contribution of each feature to the predicted risk [5].

It is thus possible to compare the traditional linear Cox model and its neural network extension using a single clinical sampling. This will allow evaluation of the potential of machine learning methods in the survival prediction tasks, and study the possibilities of interpretation of results in a clinically significant context.

AIM

To compare the predictive accuracy of Cox regression and machine learning (ML) methods regarding recurrence-free survival in patients with locally advanced renal cell carcinoma after radical treatment, and to investigate an extended Cox model in which the risk function is formed using a neural network approximator (DeepSurv).

MATERIAL AND METHODS

This study included a retrospective analysis of records of patients diagnosed with renal cell carcinoma who had undergone radical nephrectomy with thrombectomy from the renal vein and the lower hollow vein in the period from 2007 to 2024 at the Federal State Budgetary Institution "RSC for Radiology and Surgical Technologies named after Acad. A.M. Granov". The study included 100 patients (54 men and 46 women). The median age was 61.5 years (IQR: 59.7–63). Of the total observations, disease progression was recorded in 41 cases, while in the remaining 59 cases, the data were censored.

Exclusion criteria were level III–IV tumor thrombosis (Mayo classification), severe intraoperative complications that required access conversion, and lack of morphological verification of the tumor. The patients in which no progression had been recorded by the end of the study, were regarded as censored cases.

The statistical analysis comprised three successive stages. The primary analysis included an assessment of recurrence-free survival with the Kaplan-Meier method and the log-rank test to compare subgroups. Besides, a set of single-factor Cox regression models was constructed, which enabled a preliminary assessment of significance of clinical and morphological predictors [1].

On the stage of multivariate analysis, the classic Cox model of proportionate risks was developed. It included the clinically significant predictors, and those predictors that had $p < 0.1$ following the outcomes of the univariate analysis. The statistical significance of the factors was assessed with the Wald test, and the analysis was performed with the use of MedCalc and Statistica software suites.

On the final stage, two survival models were built and compared: the classis linear Cox model and the DeepSurv neural network [6]. The two models were trained only on predictors that proved statistically significant in the multivariate analysis ($p < 0.05$). DeepSurv is executed as a neural network approximating the risk function.

In order to assess the quality of the Cox linear model the following were used: Overall Model Fit, Likelihood Ratio Test, and the Wald test. To compare the Cox linear model and the DeepSurv model on the final stage, the concordance index (C-index) was used that measured the model's capability of properly ranking the patients by risk of progression [7]. To interpret the results of the DeepSurv model, the SHAP method was used that enabled a quantitative assessment of contribution made by each predictor to the individual prognosis and the identification of the most valuable risk predictors in the context of the neural network model [5].

RESULTS

On the first stage, the univariate analysis of predictors was performed using the Cox proportionate regression. The following were considered significant factors associated with decrease of time to progression: ISUP degree of malignity ($p = 0.0058$), tumor size ($p < 0.0001$), lymphatic node involvement ($p = 0.0070$), venous invasion ($p = 0.0074$), anemia status ($p = 0.0003$), thrombocytosis ($p = 0.0008$), Charlson comorbidity index ($p = 0.0105$), disease stage ($p < 0.0001$), and the level of tumor thrombosis (level 1: $p = 0.0016$; level 2: $p < 0.0001$). Some variables, such as age and arterial hypertension, did not demonstrate significant influence and were excluded from subsequent analysis (**Table 1**).

Predictors	P (value)
Hemoglobin	0.5087
Age	0.3034
Grade (ISUP)	0.0058
Tumor size, cm	<0.0001
Lymph nodes: indicator 2	0.0070
Level 1	0.0016
Level 2	<0.0001
Venous wall invasion: indicator 2	0.0074
Anemia (Hb <120): indicator 2	0.0003
Thrombocytosis (PLT>400): indicator 2	0.0008
Charlson (index) score	0.0105
Stage	<0.0001
Body mass index	0.1047
LDH_N (lactate dehydrogenase)	0.0520

Table 1. *Results of the Cox Univariate Model*
Таблица 1. *Результаты однофакторной модели Кокса*

On the second stage, the multivariate Cox model was constructed that included the predictors with clinical significance and $p < 0.1$ as per outcomes of the univariate analysis. The resulting model was statistically significant ($\chi^2 = 70.686$, $p < 0.0001$). The following covariates retained their impact on the decrease of recurrent-free survival: ISUP grade ($p = 0.0472$), morphological tumor type ($p = 0.0195$), tumor size ($p = 0.0031$), and the level of tumor thrombosis (level 1: $p = 0.0236$; level 2: $p = 0.0406$) (**Table 2**). Some variables were losing significance, likely due to multicollinearity and probable nonlinear interactions between parameters [8].

To compare the prediction accuracy of survival models, the entire sampling was randomly divided 80:20 into the training ($n = 80$) and testing ($n = 20$) subsamples. Based on the training subsample, both models were built: the classis linear Cox model and the neural network DeepSurv model. Both models were trained on the same subset of predictors chosen as statistically significant following the outcomes of the multivariate analysis ($p < 0.05$), which ensured the correct matching of their prognostic capabilities. In the process of training of the model, steps were taken to control overfitting.

The comparative analysis of prognostic accuracy of survival models is shown in **Table 3**.

Covariate	B	SE	Wald	P	Exp(b)
Charlson index, score	0.118	0.182	0.425	0.514	1.126
ISUP grade	0.3586	0.1807	3.9378	0.0472	1.431
Anemia (Hb<120)	0.6395	0.4694	1.8564	0.1730	1.8956
Body mass index	0.1468	0.09001	2.6593	0.1029	1.15810
Venous wall invasion	0.7418	0.7065	1.1023	0.2938	2.0996
LDH_N (lactate dehydrogenase)	0.3413	0.5506	0.3842	0.5354	1.4067
Lymph nodes	0.5176	0.5597	0.8553	0.3561	1.6781
Morphology	1.3723	0.5874	5.4572	0.0195	3.9445
Tumor size, cm	0.4665	0.1576	8.7603	0.0031	1.5943
Thrombocytosis, PLT_400	0.6035	0.5325	1.2845	0.2571	1.8284
Level_1	1.0505	0.4642	5.1223	0.0236	2.8591
Level_2	1.3413	0.6549	4.1943	0.0406	3.8239

Table 2. *Coefficients and Standard Errors in the Multivariate Model*
Таблица 2. *Коэффициенты и стандартные ошибки в многофакторной модели*

	C_index (training)	C_index (testing)
Cox linear model	0.8500	0.7917
DeepsurvK	0.8537	0.8056

Table 3. *Comparison of the Results of the Cox Linear Model and DeepSurvK*

Таблица 3. *Сравнение результатов построения линейной модели Кокса и DeepSurvK*

The Cox linear model demonstrated a high concordance index on the training sample (C-index = 0.8500) and a moderate decrease on the testing sample (C-index = 0.7917), which meets the expected degree of generalizing capability of linear models. The DeepSurv neural network model showed a similar level of prediction on the training sample (C-index = 0.8537), while showing a higher accuracy on the testing sample (C-index = 0.8056).

Significance of features in the DeepSurv model was visualized with the SHAP method [9]. The respective graph shows a distribution of SHAP-values for each included feature. The higher the absolute SHAP value, the greater the contribution of this feature to the resulting prediction of the risk. The color scale shows the significance of the feature in a specific patient, from low (blue) to high (red). The features are organized by the degree of their influence on the model (**Fig. 1**).

In the course of our study, we confirmed the applicability of the neural network extension of the Cox model (DeepSurv) for survival analysis and compared it with the classic model using a clinical sampling of patients with renal cell carcinoma and thrombosis of veins. Both approaches demonstrated high prediction accuracy (C-index ~0.80), notably, DeepSurv showed a slightly better result on the testing sample (0.8056 vs. 0.7917 in the Cox model). The increase matches the literature data: modern deep neural networks may be similar or even surpass the classic Cox regression in prediction accuracy when analyzing survivability [6, 10]. In particular, a large multicenter study involving 2139 patients with non-metastatic renal cell carcinoma performed by S.-S. Byun *et al.* (2021) showed that DeepSurv is better at predicting recurrence-free and specific survival that the Cox model (e.g., C-index for recurrence-free survival is 0.802 vs. 0.794) [11].

The major advantage of DeepSurv is the absence of the strict prerequisite of linear influence of covariates on the log-risk inherent in the Cox model [6]. The classic Cox regression describes the logarithm of the base risk as the sum of products

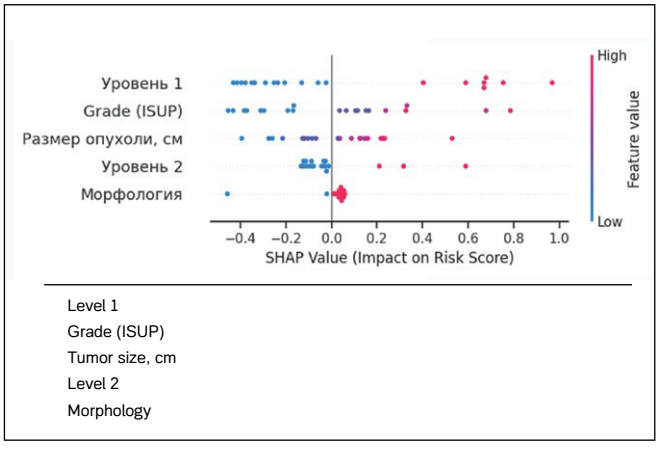

Figure 1. *Results of predictor analysis using the SHAP method.*

Рисунок 1. *Результат анализа предикторов методом SHAP.*

of coefficients multiplied by predictor values, which simplifies interpretation but limits the capability of identifying nonlinear effects and interactions between features. In our multivariate analysis, this was manifested in the following: some variables significant in a univariate analysis (e.g., anemia, thrombocytosis) lost significance on simultaneous inclusion in the model likely due to multicollinearity and overlapping information between related factors. Indeed, high correlation of predictors is known to result in an unstable assessment of coefficients in the Cox regression and their complicated interpretation [12]. The neural network approach of DeepSurv, conversely, is capable of flexible approximation of the connection between the features and survival without the prerequisite of additive nonlinearity. The multilayer network may identify underlying nonlinear dependencies not accessible to the classic model thereby taking into account the multifactor interactions (e.g., mutual influence of correlated clinical and morphological features). Furthermore, implementation of methods of regularization and decrease of feature dimensions improves the stability of deep models towards noise and data multicollinearity [6].

Interpretability remains a significant issue of implementation of deep learning methods into clinical practice. We solved this problem by using SHAP, a contemporary approach facilitating quantitative assessment of the contribution of each feature to the prediction of the model [13]. The results of the SHAP-analysis (Fig. 1) show that the greatest influence on the progression risk in the DeepSurv model came from the tumor size, degree of malignity (ISUP grade), level of tumor thrombosis and histological subtype of the tumor. These features are plotted in the top part of the graph and are characterized with the greatest scattering of the SHAP-values. Contribution of factors agrees with clinical concepts: the larger size of the tumor was associated with the increased risk of recurrence (red dots on the right of the graph), which reflects the higher tumor burden and the aggressiveness of the disease. Higher degrees of malignity (ISUP 3–4) also significantly increased the predicted risk; this fact matches the well-known predictive significance of the degree of nuclear atypia of the renal carcinoma, in which the badly differentiated tumors have worse outcomes [11]. The presence of level II tumor thrombus (with proliferation to the inferior vena cava) resulted in a significant increase of progression risk as compared to levels 0 and I. This coincides with literature data, according to which the tumor invasion of the venous system per se, especially with the involvement of the inferior vena cava, is an independent adverse prediction factor for patients with renal cell carcinoma.

In is noteworthy that according to SHAP-analysis the influence of level I thrombosis was even more pronounced than that of level II. This may reflect the statistical peculiarities of the specific sample: in this study, there were significantly less patients with level II (n=16), which might have resulted in the decrease of stability of assessments in the training of the DeepSurv model. Besides, tumors with level II thrombosis could be combined, in individual cases, with less aggressive morphological characteristics (e.g., smaller size or lower ISUP grade), which the neural network could have considered in a cumulative way and partially compensate the total risk.

According to H. Park *et al.* (2019), the presence of the venous thrombus in the renal cell carcinoma (RCC) is associated with almost two-fold risk of progression (HR ~1.9) [14]. In our study, the higher level of thrombosis decreased the recurrence-free survival in a similar way. Finally, the neural network identified the significance of the histological type of the tumor: while the non-clear cell forms (papillary, chromophobe, and other forms) are usually associated with a negative outcome of the RCC with venous thrombosis, in our model the clear-cell histotype showed some increase of the risk, even though the SHAP scattering was narrow.

A possible explanation of the observed increase of the risk in the clear-cell RCC could be that this histotype prevailed in the studied sample, whereas the rare forms (papillary, chromophobe, medullar) were represented only by a small sample. This decreases the statistical capacity for the assessment of their influence and may result in a lowered assessment of risk associated with them. Besides, clear cell tumors may be combined with other adverse characteristics, namely, larger size, high ISUP grade, extended venous thrombosis, which, in aggregate, increased the predicted progression risk. Finally, the deep learning model DeepSurv, capable of considering the nonlinear interactions between variables, was able to identify the characteristic combinations of features, more typical of the clear-cell type, and to interpret them as an integral prognostic marker augmenting the contribution from this histotype.

In our study, the benefit of DeepSurv over the classic approach in the concordance metrics was rather modest (difference of ~0.01–0.02), which may be explained by a limited size of sample (n=100) and the fact that the key risk drivers for this group of patients are identified quite well by the linear model. At the same time, even a minor increase in accuracy assisted by the neural network may be clinically significant in boundary cases (e.g., in stratification into groups of high or low risk); what is most important, DeepSurv became a tool for a deeper understanding of structure of patient data. On the other hand, the downsides of deep learning include a more complicated learning process requiring selection of hyper-parameters and, quite often, large arrays of data for a reliable generalization. Besides, the "black box" of the neural networks makes it difficult to provide a direct explanation why some patient of the other received a certain prognosis. We demonstrated that this problem may be solved with SHAP methods. This allowed to make the model conventionally interpretable, making it close in terms of information value to the Cox regression known to medical professionals.

The obtained results have practical implications for clinical practice. The ability to stratify risk in patients with renal cell carcinoma and tumor thrombosis in a more accurate way may help optimize treatment strategies and follow-up care. Firstly, identification of patients with extremely high risk of progression after surgical treatment may facilitate addressing the question of adjunctive therapy. The present-day standard for localized RCC with thrombus remains the radical nephrectomy with thrombectomy [15]. At the same time, five-year survival in this group varies greatly (from ~23% to 70% depending on the tumor volume, level of thrombosis, and accompanying factors) [15]. Currently, there is no universally accepted single criterion to identify which patients from this heterogeneous group would truly benefit from adjuvant therapy, such as postoperative immunotherapy, to improve clinical outcomes [16]. It follows from our data that a combined model based on DeepSurv may serve as the basis for such a prognostic tool. Individual risk prognosis calculated by a neural network with consideration of a set of clinical and morphological features may potentially serve as the integral criterion that is used to select the patients for additional interventions. For instance, a patient with a large-sized tumor, high ISUP grade and level II thrombus will be identified as having a model-predicted high risk of early progression, this warrants both the intensified surveillance and the consideration of adjuvant systemic therapy through multidisciplinary team discussion. Secondly, such models will assist in informing the patients and planning the follow-up care. Conventional prognostic schemes (TNM-staging, gradation type factors, involvement of lymphatic nodes, etc.) do not consider many nuances, therefore, patients of one group (e.g., stage pT3a N0) may have different outcomes [11]. The use of a ML-model aggregating the data on tumor morphology, biomarkers and thrombus volume, will enable compilation of a more personalized schedule of clinical examinations: some of the low-risk patients will avoid redundant visits and check-ups, whereas the high-risk group should be given more attention. Thirdly, the use of stratification algorithms at the stage of planning of examinations and treatment will facilitate a more justified comparison of various methods. Specifically, in the context of choosing surgical access (laparoscopy vs. laparotomy) our analysis confirmed comparability of oncological outcomes, if the risk factors are spread in the same fashion. In the future, the DeepSurv type models may be used to rank patients according to their prognostic index even before the operation: this will assist correct comparison of new methods of treatment thereby obtaining higher quality data for evidence-based medicine. A promising approach involves integrating clinical variables with molecular and radiological tumor characteristics (genomic markers, CT/MRI data) within a unified neural network model [16-18]. Existing examples demonstrate how combining radiomics with DeepSurv algorithms improves prognostic accuracy and therapy selection in lung cancer [16]; similarly, adopting such comprehensive models in renal cell carcinoma could significantly enhance risk stratification precision.

CONCLUSION

The neural network Cox model DeepSurv confirmed its methodological viability in the task of predicting recurrence-free survival in patients with renal cell carcinoma and thrombosis of the vein. It allowed consideration of nonlinear links of predictors and provided a higher (if marginally) prognostic rating. The use of the SHAP methods provided interpretation of the model in terms of conventional clinical categories making the results fit for practical use. These findings demonstrate the potential for broader implementation of the DeepSurv approach in oncourology, including patient selection for adjuvant therapies, development of personalized surveillance protocols, and treatment strategy decisions based on integrated prognostic indices. This aligns with the global trend of incorporating artificial intelligence in medicine to enhance prognostic accuracy and treatment personalization [5].

ADDITIONAL INFORMATION	ДОПОЛНИТЕЛЬНАЯ ИНФОРМАЦИЯ
Ethical Approval Statement. Extract from the protocol of the LEC No. 03-11/021 dated 11/19/2021.	***Этическая экспертиза.*** Выписка из протокола ЛЭК №03-11/021 от 19.11.2021 г.
Study funding. The study was the authors' initiative without external funding.	***Источник финансирования.*** Работа выполнена по инициативе авторов без привлечения финансирования.
Conflict of interest. The authors declare that there are no obvious or potential conflicts of interest associated with the content of this article.	***Конфликт интересов.*** Авторы декларируют отсутствие явных и потенциальных конфликтов интересов, связанных с содержанием настоящей статьи.
Contribution of individual authors. Mirzabekov M.K.: concept development, statistical analysis, writing of the text. Bogomolov O.A., Shkolnik M.I.: editing and approval of the text. Trukhacheva N.V., Tikhonskii N.D.: concept development, statistical analysis, preparation of graphs and editing of the text. The authors gave their final approval of the manuscript for submission, and agreed to be accountable for all aspects of the work, implying proper study and resolution of issues related to the accuracy or integrity of any part of the work.	***Участие авторов.*** Мирзабеков М.К. – разработка концепции, проведение статистического анализа, написание текста. Богомолов О.А., Школьник М.И. – редактирование и утверждение текста. Трухачева Н.В., Тихонский Н.Д. – разработка концепции, проведение статистического анализа, подготовка графиков и редактирование текста. Все авторы одобрили финальную версию статьи перед публикацией, выразили согласие нести ответственность за все аспекты работы, подразумевающую надлежащее изучение и решение вопросов, связанных с точностью или добросовестностью любой части работы.

REFERENCES / ЛИТЕРАТУРА

1. Cox DR. Regression models and life tables. *Journal of the Royal Statistical Society: Series B*. 1972;34(2):187-220. DOI: 10.1111/j.2517-6161.1972.tb00899.x

2. Reva SA, Shaderkin IA, Zyatchin IV, Petrov SB. Artificial intelligence in cancer urology. *Experimental and Clinical Urology*. 2021;14(2):46-51. [Рева С.А., Шадеркин И.А., Зятчин И.В., и др. Искусственный интеллект в онкоурологии. *Экспериментальная и клиническая урология*. 2021;14(2):46-51]. DOI: 10.29188/2222-8543-2021-14-2-46-51

3. Du M, Haag DG, Lynch JW, et al. Comparison of the tree-based machine-learning algorithms to Cox regression in predicting the survival of oral and pharyngeal cancers: analyses based on SEER database. *Cancers*. 2020;12(10):2802. DOI: 10.3390/cancers12102802

4. Qiu X, Gao J, Yang J, et al. A comparison study of machine learning (random survival forest) and classic statistic (Cox proportional hazards) for predicting progression in high-grade glioma after proton and carbon ion radiotherapy. *Frontiers in Oncology*. 2020;10:551420. DOI: 10.3389/fonc.2020.551420

5. Lundberg SM, Lee S-I. A unified approach to interpreting model predictions. *Advances in Neural Information Processing Systems*. 2017;30:4765-4774.

6. Gonen M, Heller G. Concordance probability and discriminatory power in proportional hazards regression. *Biometrika*. 2005;92(4):965-970. DOI: 10.1093/biomet/92.4.965

7. Liu Y, Zhou S, Wei H, An S. A comparative study of forest methods for time-to-event data: variable selection and predictive performance. *BMC Medical Research Methodology*. 2021;21(1):193. DOI: 10.1186/s12874-021-01386-8

8. Katzman JL, Shaham U, Cloninger A, et al. DeepSurv: personalized treatment recommender system using a Cox proportional hazards deep neural network. *BMC Medical Research Methodology*. 2018;18(1):24. DOI: https://doi.org/10.1186/s12874-018-0482-1

9. Alabi RO, Elmusrati M, Leivo I, et al. Machine-learning explainability in nasopharyngeal cancer survival using LIME and SHAP. *Scientific Reports*. 2023;13(1):8984. DOI: 10.1038/s41598-023-35795-0

10. Kantidakis G, Putter H, Lancia C, et al. Survival prediction models since liver transplantation – comparisons between Cox models and machine-learning techniques. *BMC Medical Research Methodology*. 2020;20(1):277. DOI: 10.1186/s12874-020-01153-1

11. Byun S-S, Heo TS, Choi JM, et al. Deep-learning-based prediction of prognosis in non-metastatic clear cell renal cell carcinoma. *Scientific Reports*. 2021;11(1):1242. DOI: 10.1038/s41598-020-80262-9

12. GraphPad Software. Multicollinearity in Cox proportional hazards regression. URL: https://www.graphpad.com/guides/prism/latest/statistics/stat_cox_reg_results_multicollinearity.htm

13. Moncada-Torres A, van Maaren MC, Hendriks MP, et al. Explainable machine learning can outperform Cox regression predictions and provide insights in breast-cancer survival. *Scientific Reports*. 2021;11(1):6968. DOI: 10.1038/s41598-021-86327-7

14. Park H, Jeong CW, Yuk H, et al. Influence of tumor thrombus on occurrence of distant venous thromboembolism and survival in patients with renal cell carcinoma after surgery. *Clinical and Applied Thrombosis/Hemostasis*. 2019;25:1076029618823288. DOI: 10.1177/1076029618823288

15. Shin D, Lim B, Song C, et al. Comparative analysis of oncologic outcomes in surgically treated patients with renal cell carcinoma and renal-vein thrombosis by pathologic subtypes. *Scientific Reports*. 2025;15(1):15946. DOI: 10.1038/s41598-025-00452-1

16. Yang B, Liu C-X, Wu R, et al. Development and validation of a DeepSurv nomogram to predict survival outcomes and guide personalized adjuvant chemotherapy in non-small-cell lung cancer. *Frontiers in Oncology*. 2022;12:895014. DOI: 10.3389/fonc.2022.895014

17. Schulz S, Woerl A-C, Jungmann F, et al. Multimodal deep learning for prognosis prediction in renal cancer. *Frontiers in Oncology*. 2021;11:788740. DOI: 10.3389/fonc.2021.788740

18. Mahootiha M, Qadir HA, Aghayan D, et al. Deep-learning-assisted survival prognosis in renal cancer: a CT-scan-based personalized approach. *Heliyon*. 2024;10(2):e24374. DOI: 10.1016/j.heliyon.2024.e24374

Original research | Оригинальное исследование
DOI: https://doi.org/10.35693/SIM678381

Comparative analysis of *Streptococcus pyogenes* sensitivity and effectiveness of antibacterial therapy in chronic tonsillitis

Evgenii S. Burenkov, Pavel N. Zolotarev
Medical University "Reaviz" (Samara, Russian Federation)

Abstract

Background. The rise in antibiotic resistance of *Streptococcus pyogenes* in chronic tonsillitis remains a global issue, exacerbated by irrational use of antibacterial drugs, low patient adherence to therapy, and the spread of resistant strains. The discrepancy between the relatively high *in vitro* sensitivity of microorganisms and the reduced clinical efficacy of drugs *in vivo* is of particular concern and requires an in-depth analysis of the causes of such disparities.

Aim. The study aims to evaluate the efficacy of various groups of antibacterial drugs *in vitro* and *in vivo* used to treat chronic tonsillitis during exacerbations.

Material and methods. Based on outpatient records and microbiological studies, a group of patients was identified in whom *S. pyogenes* was the primary significant factor in the development of chronic tonsillitis. The sensitivity of the pathogen to commonly used antibacterial drugs was assessed using the disk-diffusion method. Clinical efficacy of antibiotic therapy was evaluated based on objective criteria. Additionally, isolates of *S. pyogenes* co-incubated with antibacterial agents were analyzed using Raman spectroscopy.

Results. The analysis revealed discrepancies between in vitro disk-diffusion data and clinical outcomes. According to the disk-diffusion test, 87.6% of patients showed sensitivity to semi-synthetic penicillins, yet incomplete or absent clinical efficacy was observed in 28.2% of cases. Slightly better results were obtained with inhibitor-protected penicillins. Macrolides, demonstrating 88.5% efficacy *in vitro*, failed to achieve full therapeutic effects in 26.6% of patients. Comparable results were observed with cephalosporins. The lowest *in vitro* sensitivity of *S. pyogenes* was noted for fluoroquinolones, leading to inadequate clinical efficacy in 28.0% of patients. Raman spectroscopy enabled the assessment of sensitivity to one of the most frequently used antibacterial agents.

Conclusions. The significant gap between laboratory and clinical data is attributed not only to potential antibiotic resistance mechanisms (which are also discussed) but also to the influence of internal factors that must be considered when selecting etiotropic therapy for chronic tonsillitis during exacerbations.

Keywords: chronic tonsillitis, antibiotic resistance, clinical efficacy, Raman spectroscopy.

Conflict of interest: nothing to disclose.

Citation
Burenkov ES, Zolotarev PN. **Comparative analysis of *Streptococcus pyogenes* sensitivity and effectiveness of antibacterial therapy in chronic tonsillitis.** *Science and Innovations in Medicine.* 2025;10(3):243-247.
DOI: https://doi.org/10.35693/SIM678381

Information about authors
***Evgenii S. Burenkov** – senior lecturer at the Department of Pharmacy.
ORCID: https://orcid.org/0000-0003-0045-7046
E-mail: evgburenkov@mail.ru

Pavel N. Zolotarev – MD, Dr. Sci. (Medicine), Professor of the Department of Morphology and Pathology.
ORCID: https://orcid.org/0000-0003-4020-0720
E-mail: zolotareff@list.ru
Corresponding Author

Received: 11.04.2025
Accepted: 25.05.2025
Published: 12.08.2025

Сравнительный анализ чувствительности *Streptococcus pyogenes* и эффективности антибактериальной терапии при хроническом тонзиллите

Е.С. Буренков, П.Н. Золотарев
ЧУО ОВО «Медицинский университет «Реавиз» (Самара, Российская Федерация)

Аннотация

Обоснование. Рост антибиотикорезистентности *Streptococcus pyogenes* при хроническом тонзиллите остается глобальной проблемой, усугубляемой нерациональным использованием антибактериальных препаратов, низкой приверженностью пациентов к терапии и распространением устойчивых штаммов. Особую тревогу вызывает противоречие между относительно высокой чувствительностью микроорганизмов *in vitro* и сниженной клинической эффективностью препаратов *in vivo*, что требует углубленного анализа причин таких расхождений.

Цель. Исследование направлено на оценку эффективности различных групп антибактериальных препаратов *in vitro* и *in vivo*, применяемых для лечения хронического тонзиллита в период обострения.

Материал и методы. По данным амбулаторным карт и микробиологического исследования определена группа пациентов, у которых *S. pyogenes* был основным значимым фактором развития хронического тонзиллита. Проведена оценка резистентности возбудителя диско-диффузионным методом. Изучена клиническая эффективность антибиотиков на основании

объективных критериев. Выполнено исследование изолятов *S. pyogenes*, совместно инкубированных с антибактериальным препаратом методом спектроскопии комбинационного рассеяния.

Результаты. Проведенный анализ выявил несоответствия между полученными данными диско-диффузионного метода *in vitro* и клиническими результатами. По данным диско-диффузионного теста к полусинтетическим пенициллинам были чувствительны только 87,6% пациентов, при этом в 28,2% случаев клинический эффект был неполным или отсутствовал. Незначительно, но лучшие результаты получены в случае применения ингибиторозащищенных пенициллинов. Макролиды, демонстрирующие 88,5% эффективности *in vitro*, не позволяли достигать полного эффекта от лечения у 26,6% пациентов. Сопоставимые результаты были получены при анализе цефалоспоринов. Наименьшая чувствительность *S. pyogenes in vitro* выявлена к фторхинолонам, что не позволяло достигать адекватного клинического эффекта у 28,0% пациентов. Спектроскопия комбинационного рассеяния позволила оценить чувствительность к одному из наиболее часто применяемых антибактериальных препаратов.

Выводы. Значимая разница между лабораторными и клиническими данными обусловлена не только возможной антибиотикорезистентностью, механизмы которой также рассмотрены, но и влиянием внутренних факторов, которые следует учитывать при выборе этиотропной терапии хронического тонзиллита в период обострения.

Ключевые слова: хронический тонзиллит, антибиотикорезистентность, клинический эффект, спектроскопия комбинационного рассеяния.

Конфликт интересов: не заявлен.

Для цитирования:
Буренков Е.С., Золотарев П.Н. **Сравнительный анализ чувствительности *Streptococcus pyogenes* и эффективности антибактериальной терапии при хроническом тонзиллите.** *Наука и инновации в медицине.* 2025;10(3):243-247.
DOI: https://doi.org/10.35693/SIM678381

Сведения об авторах
***Буренков Евгений Сергеевич** – старший преподаватель кафедры фармации.
ORCID: https://orcid.org/0000-0003-0045-7046
E-mail: evgburenkov@mail.ru

Золотарев П.Н. – д-р мед. наук, профессор кафедры морфологии и патологии.
ORCID: https://orcid.org/0000-0003-4020-0720
E-mail: zolotareff@list.ru
Автор для переписки

Список сокращений
СКР – спектроскопия комбинационного рассеяния.

Получено: 11.04.2025
Одобрено: 25.05.2025
Опубликовано: 12.08.2025

INTRODUCTION

Chronic tonsillitis remains one of the prevalent chronic diseases among active population [1]. Viruses, bacteria (*Streptococcus pyogenes, Staphylococcus aureus, Haemophilus influenzae, Streptococcus pneumoniae*) and some fungi are well known as potential causative agents maintaining the inflammatory reaction in the tonsils, combined with the action of other exogenous and endogenous adverse factors [2]. *Streptococcus pyogenes (S. pyogenes)* plays the leading role in the development of chronic tonsillitis. Being an extracellular pathogen, it persists in tonsillar tissue by expressing a broad spectrum of virulence proteins that modify immune cell response mechanisms [3].

Antibacterial drugs form the base of treatment of chronic tonsillitis. Their efficiency depends on the structure of the main substance, dosage, frequency of administration, paths and duration of administration as well as characteristics of pathogens showing susceptibility to them [4, 5]. According to the effective clinical recommendations for the diagnostics and treatment of chronic tonsillitis, upon finding the S. Pyogenes in the tonsillar tissue, the drugs of choice for the conservative treatment are the β-lactams[1]. According to study data, *S. pyogenes* retains high susceptibility to inhibitor combinations and synthetic penicillins, with resistance rates not exceeding 1%. Nevertheless, the frequency of unsatisfactory clinical outcomes remains significantly higher even with properly administered antibacterial therapy, representing a persistent challenge in clinical pharmacology that warrants comprehensive evaluation [6].

AIM

To assess both *in vitro* susceptibility of *S. pyogenes* and clinical efficacy of the most commonly used antibacterial agents for treating chronic tonsillitis (simple and grade I toxic-allergic form).

MATERIAL AND METHODS

Random sampling was used to form a group of 144 patients from three urban districts of the city of Samara, registered in follow-up care by the end of 2020 with simple and grade I toxic-allergic forms of chronic tonsillitis. The form of disease was established as per patient records according to the classification of B.S. Preobrazhensky (1954) and V.T. Palchun (1977). There were 76 male (52.8%) and 68 female (47.2%) participants of the study. According to the WHO age criteria (2016), the patients were divided into two groups: Group 1 (n= 86), young patients (age 18-44); Group 2 (n= 58), middle age patients (age 45-59). The exclusion criteria were absence of a confirmed chronic tonsillitis according to patient record data; availability of objective signs of the toxic-allergic form of grade II chronic tonsillitis (decompensated form); history of low compliance with or refusal from intercurrent therapy; history of self-treatment. The groups had statistically significant differences in the duration of the disease: in Group 1 patients, it was 7.8±2.9 years, and in Group 2 patients, 14.1±2.7 years.

In both groups, standard microbiological (culture) testing was performed of palatine tonsil exudate and posterior pharyngeal wall mucosa for aerobic and facultative anaerobic microorganisms. The evaluation of the results only considered etiologically significant pathogenic microorganisms and their diagnostically significant growth (over 104 CFU/swab or CFU/mL or CFU/g). The concomitant microflora (below 104 CFU/swab or CFU/mL or CFU/g) was disregarded. For patients with S. pyogenes identified as the primary pathogen, its antibiotic susceptibility was assessed using the Kirby-Bauer disk diffusion method *in vitro*[2]. The tested antibiotics included: semi-synthetic peniccilins, inhibitor-protected penicillins, macrolides, cephalosporins, fluoroquinolones (all commonly used to treat chronic tonsillitis). The results were interpreted using the values of measured inhibition zone diameters of

[1] Chronic tonsillitis. Clinical recommendations. 2024. URL: https://diseases.medelement.com/disease/84-2024/18329 (Last retrieved: 15.03.2025)
[2] Russian national recommendations. Identification of microorganism susceptibility to antimicrobial agents. Rev. 2024-02. Smolensk: MAKMAH, SSMU, 2024. 192 p.

microbial growth (<19 mm, antibiotic-resistant; 20-27 mm, intermediate; >28 mm, antibiotic-sensitive).

For patients with *S. pyogenes* identified as the primary pathogen, a retrospective analysis of clinical efficiency of antibacterial therapy in the acute stages was performed based on the criteria of objective assessment of the inflammatory process of the oropharyngeal cavity (V.T. Palchun, A.I. Kryukov, 2001) using historical data of patient records.

Additionally, in patients (n=113) with chronic tonsillitis, sensitivity of *S. pyogenes* to Amoxiclav was assessed by Raman scattering spectroscopy (RS). The method is well known and used successfully to test the validity of medications. Amoxiclav was chosen at the most frequently prescribed drug to treat exacerbations of chronic tonsillitis, according to the patient records, in the Cmax dosage as per prescribing label, *viz.* included 105.4 mcg/ml of amoxicillin and 28.5 mcg/ml of clavulanic acid. The spectroscopy is performed in a set of samples of oral fluid and phosphate-buffer saline as solvents with added suspension of *S. Pyogenes,* compliant with concentration of 0.5 of the McFarland standard, and, later, the antibiotic in the desired dosage. The samples were incubated in a thermostat at 37 °C for 2, 4, 6 hours, following which RS was performed. The method was implemented using a set of equipment forming a test model with a spectrometer. The analysis of spectra was performed in four zones: 1155 cm^{-1}, 1525 cm^{-1}, 1033 cm^{-1} and 1611 cm^{-1}; their final processing was done in Wolfram Mathematica 9.

Statistical methods

Statistical processing of obtained data was performed in the Statistica for Windows 7.0 software suite. The methods of descriptive statistics were used for a general characterization of the obtained data. For group mean comparisons, Student's t-test was used. Correlation analysis was performed to assess relationships between quantitative variables. The strength and direction of linear associations were determined using Pearson's correlation coefficient (for normally distributed data) or Spearman's rank correlation (for non-parametric data). Normality was evaluated with the Shapiro-Wilk test. Statistical significance was set at $p<0.05$.

RESULTS

The main pathogen of chronic tonsillitis in 113 patients of both groups was *S. pyogenes*. It was identified as the etiologically significant pathogen in 82.5% patients in Group 1 and in 72.4% patients of Group 2. In 12.8% patients of Group 1 and in 19.0% patients of Group 2, this microorganism was plated with other significant pathogens, e.g. *Streptococcus pneumoniae* and/or *Staphylococcus aureus*. At the same time, in Group 2 in a credibly larger number of cases (Group 1: 19.0% vs. Group 2: 4.7%, $p<0.001$) presence of *Candida spp.* was identified.

According to patient record data, treatment of exacerbations of chronic tonsillitis of the simple and grade I toxic-allergic forms mediated by *S. pyogenes*, various antibiotics were used. Most frequently, the following were prescribed: inhibitor-protected penicillins, macrolides, cephalosporins, semi-synthetic penicillins, in some cases, fluoroquinolones. The analysis of clinical efficiency of the use of those groups of antibacterial agents in the treatment of exacerbations showed various results (**Fig. 1**).

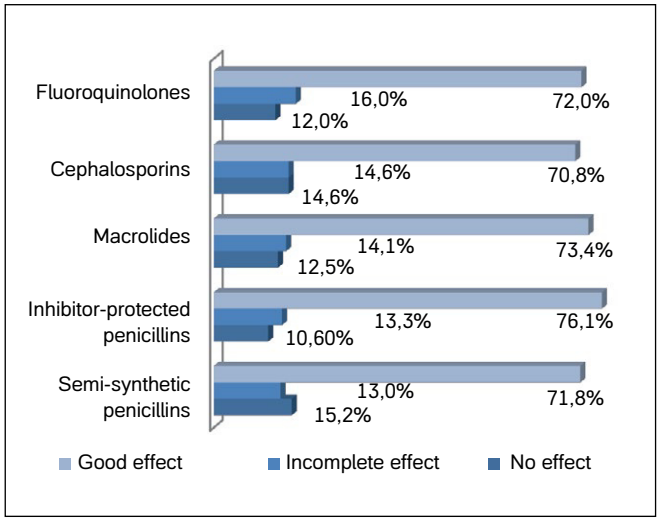

Figure 1. *Clinical efficacy of antibacterial agents in the treatment of exacerbations of chronic tonsillitis (simple and toxic-allergic grade I forms) in patients.*

Рисунок 1. *Показатели клинической эффективности терапии обострений хронического тонзиллита простой и токсико-аллергической I степени форм различными видами антибактериальных препаратов у пациентов.*

Regardless of the type of the antibacterial drug, 78 (69.0%) patients did not reach a positive clinical effect or it was incomplete and required adjustment of the scheme of therapy (increase of course duration, change of average daily dose, replacement or addition of a second antibacterial drug). Among the patients in whom a good clinical effect was reached in the treatment of exacerbation, no statistically significant variations were identified that would relate to the selection of a specific antibacterial drug.

The results of the disk-diffusion method of assessment of sensitivity of *S. pyogenes* to various types of antibacterial drugs *in vitro* did not identify a single completely resistant strain. At the same time, data was obtained indicating intermediate values of measured inhibition zone diameters of microbial growth of *S. pyogenes*, which was likely mediated by the active process of formation of antibiotic resistance (**Fig. 2**).

The results of the correlation analysis showed the presence of a moderate positive connection ($r=0.607$) between the results of the intermediate sensitivity *in vitro* and the data on incomplete or lacking clinical effect *in vivo* (**Fig. 3**).

The RS data showed that in the cases of sensitivity of *S. pyogenes* to Amoxiclav in the predominant number of samples, within the first two hours of incubation disappearance of linear values characterizing the lysis of the etiological pathogen is found. At the same time, in some patients, disappearance if linear values was identified only after six hours of incubation.

DISCUSSION

Chronic tonsillitis, particularly its toxic-allergic forms, remains a challenging clinical condition, largely due to the growing problem of antibiotic resistance. The results of this study provide direct confirmation of this hypothesis.

Semi-synthetic penicillins (amoxicillin and ampicillin) are traditionally prescribed in exacerbations of chronic tonsillitis due to their affordable price and good bioavailability. However, as the disk-diffusion test showed, in 12.4%

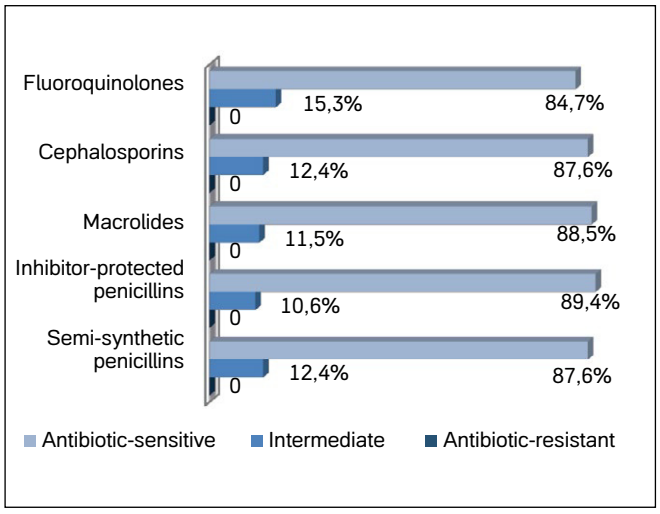

Figure 2. *Susceptibility of S. pyogenes to various antibacterial agents in patients with chronic tonsillitis (simple and toxic-allergic grade I forms) in vitro.*

Рисунок 2. *Показатели чувствительности S. pyogenes к различным видам антибактериальных препаратов у пациентов с хроническим тонзиллитом простой и токсико-аллергической I степени форм in vitro.*

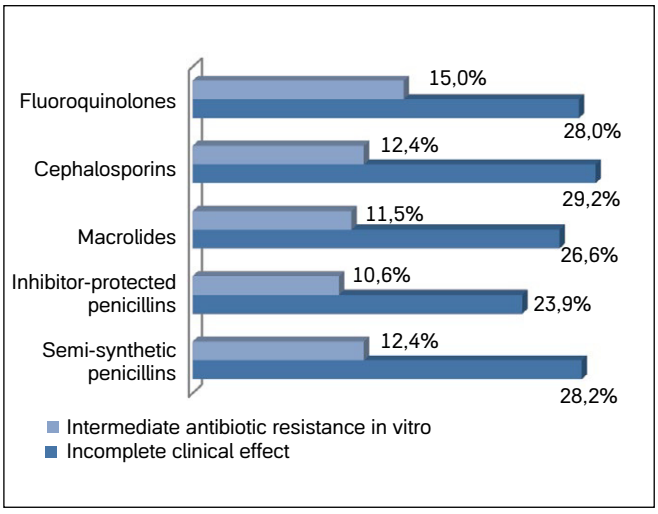

Figure 3. *Comparative analysis of intermediate inhibition zones for S. pyogenes in vitro and absent or incomplete clinical effects of antibacterial agents in the treatment of chronic tonsillitis exacerbations (simple and toxic-allergic grade I forms) in patients.*

Рисунок 3. *Сравнительные данные между показателями промежуточных зон подавления роста S. pyogenes in vitro и отсутствующим или неполным клиническим эффектом от применения различных видов антибактериальных препаратов при лечении обострений хронического тонзиллита простой и токсико-аллергической I степени форм у пациентов.*

patients, intermediate values of inhibition of bacterial growth of *S. pyogenes* were found, which indicates formation of resistance. The phenomenon may be explained by the necessity of performing a lengthy course of therapy with semi-synthetic penicillins with possible dosage adjustment and resulting low compliance of patients with the therapy regime. As little as 8% of patients are capable of keeping this regime [7]. Besides, bacterial internalization into mucosal epithelial cells renders them inaccessible to β-lactams [8]. Despite rare *in vitro* penicillin resistance (less than 5%), clinical treatment failure is typically attributed to biological and behavioral factors [9].

Transition to penicillins combined with inhibitors such as amoxicillin or clavulanic acid provided improved results of treatment of patients with chronic tonsillitis. Their clinical inefficiency, according to the results of the study, was 10.6%, which is slightly lower than that of semi-synthetic analogues. Clavulanic acid inhibits most β-lactamases, however, it is not efficient against strains with modified penicillin-binding proteins [10]. This correlates with the data of another study, in which the reasons of resistance included modification of targets or hyper-production of enzymes. In order to prevent the activation of such a mechanism of resistance, prescription of such inhibitor-protected penicillins require strict supervision [11].

Paradoxical results were seen in the analysis of macrolides. With the sensitivity of 88.5% *in vitro*, their clinical efficiency was only 73.4%. These results may be explained by several factors. First, since 2007 the intake of macrolides in Russia grew by 50%, which directly correlates with the spreading of resistance via studied mechanisms of erm-mediated modification of targets [12]. Second, the cross-resistance within a class lowers the efficiency of all macrolides, even if *in vitro* sensitivity remains high [13]. It is to be noted that in outpatient practice, this group of antibacterial agents is prescribed for their convenience (a short period of intake with a modest number of side effects).

Cephalosporins showed a level of inefficiency comparable with inhibitor-protected penicillins (14.6%). The limit to their use is related with the prevalence of strains producing extended spectrum β-lactamases (ESBL) [14]. At the same time, cephalosporins of third generation remain medications of choice in exacerbated infections since they retain their activity against most strains of streptococci.

Fluoroquinolones, despite their low clinical efficiency, demonstrate the intermediate area of growth inhibition for 15.3% strains. Their limited efficiency against *S. pyogenes* is related to the fact that fluoroquinolones are more active against gram-negative bacteria, whereas gram-positive bacteria develop resistance via mutation in the gyrA/parC genes and activation of efflux pumps. This renders their use in chronic tonsillitis less justified, especially in the regions with high levels of intake of fluoroquinolones [15].

CONCLUSION

Thus, the sensitivity analysis of pathogens isolated from chronic tonsillitis patients revealed no strains of *S. pyogenes* fully resistant to the antibiotics used for this condition. The obtained values of sensitivity of *S. pyogenes in vitro* are higher than the values of clinical efficiency in vivo for the group of semi-synthetic penicillins by 18.0%; inhibitor-protected penicillins, by 14.9%; cephalosporins, by 19.2%; fluoroquinolones, by 15.0%; macrolides, by 17.1%, respectively. Currently, inhibitor-protected penicillins and cephalosporines may remain first-line medications for the therapy of chronic tonsillitis, while the use of macrolides and fluoroquinolones in the cases of streptococcus infections should be restricted reserving them for cases of confirmed sensitivity. Raman spectroscopy proved to be an effective rapid method for personalized susceptibility testing and may find wide application in clinical practice.

ADDITIONAL INFORMATION	ДОПОЛНИТЕЛЬНАЯ ИНФОРМАЦИЯ
Ethical Approval Statement. The study was conducted at the Department of Pharmacy in 2024. A positive conclusion was received from the LEC of the Reaviz Medical University No. 08 dated 23.05.2024.	***Этическая экспертиза.*** Исследование проведено на базе кафедры фармации в 2024 году. Получено положительное заключение ЛЭК Медицинского университета «Реавиз» от 23.05.2024 г. №08.
Study funding. The study was the authors' initiative without external funding.	***Источник финансирования.*** Работа выполнена по инициативе авторов без привлечения финансирования.
Conflict of interest. The authors declare that there are no obvious or potential conflicts of interest associated with the content of this article.	***Конфликт интересов.*** Авторы декларируют отсутствие явных и потенциальных конфликтов интересов, связанных с содержанием настоящей статьи.
Contribution of individual authors. Zolotarev P.N.: concept and design of the study, editing of the manuscript. Burenkov E.S.: data collection and processing, writing of the original text. The authors gave their final approval of the manuscript for submission, and agreed to be accountable for all aspects of the work, implying proper study and resolution of issues related to the accuracy or integrity of any part of the work.	***Участие авторов.*** Золотарев П.Н. – концепция и дизайн исследования, редактирование рукописи. Буренков Е.С. – сбор и обработка данных, написание оригинального текста. Все авторы одобрили финальную версию статьи перед публикацией, выразили согласие нести ответственность за все аспекты работы, подразумевающую надлежащее изучение и решение вопросов, связанных с точностью или добросовестностью любой части работы.

REFERENCES / ЛИТЕРАТУРА

1. Kaztaeva KB, Turkhanova ZhZh. Prevalence and course of tonsillitis in adults and children. *Innova*. 2024;10(2):21-25. [Казтаева К.Б., Турханова Ж.Ж. Распространенность и течение тонзиллита у взрослых и детей. *Innova*. 2024;10(2):21-25]. URL: https://www.innova-journal.ru/jour/article/view/620/223

2. Belov VA. The continuum of chronic tonsillitis from a general pathological standpoint. *The Scientific Notes of the Pavlov University*. 2024;31(3):11-18. [Белов В.А. Континуум хронического тонзиллита с общепатологических позиций. *Ученые записки Первого Санкт-Петербургского государственного медицинского университета имени академика И.П. Павлова*. 2024;31(3):11-18]. DOI: 10.24884/1607-4181-2024-31-3-11-18

3. Iuchi H, Ohori J, Kiyama S, et al. Effectiveness of antibacterial agents against cell-invading bacteria such as *Streptococcus pyogenes* and *Haemophilus influenzae*. *BMC Microbiol*. 2021;21(1):148. DOI: 10.1186/s12866-021-02217-y

4. Madaminova NE. Choice of effective therapy for inflammatory pharyngeal diseases. *Economy and society*. 2024;2-1:1143-1146. [Мадаминова Н.Э. Выбор эффективной терапии при воспалительных заболеваниях глотки. *Экономика и социум*. 2024;2-1:1143-1146]. URL: https://cyberleninka.ru/article/n/vybor-effektivnoy-terapii-pri-vospalitelnyh-zabolevaniyah-glotki/viewer

5. Timurzieva AB. Some aspects of improving the organization of medical care for patients with ENT pathology. *Siberian Scientific Medical Journal*. 2024;44(5):61-72. [Тимурзиева А.Б. О некоторых аспектах совершенствования организации медицинской помощи пациентам с патологией лор-органов. *Сибирский научный медицинский журнал*. 2024;44(5):61-72]. DOI: 10.18699/SSMJ20240507

6. Hung TY, Phuong LK, Grobler A, et al. Antibiotics to eradicate *Streptococcus pyogenes* pharyngeal carriage in asymptomatic children and adults: a systematic review. *J Infect*. 2024;88(3):106104. DOI: 10.1016/j.jinf.2024.01.003

7. Kosyakov SYa, Pchelenok EV, Usmanova KhS. The use of combination drugs as an approach to the complex therapy of inflammatory pharyngeal diseases. *Consilium Medicum*. 2024;26(3):147-152. [Косяков С.Я., Пчеленок Е.В., Усманова Х.С. Применение комбинированных препаратов как подход комплексной терапии воспалительных заболеваний глотки. *Consilium Medicum*. 2024;26(3):147-152]. DOI: https://doi.org/10.26442/20751753.2024.3.202664

8. Guo MY, Yao KH. Research progress on the mechanism of β-lactam resistance in group A *Streptococci in vivo*. *Chinese journal of contemporary pediatrics*. 2024;26(1):92-97. DOI:10.7499/j.issn.1008-8830.2306157

9. Cosgrove SE, Sakoulas G, Perencevich EN, et al. Comparison of mortality associated with methicillin-resistant and methicillin-susceptible *Staphylococcus aureus* bacteremia: a meta-analysis. *Clin Infect Dis*. 2003;36(1):53-59. DOI: 10.1086/345476

10. Prabakar A, Palanisamy T, Kuriakose EB. Throat swabs- do they tell the entire story. *Indian J Otolaryngol Head Neck Surg*. 2025;77(2):635-638. DOI: 10.1007/s12070-024-05028-5

11. Bhadola P, Deo N. Exploring complexity of class-A Beta-lactamase family using physiochemical-based multiplex networks. *Sci Rep*. 2023;13(1):20626. DOI: 10.1038/s41598-023-48128-y

12. Chen CW, Leimer N, Syroegin EA, et al. Structural insights into the mechanism of overcoming Erm-mediated resistance by macrolides acting together with hygromycin-A. *Nat Commun*. 2023;14(1):4196. DOI: 10.1038/s41467-023-39653-5

13. Glajzner P, Szewczyk EM, Szemraj M. Phenotypic and Genotypic Characterization of Antimicrobial Resistance in Streptococci Isolated from Human and Animal Clinical Specimens. *Curr Microbiol*. 2023;80(7):228. DOI: 10.1007/s00284-023-03337-6

14. Lepe JA, Martínez-Martínez L. Resistance mechanisms in Gram-negative bacteria. *Med Intensiva (Engl Ed)*. 2022;46(7):392-402. DOI: 10.1016/j.medine.2022.05.004

15. Yan Y, Hu H, Lu T, et al. Investigation of serotype distribution and resistance genes profile in group B Streptococcus isolated from pregnant women: a Chinese multicenter cohort study. *APMIS*. 2016;124(9):794-799. DOI: 10.1111/apm.12570

Original research | Оригинальное исследование
DOI: https://doi.org/10.35693/SIM684548

Association of post-traumatic pain and knee joint changes according to magnetic resonance imaging

Andrei E. Karateev, Anastasiya A. Byalik, Vadim A. Nesterenko, Sergei A. Makarov, Daniil M. Kudinsky
Nasonova Research Institute of Rheumatology (Moscow, Russian Federation)

Abstract

Background. Chronic post-traumatic pain (CPTP) occurs in 15-50% of patients who have suffered knee joint injury (KJ). Post-traumatic pain is considered as one of the predictors of the development of post-traumatic osteoarthritis (PTOA). Early changes in the knee joint, characteristic of the development of PTOA, can be determined using magnetic resonance imaging (MRI).

Aim – to evaluate the relationship between CPTP and structural changes in the knee joint, which are determined using MRI.

Material and methods. The study group consisted of 98 patients, 48% women and 52% men, aged 39.2 ± 14.7 years, who had suffered a knee joint injury with damage to the anterior cruciate ligament (ACL) and/or meniscus (confirmed by MRI data), and experiencing pain ≥4 points on a numerical rating scale (CRS) of at least one month after the injury. The patients were followed up for 12 months. CPTP was determined with pain persistence for at least 3 months at the level of 4 points on the CRS. Repeated MRI was performed 12 months after inclusion in the study. Changes in the knee joint according to the MRI data were quantified using the WORMS system.

Results. CPTP was detected in 45.9% of patients. According to the initial MRI parameters, the groups of patients with CPTP (n=45) and without CPTP (n=53) significantly differed in cartilage morphology (minimal changes were more often detected in patients without CPTP), the presence of osteophytes, damage to the medial collateral ligament and rupture of the medial meniscus body. Almost all patients in both groups had ligament damage and meniscus rupture (with varying degrees of severity), as well as synovitis; about a third of the examined individuals had signs of bone marrow edema. After 12 months observations between patients with and without CPTP showed a significant difference in MRI parameters such as cartilage morphology, osteophytes of the medial condyle of the femur, damage to the posterior cruciate and medial collateral ligaments, rupture of the body, anterior and posterior horns of the medial meniscus, rupture of the anterior horn of the lateral meniscus, synovitis. Thus, severe cartilage damage (≥2 by WORMS) was noted in 82.1% of patients with CPTP and 43.4% without CPTP ($p < 0.05$), synovitis in 95.6% and 24.5% ($p < 0.05$).

Conclusion. CPTP, which occurs after the knee joint injury, is associated with structural changes in the joint, which can be regarded as an early stage of PTOA.

Keywords: chronic post-traumatic pain, post-traumatic osteoarthritis, magnetic resonance imaging.

Conflict of interest: nothing to disclose.

Citation
Karateev AE, Byalik AA, Nesterenko VA, Makarov SA, Kudinsky DM. **Association of post-traumatic pain and knee joint changes according to magnetic resonance imaging.** *Science and Innovations in Medicine.* 2025;10(3):248-254.
DOI: https://doi.org/10.35693/SIM684548

Information about authors
Andrei E. Karateev – MD, Dr. Sci. (Medicine), Head of the of the Laboratory of pathophysiology of pain and polymorphism of rheumatic diseases.
ORCID: 0000-0002-1391-0711
E-mail: aekarat@yandex.ru
***Anastasiya A. Byalik** – postgraduate student, traumatologist-orthopedist.
ORCID: 0000-0002-5256-7346
E-mail: nas36839729@yandex.ru
Vadim A. Nesterenko – MD, Cand. Sci. (Medicine), Junior researcher at the Laboratory of pathophysiology of pain and polymorphism of musculoskeletal diseases.
ORCID: 0000-0002-7179-8174
E-mail: swimguy91@mail.ru
Sergei A. Makarov – MD, Cand. Sci. (Medicine), Head of the Laboratory of rheumatoid orthopedics.
ORCID: 0000-0001-8563-0631
E-mail: smakarov59@rambler.ru
Daniil M. Kudinsky – MD, Cand. Sci. (Medicine), Junior researcher at the Laboratory of instrumental diagnostics, radiologist.
ORCID: 0000-0002-1084-3920
E-mail: nas36839729@yandex.ru
Corresponding Author

Received: 16.06.2025
Accepted: 04.08.2025
Published: 13.08.2025

Ассоциация посттравматической боли и изменений коленного сустава по данным магнитно-резонансной томографии

А.Е. Каратеев, А.А. Бялик, В.А. Нестеренко, С.А. Макаров, Д.М. Кудинский
ФГБНУ «Научно-исследовательский институт ревматологии имени В.А. Насоновой»
(Москва Российская Федерация)

Аннотация

Обоснование. Хроническая посттравматическая боль (ХПТБ) возникает у 15–50% пациентов, перенесших травму коленного сустава (КС). ХПТБ рассматривается как один из предикторов развития посттравматического остеоартрита (ПТОА). Ранние изменения КС, характерные для развития ПТОА, могут определяться с помощью магнитно-резонансной томографии (МРТ).

Цель – оценить взаимосвязь между ХПТБ и структурными изменениями КС, которые определяются с помощью МРТ.

Материал и методы. Исследуемую группу составили 98 пациентов, 48% женщин и 52% мужчин, возраст 39,2 ± 14,7 года, перенесших травму КС с повреждением передней крестообразной связки (ПКС) и/или мениска (подтвержденное данными МРТ) и испытывающих боль ≥4 балов по числовой рейтинговой шкале (ЧРШ) не менее месяца после травмы. Пациенты наблюдались в течение 12 мес. ХПТБ определялась при персистенции боли не менее 3 мес. на уровне ≥4 балов по ЧРШ. Повторная МРТ проводилась через 12 мес. после включения в исследование. Изменения КС по данным МРТ оценивались количественно по системе WORMS.

Результаты. ХПТБ была определена у 45,9% пациентов. По исходным параметрам МРТ группы пациентов с ХПТБ (n=45) и без ХПТБ (n=53) достоверно различались по морфологии хряща (минимальные изменения чаще выявлялись у пациентов без ХПТБ), наличию остеофитов, повреждению медиальной коллатеральной связки и разрыву тела медиального мениска. Практически у всех пациентов в обеих группах отмечались повреждение связок и разрыв мениска (с разной степенью выраженности), а также синовит; около трети обследованных лиц имели признаки отека костного мозга. Через 12 мес. наблюдения между пациентами с ХПТБ и без нее была зафиксирована достоверная разница по таким МРТ-параметрам, как морфология хряща, остеофиты медиального мыщелка бедренной кости, повреждение задней крестообразной и медиальной коллатеральной связок, разрыв тела, переднего и заднего рога медиального мениска, разрыв переднего рога латерального мениска, синовит. Так, выраженное повреждение хряща (≥2 по WORMS) было отмечено у 82,1% пациентов с ХПТБ и у 43,4% без ХПТБ (p <0,05), синовит у 95,6% и 24,5% (p <0,05).

Заключение: ХПТБ, возникающая после травмы КС, ассоциирована со структурными изменениями сустава, которые можно расценивать как раннюю стадию ПТОА.

Ключевые слова: хроническая посттравматическая боль, посттравматический остеоартрит, магнитно-резонансная томография.

Конфликт интересов: не заявлен.

Для цитирования:
Каратеев А.Е., Бялик А.А., Нестеренко В.А., Макаров С.А., Кудинский Д.М.
Ассоциация посттравматической боли и изменений коленного сустава по данным магнитно-резонансной томографии. *Наука и инновации в медицине.* 2025;10(3):248-254. DOI: https://doi.org/10.35693/SIM684548

Сведения об авторах
Каратеев А.Е. – д-р мед. наук, заведующий лабораторией патофизиологии боли и полиморфизма ревматических заболеваний.
ORCID: 0000-0002-1391-0711
E-mail: aekarat@yandex.ru
***Бялик Анастасия Андреевна** – аспирант, врач травматолог-ортопед.
ORCID: 0000-0002-5256-7346
E-mail: nas36839729@yandex.ru
Нестеренко В.А. – канд. мед. наук, младший научный сотрудник лаборатории патофизиологии боли и полиморфизма скелетно-мышечных заболеваний.
ORCID: 0000-0002-7179-8174
E-mail: swimguy91@mail.ru
Макаров С.А. – канд. мед. наук, заведующий лабораторией ревмоортопедии.
ORCID: 0000-0001-8563-0631
E-mail: smakarov59@rambler.ru
Кудинский Д.М. – канд. мед. наук, младший научный сотрудник лаборатории инструментальной диагностики, врач-рентгенолог.
ORCID: 0000-0002-1084-3920
E-mail: nas36839729@yandex.ru
Автор для переписки

Список сокращений
ПТОА – посттравматический остеоартрит; КС – коленный сустав; ПКС – передняя крестообразная связка; ХПТБ – хроническая посттравматическая боль; МРТ – магнитно-резонансная томография; ОА – остеоартрит; ОКМ – отек костного мозга; ЧРШ – числовая рейтинговая шкала; НПВП – нестероидный противовоспалительный препарат; БК – бедренная кость; ББК – большеберцовая кость.

Получено: 16.06.2025
Одобрено: 04.08.2025
Опубликовано: 13.08.2025

INTRODUCTION

Post-traumatic osteoarthritis (PTOA) is a prevalent complication of traumas manifested by chronic pain, persisting inflammation and progressing disorder of articular biomechanics. PTOA is most typically localized in the knee joint [1, 2]. In the event of injury of the anterior cruciate ligament (ACL) and the menisci of the knee joint, PTOA is developing in 20–50% cases 5–15 years after the injury. From the medical and social perspectives, this pathology has a high impact primarily due to the young age of patients: with traumas suffered at the age of 20–30, the characteristic clinical manifestations of PTOA and pronounced structural alterations severely impairing functional capabilities and working capacity occur as early as at the age of 35–45, i.e. at the most active age of members of modern society [3, 4].

Early identification of signs of PTOA prior to the onset of irreversible structural changes of the joint ('pre-radiographic stage') and active preventive therapy are the major vector of improvement of medical aid to patients suffering a trauma of the knee joint. To that end, PTOA predictors are sought and target groups of patients are identified among patients that suffered injuries of the knee joint and underwent orthopedic surgeries for ACL and meniscus ruptures and are in need in close supervision, treatment and rehabilitation [1–4].

The first manifestation of PTOA is the chronic post-traumatic pain (CPTP). It appears due to biomechanical disorders persisting after the trauma and/or respective orthopedic intervention, inflammatory process involving the synovia, subchondral bone, ligaments and entheses, degenerative changes (neoangiogenesis, nerve fiber sprouting), dysfunction of the nociceptive system and psycho-emotional problems. In essence, the same mechanisms underlie the development of PTOA, which opens the possibility of viewing the CPTP not only as a symptom but as a predictor of the disease [5, 6].

The analysis of correlation of painful sensations and structural changes of the joint persisting (or progressing) after the sustained energy are of principal importance for the evaluation of the role of CPTP as the factor indicating the high risk of PTOA development. The major method ensuring quality visualization of pathology of soft tissues of the knee joint is the magnetic resonance imaging (MRI). It is important that MRI allows identification of alterations in the ligaments, menisci, cartilage and subchondral bone long before the development of typical radiographic features of PTOA. Apart from the qualitative assessment of the pathology (presence or absence of changes), MRI allows its quantitative analysis using such systems as WORMS (Whole Organ Magnetic Resonance Imaging Score), MOAKS (MRI Osteoarthritis Knee Score), ICRS (International Cartilage Regeneration and Joint Preservation Society) and others [7, 8].

The characteristic features identified on the MRI of the knee joint in the post-trauma period are ruptures (with subsequent degenerative changes) of the ACL and menisci, as well as general inflammatory changes in the

articular tissue in the form of synovitis and bone marrow edema (BME) as a manifestation of the bone 'contusion' [9, 10]. There are series of clinical studies and respective meta-analyses confirming the correlation between this MRI-identified pathology and the manifestation of CPTP. Thus, the availability of correlation between the alterations identified in the MRI and the osteoarthritic (OA) pain was the subject of the work of P. Dainese *et al*. [11] who performed a meta-analysis of 37 studies in 17 of which the correlation of the clinical manifestations with the status of synovitis or bone marrow edema was evaluated. Six papers showed that contrast-enhanced MRI identified moderate positive correlation between the visualized features of inflammation and pain status. The systematic review of A. Ghouri *et al*. [12] evaluated the correlation between the MRI features of meniscal rupture and severity of pain. According to the data of 11 studies, in single-timepoint analyses pain and meniscal injury were interrelated.

It is to be noted that the combination of MRI-identifiable alterations of the knee joint and the chronic pain are assessed by some experts as criteria of the early stage of OA. Specifically, the evaluation of these features were listed in the early version of criteria of F. Luyten *et al*. (as of 2012) [13].

To date, no domestic studies have investigated the correlation between chronic post-traumatic bone changes and knee joint alterations using MRI.

AIM

To evaluate the relationship between CPTP and structural changes in the knee joint, which are determined using MRI.

MATERIAL AND METHODS

The study group comprised 98 patients meting the following *inclusion criteria:* age 18 to 50 years; traumatic injury of the knee joint due to which the patient had to seek medical aid; trauma of soft tissue elements of the knee joint confirmed by MRI findings; moderate or severe pain in the knee joint area (>4 points on the numerical rating scale, NRS 0–10, where 0 = no pain, 10 = worst imaginable pain) for ≥ 1 months after the injury; availability of the patient's informed consent.

Exclusion criteria were confirmed fracture of bone structures in the knee joint area (confirmed clinically and radiologically), availability of credible signs of a rheumatic disease (including previously diagnosed OA and fibromyalgia), severe disorders of the musculoskeletal system and comorbid pathologies precluding regular visits required by the study protocol.

The study group mainly consisted of young persons with approximately equal number of male and female patients with injuries of the ACL, menisci or a combination thereof, with moderate or severe pain in the knee joint; almost half of patients required orthopedic intervention (**Table 1**).

All study participants were advised to use knee braces, perform regular physical exercise and administer systemic and/or local non-steroid anti-inflammatory drugs (NSAIDs) as ointment or gels upon pain onset in compliance with 2024 clinical recommendations on injury of knee joint ligaments and the Order of the Ministry of Health of the Russian Federation dated 29.06.2023 No. 331n "On Approval of the Medical Care Standard for Adults with Knee Joint Meniscus Injury (Diagnosis and Treatment)".

The analysis of clinical manifestations was performed during the first visit, and 3, 6 and 12 months later. CPTP was identified during the second visit, 3 months after the follow-up started. The CPTP criteria was moderate or severe pain in the knee joint on activity or at rest (>4 on the numeric rating scale (NRS), where 0 = no pain, 10 = worst imaginable pain), that persisted for the majority of days in the 3 months before the evaluation.

All patients underwent MRI at the moment of inclusion and 12 months after the start of the study with a semi-quantitative analysis of structural changes as per WORMS system. The following was assessed: signal intensity and cartilage morphology in the center of the medial tibiofemoral joint and lateral tibiofemoral joint in coronary projection; proximal part of the patellofemoral joint in lateral projection (0 = norm, 1 = thinning of cartilage, without defects, 2 = one individual non full-thickness defect, 3 = several partial defects, 4 = full-thickness defect <50% of cartilage length, 5 = full-thickness defect >50%); OCD in the medial and lateral femoral condyles (FC), medial and lateral tibial condyles (TC), and central tibial plateau (0 = none, 1 = < 25% or the region area, 2 = 25–50%, 3 > 50%); subchondral cysts in the medial and lateral FC, medial and lateral TC (0 = none, 1 = < 25% of the region area, 2 = 25–50%, 3 = > 50%); subchondral edema in the medial and lateral FC, medial and lateral TC (0 = none, 1 = mild, 2 = severe); osteophytes of the medial and lateral FC, medial and lateral TC (0 = none, 1 = small, 2 = medium, 3 = large); damage of the anterior cruciate ligament, posterior cruciate ligament, medial collateral ligament, lateral collateral ligament (0 = intact, 1 = damaged); tear of the

Parameter	Value
Sex (F/M, %)	47 (48,0) /51 (52,0)
Age, years; M±σ	39,2 ± 14,7
Body mass index, kg/m2; M±σ	27,1 ± 6,3
Injury of knee joint tissues as per MRI data, %	ACL 42.0, meniscus 56,0, combined injury of ACL + meniscus 15.0, ACL + other injury (tendinitis, cysts, strained ligaments, etc.) 28.0
Surgical intervention (ACL reconstruction, meniscal repair, meniscal resection, combined surgery), %	39,0
Pain on activity; Me [25th; 75th percentiles]	5,0 [3,5; 6,5]
Pain at rest; Me [25th; 75th percentiles]	2,0 [1,0; 4,0]
Pain at nighttime; Me [25th; 75th percentiles]	2,0 [0,5; 3,5]
Functional disorder; Me [25th; 75th percentiles]	5,0 [2,0; 5,5]
KOOS total; M±σ	48,6 ± 19,1
KOOS symptoms; M±σ	58,7 ± 22,3
KOOS pain; M±σ	57,4 ± 18,1
KOOS activity; M±σ	65,6 ± 20,4
KOOS sports; M±σ	30,5 ± 21,7
KOOS quality of life; M±σ	39,1 ± 19,8

Table 1. *Clinical characteristics of patients at inclusion in the study (n=98)*

Таблица 1. *Клиническая характеристика пациентов на момент включения в исследование (n=98)*

MRI-symptom >1, n (%)		CPTP+ (n=45)	CPTP- (n=53)	p-value
Cartilage morphology		26,7	66,7	**0,012**
Bone marrow edema	Medial TC	26,7	30,2	0,61
	Lateral TC	20,0	20,8	0,401
	Medial FC	22,2	13,2	0,508
	Lateral FC	20,0	13,2	0,803
	Central part of femur	20,0	20,8	0,597
SC	Medial TC	11,1	5,7	0,521
	Lateral TC	4,4	10,0	0,078
	Medial FC	6,0	9,4	0,703
	Lateral FC	6,0	4,9	0,814
	Central part of femur	4,4	4,9	0,612
SO	Medial TC	15,6	7,1	0,332
	Lateral TC	2,2	1,9	0,891
	Medial FC	22,2	9,4	0,081
	Lateral FC	4,4	3,8	0,901
Osteophytes	Medial TC	44,4	20,8	**0,042**
	Lateral TC	31,1	15,1	0,064
	Medial FC	37,8	20,8	0,061
	Lateral FC	35,6	13,2	**0,041**
Ligament damage	Anterior cruciate	82,2	86,8	0,533
	Posterior cruciate	37,8	24,5	0,469
	Medial collateral	24,4	9,4	**0,048**
	Lateral collateral	8,9	1,8	0,112
Meniscus tear (>2)	Body of medial meniscus	75,6	49,1	**0,008**
	Anterior horn of medial meniscus	48,9	37,8	0,549
	Posterior horn of medial meniscus	75,6	56,7	0,063
	Body of lateral meniscus	44,4	32,0	0,382
	Anterior horn of lateral meniscus	44,4	28,3	0,204
	Posterior horn of lateral meniscus	44,4	28,3	0,311
Synovitis		97,8	88,7	0,204
Osteonecrosis		4,4	1,8	0,611

Table 2. *Comparison of structural changes in the knee joint in patients with and without CPTP (MRI data at the beginning of the study)*

Таблица 2. *Сравнение структурных изменений коленного сустава у пациентов с хронической посттравматической болью и без нее (данные МРТ в начале исследования)*

medial meniscus body, anterior horn of the medial meniscus, posterior horn of the medial meniscus, body of the lateral meniscus, anterior horn of the lateral meniscus, posterior horn of the lateral meniscus (0 = intact, 1 = minor radial or parrot-beak tear, 2 = non-displaced tear, 3 = displaced tear or partial resection, 4 = total destruction); synovitis (0 = absent, 1 = present); osteonecrosis (0 = absent, 1 = present).

Frequency and severity of MRI changes (baseline and after 12 months) was performed between groups of patients with and without CPTP.

The statistical analysis of obtained data was performed in the IBM SPSS Statistics 23 software suite. Quantitative variables were tested to meet the normal distribution law. Quantitative variables were described as median values with respective standard deviation (M±σ), in the event of absence of normal distribution in groups, as medians with the interquartile interval Me [25th; 75th percentiles] and verified using the Shapiro-Wilk test. Qualitative variables were presented as absolute values and their respective rates (%). The following statistical analysis methods were used to assess the obtained results: χ^2 Pearson's test (contingency table analysis), unpaired Student's t-test, paired comparisons of quantitative values, Wilcoxon signed-rank test (χ^2) was used. Differences were considered statistically significant at $p<0.05$.

The study was conducted in accordance with the principles of the Declaration of Helsinki. All patients provided written informed consent to participate. The protocol was approved by the Local Ethics Committee of the V.A. Nasonova Research Institute (protocol No. 23, dated 23.11.2022).

RESULTS

Chronic post-traumatic pain, or persistent sensation of pain ≥4 NRS for 3 months of follow-up, was diagnosed in 45 or 98 patients (45.9%). By the third month of the follow-up, CPTP+ patients, as compared to non-CPTP patients, demonstrated credibly higher pain intensity during movement, at rest and at nighttime, and functional disorders (NRS scale): 5.138 ± 1.512 and 1.771 ± 0.901 ($p<0.000$); 2.27 ± 0.691 and 0.803 ± 0.453 ($p<0.001$); 2.00 ± 1.766 and 0.405 ± 0.342 ($p<0.000$); 4.208 ± 1.356 and 1.898 ± 1.627 ($p<0.0302$). Similarly, in the third month of the follow-up, statistically significant difference between CPTP+ and CPTP- patient groups in all scores of the KOOS scale: the average value of the KOOS total was 58.4 ± 22.1 and 75.7 ± 23.4 ($p=0.012$); KOOS symptoms 58.1 ± 25.5 and 78.3 ± 29.2 ($p<0.018$); KOOS pain 54.6 ± 19.7 and 78.5 ± 28.4 ($p<0.02$); KOOS activity 57.8 ± 18.6 and 80.3 ± 30.3 ($p<0.004$), KOOS sports 51.9 ± 23.2 and 77.8 ± 20.4 ($p<0.009$), KOOS quality of life 46.3 ± 16.8 and 67.2 ± 21.1 ($p<0.025$).

In the baseline MRI parameters, the CPTP+ patient group (n=45) and CPTP- group (n=53) had statistically significant differences in the cartilage morphology (minimal alterations were more frequently identified in the CPTP- group), status of osteophytes of the medial tibial condyle and the lateral femoral condyle, damage of the medial collateral ligament and tear of the medial meniscus body. Practically all of patients in both groups showed injury of the ligaments of the knee joint (most frequently, the ACL) and tear of some meniscus or other (with varying severity), as well as synovitis; about a third of studies patients showed signs of OCD (**Table 2**).

After 12 months of follow-up, the differences in the MRI findings between the CPTP+ and CPTP- groups became more noticeable. Statistically significant difference was registered in such parameters as cartilage morphology, osteophytes of the medial TC, damage of the posterior cruciate and medial collateral ligaments, tear of the body, anterior and posterior horn of the medial meniscus, tear of the anterior horn of the lateral meniscus, positive synovitis status (**Fig. 1**).

It is to be mentioned that while the initial changes in the cartilage structure were more pronounced in the non-CPTP group (due to minimal changes, grade1), by the 12th month the situation changed: the cartilage deterioration was seen

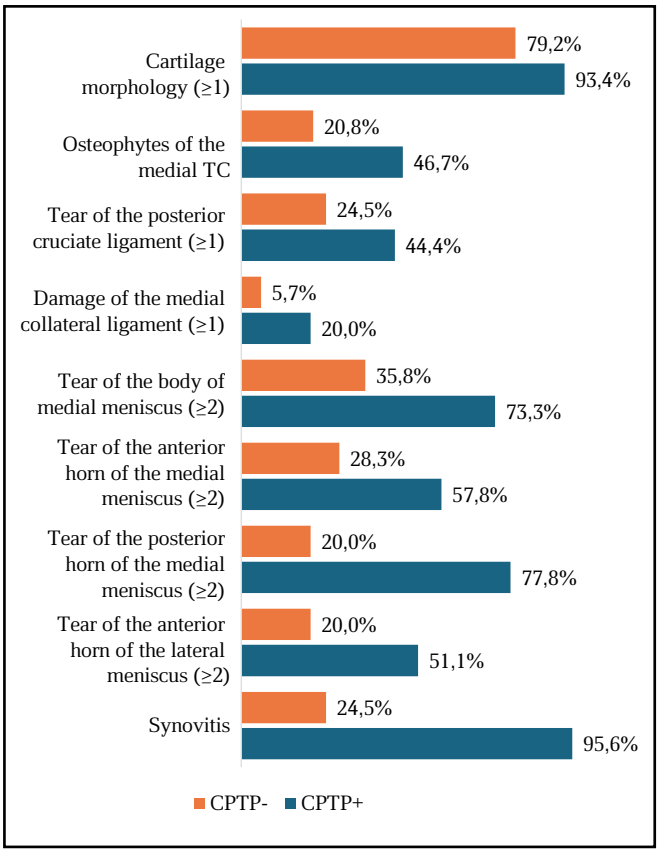

Note. Numbers in brackets designate change gradation as per WORMS; for all indicated parameters, p <0.05..

Figure 1. *Significant difference in some of structural changes in the knee joint in patients with and without CPTP (MRI data after 12 months).*

Рисунок 1. *Достоверное отличие ряда структурных изменений коленного сустава у пациентов с хронической посттравматической болью и без нее (данные МРТ через 12 мес.).*

more frequently and in more severe forms in the CPTP+ group (**Fig. 2**).

DISCUSSION

According to the obtained data, initially, the CPTP+ patients, as compared to CPTP- patients, had statistically significant difference just in several MRI features reflecting the post-traumatic changes of the knee joint. In CPTP+ patients, the more frequently identified features were the osteophytes of the medial TC and lateral FC, and damage of the medial collateral ligament and tear of the body of the medial meniscus. Meanwhile, the cartilage alterations (minimally pronounced) were more pronounced in patients without history of CPTP.

Twelve months later, the MRI findings changed significantly. The number of patients with changes in the ligaments and, specifically, menisci of the knee joint among CPTP+ patients considerably exceeded the number of individual with the same pathology in the CPTP- patient group. A particularly significant difference was observed in both synovitis detection frequency and the dynamic changes of articular cartilage. Initially, cartilage damage was registered in CPTP+ patients only in 26.7%, but after 12 months in 93.4%, and in the majority of them (82.1%), the damage was substantial (≥2 WORMS). In CPTP- patients, such changes were registered only in 43.4%.

The obtained results show a clear correlation between the CPTP and the structural alterations in the knee joint. Our data align with the results obtained by foreign colleagues. K. van Oudenaarde *et al.* [14] compared the clinical manifestations and the MRI findings in 174 patients with an injury of the knee joint (follow-up period up to 6 months). Alterations identified by the MRI are predominantly trauma of ACL and menisci were found in 39%. There was credible correlation between changes in the MRI, severity and duration of symptoms persistence. The correlation between post-traumatic alterations found in the MRI and clinical manifestations of the knee joint injury was demonstrated in the works of O. Babalola *et al.* [15] and J.Wasser *et al.* [16].

Correlation of the MRI findings and OA symptoms was shown in a series of clinical studies. According to D. Felson *et al.* [17], who evaluated progression of OA in 110 patients, the pain in the knee joint was credibly more frequently observed in cases when bone marrow edema was identified by MRI: for grades ≥2 WORMS the odds ratio (OR) was

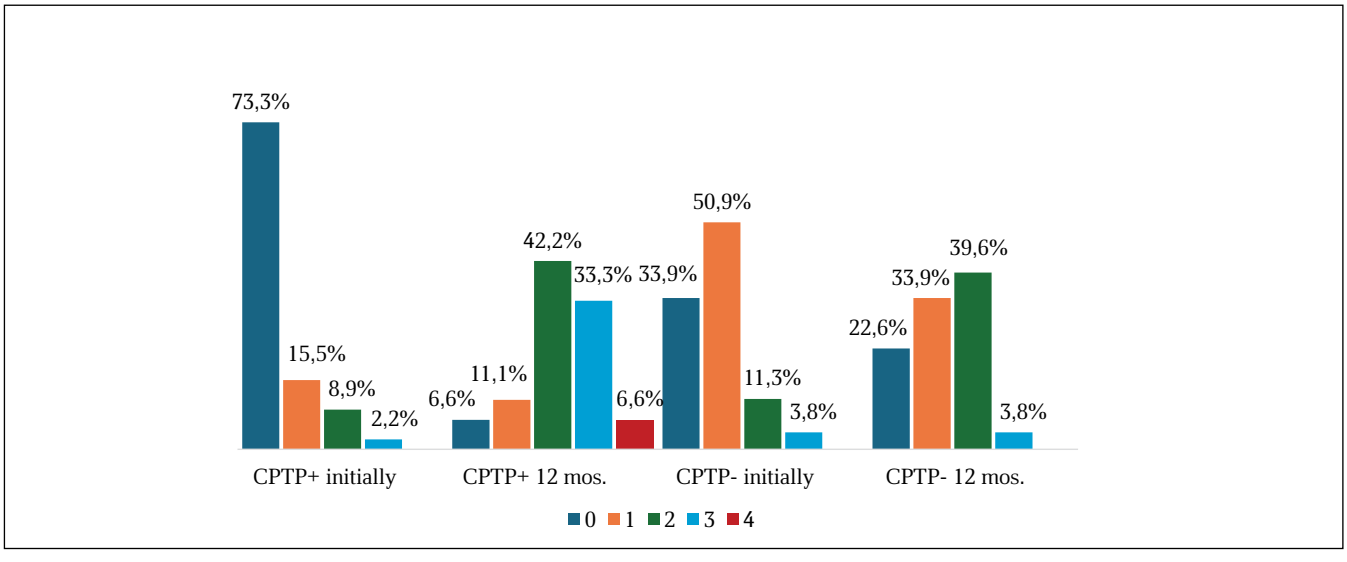

Figure 2. *Dynamics of changes in articular cartilage in the CPTP+ and CPTP- groups (MRI data after 12 months).*

Рисунок 2. *Динамика изменений суставного хряща в группах ХПТБ+ и ХПТБ- (данные МРТ через 12 мес.).*

3.2 (95% CI 1.5–6.8, p<0.002). The study of C. Hill *et al.* [18], which involved 270 patients with OA, showed a correlation between severity of MRI-identified signs of synovitis and pain: r = 0.21, p<0.0003. According to the MOST study, lateral osteophytes of the patellofemoral joint, synovitis of the knee joint and infrapatellar synovitis correlated with pain in the anterior part of the knee joint: OR 5.0 (95% CI 1.7-14.6]); 4.7 (95% CI 1.3-16.2), 2.8 (95% CI 1.0-7.8) [19]. Moreover, the follow-up of 1185 patients in the MOST study showed that MRI findings of the cartilage damage (≥2) and of osteophytes (≥2), with signs of bone marrow edema or synovitis (≥1) have higher sensitivity and specificity (over 90%) for the identification of both symptomatic and radiologic progression of OA [20]. According to the study program "Osteoarthritis Initiative", MRI features of meniscus damage in patients with OA correlate with presence of pain in the joint (OR = 2.82, 95% CI 1.79-4.43) [21]. In the study of Z. Zhao *et al.* [22], who used the method of computer-assisted analysis (a total of 421 affected knee joints), correlation was shown between the pain and such MRI findings as bone marrow edema and destruction of the joint cartilage.

The correlation between symptoms and structural alterations of the knee joint confirms significance of CPTP as a predictor of PTOA development. It is evident that the persistence and progression of MRI-identified alterations in the CPTP+ patient group may be regarded as a manifestation of the early stage of the disease. Especially important is the increase in the alterations of the joint cartilage. This MRI-identified feature seems important for the development of early OA even with the absence of manifested pain in the joint. Cartilage deterioration has even greater predictive value if symptoms indicating damage of the knee joint persist and progress [23].

It is to be noted that persistence of symptoms assessed with a standard KOOS questionnaire is one of the major classification criteria of early OA as defined by the research group of F. Luyten *et al.* (updated in 2018: assessment using two scales KOOS ≤ 85 and presence of pain, functional disorder or crepitation of the knee joint) [24]. Recently, two papers were published that assess the outcome of the ACL trauma in which changes after 1 and 3 years were analyzed in accordance with the updated criteria of Luyten. In the study of A. Cronström *et al.* [25], 106 patients were involved after an injury of the knee joint and surgical reconstruction of the ligament. After 1 year and 3 years, the number of persons meeting the Luyten criteria for early OA was 82% and 78%. The study of M. Harkey *et al.* [26] assessed the condition of 82 patients (aged from 13 to 35) after the trauma and subsequent reconstruction of the ACL. Their meeting the Luyten criteria for early OA in the follow-up visits after 6 and 12 months was registered in 22% patients.

CONCLUSION

Development of CPTP after knee joint injury is related to higher rate of progression of structural changes of the affected joint. Persistence of mild or severe pain in the knee joint for over three months after the trauma may be seen as an important predictor of development of early stages of post-traumatic osteoarthritis.

ADDITIONAL INFORMATION	ДОПОЛНИТЕЛЬНАЯ ИНФОРМАЦИЯ
Ethical review. This work was carried out in compliance with human rights defined by the Helsinki Accords. All patients gave informed consent to participate in the study. The study was approved by the Ethics Committee of the V.A. Nasonova Research Institute of Rheumatology (Protocol No. 8 dated 10/25/2022).	***Этическая экспертиза.*** Настоящая работа проводилась с соблюдением прав человека, определенных Хельсинкским соглашением. Все пациенты дали информированное согласие на участие в исследовании. Исследование было одобрено этическим комитетом ФГБНУ «НИИ ревматологии имени В.А. Насоновой» (протокол № 8 от 25.10.2022).
Study funding. The work was carried out using budgetary funding for the implementation of the state assignment on topic FURS-2022-0009 (state assignment number 1021062512064-0).	***Источник финансирования.*** Работа выполнена за счет средств бюджетного финансирования на выполнение государственного задания по теме FURS-2022-0009 (номер государственного задания 1021062512064-0).
Conflict of interest. The authors declare that there are no obvious or potential conflicts of interest associated with the content of this article.	***Конфликт интересов.*** Авторы декларируют отсутствие явных и потенциальных конфликтов интересов, связанных с содержанием настоящей статьи.
Contribution of individual authors. Byalik A.A.: collection of database, writing of the text of article. Makarov S.A.: patient selection. Karateev A.E.: idea of the study, editing of the article. Nesterenko V.A., Kudinsky D.M.: statistical processing of results. The authors gave their final approval of the manuscript for submission, and agreed to be accountable for all aspects of the work, implying proper study and resolution of issues related to the accuracy or integrity of any part of the work.	***Участие авторов.*** А.А. Бялик – сбор базы данных, написание текста статьи. С.А. Макаров – отбор пациентов. А.Е. Каратеев – идея исследования, редактирование статьи. В.А. Нестеренко, Д.М. Кудинский – статистическая обработка результатов. Все авторы одобрили финальную версию статьи перед публикацией, выразили согласие нести ответственность за все аспекты работы, подразумевающую надлежащее изучение и решение вопросов, связанных с точностью или добросовестностью любой части работы.

REFERENCES / ЛИТЕРАТУРА

1. Zubavlenko RA, Ulyanov VYu, Belova SV. Pathogenic peculiarities of post-traumatic knee osteoarthrosis: analysis of diagnostic and therapeutic strategies (review). *Saratov Journal of Medical Scientific Research*. 2020;16(1):50-54. [Зубавленко Р.А., Ульянов В.Ю., Белова С.В. Патогенетические особенности посттравматического остеоартроза коленных суставов: анализ диагностических и терапевтических стратегий (обзор). *Саратовский научно-медицинский журнал*. 2020;16(1):50-54]. URL: https://ssmj.ru/system/files/archive/2020/2020_01_050-054.pdf

2. Fogarty AE, Chiang MC, Douglas S, et al. Posttraumatic osteoarthritis after athletic knee injury: A narrative review of diagnostic imaging strategies. *PM&R*. 2025;17(1):96-106. DOI: 10.1002/pmrj.13217

3. Whittaker JL, Losciale JM, Juhl CB, et al. Risk factors for knee osteoarthritis after traumatic knee injury: a systematic review and meta-analysis of randomised controlled trials and cohort studies for the OPTIKNEE Consensus. *Br J Sports Med*. 2022;56(24):1406-1421. DOI: 10.1136/bjsports-2022-105496

4. Gupta S, Sadczuk D, Riddoch FI, et al. Pre-existing knee osteoarthritis and severe joint depression are associated with the

need for total knee arthroplasty after tibial plateau fracture in patients aged over 60 years. *Bone Joint J*. 2024;106-B(1):28-37. DOI: 10.1302/0301-620X.106B1.BJJ-2023-0172.R2

5. Andersen TE, Ravn SL. Chronic pain and comorbid posttraumatic stress disorder: Potential mechanisms, conceptualizations, and interventions. *Curr Opin Psychol*. 2025;62:101990. DOI: 10.1016/j.copsyc.2025.101990

6. Ashoorion V, Sadeghirad B, Wang L, et al. Predictors of Persistent Post-Surgical Pain Following Total Knee Arthroplasty: A Systematic Review and Meta-Analysis of Observational Studies. *Pain Med*. 2023;24(4):369-381. DOI: 10.1093/pm/pnac154

7. Kijowski R, Roemer F, Englund M, et al. Imaging following acute knee trauma. *Osteoarthritis Cartilage*. 2014;22(10):1429-43. DOI: 10.1016/j.joca.2014.06.024

8. Mahmoudian A, Lohmander LS, Mobasheri A, et al. Early-stage symptomatic osteoarthritis of the knee - time for action. *Nat Rev Rheumatol*. 2021;17(10):621-632. DOI: 10.1038/s41584-021-00673-4

9. Villari E, Digennaro V, Panciera A, et al. Bone marrow edema of the knee: a narrative review. *Arch Orthop Trauma Surg*. 2024;144(5):2305-2316. DOI: 10.1007/s00402-024-05332-3

10. Fogarty AE, Chiang MC, Douglas S, et al. Posttraumatic osteoarthritis after athletic knee injury: A narrative review of diagnostic imaging strategies. *PM&R*. 2025;17(1):96-106. DOI: 10.1002/pmrj.13217

11. Dainese P, Wyngaert KV, De Mits S, et al. Association between knee inflammation and knee pain in patients with knee osteoarthritis: a systematic review. *Osteoarthritis Cartilage*. 2022;30(4):516-534. DOI: 10.1016/j.joca.2021.12.003

12. Ghouri A, Muzumdar S, Barr AJ, et al. The relationship between meniscal pathologies, cartilage loss, joint replacement and pain in knee osteoarthritis: a systematic review. *Osteoarthritis Cartilage*. 2022;30(10):1287-1327. DOI: 10.1016/j.joca.2022.08.002

13. Luyten FP, Denti M, Filardo G, et al. Definition and classification of early osteoarthritis of the knee. *Knee Surg Sports Traumatol Arthrosc*. 2012;20(3):401-6. DOI: 10.1007/s00167-011-1743-2

14. van Oudenaarde K, Swart NM, Bloem J, et al. Post-traumatic knee MRI findings and associations with patient, trauma, and clinical characteristics: a subgroup analysis in primary care in the Netherlands. *Br J Gen Pract*. 2017;67(665):e851-e858. DOI: 10.3399/bjgp17X693653

15. Babalola OR, Itakpe SE, Afolayan TH, et al. Predictive Value of Clinical and Magnetic Resonance Image Findings in the Diagnosis of Meniscal and Anterior Cruciate Ligament Injuries. *West Afr J Med*. 2021;38(1):15-18. PMID: 33463701

16. Wasser JG, Hendershot BD, Acasio JC, et al. A Comprehensive, Multidisciplinary Assessment for Knee Osteoarthritis Following Traumatic Unilateral Lower Limb Loss in Service Members. *Mil Med*. 2024;189(3-4):581-591. DOI: 10.1093/milmed/usac203

17. Felson DT, Niu J, Guermazi A, et al. Correlation of the development of knee pain with enlarging bone marrow lesions on magnetic resonance imaging. *Arthritis Rheumatol*. 2007;56(9):2986-92. DOI: 10.1002/art.22851

18. Hill CL, Hunter DJ, Niu J, et al. Synovitis detected on magnetic resonance imaging and its relation to pain and cartilage loss in knee osteoarthritis. *Ann Rheum Dis*. 2007;66(12):1599-603. DOI: 10.1136/ard.2006.067470

19. Macri EM, Neogi T, Jarraya M, et al. Magnetic Resonance Imaging-Defined Osteoarthritis Features and Anterior Knee Pain in Individuals With, or at Risk for, Knee Osteoarthritis: A Multicenter Study on Osteoarthritis. *Arthritis Care Res (Hoboken)*. 2022;74(9):1533-1540. DOI: 10.1002/acr.24604

20. Liew JW, Rabasa G, LaValley M, Collins J, Stefanik J, et al. Development of a Magnetic Resonance Imaging-Based Definition of Knee Osteoarthritis: Data From the Multicenter Osteoarthritis Study. *Arthritis Rheumatol*. 2023;75(7):1132-1138. DOI: 10.1002/art.42454

21. Antony B, Driban JB, Price LL, et al. The relationship between meniscal pathology and osteoarthritis depends on the type of meniscal damage visible on magnetic resonance images: data from the Osteoarthritis Initiative. *Osteoarthritis Cartilage*. 2017;25(1):76-84. DOI: 10.1016/j.joca.2016.08.004

22. Zhao Z, Zhao M, Yang T, et al. Identifying significant structural factors associated with knee pain severity in patients with osteoarthritis using machine learning. *Sci Rep*. 2024;14(1):14705. DOI: 10.1038/s41598-024-65613-0

23. Pius AK, Beynnon BD, Fiorentino N, Gardner-Morse M, Vacek PM, et al. Articular cartilage thickness changes differ between males and females 4 years following anterior cruciate ligament reconstruction. *J Orthop Res*. 2022;40(1):65-73. DOI: 10.1002/jor.25142

24. Luyten FP, Bierma-Zeinstra S, Dell'Accio F, et al. Toward classification criteria for early osteoarthritis of the knee. *Semin Arthritis Rheum*. 2018;47(4):457-463. DOI: 10.1016/j.semarthrit.2017.08.006

25. Cronström A, Risberg MA, Englund M, et al. Symptoms indicative of early knee osteoarthritis after ACL reconstruction: descriptive analysis of the SHIELD cohort. *Osteoarthr Cartil Open*. 2025;7(1):100576. DOI: 10.1016/j.ocarto.2025.100576

26. Harkey MS, Driban JB, Baez SE, et al. Persistent Early Knee Osteoarthritis Symptoms From 6 to 12 Months After Anterior Cruciate Ligament Reconstruction. *J Athl Train*. 2024;59(9):891-897. DOI: 10.4085/1062-6050-0470.23

Editorial | Редакционная статья
DOI: https://doi.org/10.35693/SIM689011

Scientific and pedagogical school of Professor A.A. Lebedev (commemorating the 95th anniversary of his birth)

Aleksei V. Dubishchev, Elena N. Zaitceva, Elena V. Avdeeva
Samara State Medical University (Samara, Russian Federation)

Abstract

August 28, 2025 marks the 95th anniversary of the birth of Aleksei A. Lebedev, the founder of the Samara Scientific and Pedagogical School of Pharmacologists, which has all-Russian and international recognition in the field of "Pharmacology of the Kidneys and Water-Salt Metabolism".

The milestones of A. A. Lebedev's biography are presented. His influence on the development of pharmacology, training of scientific and pedagogical personnel in the field of pharmacology, clinical pharmacology and clinical medicine in Russia is analyzed.

Keywords: experimental and clinical pharmacology; drugs; teaching pharmacology; scientific research.

Conflict of interest: nothing to disclose.

Citation
Dubishchev AV, Zaitceva EN, Avdeeva EV. **Scientific and pedagogical school of Professor A.A. Lebedev (commemorating the 95th anniversary of his birth).** *Science and Innovations in Medicine.* 2025;10(3):255-258.
DOI: https://doi.org/10.35693/SIM689011

Information about authors
Aleksei V. Dubishchev – MD, Dr. Sci. (Medicine), Professor, Professor of the Department of Pharmacology named after Honored Scientist of the Russian Federation Professor A.A. Lebedev.
ORCID: 0000-0002-4430-6672
E-mail: a.v.dubischev@samsmu.ru
Elena N. Zaitceva – MD, Dr. Sci. (Medicine), Associate Professor, Professor of the Department of Pharmacology named after Honored Scientist of the Russian Federation Professor A.A. Lebedev.
ORCID: 0000-0001-5689-2077
E-mail: e.n.zaitceva@samsmu.ru

***Elena V. Avdeeva** – MD, Dr. Sci. (Medicine), Professor, Head of the Department of Pharmacology named after Honored Scientist of the Russian Federation Professor A.A. Lebedev.
ORCID: 0000-0003-3425-7157
E-mail: e.v.avdeeva@samsmu.ru
Corresponding Author

Received: 01.08.2025
Accepted: 13.08.2025
Published: 15.08.2025

Научно-педагогическая школа профессора А.А. Лебедева (к 95-летию со дня рождения)

А.В. Дубищев, Е.Н. Зайцева, Е.В. Авдеева
ФГБОУ ВО «Самарский государственный медицинский университет» Минздрава России (Самара, Российская Федерация)

Аннотация

28 августа 2025 года исполнилось 95 лет со дня рождения Алексея Александровича Лебедева, основоположника Самарской научно-педагогической школы фармакологов, имеющей общероссийское и международное признание по направлению «Фармакология почек и водно-солевого обмена». В статье представлены основные этапы биографии А.А. Лебедева. Проведен анализ его влияния на развитие фармакологии, подготовку научно-педагогических кадров в области фармакологии, клинической фармакологии и клинической медицины в Российской Федерации.

Ключевые слова: экспериментальная и клиническая фармакология; лекарственные средства; преподавание фармакологии; научные исследования.

Конфликт интересов: не заявлен.

Для цитирования:
Дубищев А.В., Зайцева Е.Н., Авдеева Е.В. **Научно-педагогическая школа профессора А.А. Лебедева (к 95-летию со дня рождения).** *Наука и инновации в медицине.* 2025;10(3):255-258. DOI: https://doi.org/10.35693/SIM689011

Сведения об авторах
Дубищев А.В. – д-р мед. наук, профессор, профессор кафедры фармакологии имени заслуженного деятеля науки РФ профессора А.А. Лебедева.
ORCID: 0000-0002-4430-6672
E-mail: a.v.dubischev@samsmu.ru
Зайцева Е.Н. – д-р мед. наук, доцент, профессор кафедры фармакологии имени заслуженного деятеля науки РФ профессора А.А. Лебедева.
ORCID: 0000-0001-5689-2077
E-mail: e.n.zaitceva@samsmu.ru

***Авдеева Елена Владимировна** – д-р фарм. наук, профессор, заведующая кафедрой фармакологии имени заслуженного деятеля науки РФ профессора А.А. Лебедева.
ORCID: 0000-0003-3425-7157
E-mail: e.v.avdeeva@samsmu.ru
Автор для переписки

Список сокращений
ОЦК – объем циркулирующей крови.

Получено: 01.08.2025
Одобрено: 13.08.2025
Опубликовано: 15.08.2025

Aleksei Aleksandrovich LEBEDEV (28.08.1930 – 09.03.2008)

A GLIMPSE INTO A REMARKABLE LIFE

Aleksei Aleksandrovich Lebedev, Honored Scientist of the Russian Federation, Doctor of Medicine, Professor Emeritus of the Ivanovo State Medical Academy and Samara State Medical University, was born on 28 August 1930, in the town of Suzdal of the Vladimir Region in a family of doctors. Having moved to the town of Ivanovo, Aleksei Aleksandrovich followed the family traditions and entered the Ivanovo State Medical University; in 1953, he graduated with honors.

He chose his field of scientific interest in the third year of studies, when he joined the students' club of the pharmacology department; he kept the interest to pharmacological science until the very end. His formation as a scientist was greatly influenced by his tutor, Georgy Mikhailovich Shpuga, who had developed the method of kidney autotransplantation to the cervical vessels as early as in 1937. The method involves anastomosing the carotid artery to the renal artery, and the jugular vein with the renal vein. It was found that the kidney transplanted to the neck functioned 30–40% worse compared to the intact kidney, which was likely due to denervation occurring during organ transplantation. The idea suggested by Prof. G.M. Shpuga, on the necessity of reinnervating the transplanted kidney to improve its function and trophicity, later formed the basis of the doctoral dissertation of A.A. Lebedev.

It proposed an original idea of restoring the innervation during surgery by anastomosing the central end of the vagus nerve with the peripheral ends of the renal nerves severed during transplantation. A brilliant experimenter, Aleksei Aleksandrovich proved that both afferent and efferent innervation of the kidneys recover after anastomosing of the nerves. Reinnervation was confirmed in the works of his students: long-term monitoring of test animals demonstrated gradual adequation of the functions of the intact and the auto-transplanted kidneys. Owing to the works of A.A. Lebedev and his students one of the debatable issues of organ physiology found its solution: the question of the role of renal nerves in the kidney physiology.

SCIENTIFIC SCHOOL OF A.A. LEBEDEV

In 1964, A.A. Lebedev was elected as the Chair of the Department of Pharmacology of the D.I. Ulyanov Kuybushev Medical Institute (now the Samara State Medical University). He worked in this position for 36 years. Under his guidance, there started a large-scale research in the areas of kidney physiology and salt and water metabolism. One of strategic areas that had to be developed and justified was the research of the very close connection between the kidney function and the blood circulation system. Even at the time, it was established that while performing the excretory function kidneys perform a not less important homeostatic function maintaining adequacy of the blood circulation. It meant that the obvious excretion of salt, water and metabolites from the body is appended on a not less crucial yet invisible function of retaining electrolytes and liquid in the body, which ensures the bodily homeostasis: volume of the circulating blood, its composition, arterial blood pressure and other parameters. When studying the activity of acetylcholine, nitroglycerin, benzohexonium and hygronium a decrease in the peripheral resistance of the vessels was established. Despite the different chemical structure and the mechanism of action of the substances, they cause a unidirectional reaction of keeping sodium and water in the body by increasing reabsorption of these components in the renal tubules. At the same time, the circulatory blood volume (CBV) increases. It was found that due to the effect of ephedrine, adrenaline, noradrenaline, occlusion of the common carotid arteries the peripheral resistance of vessels increases, as well does the excretion of sodium, potassium and water with a decrease of the CBV.

Manipulations with CBV also demonstrated the homeostatic function of the kidneys: volume reduction induced by phlebotomy elicits antinatriuretic and antidiuretic effects; conversely, increased blood volume produces the opposite renal response. These investigations led to the formulation of the theory of blood volume vascular capacity matching as a regulator of renal homeostatic function. Subsequent studies focused on elucidating specific

renal and extrarenal mechanisms mediating these responses, including the roles of renal nerves, the sympathoadrenal system, and the renin-angiotensin system, under both pharmacological interventions and pathological conditions. In all of these cases, excretion of sodium and water correlates more with the level of peripheral resistance of vessels than with the level of arterial blood pressure. Homeostatic reactions of the kidneys drastically change under hypertensive disease, myocardial infarction, heart failure, and under intervention of pathogenic factors into this process.

In the course of analysis of homeostatic reactions of the kidneys ensuring maintenance of the blood circulation adequacy, Prof. Lebedev clearly saw that the intricate mechanisms of kidney excretion could not be understood without an in-depth study of the nephron functions. It was necessary to study the tubule reabsorption of the principal ion of the internal medium, sodium, which determines its osmotic concentration, alkaline potential, volume of intravascular and extracellular fluid. Research in this direction assumed a large-scale character. It became necessary to re-conceptualize the transport of sodium and chloride in the nephron. The existing model of sodium transfer from the lumen to the interstitium at the start of the work stated that the ion moves passively through sodium channels in the luminal membrane of nephrocytes along the concentration gradient, while across the basolateral membrane, sodium was believed to be transported against the electrochemical gradient via an active transport mechanism. Chlorine follows the sodium ion, creates an oncotic gradient in the basal labyrinth, mediates the fluid flow in the extracellular pathways from the tubule lumen to the interstitium. In this way, cell reabsorption of water occurs due to primary reabsorption of sodium.

Aleksei Aleksandrovich made a proposition that the ion transport may fulfil not only in a transcellular way but also by transfer in the intercellular space. There appeared the theory of fixed charges of the nephron wall that explained and proved the possibility of transcellular transport. In the experiments using biomembranes performing sodium transfer from the internal surface to the external (wall of the urinary bladder of a frog), the possibility of transfer of sucrose, ions of iodide, chloride, lithium and fluoresceine in the intercellular space was demonstrated multiple times. Subsequently, it was established that cations are always transported in greater quantity from the mucosal to the serosal surface, while anions move in the opposite direction. The charge hypothesis provided an explanation for this phenomenon, attributing it to fixed charges creating flow asymmetry. It was hypothesized that within the nephron, at the entrance to the intercellular spaces on the luminal side, negative charges are present, promoting cation movement and hindering anion transport, while on the basolateral surface in the region of the intercellular spaces, positive charges exist, facilitating the opposite phenomenon. This mechanism contributes to the generation of a transepithelial potential across the nephron wall.

The theory of gate charges of cell junctions proved very useful for the interpretation of mechanism of action of some diuretics. Such diuretics as etacrynic acid, osmotic diuretics, mercurial diuretics expand the gates of the cell junctions, while the gate charges lose their role and the selectivity of ion flows decreases.

The problem of localization and tubular effect of diuretics became the center of many dissertations supervised by the professor. However, this path was full of methodological complications. The nephron, the main structural unit of the kidney, is microscopic in size, it is not possible to study it directly; therefore, model experiments were performed on epithelial structures performing directed transfer of sodium: the skin and the wall of the urinary bladder of a frog, the wall of large intestine of mammals.

Early research performed in the laboratory of A.A. Lebedev in 1970s demonstrated that the inhibitors of metabolic processes, such as strophantine, directly blocked the active transfer of sodium through biological membranes, and some diuretics, such as Mercusal, Novurit, Hypothiazid caused a significant increase in the permeability of cell membranes. The effect of Novurit was confirmed in experiments with micropuncture examination of the rat nephron, and in experiments utilizing the Na24 radioactive isotope. The obtained data demonstrated the capability of diuretics to influence bypassing sodium flows in the nephron presumably traveling through intercellular spaces. This proposal was later confirmed in multiple experiments.

The doubts completely vanished when micropuncture experiments on rat nephrons with fluorescein, marker of intercellular permeability, showed that Novurit and Mannitol significantly change the paracellular transport, while Furosemide had no effect on it. Expansion of intercellular spaces increases the bypassing flow of sodium from the interstitium to the nephron lumen, which balances the active transport and leads to an increase of natriuresis. Furosemide does not affect the intercellular transport of ions, and its effect is mediated by binding to one of the enzymes of the renal epithelium and secondary effect on the Na+-2Cl--K+ cotransporter of the luminal membrane of the ascending limb of Henle's loop. Based on the obtained data, A.A. Lebedev proposed an original classification of diuretics based on the mechanism of their action.

The search for new agents with a diuretic effect has always been the focus of interest of the department of pharmacology. This involved establishment of contacts with chemists of Kuybyshev (today, the city of Samara) and other regions to study the pharmacology of heterocyclic spirans and isoindoles (Saratov State University), triazines (Leningrad Institute of Chemistry and Pharmacology), sulfamoylbenzoic acid (Research Institute of Medicinal Products of Kupavna). Active diuretics were identified for future in-depth research. It was found that the lithium and furfurylamin salts of furosemide have especially high activity surpassing the effect of Furosemide. The Department of Pharmaceutical Chemistry of the Kuybyshev Medical Institute synthesized several compounds based on etacrynic acid and bumetanide that had a marked diuretic effect. These works had very high theoretical importance for they opened ways of synthesis of new biologically active compounds.

In the late 1980s, the Department of Pharmacology of the Kuybyshev Medical Institute became the base for research of diuretic agents. The All-Union Research Institute of Chemistry and Pharmacology (Moscow) received the state order for the development of domestic diuretic agents that involved novel synthesis of Furosemide, Hypothiazid, Triamterene, Spironolactone, and the Department performed a comparative assessment of their diuretic properties. The analysis showed that the protective action of the products is not related to their structure (they belong to different chemical classes) but was determined by the diuretic effect itself. The scientists concluded that the prophylactic action of the drugs stems from the hemodynamic effect developing on the nephron level. Thus, Furosemide

increases the lumen of proximal and distal tubules, reduces the swelling and deterioration of nephrocytes, increases the tubule flow of the fluid, and increases the hydrostatic pressure in the lumen: this enables the tubules resist the ischemic stress. The similar effect of Furosemide was confirmed in the experiments with acute hemorrhagic hypotension and toxic nephropathy. It was demonstrated that the domestically produced Furosemide does not differ from the imported analogs. After that, domestic production of Furosemide started in the country. At present, diuretics are used in acute kidney failure both as prevention and treatment drugs, in the initial period of development of kidney failure, if the arterial blood pressure and the circulating blood volume are normalized. It is to be remembered that the clinical use of diuretics was justified experimentally.

The method of nephron micropuncture, biological modeling of sodium transport, methods of fluorescent analysis of individual nephrons facilitated development of a classification of diuretics described in the article "Diuretic Agents" in the Great Medical Encyclopedia. Prof. Lebedev was the editor of five monothematic collections of articles.

A.A. Lebedev is the co-author of 16 patents on biologically active substances, including those with a diuretic action. He wrote 240 scientific works, among them 4 monographs.

TRAINING OF SCIENTIFIC AND PEDAGOGICAL STAFF

A.A. Lebedev gave great attention to training of scientific research and pedagogical staff; he initiated and pioneered the Pharmaceutical Faculty of the Kuybyshev Medical Institute. He was the tutor of 11 doctors of science and 28 candidates of science. In the course of his work in Samara, he created a scientific school of pharmacologists within a single scientific field, "Pharmacology of the kidneys and salt and water metabolism". To date, this school shapes the development of this area of research in the country. In 1964, A.A. Lebedev organized the Regional Society of Pharmacologists and chaired its work for many years. He was also a member of the Russian Society of Pharmacologists, and a member of the editorial board of the "Journal of Experimental and Clinical Pharmacology". In the Scientific Council on Pharmacology and Pharmacy, A.A. Lebedev supervised the "Pharmacology of the Kidneys" branch. Aleksei Aleksandrovich spared no effort and energy in working with aspiring specialists: for 35 years, he was the academic advisor of the Students' Scientific Society of the Samara State Medical University. Under his leadership, five national conferences on kidney pharmacology and salt and water metabolism, and one national symposium. For his constructive academic and pedagogical activity, training of academic staff A.A. Lebedev was awarded with the Order of Peoples' Friendship, second-class Medal of the Order of "Merit for the Motherland", signs of the "Expert of Healthcare", "Foe Exceptional Achievement in the Work", and the Medal of "Veteran of Labor". Cambridge International Bibliographic Database awarded him with a prize for exceptional contributions to science. In 1978, for his merit in the development of Soviet pharmacology, the Academic Council of the Institute of Pharmacology of the Academy of Medical Sciences of the USSR awarded A.A. Lebedev with the medal of the founder of Russian pharmacology, Nikolay Pavlovich Kravkov.

A.A. Lebedev was Professor emeritus of the Samara State Medical University and Ivanovo State Medical Academy. He was elected as a Fellow of the Eurasia International Academy of Sciences. In 1999, the American Biographical Institute, following the recommendation of Academy Fellow D.A. Kharkevich, listed A.A. Lebedev on the International Directory of Distinguished Leadership.

Aleksei Aleksansrovich Lebedev passed away on 9 March, 2008 at the age of 78 years. The cherished memory of him stays in our hearts.

CONCLUSION

In 2008, the Rectorate of the Samara State Medical University gave the name of the Honored Scientist of the Russian Federation Prof. A.A. Lebedev to the Department of Pharmacology. The staff and faculty of the Department of Pharmacology, students of Prof. Lebedev, continue developing the lines of science pioneered by Aleksei Aleksandrovich, and, inspired by the vigor and the range of thought of the scientist, they blaze new trails. The contribution of A.A. Lebedev in the national medicine constitutes a solid foundation of ongoing research in the area of pharmacology of the kidneys and related fields of experimental pharmacology.

ADDITIONAL INFORMATION	ДОПОЛНИТЕЛЬНАЯ ИНФОРМАЦИЯ
Provenance and peer review. This paper was commissioned by the journal's Editorial Board and underwent prioritized internal peer review.	***Рассмотрение и рецензирование.*** Настоящая работа подготовлена по просьбе редакции журнала, была рассмотрена во внеочередном порядке без участия внешних рецензентов.
Study funding. The study was without external funding.	***Источник финансирования.*** Работа выполнена без привлечения финансирования.
Conflict of interest. The authors declare that there are no obvious or potential conflicts of interest associated with the content of this article.	***Конфликт интересов.*** Авторы декларируют отсутствие явных и потенциальных конфликтов интересов, связанных с содержанием настоящей статьи.
Contribution of individual authors. Dubishchev A.V.: definition of the concept, editing of the manuscript. Zaitseva E.N., Avdeeva E.V.: collection and processing of materials, writing of the original text, editing of the manuscript. The authors gave their final approval of the manuscript for submission, and agreed to be accountable for all aspects of the work, implying proper study and resolution of issues related to the accuracy or integrity of any part of the work.	***Участие авторов.*** Дубищев А.В. – определение концепции, редактирование рукописи. Зайцева Е.Н., Авдеева Е.В. – сбор и обработка материалов, написание оригинального текста, редактирование рукописи. Все авторы одобрили финальную версию статьи перед публикацией, выразили согласие нести ответственность за все аспекты работы, подразумевающую надлежащее изучение и решение вопросов, связанных с точностью или добросовестностью любой части работы.